CHAPTER ONE

INTRODUCTON

1.1 Background of Study

Water pollution, particularly of surface water results from all activities of man which include indiscriminate waste disposal from industries such as effluents into waterways. Municipal wastes and Industrial sewages have been continuously added to water bodies which affect the physico-chemical quality of water, making them unfit for use by human, livestock and other organisms (Dwivedi and Pandey, 2002). Pollution is caused when a change in the biological, chemical or physical condition in the environment harmfully affect quality of human life including other animals' life and plant (Lowel and Thompson, 1992; Okoye et al, 2002). Water quality models can be useful tools for simulating and predicting pollutant transport (Bai et al, 2011).

Industrial effluents are unwanted fluids generated from industrial activities and are inappropriately discharged into the environment or receiving surface water. Its characteristics provide basic information about the utility of the rivers and streams into which they are discharged (Kanu et al, 2006). The problem posed by environmental pollution due to man's (anthropogenic) activities is fast becoming a point that should be taken seriously in today's world (Okereke, 2007).

Effluent discharges into the environment with enhanced concentration of nutrients and sediments will have serious negative impact on the quality and life forms of the receiving water body when discharged untreated or partially treated (Forenshell, 2001; Schulz and Howe, 2003). Water pollution by industrial effluents has become a question of

considerable public and scientific concern in the light of evidence of their extreme toxicity to human health and to biological ecosystems (Katsuro et al, 2004). The occurrence of heavy metals in industrial effluents and municipal sewage constitute a major source of the pollution entering aquatic ecosystem.

It is noteworthy that Industries play an important role in the socio-economic development of any nation. However, global industrialization especially in Africa has put much demand on natural resources. It is generally recognized that in many developing countries, industrial environmental standards are lacking and where they exist, the instruments of control are not efficient. This is largely explained by the absence of reliable and comprehensive system of monitoring industrial emissions and enforcement of compliance with the industrial standards (Aluyor and Badmus, 2003a). The ultimate recipient of all forms of pollution is the natural water body.

Many industries are located near water bodies, presumably to facilitate easy disposal of effluents and other wastes into them. The perceived consequences of unregulated waste disposal into water bodies used for potable water sources has stimulated various studies on industrial effluent (Aluyor and Badmus, 2003a; Aluyor and Badmus, 2003b; Eletta et al, 2005; Otukunefor and Obiukwu, 2005; Aisien et al, 2003); Nkwocha and Okoye, 2007; Nkwocha and Okoye, 2008; Nkwocha et al, 2010)

Ele River Nnewi, Anambra State is surrounded by several industries such as Chicason Group, Tummy-Tummy Industries, Innoson Vehicle Manufacturing, Godwin Kris Industries etc. These industries, contribute so much to the pollution of this water body since it is a surface water source where industrial effluents from several industries are discharged. The pollution has adversely affected the aquatic ecosystem which calls for

serious concern and needs urgent attention since Ele River is a water source for irrigation and many other domestic purposes. To predict pollution level of these effluents, a hydrodynamic and surface water quality model will be used to ascertain the pollution level of the River from the point source of discharge to several points from the discharge point. This is determine its suitability for irrigation purposes towards enhancing Agricultural production. Water quality models are very important in evaluating the impacts of wastewater discharge into surface waters in recent years (Yetik et al., 2014).

Hydrodynamic and water quality models have been widely developed and used for evaluating the characteristics of rivers, lakes or reservoirs through simulating and forecasting the complex processes in the aquatic ecosystem. This research applies the principles of hydrodynamic and surface water quality modeling through the application of Artificial intelligence and computational fluid dynamics model. Thus, it helps to study sediment transportation and water quality processes respectively to enable prediction of industrial pollution which will facilitate decision making for irrigation water quality assessment.

A common approach of controlling point source discharges, such as from storm-water outfalls, municipal wastewater treatment plants or industries, is to impose standards specifying maximum allowable pollutant loads or concentrations of effluents. The goal of an ambient water quality management program is to establish appropriate standards for water quality in water bodies receiving pollutant loads and then to ensure that these standards are met. Realistic standard setting takes into account the basin's hydrologic, ecological, land use conditions and the potential uses of the receiving water body. Ambient-based water quality prediction and management involves considerable

uncertainty since no one can predict the future occurrence of pollutant contamination in the River especially from non-point sources of the surface water. In addition to uncertainties inherent in measuring the attainment of water quality standards, there are uncertainties in models used to determine sources of pollution, to allocate pollutant loads and to predict the effectiveness of implementation actions on meeting water quality standards. The models available to help managers predict water quality impacts are relatively simple compared to the complexities of actual water systems. These limitations and uncertainties should be understood and addressed as water quality management decisions are made based on their outputs.

1.2 Problem Statement

Surface water has been adversely affected by pollution from point and non-point sources. These natural water bodies are used for domestic, drinking and irrigation purposes. Standards specifying minimum acceptable levels of quality are commonly set for most ambient waters. Ele River in Nnewi which serves as a discharge basin for effluents from surrounding industries has to be investigated to ascertain the pollution level due to the adverse effects it poses in farm irrigation. This research will lead to the development of water quality model so as to determine the pollution level at several points in Ele River during rainy/dry season for irrigation water quality assessment.

1.3 Aim and Objectives

1.3.1 Aim

The study aims at using Hydrodynamic and Surface water Quality Models for Industrial Pollution Prediction for Ele River Nnewi, Anambra State, Nigeria.

1.3.2 Objectives

The specific objectives are to:

1) Develop time series using artificial neural network model for water quality simulation of the River system.

2) Forecast the quality of the river system at spatial and temporal intervals using the developed ANN model.

3) Model sediment transport of Ele River using computational fluid dynamics method.

4). Evaluate the Water quality of the River system for Irrigation purpose.

1.4 Significance of Study

This study gives an insight into the development of water quality model for pollution prediction of Ele River so as to predict the pollution level at various points of water transport in the river using irrigation water quality parameters. This study will be of great importance to Ecologists, Environmental Scientists, Agricultural Engineers and other professionals whose jobs are to enhance the health and quality of the aquatic ecosystem so as to be able to utilize the River water for irrigation purposes.Additionally, this research will also serve as a guide for other researchers studying the impact of pollution on water body since water quality models are very useful in describing the ecological state of a river system and to predict the change in this state when certain boundary or initial conditions are altered

1.5 Scope and Limitation

The scope of this study is to model the Hydrodynamic and Surface Water Quality of Ele River, Nnewi for Industrial Pollution Prediction considering the irrigation water quality parameters. This study is only limited to Ele River and using the irrigation water quality parameters to achieve the desired results in modeling the Hydrodynamic and Surface Water Quality of the River.

CHAPTER TWO

LITERATURE REVIEW

2.1 Preamble

Industrialization has been of paramount importance to economic development in most developing nations. It has provided much needed jobs and improved livelihood for the ever-growing populations, especially in sub-saharan Africa (Ogunkunle et al, 2016). However, development through industrialization carries price tags, one which is environmental degradation through waste discharges (FEPA, 1991; Oketola and Osibanjo, 2009). Another downside to industrialization is the encouragement of rural-urban migration which leads to growing peri-urban centers and their attendant waste generation issues (Omole et al, 2014) as exemplified by Lagos State in Nigeria which is arguably the most populated and fastest growing City-State in Africa (Oketola and Osibanjo, 2009; Omole and Ndambuki, 2014). With a population of over 21 million people, growth rate of 3.2%, rural-urban ratio of 10:90 and density of over 5,870 persons per square kilometer, Lagos State represents the economic hub of Nigeria which is the most populous Black nation on earth (Omole and Isiorho, 2011; Omole et al, 2014).

Aside the huge population, Lagos State is also home to about 70% of most industries in Nigeria (Omole and Isiorho, 2011). These industries, by sectoral classification, include electrical and electronics, food, beverages and tobacco; chemicals and pharmaceuticals; foam and asbestos; metals and alloys; textiles and fabrics; pulp and paper; plastics among others (FEPA, 1999; Oketola & Osibanjo, 2009; Omole and Isiorho, 2011). Just like Lagos, Nnewi is the second largest industrial city in Anambra State which has attracted urbanization through industrial and population clusters.

The need to control toxic materials from the industrial effluents is currently increasing to avert causing serious health problems like cancer and diseases. Water is the most vital resource for all kinds of life on this planet, but it is being adversely affected both quantitatively and qualitatively. Today, most of the rivers receive sewages, domestic waste and industrial effluents varying in characteristics from simple nutrient to highly toxic substances. In recent years, increasing industrialization, urbanization and developmental activities with the population explosion has led to generation of large amount of waste water from domestic, commercial, industrial and other sources. Industrial waste waters directly discharged into rivers or lakes have created serious pollution problem which is found in large amount in some industrial areas in Nigeria like Lagos, Ogun, Anambra, Abia, Enugu, Rivers, Akwa-Ibom States etc. The data collected by various agencies like Spring Board Laboratories, Greenpeace Research Laboratories and Center for Science and Environment (CSE) reveals that these Industrial areas deteriorate the quality of the surface water as a result of indiscriminate effluent discharges.

2.2 Industrial Effluents

The effluents released from industrial activities vary so greatly in both flow and pollution strength (Beal and Raman, 2000). In general, industrial effluents may contain suspended, colloidal and dissolved (mineral and organic) solids. In addition, they may be either excessively acidic or alkaline and may contain high or low concentrations of coloured matter. These effluents may contain inert, organic or toxic materials and possibly pathogenic bacteria.

Industrial waste is the most common source of water pollution in the present day (Ogedengbe and Akinbile, 2004) and it increases yearly due to the fact that industries are

increasing as most countries are getting industrialized. The extent of industrial waste discharges in most developing countries is such that rivers receiving untreated effluents cannot give natural dilution necessary for their survival as good quality water sources. There is thus a challenge of providing water in adequate quantity and of required quality to minimize hazards to human health while conserving the water bodies and the environment.

Effluent discharges into the environment have been on the increase in Nigeria since 1960 due to active industrialization, urbanization and the accompanying increase in commercial activities. The discharge of industrial effluents into water bodies is one of the main causes of environmental pollution and degradation in many cities, especially in developing countries. Many of these industries lack liquid, solid waste regulations and proper disposal facilities for harmful wastes. Such wastes might be infectious, toxic or radioactive (Jimena *et al*., 2008; WHO, 2004). On the other hand, waste or effluent management has remained underdeveloped and very unsatisfactory leading to environmental pollution, global warning, deforestation, shoreline erosion or degradation of natural ecosystems. As a result, many potential pollutants have found their way into natural waters, especially in the urban areas upsetting the ecological balance.

Surface waters are usually exposed to negative impacts as well as microbial contamination from run-off inputs, soils and any waste deliberately or inadvertently dumped into such waters (Eremektar *et al*., 2002). These result in pollution increase in microbial load, eutrophication, visible aesthetic nuisance and loss of recreational amenities. Government awareness and interest in solving these problems have led to the establishment of

Environmental Protection Agencies (EPA) which is in the infant stage of operation in most African countries.

2.3 Classification of Industrial Effluents

There are many types of industrial effluents based on the type of industry releasing the effluent. Basically, industrial effluents can be divided into two types namely inorganic and organic effluents.

2.3.1 Inorganic Industrial Effluent

Inorganic industrial effluent is produced mainly in the coal and steel industry, non-metallic minerals industry, commercial enterprises and manufacturing industries (Gbadebo *et al*., 2010). These effluents contain a large proportion of suspended matter and chemical compounds, which can be eliminated by sedimentation often together with chemical flocculation through the addition of iron or aluminum salt, flocculation agents and different kinds of polymers. The purification of warm and dust laden waste gases from blast furnace, converters, cupola furnace, refuse and sludge incineration plants and aluminum works results in wastewater containing mineral and inorganic substance in dissolved and un dissolved forms (Aydin *et al*., 2010).

2.3.2 Organic Industrial Effluents

These are industrial effluent flow from those industries and large scale chemical works, which mainly use organic substances for chemical reaction. The effluents contain organic substances having various origins and properties (Sevimli *et al*., 1999). These organic substances can only be removed by special pretreatment of the wastewater, followed by biological treatment. Most organic industrial wastewater are produced by the following industries and plants such as the factories manufacturing pharmaceuticals, cosmetics,

organic dye-stuffs, glue and adhesive, soap, synthetic detergent, pesticide and herbicides releases large amount of organic industrial effluents; tanneries and leather factories, textile factories, cellulose and paper manufacturing plant, factories of oil refining industries, brewery and fermentation factories and metal processing industries produces large amount of organic industrial effluents.

2.4 Major Sources of Industrial Effluents in Nigerian Environment

The different sources of industrial effluents peculiar to Nigerian environment are discussed below:

2.4.1 Pharmaceutical Industry

Pharmaceutical and personal care products (PPCPs) industries suffer from inadequate effluent treatment due to the presence of recalcitrant substances and insufficient carbon sources and nutrients (Kanu and Achi, 2011). A large number of pre-treatment systems are employed to remove these pollutants to prevent a host of problems that may otherwise arise in the biological process and reduce the efficiency of the treatment plant. Problems caused by excessive PPCPs in the environment include possible inhibition on microorganisms, a reduction in the cell-aqueous phase transfer rates, a sedimentation hindrance due to the development of filamentous microorganisms, development and flotation of sludge with poor activity, clogging and the emergence of unpleasant odours.

Therefore, it is not surprising that research efforts have been directed towards the development of efficient treatment technologies including various physicochemical and biological processes. Some of the most representative pharmaceutical and personal care products found in receiving waters include antibiotics, lipid regulators, anti-inflammatory, anti-epileptics, tranquilizers and cosmetic ingredients containing oil and grease with very

different chemical structures ,conventional biological processes (activated sludge, trickling filters) can effectively accomplish carbon and nitrogen removal, as well as microbial pollution control.

However, pharmaceutical and personal care products contain many different compounds for which conventional technologies have not been specifically designed. Their removal efficiencies are influenced, apart from the chemical properties of specific compounds, by the microbial activity and environmental conditions (Kanu and Achi, 2011). The application of a pretreatment to hydrolyze the effluents and bio-augmentation, may improve the biological degradation.

2.4.2 Soap and Detergent Industry

Alkyl sulfates (AS) are anionic surfactants widely used in household and personal cleansing applications. Aquatic toxicity of AS under laboratory conditions indicated effects at relatively low concentrations (50-230 μg/L) for some sensitive species. Industrial effluents from soap manufacturing industries are known to contain complex chemicals most of which are very toxic and capable of destroying the microbial habitats in a serious adverse way (Kanu and Achi, 2011). For example, characterization of the composite wastewater from both soap and food processing plants indicated that the waste was highly contaminated with organic compounds as indicated by COD and BOD values.

2.4.3 Paper Mill Industry

Process water in paper and board mills contains a lot of sugars and lignocelluloses, which support the growth of bacteria, mold and some yeast. The occurrence of these microbes in the effluents lead to excessive oxygen demand loading and also disturb the ecological equilibrium of the receiving waters with much loss of aquatic life and intense consequences like water pollution, blockage of irrigation nozzles and orifice.

2.4.4 Textile Mill Effluent

The textile industry is distinguished by raw materials used and this determines the volume of water required for production as well as waste generated. Heavy metals such as Nickel, cobalt, molybdenum have been associated with the textile effluents. The nature of the processing exerts a strong influence on the potential impacts associated with textile manufacturing operations due to the different characteristics associated with these effluents (Kanu and Achi, 2011).

2.4.5 Brewery Industry

Wastewater from Brewery Industry originates from liquors pressed from grains and yeast recovery possessing the characteristic odour of fermented malt and slightly acidic. Brewery effluents are high in carbohydrates; nitrogen and the cleaning /washing reagents which have been proved to be water pollutants. The introduction of wastewater with high in-organic matter and organic nutrients into water bodies bring about changes in the micro-flora.

2.4.6 Soft Drink Effluent

Wastewater was analyzed in the accumulation pond and final discharge point of Nigerian Bottling Company PLC in Owerri, Nigeria to determine their bacteriological and physico-chemical characteristics (Ibekwe et al, 2004). Species of organisms isolated included *Staphylococcus*, *Bacillus*, *Lactobacillus*, and *Streptococcus.* Others include *Klebsiella*, *Escherichi*a, *Proteu*s and *Serratia*. However, species of *Lactobacillus* and *Proteus* were isolated from the final discharge point only. Bacterial count after 72 hours was higher with a maximum count of 6 x 10^7cfu/ml in the final discharge point. The waste water from both points were clear and had the same residual chlorine (1ppm) and iron (1ppm) concentration, while the accumulation pond showed more acidity with a pH of 6.6±1.2. The final discharge contained more dissolved solids (20±1.8ppm) which was double that of the accumulation pond (10±2.2ppm). It was also found that dissolved oxygen was slightly higher (6.0±0.26mg/ml) in the final discharge point than accumulation pond (5.0±0.33mg/ml). Although, these findings were found to be within the permissible limits of effluent discharge specified by the Federal Ministry of environment in Nigeria. The consequent long-term bioaccumulation effects on microbial ecosystem were not reported.

2.4.7 Chemical Industry Effluent

Chemical industry releases large amount of inorganic and organic effluent. The toxicity of benzene, hydroxylbenzene (phenol), chlorobenzene, methylbenzene (toluene) and dimethylbenzene (xylene) to four chemolithotrophic bacteria (Nitrosomonas, Nitrobacter, Thiobacillus and Leptothrix isolated from the New Calabar River water were investigated by Odokuma and Oliwe, 2003). The static method of acute toxicity assessment was

employed. Mortality within a period of 5 hours exposure to toxicant was the index of assessment.

Toxicity of the methyl and dimethyl substituted derivatives of benzene was probably a function of the genetic make-up of the bacteria. The toxicity generally decreased with increased methyl substitution in the case of Nitrobacter and Thiobacillus, but increased with increased methyl substitution in the case of Nitrosomonas and Leptothrix. Hydroxyl and halogenated substituted derivatives were more toxic than methyl substituted derivatives. These results indicate that wastes containing hydroxyl and chloro-substituted derivatives of benzene may pose a greater toxicity problem to microbiota than wastes containing methyl-substituted derivatives. The nitrification stage of the nitrogen cycle will also be greatly impaired in the presence of these groups of chemicals in a river.

2.4.8 Palm / Vegetable Oil Mill Effluent

Palm oil mill effluent and vegetable oil effluent are important sources of inland water pollution when released without treatment into local rivers or lakes. In Nigeria, palm oil is processed locally and industrially through the oil palm belt stretching from Cross River to Lagos State such as Ikom, Ikorodu etc. Besides the main product which is the crude palm oil (CPO), the mills also generate many by-products and liquid wastes, which may have significant impacts on the environment if they are not treated/ handled properly.

The palm oil mill effluent (POME) is generated from three major sources, namely sterilizer condensate, hydro-cyclone waste and separator sludge (Kanu and Achi, 2011). On an average 0.9–1.5m^3 of POME is generated for each ton of crude palm oil produced (Davis and Reilly, 1980). POME is rich in organic carbon with a biochemical oxygen demand (BOD) higher than 20 g/L and nitrogen content about 0.2 g/L as ammonia

nitrogen and 0.5 g/L total nitrogen (Ma, 2004). Also, palm oil mill wastewater treatment systems are one of the major sources of greenhouse gases due to their biogas emission (36 % CH_4 with a flow rate of 5.4 l/min.m^2) from open digester tanks and/or anaerobic ponds (Ma, 2004). POME has generally been treated by anaerobic digestion, resulting to improved water quality.

The characteristic problems associated with palm oil mill effluents are pH, dark color, high levels of biochemical oxygen demand (BOD), chemical oxygen demand (COD), color, and suspended solids (Kanu and Achi, 2011). High values of COD also indicate the recalcitrance of chemicals that have escaped biodegradation. These chemicals may be persistent in nature and may cause severe environmental problems like bioaccumulation**.**

2.5 Water Bodies as Sink for Industrial Effluents

Industrial effluents are main source of direct and often continuous input of pollutants into aquatic ecosystems with long-term implications on ecosystem functioning including changes in food availability and an extreme threat to the self-regulating capacity of the biosphere. These industrial discharges or wastes include heavy metals, pesticides, polychlorinated biphenyls (PCBs), dioxins, poly-aromatic hydrocarbons (PAHs), petrochemicals, phenolic compounds and microorganisms (Kanu and Achi, 2011). These wastes are usually discharged into water bodies and the cumulative hazardous effects on the environment have received much attention.

Industrial wastes containing high concentration of microbial nutrients would obviously promote an after-growth of significantly high coliform types and other microbial forms. Some heavy metals contained in these effluents have been found to be carcinogenic while other chemicals equally present are poisonous depending on the dose and duration of

exposure. Undoubtedly, wastewaters from industries and residential areas discharged into another environment without suitable treatment could disturb the ecological balance.

The industrial discharge, therefore contribute a larger portion of the flow of the river during the dry season, with the result that the water quality of the river is further deteriorated. Uses, for which the river is employed involving body contact, expose users to serious hazards due to the bacterial contamination. Many water bodies in Nigeria experience seasonal fluctuations, because high concentration should be a consequence of reduced rainfall/ residual inflow of water into the water bodies.

2.6 Effects of Water Pollutants

Water pollutants and their effects differ significantly according to the pollutants which include:

2.6.1 Heavy Metals

Heavy metals are those chemical elements with a specific gravity that is at least five times the specific gravity of water (Odemealam, 2005). Examples include cadmium, lead, arsenic, iron and mercury.

Heavy metals occur naturally in the environment as constituents of earth's crust and fulfill the criteria of persistence but are however dispersed over large area and in the process are often diluted or broken down to harmless level by natural process. However, due to anthropogenic activities, metal distribution patterns can be rearranged, resulting in site specific elevated concentrations (Merian, 1991). Heavy metals are common in industrial applications such as in the manufacture of pesticides, batteries, alloys, electroplated metal parts, textiles dyes, steel amongst others.

Heavy metals that enter water bodies affect fish and other aquatic organisms consequently endangering public health through consumption of contaminated seafood and irrigated food crops. Chronic toxicity of heavy metals results from repeated or continuous exposures leading to an accumulation in the body. Symptoms of chronic toxicity may be similar to many common conditions and may not be readily recognized.

Another adverse health effect of heavy metal is associated with copper, mercury and cadmium. Copper poisoning is known to have a damaging effect on the brain of higher animals at 0.5ppm level (Brown et al, 1998).

2.6.2 Sediments

These suspended solid particles in water body make water turbid or cloudy and unpleasant for various uses thus necessitating water treatment (Marquita, 2004). It is worthy to note that sediment reduces light available to algae and aquatic plants, kill or injure fish by damaging their gills, cover spawning gravel and smother fish eggs. It also reduces the quality of recreational activities such as swimming and boating.

2.6.3 Oil and Grease

Crude oil consists of hydrocarbon, with carbon and hydrogen in the ratio 1:6 by weight and other related inorganic metals. Oil spill is a major source of oil and grease pollution in a water body. Oil spill is an accidental discharge of crude oil, refined oil products as well as the disposal of used or exhausted lubricants and waste oil. It is noteworthy that depending upon the amount and type oil spilled, weather condition, ecosystem recovery can be quick or painfully slow. Floating oil reduce or prevent oxygenation of the water and without an adequate supply of oxygen, the self-purification property of water is

entirely prevented from operating (Egborge, 1994). Marine life from the simple algae to fish is endangered and the delicate ecological balance is destroyed.

2.6.4 Acids and Alkalis

Acids and alkalis directly affect the pH of the receiving water body. The wide changes in pH affect enzymes and other proteins, altering the course of natural physiological processes of water (Ubawuike, 2010).

2.6.5 Excess Nitrate

It has been shown that excess nitrate in the body causes blood problems such as anemia and hepatitis. Increased heart rate, decreased blood pressure and circulatory collapse have also been reported it was also shown that high concentration of nitrate in water result in eutrophication. Sources of nitrogen and nitrates may include runoff or seepage from fertilized agricultural lands, municipal and industrial waste water, refuse dumps, animal feedlots, septic tanks and private sewage disposal systems, urban drainage and decaying plant debris.

2.7 Effects of Industrial Effluents on the Environment

Industrial effluents may impact negatively on the environment. These impacts might be seen on the plants, animals and even human.

2.7.1 Effects of Industrial Effluents on Plants

Industrial effluents when released in the open or on agricultural land contaminate the soil with heavy metals and organic pollutants. (Mahata and Antil, 2004) observed that the morphometric analysis showed that the height of seedling and length of root were also reduced with the application of effluent. Thus, effluents must be diluted either with canal water or tube well water to avoid their adverse effect on plant growth.

Impact of Industrial Effluents on the Soil (Lithosphere)

Sometimes, effluents especially sludge from the water or wastewater treatment facility are disposed of by using them as soil amendment, or just indiscriminately to dump sites. When these effluent or sludge (as the case may be) contain toxic materials and heavy metals, they immediately become part of the soil; when these toxic materials and heavy metals become ionized (i.e. in soluble form), they could be picked by the root of the plant and bioaccumulation in the tissues of the plant (Mura et al., 2013). These toxic materials and heavy metals may also disrupt the natural activities of both the flora and fauna components of the soil.

Impacts of Industrial Effluent on the Air (Atmosphere)

Effluent especially when it contains high BOD and other organic pollutant tends to give off foul smell. This worsens when the waste is not properly dosed with the required oxygen to effectively digest the complex organic matter to simpler form. Pungent gases like hydrogen sulphide (H_2S), cyanide (CN) among others are` very notorious in this regards (Ghosh, 2002). With uncontrolled release of effluent / wastewater, the undesirable foul smell could become a threat to the inhabitants of such locality.

Impacts of Industrial Effluents on Human

In non-ferrous metal industries and industries that produce batteries, pigments, stabilizers and plastics, the primary heavy metals discharged are lead, zinc, and cadmium. Cement manufacture results in high emission of mercury as well as these heavy metals except zinc (Scoullos et al., 2012). Arsenic and Zinc gain access to the water environment through mining operations. Nickel and Cobalt are used in the electroplating industry. Effluents contain these heavy metals which are harmful to human health either through direct ingestion or from fish and other animals or plants. Heavy metals particularly arsenic, mercury and lead are environmental pollutants threatening the health of human population and natural ecosystem (Castro-González and Méndez-Armenta, 2008). The untreated effluents when released to the environment would interact with all components of the environment. The effect would not only be felt in the water bodies alone, but across all the components of the biosphere. The toxic component would definitely move round polluting the food web / trophic level (Förstner and Wittmann, 2012).

2.7.2 Effects of Industrial Effluents on Animals

Pollution is caused when a change in the physical, chemical or biological condition in the environment harmfully affect quality of human life including other animals' life and plant. .Industrial, sewage and municipal wastes are being continuously added to water bodies hence affect the physiochemical quality of water making them unfit for use of livestock and other organisms, (WHO, 2004).

Uncontrolled industrial effluent discharges into aquatic body has resulted in eutrophication of ponds as evidenced by substantial algal bloom and dissolved oxygen depletion in the subsurface water, (Ubawuike, 2010). This leads to large fish kill and other

oxygen requiring organism. Effluent discharged into aquatic environment with enhanced concentration of nutrient, sediment and toxic substances may have a serious negative impact on the quality and life forms of the receiving water body when discharge untreated or partially treated.

Water pollution by effluent has become of considerable public and scientific concern in the light of evidence of their extreme toxicity to the health of animals and biological ecosystems (WHO, 2004a). The occurrence of heavy metals in industrial and municipal sewage effluents constitute a major source of the heavy metals entering aquatic media which adversely affects lives of aquatic animals. Hence, there should be regular assessment of these sewage effluents to ensure that adequate measures are taken to reduce pollution level to the minimum. Worldwide water bodies are primary means for disposal of waste, especially the effluents from industrial, municipal sewage and agricultural practices that are near them. This effluent can alter the physical, chemical, and biological nature of receiving water body. The initial effect of waste is to degrade physical quality of the water.

2.8 Effects of Industrial Effluents on Water Quality

Over the last three decades, there has been increasing global concern over the public health impacts attributed to water pollution, in particular, the global burden of disease. The World Health Organization (2004) estimated that about a quarter of the diseases facing mankind today occur due to prolonged exposure to water pollution. Most of these water pollution-related diseases are however not easily detected and may be acquired during childhood and manifest later in adulthood.

The discharge of industrial effluents into water bodies is one of the main causes of environmental pollution and degradation in many cities, especially in developing countries. Many of these industries do not adhere to liquid and solid waste regulations and proper disposal facilities, including for harmful waste. Such waste may be infectious, toxic or radioactive (WHO, 2004). In most countries, the principal risks to human health associated with the consumption of polluted water are microbiological in nature.

The risk of acquiring a waterborne infection increases with the level of contamination by chemicals and pathogenic microorganisms. Unfortunately, polluted rivers by industrial effluents are common throughout the world. The WHO (2004) stated that one sixth of the world's population, approximately 1.1 billion people do not have access to safe water and 2.4 billion lack basic sanitation. Polluted water which consists of industrial discharged effluents, sewage water, pollution from rainwater, agriculture or households causes damage to human health or the environment. This water pollution affects the health and quality of soils and vegetation. Some water pollution effects are recognized immediately, whereas others do not show up for months or years.

Estimation indicates that more than fifty countries of the world with an area of twenty million hectares area are treated with polluted or partially treated polluted water including parts of all continents and this poor quality water causes health hazard and death of human being, aquatic life and also disturbs the production of different crops, (Kanu and Achi, 2011). In fact, the effects of water pollution are said to be the leading cause of death for humans across the globe, moreover, water pollution affects our oceans, lakes, rivers, and drinking water, making it a widespread and global concern.

Surface water is used in various ways such as drinking, commercial, agricultural and industrial activities (Akan et al., 2009). Despite the importance of surface water to human life, it is the most poorly managed resources in the world (Fakayode, 2005). The increase in demand of water for various uses arose from increase in global population and fast growth of industries around the world which amounted to pressure on limited water resources (Norman and Michel, 2000, Phiri et al, 2005 and NPDES, 2008). The principal cause of water scarcity is water quality degradation, which critically reduces the quantity and quality of water available for potable, agricultural and industrial uses (Norman and Michel, 2000). Thus, the quantity of available water is closely linked to the quality of water, which may limit its uses. However, industrial survey carried out in Nigeria by Dada, (1997) showed that more than 60% of the industries discharged untreated effluents into surface water and it is attributed to the increase in concentration of industries around rivers in Nigeria. The concentrations of industrial activities around rivers and the release of effluents from industries into surface waters have led to deterioration of surface water quality, (Bichi, 2000; Ajibola and Ladipo, 2011).

Nkwocha et al, (2010), assessed the quality of effluent discharges from vegetable oil plant, located in Anambra State, which was evaluated relative to regulatory body – Federal Environmental Protection Agency (FEPA) standard. Wastewater quality parameters namely; biochemical oxygen demand (BOD), dissolved oxygen (DO), total hydrocarbon content (THC), oil and grease, total dissolved solids (TDS), pH and temperature were determined weekly on effluent samples, for a period of 12 weeks, using standard methods. The effluent data were subjected to statistical correlation. BOD values ranged from 10.80 – 94.20 mg/L with 90% occurrence value of 81.20 mg/L, which exceeded FEPA set limit

of 50mgLl by 62.40% for about 14% of the time. DO level ranges from 2.70 – 4.60 mg/L which was below the saturation point of 7.5mg/L at 300C. THC, Oil and Grease consistently exceeded the set limit of 10 mg/L. Effluent pH range of 4.60 - 9.60 was outside FEPA range of 6-9. However, TDS and temperature levels were consistently within permissible limits throughout the period under investigation. Thus, there is need for proper treatment and monitoring of effluent to ensure consistent quality that meets environmental standard.

Onuigbo and Madu, (2013) assessed the impacts of industrial effluents discharge on the quality of Emene River in Enugu State. Samples were collected from the river at three sampling points in order to evaluate the spatial concentration of industrial effluents in Emene River. Samples were analyzed following the procedure described by America Public Health Association (APHA). The results showed that TDS, TSS, ion, calcium, nitrate, chloride, magnesium, electrical conductivity, BOD, turbidity, color, temperature, zinc, odour and total hardness are significantly different ($p<0.05$) at point source when compared with values obtained at upstream. Nine variables exceeded maximum permissible limit (MPL) in all the sample points, while seven variables exceeded MPL at control point of Emene River. All the variables except chloride exceeded MPL of industrial effluent discharge as recommended by World Health Organization (WHO) and Nigeria Industrial Standard (NIS).

Okoye et al, (2011) conducted analysis of untreated effluents from soap factories in Aba, Abia State, Nigeria. Effluent waters from three soap producing industries were collected and analyzed with the aim of ascertaining their potential and environmental impact on receiving water bodies. Their physico-chemical characteristics were investigated and the

concentration of the metals determined using AAS analysis. Results obtained showed that the parameters of the effluents were below WHO and FEPA standards except for turbidity which was high ranging between 6 and 12. The following metals were detected in the increasing order Cr, Cd<Pb<Zn<Fe<Cu<As<Na<Ca<Mg. Thus, regulatory bodies are bound to maintain steady control measures as this will greatly reduce the pollution and environmental hazards.

Egwuonwu et al, (2012) evaluated the effects of Industrial wastewater discharge on surface water using Nigeria Breweries Plc Enugu as a case study. This was done to ascertain the level of Biochemical Oxygen Demand (BOD), Chemical Oxygen Demand (COD), Total Suspended Solids (TSS) etc and other characterized effluent being discharged into the water body that determines the level of use and quality of this water for irrigation purposes, human consumption and safe ecological habitation of aquatic lives. The water samples used for these analyses were those collected from Nigeria Brewery Enugu effluent discharge point and water from Ajali River some miles away from the discharge point. Pollution of the aquatic ecosystem was detected, thus treatment measures and regulatory policies were suggested to checkmate the abuse of the water body and the danger it might likely pose to aquatic ecological system if regulatory standards were not complied with.

Ubah et al, (2015) determined the Seasonal Impacts of Industrial Effluents from Chicason Industries Limited on Ele-river Nnewi, Anambra State, Nigeria. Physico-chemical and heavy metal analysis were conducted which showed the concentration of different parameters at various points analysed during the rainy and dry season in comparison with the WHO standards. Most parameters including BOD, Magnesium and Calcium exceeded

the WHO permissible standard at different points especially in the dry season. Where heavy metals were observed to be high at most sampling points, it could be as a result of the presence of ions from the soil. Thus, the pollution poses great threat to lives of aquatic organisms and also the river cannot serve the purpose for dry season irrigation.

2.9 Physico-chemical Properties of Industrial Effluents

An important pollution index of industrial wastewaters is the oxygen function measured in terms of chemical oxygen demand (COD), and biological oxygen demand (BOD), while the nutrient status of wastewater is measured in terms of nitrogen and phosphorus. In addition, other important quality parameters include pH, temperature and total suspended solids (Kanu and Achi, 2011). Industrial effluents are characterized by their abnormal turbidity, conductivity, chemical oxygen demand (COD); total suspended solids (TSS) and total hardness.

Total Solids

The total solids in a wastewater consist of the suspended solids and the soluble compounds dissolved in water. Volatile solids are presumed to be organic matter, although some organic matter will not burn and some inorganic salts break down at high temperatures. The organic matter consists mainly of proteins, carbohydrates and fats. Soluble solids, expressed as milliliters per litre are those that can be removed by sedimentation.

Water Hardness

Water hardness is the traditional measure of the capacity of water to react with soap since hard water requires considerably more soap to produce lather. Hard water often produces a

noticeable deposit of precipitate (e.g. insoluble metals, soaps or salts) in containers, including “bathtub ring”. The principal natural sources are varieties of dissolved polyvalent metallic ions from sedimentary rocks, seepage and runoff from soils, predominantly calcium and magnesium cations, although other cations (e.g. aluminum, barium, iron, manganese, strontium and zinc) also contribute. Hardness is most commonly expressed as milligrams of calcium carbonate equivalent per litre. Although hardness is caused by cations, it may also be discussed in terms of carbonate (temporary) and non-carbonate (permanent) hardness. Calcium and magnesium, the two principal ions, are present in many sedimentary rocks, the most common being limestone and chalk. They are also common essential mineral constituents of food.

Turbidity

Turbidity is a measure of water clarity which boils down on how much the material suspended in water decreases the passage of light through the water. Suspended materials include soil particles (clay, silt, and sand), algae, plankton, microbes, and other substances. Turbidity can be caused by:

- silt, sand and mud;
- bacteria and other germs;
- Chemical precipitates.

It is very important to measure the turbidity of domestic water supplies, as these supplies often undergo some type of water treatment which can be affected by turbidity. For example, during the rainy season when mud and silt are washed into rivers and streams, high turbidity can quickly block filters and stop them from working effectively. High turbidity will also fill tanks and pipes with mud and silt, and can damage valves and taps. Where chlorination of water is practiced, even quite low turbidity will prevent the chlorine

killing the germs in the water efficiently. Some treatment systems, such as sedimentors, coagulators and gravel pre-filters are designed to remove turbidity. It is important for operators of both large and small treatment systems to know how well these systems are working. Measuring the turbidity of the water before and after each part of a system can tell the operator where maintenance or cleaning is needed.

Nutrients

The principal limiting nutrients in water include free ammonia, organic nitrogen, nitrites, nitrates, organic phosphorus and inorganic phosphorus. Nitrogen and phosphorus are important because these two nutrients are responsible for the growth of aquatic plants. All living organisms require varying amounts of some trace elements, such as iron, copper, zinc and cobalt, for proper growth.

Dissolved Oxygen

The solubility and the dynamics of dissolved oxygen distribution in water bodies are basic to the understanding of the abundance and distribution of aquatic organisms. Dissolved oxygen is essential for the metabolism of all aquatic organisms that undergo aerobic biochemistry. Seasonal changes of dissolved oxygen were positively correlated with the density of phytoplankton but inversely with the zooplankton. Dissolved oxygen is not only an important water quality criterion in supporting well balanced aquatic fauna but insufficient amount in water causes anaerobic decomposition of organic materials in a water body.

pH and Alkalinity

The acidity or basicity of irrigation water is expressed as pH (acidic < 7.0 > basic). The normal pH range for irrigation water is from 6.5 to 8.4. Low pH may cause accelerated irrigation system corrosion where they occur. High pH above 8.5 are often caused by high bicarbonate (HCO_3^-) and carbonate (CO_3^{2-}) concentrations, known as alkalinity. High carbonates cause calcium and magnesium ions to form insoluble minerals leaving sodium as the dominant ion in solution. Excessive bicarbonate concentrates can also be problematic for drip or micro-spray irrigation systems when calcite or scales build up causes reduced flow rates through orifices or emitters. When these occur, injection of sulfuric or other acidic materials into the system may be required for correction.

Nitrogen

Nitrogen in irrigation water (N) is largely a fertility issue. The nitrate ion often occurs at higher concentrations than ammonium in irrigation water. Waters high in N can cause quality problems in crops such as barley and sugar beets and excessive vegetative growth in some vegetables. However, these problems can usually be overcome by good fertilizer and irrigation management.

Total Dissolved Solids (TDS)

Water has the ability to dissolve a wide range of inorganic and some organic minerals or salts such as potassium, calcium, sodium, bicarbonates, chlorides, magnesium, sulfates etc. These minerals produce unwanted taste and dilute color in appearance of water. This is an important parameter for the use of water. Water with high TDS value indicates that water is highly mineralized. High values of TDS in ground water are generally not harmful to human beings, but high concentration of these may affect persons who are

suffering from kidney and heart diseases. Water containing total dissolved solids may cause laxative or constipation effects and when used for irrigation and will likely increase salinity in the soil thereby reducing nutrient and moisture absorption, Onuigbo and Madu, (2013).

Electrical conductivity (EC)

Clean water is not a good conductor of electric current rather it is a good insulator. Increase in ions concentration enhances the electrical conductivity of water. Generally, the amount of dissolved solids in water determines the electrical conductivity. Electrical conductivity (EC) actually measures the ionic process of a solution that enables it to transmit current. According to WHO standards, EC value should not have exceeded 400 μS/cm for drinking water and for FAO maximum permissible standard for Irrigation water quality the 3 dS/m.

Nitrate (NO_3):

Nitrate one of the most important disease causing parameters of water quality particularly blue baby syndrome in infants. The sources of nitrate are nitrogen cycle, industrial waste, nitrogenous fertilizers etc. The FAO allows maximum permissible limit of Nitrate-Nitrogen for irrigation as 10 mg/l for irrigation water.

Sodium (Na):

Sodium is a silver white metallic element and found in less quantity in water. Proper quantity of sodium in human body prevents many fatal diseases like kidney damages, hypertension, headache etc. In most of the countries, majority of domestic water supply

bear less than 20 mg/l while FAO maximum permissible standard for irrigation water quality is 40 me/l.

Heavy Metals Concentrations

Bioaccumulation of metals occurs in fauna and flora if the rate of uptake of heavy metals by the organisms is more than the excretion. Unlike food that when assimilated into the body digest or biodegrade, heavy metals are not biodegradable so they accumulate in primary organs in the body and over time begin to fester, leading to various symptoms of diseases. Heavy metal distributions in seawater and sediment samples were found in high concentrations when compared to regulatory standards. This development is as a result of introduction of heavy metals into the sea through runoff from residential, urban and industrial sources (Rein, 2005).

Many of the pollutants entering aquatic ecosystems (e.g., mercury lead, pesticides, and herbicides) are very toxic to living organisms. They can lower reproductive success, prevent proper growth and development, and even cause death. Heavy metals may also precipitate phosphate bio-compounds or catalyze their decomposition. For example, among the toxicological effects of mercury were neurological damage, including irritability, paralysis, blindness, insanity, chromosome breakage and birth defects (Rein, 2005). Heavy metals can also produce toxic effects; therefore, determination of the amounts of heavy metals is especially important where the further use of treated effluent or sludge is to be evaluated. Many of metals are also classified as priority pollutants such as arsenic, cadmium, chromium, mercury, etc. Measurements of gases, such as hydrogen sulphide, oxygen, methane and carbon dioxide, are made to help the system to operate. The presence of hydrogen sulphide needs to be determined not only because it is an

odorous and very toxic gas but also because it can affect the maintenance of long sewers on flat slopes, since it can cause.

2.10 Water Pollution

Water pollution is unarguably one of the most fundamental environmental issues globally and locally, as untreated or inadequately treated wastes is being discharged into streams, estuaries and seas (Novotny, 2003). Pollution of water bodies in Nigeria is further worsening with lack of adequate environmental monitoring schemes; weak enforcement of environmental regulations and worst of all bribery and corruption (Nwabuzor, 2005; Winbourne, 2002). Numerous studies have been and are being conducted to help define this problem so as to determine the amounts of pollutant substances released to the environment, their sources, their impacts, and possible means of control (Kim et al., 2013). Water is considered polluted if some substances or condition is present to such a degree that the water cannot be used for a specific purpose. Water pollution occurs when unwanted materials with potentials to threaten human and other natural systems find their ways into rivers, lakes, wells, streams, boreholes or even reserved fresh water in homes and industries (Rice et al., 2012). The pollutants are usually pathogens, silt and suspended solid particles such as soils, sewage materials, disposed foods, cosmetics, automobile emissions, construction debris and eroded banks from rivers and other waterways (Bakare and Akintan, 2016). Pollution by organic and inorganic contaminant such as pesticide and heavy metals respectively is a serious threat to aquatic ecosystems because some of these contaminants are potentially toxic, even at very low concentrations. Additionally, heavy metals and pesticides are not biodegradable and tend to accumulate in living organisms,

and they can cause severe problems to both human health and wildlife (Crini, 2005). Water Pollutants can be grouped into three broad categories according to their nature:

I. Organic pollutants

II. Inorganic pollutants

III. Biological pollutants

Water pollutants can also be grouped according to source:

I. Point source

II. Non-point source

2.10.1 Point Source Pollution

Point source pollution comes directly from a known source like an industrial or sewage outflow pipe. It can also be from factories, wastewater treatment facilities, septic systems, and other sources that are clearly discharging pollutants into water sources (Rehman et al., 2008). Point sources are typically associated with manufacturing processes. However, point sources also include discharges from water treatment plants and large animal feeding operations (Knight et al., 2000).

2.10.2 Non-Point Source Pollution

Non-point source pollution can be defined as pollution that comes from many miscellaneous or diffuse sources rather than from an identifiable, specific point. Non-point source pollution can originate from urban environments such as yards in neighborhoods or from agricultural production areas such as crop fields (Robbins et al., 2001). Chemicals, waste products and soil that are carried by rain into streams or rivers become a part of non-point source pollution (Alloway and Ayres, 1997). Common examples are fertilizers,

herbicides, pesticides, spilled motor oil and wastes from pets, wildlife and livestock. Other significant sources of non-point source pollution include: Litters, Hazardous waste improperly stored or discarded, Erosion from construction sites, farms or home sites, Pollution from roadways and road salting activities, Discharge of sewage and garbage from ships and boats, Cleansers and other compounds used on ships in the urban or agriculture environment and boats to prevent barnacles and algae from accumulating, Disposal of wastes in catch basins, Improperly operating septic systems , Acid deposition including acid rain and fog, Leaking sewer lines, Improper use of fertilizers and pesticides and Animal feeding operations.

Non-point sources are more difficult to identify, because they cannot be traced back to a particular location (Sigel et al., 2010). Treatment of polluted water from non-point sources can also be very difficult. Best management measure to non-point source pollution is the Watershed Management system (Ritter and Shirmohammadi, 2000). Riparian community must act as stakeholder in watershed management (Bulkley, 2011).

2.11 Water Quality Modeling

Water quality models can be effective tools to simulate and predict pollutant transport in water environment (Bai and Cui, 2011; Wang et al, 2009) which can contribute to saving the cost of labour and materials for a large number of chemical experiments to some degree. They are commonly applied for management, planning and pollution control. Water quality models become an important tool to identify water environmental pollution, the final fate and behaviors of pollutants in water environment (Wang et al, 2009). The water quality models available today are multipurpose and it can be used for river and

reservoir modeling, runoff modeling, hydrology and hydrodynamic modeling, water quality modeling, ground water and ecological modeling.

These construction projects such as petrochemical, hydrological, and paper-making projects can bring serious effects on aquatic environment after enforcement (Liou et al, 2003; Xiao et al, 2012). With the influence of human economic activity, environmental degradation and activity zones (e.g., household water supply, agriculture, hydropower and fisheries), the water quality is threatened by point (PS) and non-point (NPS) source pollution, thus, hydrologic/water quality models are important tools for water quality decision analysis (Susilowati et al, 2004)

These environmental effects have to be simulated, predicted, and assessed using numerical models before these construction projects are implemented. These modeling results under different pollution scenarios using water quality models are very important components of environmental impact assessment. Moreover, they are also the important basis for environmental management decisions as they not only provide data assistance for environmental management agencies to authorize the construction projects but also provide technical supports for water environmental protection agencies (Bai et al ,2012b; Bai et al 2012b)

With the development of model theory and the fast updating computer technique (Ashraf et al, 2012), more water quality models have been developed with various model algorithms (Wang et al 2009; Liou et al, 2003). Up to date, tens of types of water quality models including hundreds of model softwares have been developed for different topography, water bodies, and pollutants at different space and time scales (Wang et al, 2009; Wang et al, 2004).

However, there are often large differences between these modeling results due to different theories and algorithms of these models, which can lead to the inconsistency of the predicted results using different models, and thus bringing different environment management decisions as these modeling results cannot be referred or compared to each other (Obropta et al, 2008). Therefore, it is very necessary for most developing countries to have better understanding of the availability and precisions of different water quality models as well as their methods of calculation and calibration in order to determine the model standardization for effective application of these models to enable good model regulation system (Cao and Zhang, 2006 ; Politano et al, 2008).

2.11.1 Development of Surface Water Quality Models

Surface water quality models have made a big progress from single factor to multifactor of water quality, from steady-state model to dynamic model; from point source model to the coupling model of point and nonpoint sources and from zero-dimensional mode to one-dimensional, two-dimensional, and three-dimensional models (Xu and Lu, 2003). More than 100 surface water quality models have been developed up till now. Cao and Zhang, (2006) classified these models based on water body types, model-establishing methods, water quality coefficient, water quality components, model property, spatial dimension, and reaction kinetics.

2.11.2 A Concise History of Water Quality Models

Water quality models have been used for many years to predict the effect of external influences on water quality. Initial water quality variables studied were dissolved oxygen and biological oxygen demand in order to manage the impacts of effluents. Once

computers became commercially available, complex mathematical formulae were applied and calculated parameters now included temperature. As other constituents of water quality are considered important due to their interactive effect on water quality, more complex models were developed and since the 1980's, there has been a growing emphasis on hydrodynamic models coupled to water quality processes. Interactions with the sediment are also modeled as well as some form of algal modeling (Nitsche, 2000). With the increasing power of computers, the models being developed now are more complex and computer runtime intensive.

A model is an invaluable tool for water quality managers since it can assist in the decision for varying scenarios. A model for a catchment may be categorized according to the processes they address such as:

- Hydrodynamic and hydraulic models (H/H)
- Hydrological and watershed models (H/W)
- Surface water quality models (SWQ)
- Groundwater models (GW)
- Ecological models (E).

Water quality models may be one dimensional, two-dimensional or three-dimensional, this progression usually indicate the degree of accuracy of the model used. A one-dimensional model will usually oversimplify the hydrodynamics with constant volumes of each segment in the water column. A more accurate representation of the water-body would be obtained using a two dimensional model, whereas three-dimensional modeling produce results that mimic the real system. The aim of hydrodynamic water quality modeling is

to describe interactions between the hydraulics of a system and its chemical and biological components.

Hydrodynamic and hydraulic models (H/H)

Over the past few years, hydrodynamic modeling of lakes, lagoons and rivers has become an important tool for managing water resources, especially in modeling the dispersion of pollutants and morphological analysis, Holanda et al, (2011).

Hydrodynamic models use numerical solutions for fundamental governing equations for the conservation of momentum and/or mass to predict water movements. Hydrodynamic models such as CH3D-WES are distributed as standalone models and can be coupled internally or externally with WASP5 or CE-QUAL-W2 water quality models. Hydrodynamic models may also form the transport foundation for lake or river mass balance models. (Limno-Tech, 2002). Hydrodynamic models were commonly used for flood risk management in urban area. Coupling of the 1D and 2D hydrodynamic model aids to accurately simulate detailed urban flood propagation and inundation of the ground's surface; simulate flows in the pipe/river drainage system and surface inundation, respectively Yuyan et al, (2017).

Purpose of Model

Hydrodynamic models which addresses issues related to waves, sediment and water quality, normally forms one of the key components of any impact assessment in the ocean environment. Typically, models are developed over a wide regional extent, such that a much wider understanding can be obtained of processes (e.g. tidal characteristics) within that extent than could be provided through monitoring alone. Effectively, models allow two key advantages over monitoring:

a. The ability to consider characteristics and impacts anywhere within the model extent; and

b. The ability to predict how characteristics might change in response to actions within the extent. Such actions could include the dredging of a channel, the construction of a reclamation Area, or the creation of a plume.

In order for models to be able to realize these advantages, a staged process must be adopted. This comprises:

a. The collection of data to drive model boundaries (e.g. water levels, wave conditions, wind fields);

b. The collection of data for calibration purposes (e.g tidal currents and wave heights within the model extent, and typically within the general extent of one or more of the primary points of interest);

c. The assembly of bathymetric and land boundary data, such that the physical characteristics of the seabed can be replicated;

d. Creation of a model mesh;

e. Model calibration;

f. Model verification (i.e. to an additional dataset, where available);

g. Determination of baseline conditions; and

h. Assessment of proposed infrastructure or dredging activities through changes to the model mesh, boundaries, or bathymetry.

Hydrological and Watershed Models (H/W)

Hydrologic and watershed models are useful for assessing hydrology to manage the water resources of a watershed. This category of models can simulate the generation and dispersion of a constituent of concern from the point of origin to its discharge into receiving waters. These models can be used to quantify total watershed contributions of flow, sediment, nutrients and other constituents of interest. These models require hydro-meteorological data such as rainfall, temperature, humidity and solar intensity. The watershed models evaluate the effects of different land uses and practices, land cover and soil properties on pollutant loadings to water-bodies. Available hydrologic/watershed models vary from simple methods to detailed loading models depending on their capabilities. Simple methods have very limited predictive capabilities and generally provide rough estimates since they are derived from empirical relationships. Detailed models are complex models with greater spatial and temporal resolutions and they use storm events or continuous simulation to predict flow and pollutant concentrations for a range of flow conditions. They include physical processes of infiltration, runoff, pollutant affects, groundwater and surface water interactions. Applications for these models vary depending on data availability and modeling needs (Limno-Tech, 2002).

According to Gayathri et al, 2015, the most important major classifications under hydrological model are empirical model, conceptual models and physically based models.

Empirical models (Metric model):

These are observation oriented models which take only the information from the existing data without considering the features and processes of hydrological system and hence these models are also called data driven models. It involves mathematical equations

derived from concurrent input and output time series and not from the physical processes of the catchment. These models are valid only within the boundaries. Unit hydrograph is an example of this method.

Conceptual methods (Parametric models): This model describes all the components of hydrological processes. It consists of a number of interconnected reservoirs which represents the physical elements in a catchment in which they are recharged by rainfall, infiltration and percolation and are emptied by evaporation, runoff, drainage etc. Semi empirical equations are used in this method and the model parameters are assessed not only from field data but also through calibration. Large number of meteorological and hydrological records is required for calibration.

Physically based model: This is a mathematically idealized representation of the real phenomenon. These are also called mechanistic models that include the principles of physical processes. It uses state variables which are measurable and are functions of both time and space. The hydrological processes of water movement are represented by finite difference equations. It does not require extensive hydrological and meteorological data for their calibration but the evaluation of large number of parameters describing the physical characteristics of the catchment are required (Abbott et al. 1986). In this method huge amount of data such as soil moisture content, initial water depth, topography, topology, dimensions of river network etc. are required.

Surface Water Quality Models (SWQ)

Surface water quality models predict scenarios associated with water quality constituents that result in killing fishes, taste and odour problems, human health impacts and other ecosystem disturbances. This category of models includes models that predict dissolved

oxygen, nutrient eutrophication, sediment transport and the fate and transport of constituents. Surface water quality models are used to analyze water quality related problems concerning inputs; reactions and physical transport as well as outputs. The analysis of pollutants in surface waters describes load response relationships, cause-effect mechanisms, and in some cases, the impact of pollutants on biota in the system. The parameters simulated include nutrients (generally phosphorus, nitrogen and silicon), dissolved oxygen, biochemical oxygen demand (BOD), chlorophyll, temperature, phytoplankton, zooplankton, and faecal coliforms. These models simulate physical (dilution, advection, and dispersion), chemical and biological processes (for example, nutrient-algal cycle, algal growth and kinetics, DO-BOD cycle, decay, benthic algae, and sediment diagenesis). Eutrophication models predict the production, transformation and decay of phytoplankton biomass in response to changes in nutrients, temperature and light.

A brief description of selected models of surface water is given below according to Wang et al, 2013:

Table 2.1: Brief Description of Selected Surface Water Models			
	Models	Model version	Characteristics
1.	Streeter-Phelps models	QUAL I QUAL II QUAL2E QUAL2E UNCAS QUAL 2K	Thomas Streeter and Phelps established the first S-P model in 1925. S-P models focus on oxygen balance and one-order decay of BOD and they are one dimensional steady-state models
2.	QUAL models	QUAL I QUAL II QUAL2E QUAL2E UNCAS QUAL 2K	The USEPA developed QUAL I in 1970.QUAL models are suitable for dendritic river and non-point source pollution, including one-dimensional steady-state or dynamic models.
3.	WASP models	WASP1-7 models	The USEPA developed WASP model in 1983.WASP models are suitable for water quality simulation in rivers, lakes, estuaries, coastal wetlands, and reservoirs, including one-, two-, or three-dimensional models.
4.	QUASAR model	QUASAR model	Whitehead established this model in 1997. QUASAR model is suitable for dissolved oxygen simulation in larger rivers, and it is a one dimensional dynamic model including PC QUA SAR, HERMES, and QUESTOR modes.
5.	MIKE models	MIKE11 MIKE 21 MIKE 31	Denmark Hydrology Institute developed these MIKE models, which are suitable for water quality simulation in rivers, estuaries, and tidal wetlands, including one-, two-, or three dimensional models.

6.	BASINS models	BASINS 1 BASINS 2 BASINS 3 BASINS 4	The USEPA developed these models in 1996. BASINS models are multipurpose environmental analysis systems, and they integrate point and nonpoint source pollution. BASINS models are suitable for water quality analysis at watershed scale
7.	EFDC model	EFDC model	Virginia Institute of Marine Science developed this model. The USEPA has listed the EFDC model as a tool for water quality management in 1997. EFDC model is suitable for water quality simulation in rivers, lakes, reservoirs, estuaries, and wetlands, including one-, two-, or three-dimensional models.

(Source: Wang et al, 2013)

Groundwater models (GW)

Groundwater is a crucial resource for sustaining life, especially in semi-arid regions. It tends to be more stable in terms of quality and size than surface water, and as such it serves as the primary drinking water source for approximately 2 billion people (WWAP, 2014; Morris et al., 2003). Groundwater models address issues related to water supply, sub-surface contaminant transport, remediation and mine dewatering. These models can be used for tracking pollutants in the saturated and unsaturated zones as well as evaluating the transport of pollutants due to migration and interactions of groundwater and surface water. Groundwater withdrawals can result in lower river and stream water levels. Groundwater models generally require a large amount of information and a complete description of the flow system. Most of the groundwater models require a high level of expertise by the operator (Limno-Tech, 2002). Groundwater is estimated to irrigate 98 million hectares of land, approximately 38% of all irrigated land (Siebert et al., 2010).

Because groundwater is a ready source of water year-round, it may become a more prominent source of irrigation water in the face of a changing climate (WWAP, 2014). Groundwater models are most widely used tools for efficient management of precious groundwater resources and to predict different future scenarios A. Ashraf and Z. Ahmad, (2008). Different groundwater modeling codes are available, each with their own capabilities, operational characteristics, and limitations such as PMWIN, FEFLOW, SVFlux, and GWVistas.

Ecological models (E)

An ecological system or subsystem is demarcated as an identifiable place by the system boundary. It can be physical or conceptual, natural or arbitrary, but it is necessary for distinguishing the system from non-system. All space and activity outside the system boundary is known collectively as the surroundings, (Fath et al, 2011).

This category includes a wide variety of models and techniques for the ecological assessment of the aquatic system. It includes habitat and species classification, index systems, as well as toxicological and ecological models that simulate the effect of stressors on habitats. These types of models can examine or predict the status of a habitat, biological population or biological community. Ecological effects models for addressing the impacts of water withdrawals include a wide range of evaluation and assessment techniques that affect the ecosystem structure and function (Limno-Tech, 2002). . Changes in water quantity, water quality and sediment dynamics driven by water withdrawals can affect the following components and interactions in an aquatic ecosystem: Species habitat; production and diversity of flora; acute and chronic toxicity to

any species; population levels; growth of species (that can affect the bioenergetics costs); predator-prey relationships; food web structure; energy flow and nutrient cycling; bioaccumulation of contaminants.

Ecological models can be expressed as having advantages such as

i) to provide a way to synthesize observations, theoretical knowledge, and information about the stocks, flows, rates, and interconnections of many parts of the system;

ii) to provide a formal representation of conceptualized systems

iii) to reveal the gaps in our knowledge and therefore can be used to establish research directions

iv) to be a useful way to test scientific hypotheses, in that each model equation itself is a hypothesis about the way the system functions which can be compared with observations

v) to allow for the generation of scenarios to be developed and investigated

vi) to reveal indirect pathways and connections between system components

vii) to force one to understand dimensional consistency particularly between model domains in interdisciplinary systems.

2.11.3 Model Selection

Water quality predictive models include both mathematical expressions and expert scientific judgement. These include process-based (mechanistic) models and data-based (statistical) models. These models are meant to link management options to meaningful response variables (such as pollutant sources and water quality standard

parameters). They should incorporate the entire 'chain' from stressors to responses. Process-based models should be consistent with scientific theory, Fath et al, (2011).

The selection of the appropriate models to address a particular management question was based on many considerations, including management objectives, data availability and available resources. The model inventory provides useful information to support the model selection process. The data needs associated with many of these models may require significant resources to apply them on a site-specific basis; resource and data availability for a given site are critical considerations in the model selection process.

Simple models require less expertise and less data, so they can be used by a wider community, but often they are limited in the management questions that they can credibly address. Complex models generally have high spatial, temporal and process resolutions, require large data sets, and involve extensive computation time. These models, however, can only be used by a limited number of experts. In addition, in some cases, these more complex models have undergone limited field testing and great care should be taken in applying them on a site-specific basis without rigorous calibration. Model selection is the task of selecting a statistical model from a model class, given a set of data.

For example, we may be interested in the selection of

i. variables for linear regression,
ii. basic terms such as polynomials, splines, or wavelets in function estimation,
iii. order of an autoregressive process,
iv. number of components in a mixture model,
v. most appropriate parametric family among a number of alternatives,
vi. number of change points in time series models,

vii. number of neurons and layers in neural networks,

viii. best choice among logistic regression, support vector machine, and neural networks,

ix. best machine learning techniques for solving real data challenges on an online competition platform

Selection of a model which comes with the development of water quality model involves the following two stages:

- **Analysis of the system** - this may be theoretical, observational, or experimental;
- **Synthesis of a mathematical replica** of the system.

The main steps of model building may be explained as follows (James, 1996):

- **Formulation of objectives** - As more precisely the objectives are formulated, preferably in quantitative terms, the more satisfactory model is possible to be created and adapted;
- **Review of theoretical background** - It should include an analysis of the processes affecting water quality, method of representation, and appropriate ranges for any model parameter, review and compile all relevant information at both local and regional scales;
- **Formulation of the model** - This step involves a decision about the type of model, elimination of the relationships that do not affect the output results, examination of alternative types of models and careful relationships of base data collection. This information is integrated into a conceptual model, in general through the introduction of simplifying assumptions and qualitative interpretations regarding the flow and the transport process.

- **Creation of a model structure** - Generally the process begins by identifying the large subdivisions of a model and proceeds by fitting these together in diagrammatic form with a flow chart. It is better the model to be created from different modules (separated parts) and every part to be developed, tested and calibrated apart.

- **Formulation of equations** - On the basis of the review of theory and the model structure it is possible to state the relationships involved in some formal mathematical or statistical way. Adoption of a hierarchical approach to this process often results in a clearer set of equations in which the influence of primary and secondary relations can be more easily appreciated. Some preliminary data may be needed to guide the choice.

- **Formulation of methods of solution** - Only in a few special cases it may be possible to solve the equations analytically, but most models involve the use of numerical methods for solving partial differential equations, interpolation, etc. The choice of the appropriate numerical technique is crucial for numerical stability and accuracy and also for minimizing computational effort.

- **Selection of a computer code** - The decision depends on the project goals. If a modeling is intended only to provide a first approximation, a simple code may be appropriate. The form of input and output results, and the choice of the language, is in dependence of the available facilities. The simplest programming language is BASIC, which together with QBASIC is a power tool for many modeling purposes.

- **Calibration of the model** - It is essential that completely independent data sets are used for the calibration procedure. Calibration is one of the most critical, difficult, and valuable steps in the model application process. After a pollutant transport model is

calibrated to a satisfactory degree, it is often applied to predict and simulate the future contaminant migration.

- **Validation of the model -** It is impossible to apply the model as representative without suitable proof. The validation of the model depends on the local possibilities. Model validation, evaluation, confirmation, or testing is the process of assessing the degree of reliability of the calibrated model using one or more independent data sets. Ideally it is possible to compare the output results from the model with the observed data.

- **Statistical assessment of paired observations and simulations -** The basic statistical parameters and goodness-of-fit criteria are: average error, standard deviation, correlation coefficient, index of agreement, per cent deviation per year by flow and pollutants, and others.

- **Sensitivity analysis** -This procedure is used before and after calibration mainly to test the responsiveness and sensitivity of the numerical model to every input parameter. The sensitivity analysis is useful for: examining the likely uncertainty in simulation results due to uncertainty in model input parameters, and examining how well parameters are likely to be estimated from the available data for model calibration. Sensitivity analysis provides important information on how uncertainties in the model parameters affect the model results. If the model results are highly sensitive to a particular parameter, the uncertainty associated with that parameter will significantly affect the ability of the model to make meaningful interpretations and predictions. Sensitivity analysis is the mean of determining the model parameters.

In considering criteria for model selection, there is need to evaluate the general classifications of water quality models by their types which include:

a) Mechanistic models

Mechanistic water quality models are models that by means of mathematical tools express the mechanisms of the process that cause changes on water quality and lead to the establishment of the relationship "cause-and-effect". The mechanistic models have some advantages:

- To gain insights and increased understanding of the water quality of a particular stream;
- To provide information on "cause-and-effect" relationships;
- To indicate what is not understood;
- To provide a predictive capability.

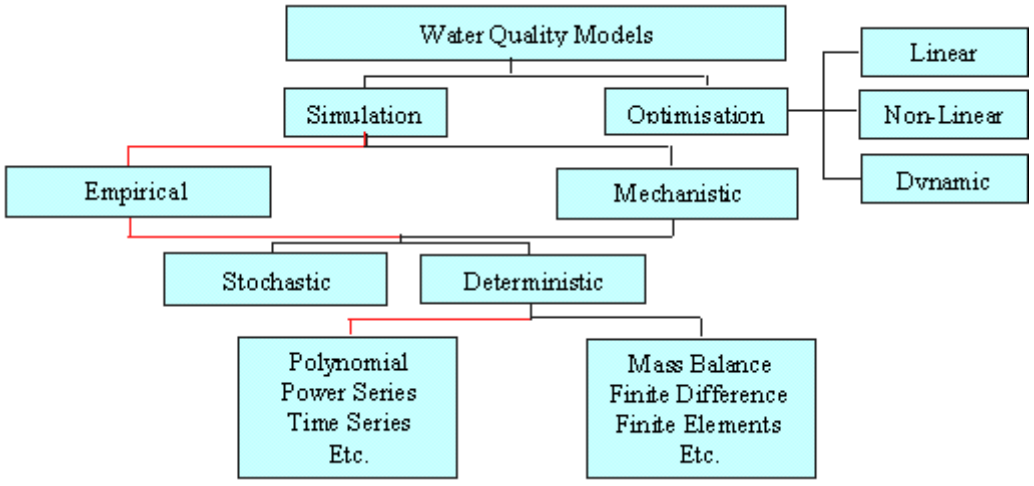

Figure 2.1 Classifications of Water Quality Models (SKM, 2011)

b) Empirical models

Empirical models are "black-box" models. Purely empirical models, such as many statistical models, allow description of the fixed relationships between input data and output results with a minimum of understanding about how the system works. Statistical models estimate the parameters through statistical analysis and then check the adequacy of the model. One of the principal restrictions of the empirical models is that they cannot be implemented to other close systems or for data out of the range used for creation of the model (Martin, 1999).

c) Deterministic/Predictive models

Deterministic models have a fixed relationship between input data and output results, which may be empirical or mechanistic. Predictive models are quantitative mathematical projections that use statistical classifiers to determine the probability of a specific water quality event in the future.

d) Stochastic models

Stochastic models contain some random elements. They are divided into: steady-state Monte-Carlo simulation models, using a mass balance model, which generate an output result with varying input conditions in the form of a frequency distribution of the pollutant concentration, and dynamic time series simulation models, using a dynamic finite difference model.

Among these water quality models, deterministic/predictive model will be used in this work since it perfectly models water quality predictions at several intervals. There are almost as many schemes for classifying water quality models as there are models. One useful classification scheme (SKM, 2011) describes 3 types of water quality models:

- **Catchment models** — derive flows from rainfall runoff and simulate associated pollutant loads
- **In-stream models** — simulate hydrodynamic behaviour of flows and in-stream water quality processes
- **Ecological response models** — simulate the ecosystem response to stressors, such as flow and water quality.

Moreover, the artificial neural network is the predictive model to be used in this work considering its high efficiency in computing multiple/complex data over time.

2.12 Artificial Neural Network (ANN) Model

Artificial Neural Networks is a time series computational model inspired by the human brain. Many of the recent advancements have been made in the field of Artificial Intelligence, including Voice Recognition, Image Recognition, and Robotics using Artificial Neural Networks, (Gill, 2019). The term 'Neural' is derived from the human nervous system's basic functional unit 'neuron' or nerve cells that are present in the brain and other parts of the body. An Artificial Neural Network is an information processing model that is inspired by the way biological nervous systems, such as the brain processes information. They are loosely modeled after the neuronal structure of the mammalian cerebral cortex but on much smaller scales. In simpler terms, it is a simple mathematical model of the brain which is used to process non-linear relationships between inputs and outputs in parallel like a human brain does every second, (Dacombe, 2017).

Artificial neural networks are able to accurately approximate complicated non-linear input–output relationships. The ANN technique is flexible enough to accommodate additional

constraints that may arise during its application. Moreover, the ANN model can reveal hidden relationships in historical data, thus facilitating the prediction and fore-casting of water quality, (Najah et al, 2012). ANN is best suited to model the irrigation water quality parameters considering the spatial and temporal resolutions in the water sampling. Here are some of the most important types of neural networks and their applications according to Anukrati, 2020.

2.12.1 Radial Basis Function Neural Network

A radial basis function considers the distance of any point relative to the centre. Such neural networks have two layers. In the inner layer, the features are combined with the radial basis function. Then the output of these features is taken into account when calculating the same output in the next time-step. Here is a diagram which represents a radial basis function neural network.

Fig. 2.2 Radial Basis Function Neural Network
(Source: Anukrati, 2020)

The radial basis function neural network is applied extensively in power restoration systems. In recent decades, power systems have become bigger and more complex. This increases the

risk of a blackout. This neural network is used in the power restoration systems in order to restore power in the shortest possible time.

2.12.2 Multilayer Perceptron

A multilayer perceptron has three or more layers. It is used to classify data that cannot be separated linearly. It is a type of artificial neural network that is fully connected. This is because every single node in a layer is connected to each node in the following layer. A multilayer perceptron uses a nonlinear activation function (mainly hyperbolic tangent or logistic function). Here's what a multilayer perceptron looks like.

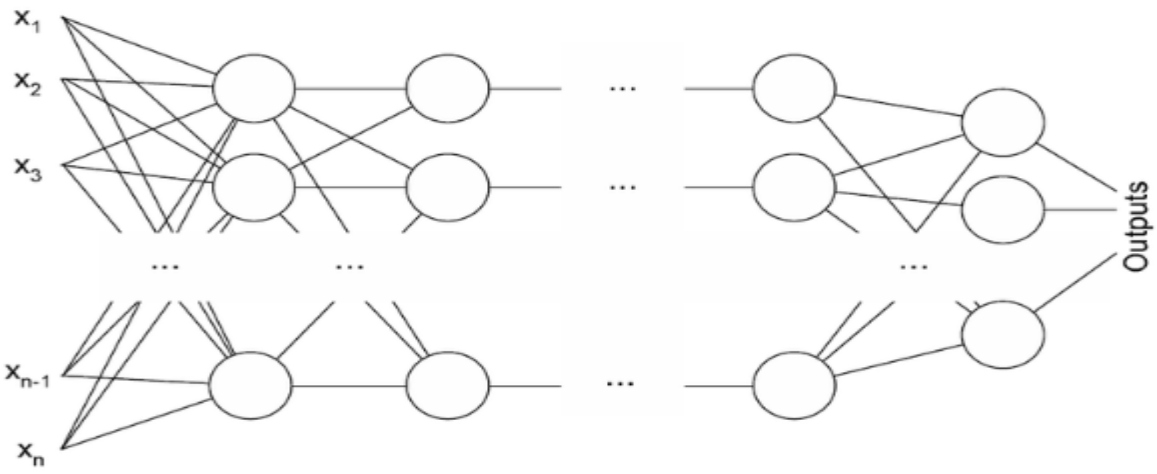

Fig 2.3 Multilayer Perceptron
(Source: Anukrati, 2020)

This type of neural network is applied extensively in speech recognition and machine translation technologies.

2.12.3 Convolutional Neural Network

A convolutional neural network (CNN) uses a variation of the multilayer perceptrons. A CNN contains one or more than one convolutional layers. These layers can either be completely interconnected or pooled. Before passing the result to the next layer, the convolutional layer uses a convolutional operation on the input. Due to this convolutional operation, the network can be much deeper but with much fewer parameters.

Due to this ability, convolutional neural networks show very effective results in image and video recognition, natural language processing, and recommender systems. Convolutional neural networks also show great results in semantic parsing and paraphrase detection. They are also applied in signal processing and image classification. CNNs are also being used in image analysis and recognition in agriculture where weather features are extracted from satellites like LSAT to predict the growth and yield of a piece of land. Here's an image of what a Convolutional Neural Network looks like.

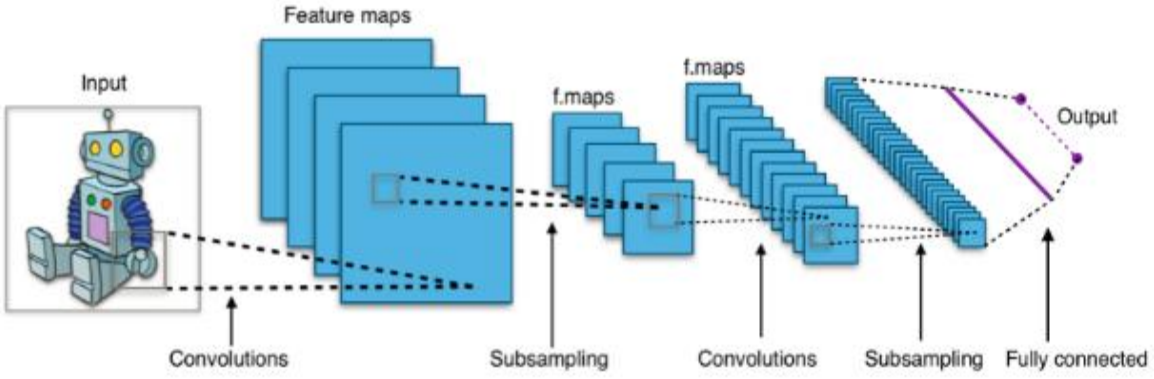

Fig. 2.4 Convolutional Neural Network
(Source: Anukrati, 2020)

2.12.4 Recurrent Neural Network (RNN) – Long Short Term Memory

A Recurrent Neural Network is a type of artificial neural network in which the output of a particular layer is saved and fed back to the input. This helps predict the outcome of the layer. The first layer is formed in the same way as it is in the feed-forward network. That is, with the product of the sum of the weights and features. However, in subsequent layers, the recurrent neural network process begins.

From each time-step to the next, each node will remember some information that it had in the previous time-step. In other words, each node acts as a memory cell while computing and carrying out operations. The neural network begins with the front propagation as usual but remembers the information it may need to use later. If the prediction is wrong, the system self-learns and works towards making the right prediction during the back-propagation. This type of neural network is very effective in text-to-speech conversion technology. Here's what a recurrent neural network looks like.

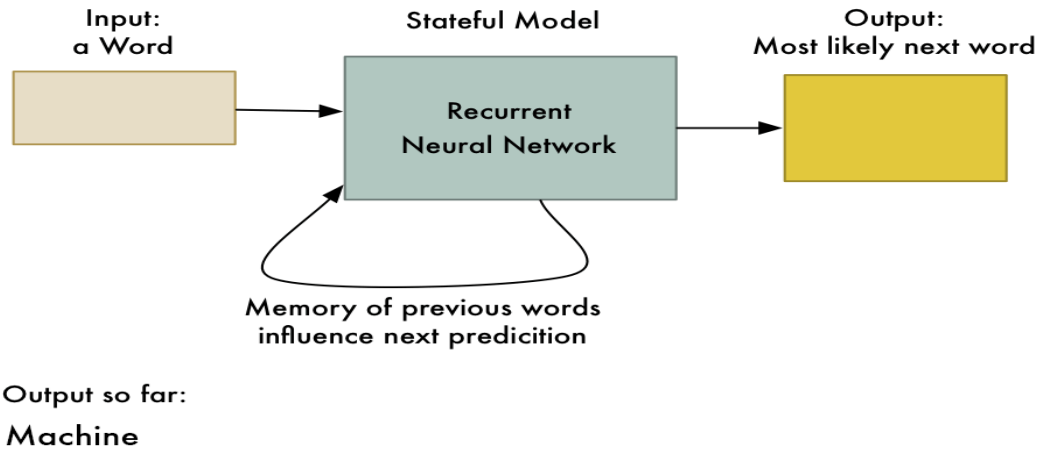

Fig. 2.5 Recurrent Neural Network (RNN) – Long Short Term Memory
(Source: Anukrati, 2020)

2.12.5 Modular Neural Network

A modular neural network has a number of different networks that function independently and perform sub-tasks. The different networks do not really interact with or signal each other during the computation process. They work independently towards achieving the output.

As a result, a large and complex computational process can be done significantly faster by breaking it down into independent components. The computation speed increases because the networks are not interacting with or even connected to each other. Here's a visual representation of a Modular Neural Network.

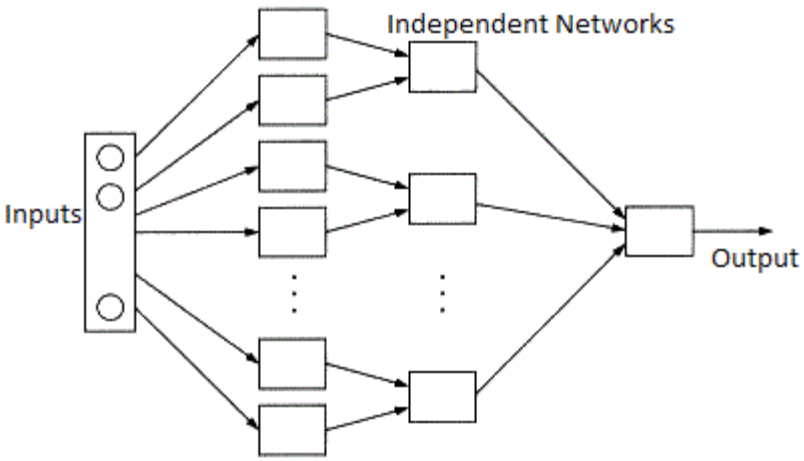

Fig. 2.6 Modular Neural Network
(Source: Anukrati, 2020)

2.12.6 Sequence-To-Sequence Models

A sequence to sequence model consists of two recurrent neural networks. There's an encoder that processes the input and a decoder that processes the output. The encoder and

decoder can either use the same or different parameters. This model is particularly applicable in those cases where the length of the input data is not the same as the length of the output data.

Sequence-to-sequence models are applied mainly in chat-bots, machine translation, and question answering systems.

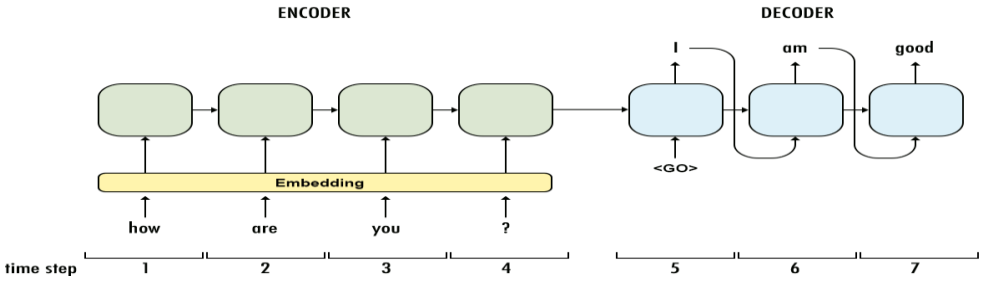

Fig. 2.7: Sequence-To-Sequence Models
(Source: Anukrati, 2020)

2.12.7 Feed-Forward Neural Networks Architecture (FFNNA)

This is a type of neural network architecture that brings inputs to a given region from another region located at an earlier stage along a particular processing pathway as shown in Figure 2.6. This neural network architecture was adopted for this study considering its ability to model the river water quality parameters efficiently. Through this connections, information flows in one direction along a connecting pathways, from the input layer via the hidden layers (in case of multilayer perceptron) to the final output layer, respectively. In feed-forward neutral network architecture, the output of any layer does not affect that same or preceding layer. Varoonchotikul (2003) reported in his study that Feed-forward neural networks architecture (FFNNA) are found to perform best for one time-step forecasting.

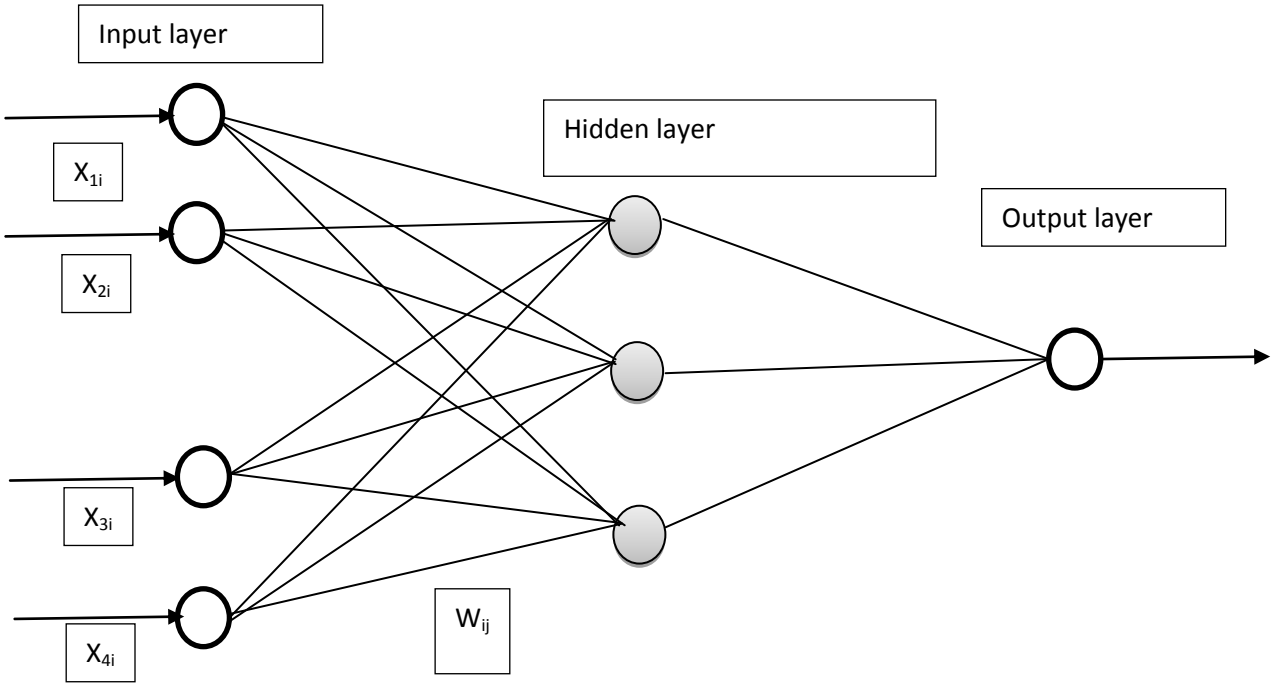

Figure 2.8: schematic diagram of Feed Forward Multilayer Neural Network Architecture. (Source: Varoonchotikul, 2003)

Feed-forward neural networks architecture is further classified as single layer or multilayer perceptron.

2.12.7.1 Feed-Forward Single Layer Network Architecture

This is the simplest kind of neural network architecture, which consists of a single layer of output neurons; the inputs are fed directly to the outputs via a series of synaptic weights (W_k) as shown in Figure 2.7. In this way, it can be considered as the simplest kind of feed-forward network. The sum of the products of the synaptic weights and the inputs is calculated in each neuron, and if the net value is above the threshold, the neuron strikes and takes the activated value; otherwise it takes the deactivated value. The neurons with this kind of activation function are also called linear threshold units. In the literature the term perceptron often refers to networks consisting of just one of these neurons. Nevertheless, it was known that a multi-layer perceptron is capable of producing

any possible Boolean function. Although a single layer perceptron is quite limited in its computational power, it has been shown that neural networks of parallel threshold units can approximate any continuous function from a compact interval of the real numbers into the interval of -1 to 1 (Auer et al., 2008).

Feed-Forward Multi-Layer Perceptron

This is a two-layer neural network that is capable of calculating XOR or any Boolean problems. A feed-forward multi-layer perceptron has a layer called hidden layer in between the input and output layers, which consist of computational units called neurons, usually interconnected in a feed-forward way. Each neuron in one layer is directly connected to the neurons of the subsequent layer as information is being propagated from the input layer through the hidden layer to the output layer. In many applications, the neurons of these networks use the sigmoid transfer function which is also known as the output function to model the inputs and outputs pattern. The sigmoidal output function has a continuous derivative function which can easily be computed and is very suitable with back propagation training algorithm.

A multi-layer neural network can compute a continuous output instead of a step function. The universal approximation theorem for neural networks states that every continuous function that maps intervals of real numbers to some output interval of real numbers can be approximated arbitrarily closely by a multi-layer perceptron with hidden layer (Awu *et al,* 2017). This theory holds for a wide range of activation functions, such as sigmoidal functions, tan function etc. A feed-forward multilayer perceptron-type of ANN is the

most suitable type of ANN for learning the stimulus-responds relationship for a given set of measured data (Minns and Halls, 1996), and this was the type employed in this study.

In feed-forward multilayer perceptron, the choice for neuron arrangement for hidden layer(s) has been by trial and error method. This could be the reason for yet-to-be breakthrough in a neural network development that behaves exactly like the human counterpart. Therefore, this study sheds more light on the adoption of finite neuron pattern architectures to optimize neural network model.

2.12.7.2 Recurrent Neural Networks (RNN)

Recurrent networks interconnect neurons within a particular region that are considered to be at the same layer along the processing pathway. This network differs from feed forward network architectures in the sense that there is at least one feedback loop. RNN propagate data from "downstream" processing elements to earlier units. Thus RNN, have feedback connections between neurons of different layers or loop type self-connections (Ahmad and Ismail, 2004). This implies that the output of the network not only depends on the external inputs, but also on the state of the network in the previous time steps as shown in Figure 2.8. Thus, in these networks, for example, there could exist one layer with feedback connections. There could also be neurons with self-feedback links, that is, the output of a neuron is feeding into itself as input. There are several advantages of RNN, the first one being that RNNs have the capability to retain values from previous cycles of processing, which can be used in current computations. This advantage allows RNN to produce complex, time varying outputs in response to simple static inputs. Since a RNN can have connections between units of any of the layers, the

output of each unit has to be identified in terms of time steps, for example outputs at time step t_{-1} can be inputs at time step t_{-n}.

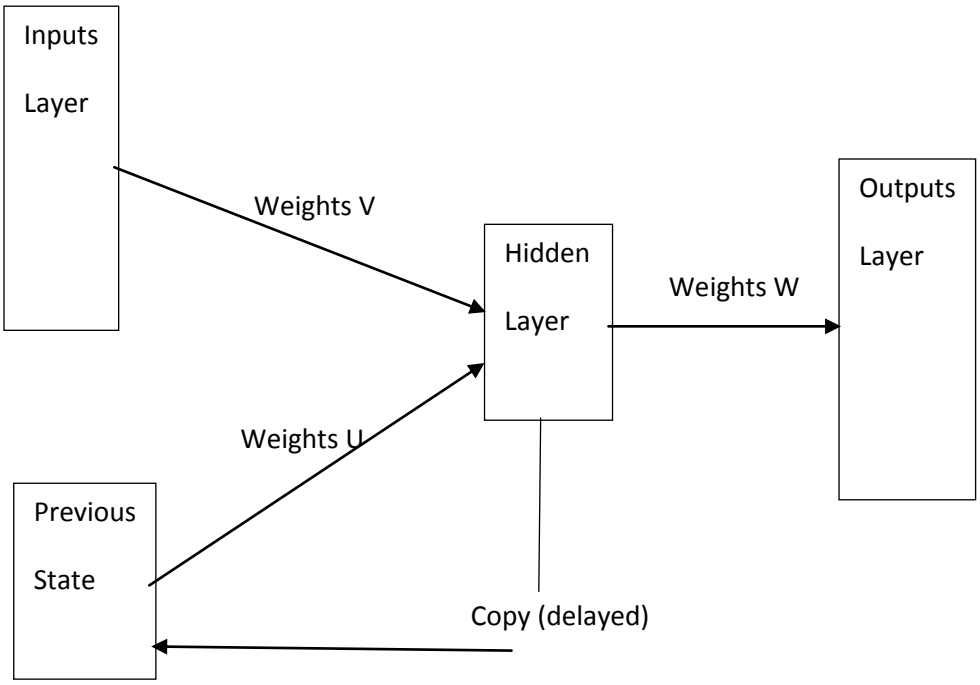

Figure 2.10: A schematic diagram of a simple recurrent network
(Source: Varoonchotikul, 2003)

2.13 Applications of Artificial Neural Network (ANN) In Water Quality Modeling

2.13.1 Working Procedures of ANN:

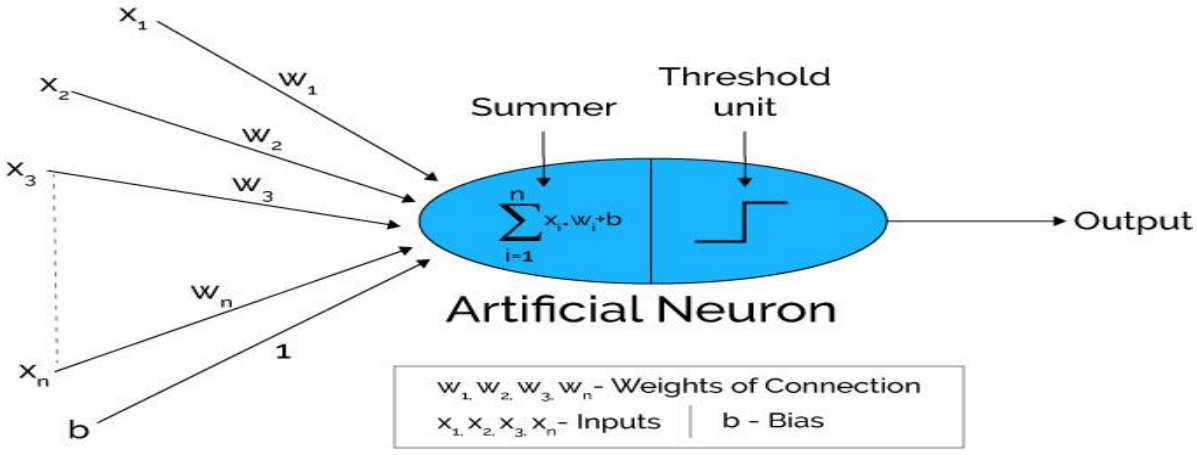

Fig. 2.11: Working procedure of Artificial Neural Network
(Source: Varoonchotikul, 2003)

Artificial Neural Networks can be viewed as weighted directed graphs, in which artificial neurons are nodes, and directed edges with weights are connected between neuron outputs and neuron inputs, (Gill, 2019). The Artificial Neural Network receives information from the external world in the form of pattern and image in vector form. These inputs are mathematically designated by the notation x (n) for n number of inputs. Each input is multiplied by its corresponding weights. Weights are the information used by the neural network to solve a problem.

Typical weight represents the strength of the interconnection between neurons inside the Neural Network. The sum corresponds to any numerical value ranging from 0 to infinity. To limit the response to arrive at the desired value, the threshold value is set up. For this, the sum is passed through an activation function, (Gill, 2019).The activation function is set to the transfer function used to get the desired output. There are linear as well as the nonlinear activation function.

Varoonchotikul (2003) stated that, ANNs are usually implemented by using electronic components or are simulated in software on a digital computer. They are characterized by

(1) Their patterns of connections between the neurons (called its architecture),

(2)Their methods of determining the weights on the connections (called their training, or learning, algorithm),

(3) Their activation function, and

(4) Their number of layers: single (Hopfield nets); bilayer (Carpenter/Grossberg adaptive resonance networks); and multilayer (most back-propagation networks).

What are neurons?

An artificial neuron is a mathematical function conceived as a model of biological neurons, a neural network. Artificial neurons are elementary units in an artificial neural network. The artificial neuron receives one or more inputs (representing dendrites) and sums them to produce an output, (Dacombe, 2017).

2.14 Case Study

1. Bowers and Shedr, (2000) predicted water quality in small streams using an Artificial Neural Network (ANN). Local precipitation, stream flow rates and turbidity for the initial prediction of suspended solids in the stream were selected as input variables. A single hidden-layer feed-forward neural network using back propagation learning algorithms was developed with a detailed analysis of model design of those factors affecting successful implementation of the model. Least-squares regression was used to compare model predictions with test data sets and most of the model configurations offered excellent predictive capabilities. Using either the logistic or the hyperbolic tangent neural activation function did not significantly affect predicted results. This was also true for the two learning algorithms tested the Levenberg-Marquardt and Polak-Ribiere conjugate-gradient descent methods. The most important step during model development and training was the representative selection of data records for training of the model.

2. Najah et al, (2012) predicted the water quality of Johor River Basin located in Johor state, Malaysia, which was degraded due to human activities and development along the river. Several methods of water modeling were adopted such as the linear regression models (LRM), multilayer perception neural networks and radial basis function neural networks (RBF-NN). From the results obtained, the use of neural networks more specifically RBF-

NN models described the behavior of water quality parameters more accurately than linear regression models. Performance evaluation of each modeling approach using 5-years worth (1998–2002) of observed data versus predicted data from each model and the performance of these three modeling approaches in terms of prediction accuracy was carried out. It was observed that RBF finds a solution faster than the MLP and is the most accurate and most reliable tool. The steps used to develop these models include the choice of performance criteria, the division and preprocessing of available data, the determination of appropriate model inputs and network architecture

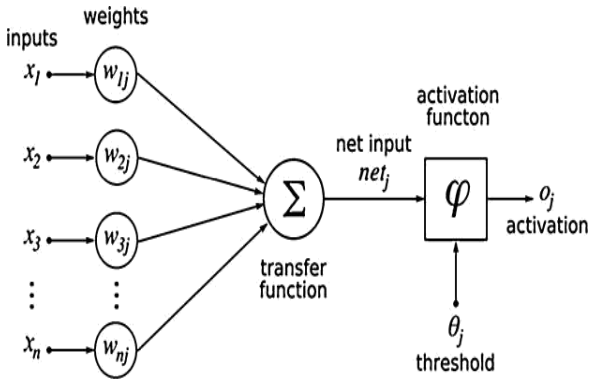

Figure 2.12: Typical multilayer perceptron neural network architecture

(Source: Najah et al, 2012)

3. Monteiro and Costa, (2018) forecasted the dissolved oxygen (DO) concentration in several monitoring sites located along the main river Vouga, in Portugal. This research was conducted from January 2002 to May 2015. Monthly DO concentration was analyzed in five water quality monitoring sites located along the Vouga River from January 2002 to May 2015. A regression model with correlated errors and a state-space model, which can be seen as a calibration model were the models compared. Results show that, the calibration model outperforms the regression model for sample modeling, that is, for a

short-term forecast, while the regression model with correlated errors has a better performance for the forecasting h-steps ahead framework. Thus, the regression model with correlated errors can be applied in order to forecast over a longer period of time while calibration model was more useful for water monitoring using an online or real-time procedure.

Table 2.2: Descriptive Statistics of Dissolved Oxygen Concentration between January 2002 and May 2015.

Monitoring Site	Abbrev	Alt. (m)	Lat. (N)	Long. (W)	Obs	Min	Max	Average St Dev
Ponte São João	de Loure	LOU 7	40.6268	−8.54329	112	5.4	11.0	8.24 1.25
Carvoeiro	CAR	18	40.68092	−8.43493	112	6.2	11.0	8.79 1.18
Ponte Vouzela	VOZ	161	40.73985	−8.09383	109	3.2	13.0	8.10 1.91
Vouguinha	VOG	441	40.75775	−7.89324	114	5.4	11.0	8.42 1.35
Aç. Maeira	MAE	495	40.7731	−7.79432	115	5.6	11.0	8.50 1.20

Alt.—altitude, Lat.—latitude, Long.—Longitude, obs.—number of monthly measurements in each water monitoring site, min—minimum, max—maximum, st dev—standard deviation.

4. Irvine et al, (2011) accomplished a study on temporal variability of turbidity, dissolved oxygen, conductivity, temperature, and fluorescence in the lower Mekong River. From the results obtained, it was shown that a strongly developed vertical variation of turbidity, DO, and conductivity in the flooded forest fringe may be related to a combination of factors, including dissolved material release from bed sediment and a floating organic-rich particulate layer near the bottom of the lake.

5. Halliday et al, (2012) studied two hydrochemical time-series derived from stream samples taken in the Upper Hafren catchment, Plynlimon, Wales. A subset of determinants such as: aluminum, calcium, chloride, conductivity, dissolved organic carbon, iron; nitrate, pH, silicon and sulphate were examined within a framework of non-stationary time-series

analysis to identify determinant trends, seasonality and short-term dynamics. The results demonstrate that both long-term and high frequency monitoring provide valuable and unique insights into the hydrochemistry of a catchment. The study also demonstrated the need for both long-term and high frequency monitoring to facilitate a thorough understanding of catchment hydro chemical dynamics. Different studies on time series analyzing in water resources management demonstrate the efficiency and necessity of this kind of modeling as it takes into account the stochastic nature of hydrological.

6. Juahir et al, (2004) predicted the water quality of Langat River basin using artificial neural network since the environmental ecosystem of Langat River basin became degraded due to poor water quality as a result of urbanization along the River. The river became seriously polluted by diffuse pollution originated from agricultural activities and untreated urban wastewater. Data from 30 sampling points of the River were monitored between (1995-2002) so as to develop ANN model consisting of 300 sets of observation and as well as to obtain WQI for six physico-chemical and biological determinants, namely Dissolved Oxygen (DO), Biochemical Oxygen Demand (BOD), Chemical Oxygen Demand (COD), Suspended Solids (SS), Ammoniacal-Nitrogen (AN) and pH. Multiple linear regression (MLR) was applied to justify the relationship between the water quality parameters and their impact on WQ. Thus, four variables namely, DO, BOD, SS and AN met the entry requirement to be included in the equation which accounted for approximately 71% of the variance in WQI. Two variables did not meet the entry requirement, namely the COD and pH, which contributed only 8% and 2%, respectively.

The summary of MLR is shown in Table: 2.3

Table 2.3: Summary of regression model

Model	R	R-square	Adjusted R-square	Std. Error of the Estimate
1	0.735[a]	0.540	0.539	13.12502
2	0.786[b]	0.617	0.615	11.99071
3	0.809[c]	0.655	0.652	11.40159
4	0.821[d]	0.673	0.669	11.11370

a. Predictors: (Constant), DO
b. Predictors: (Constant), DO, BOD
c. Predictors: (Constant), DO, BOD, SS
d. Predictors: (Constant), DO, BOD, SS, AN

7. Sahaya and Kumar, (2018) predicted the water quality index of parakai lake, India using Artificial neural network. Seven water quality parameters of Parakai Lake were chosen at four monitoring stations in the time period between December 2016 and March 2018.Artificial neural network and multiple regression model were used for modeling the lake of which from the results of the water quality index (WQI) predicted, ANN model brings better output with correlation coefficient R = 0.9907 when compared with the Multiple regression model having R = 0.7908.

8. Sirisha et al, (2008) developed empirical models based on multiple regression and artificial neural networks to predict the value of water hardness with respect to the corresponding values of chloride, fluoride and calcium contents of groundwater sample in Rajasthan, India. A thirty-point dataset was used in developing the physical models for predicting the value of hardness based on Cl, Fl and Ca. A Multiple Regression Model (MRM) was developed using the three independent variables (Calcium, Chloride and Fluoride content) and a dependent variable (Hardness). The accuracy of the model was verified using a ten-point data set by calculating the Standard Deviation (SD). The SD

value was found to be high (0.404). The Neural Network Design software, version 1.02 was also used to verify the accuracy of hardness prediction results. Artificial Neural Networks (ANNs) can be used to predict the output from the data set with better accuracy than using Regression technique. Thus, Back Propagation Network of ANN was used for the study and the results were obtained. From the Prediction, it was observed that using ANN is relatively better than that of regression model due to its flexibility to map the inputs to outputs.

9. Bisht et al, (2019) developed a river water quality forecasting model (RWQFM) created using artificial neural network (ANN) for River Ganga, India. This model development for the stream Ganga was done in the stretch from Devprayag to Roorkee, Uttarakhand, India by choosing five testing stations along this waterway which include Devprayag, Rishikesh, Haridwar, Jwalapur and Roorkee in Uttarakhan. The month to month dataset for the time arrangement was from 2001 to 2015 of which the data set comprised of four water quality parameters: temperature, pH, dissolved oxygen (DO) and biochemical oxygen demand (BOD). The objective of the work was to develop a water quality forecasting model for the river Ganga for each and every sampling station along the river through application of ANN model on the experimental dataset taken over the period of fifteen years from 2001 to 2015. Monthly forecasts into the future for a one year were made.

From the results at three stations namely, Devprayag, Rishikesh and Roorkee the quality of the Ganga River comes out as extraordinary as it was forecasted as class A throughout the year, 2016. Consequently, we can say that the water at these sites was suitable for drinking purpose. However, at the Haridwar station in general, the water quality was also forecasted

to be in class A i.e. suitable for drinking but only in nine months while in the last months of the year 2016 at the Jwalapur site the forecasting results indicated lots of uncertainty as well as critical condition of water quality in the last quarter of the year which meant that the water quality degraded significantly as a result of heavy sewage dumping at this site.

10. Pei Zhao et al, (2013) explored the changes of water quality in key channel of river Yangtze, along with the control of their relations with the water level fluctuation, which was measured through the annual encroachment processes. Mass parity budget & the integrative Water Quality indexing (WQI) approach was conducted for evaluating the total WQ status after completion of dam. The outcomes displayed that the TGR opening water (Yichang) showed high pH & COD, Mn values. Dissolved oxygen and ammonia showed low concentration. Changes in the water quality parameters showed the same tendencies for outlet & inlet water. The parameters of Water Quality displayed negative correlations due to various effects of damage to which the water body was exposed.

11. Wechmongkhonkon et al, (2012) applied ANN in classification of surface water quality. The water quality classes were evaluated using six (6) factor indices which include are pH value (pH), Dissolved Oxygen (DO), Biochemical Oxygen Demand (BOD), Nitrate Nitrogen (NO_3N), Ammonia Nitrogen (NH_3N) and Total Coliform (TColiform). The methodology involves applying data mining techniques using multilayer perceptron (MLP) neural network models. The data consisted of eleven (11) sites of canals in Dusit district in Bangkok and Thailand. The data was obtained from the Department of Drainage and Sewerage Bangkok Metropolitan Administration during 2007-2011. The results of the multilayer perceptron neural network exhibited a high accuracy multilayer perception rate

at 96.52% in classifying the water quality of Dusit district canal in Bangkok. Subsequently, this encouraging result could be applied with plan and management source of water quality.

12. Yamini and Vikas, (2019) used the ANN-based modeling approach with various training functions for the prediction of river Ganga water quality. A feed forward error back propagation neural network was used with different training functions namely trainlm (Levenberg Marquardt back propagation), trainb (Batch training with weight & bias learning rules), trainr (Random order incremental training w/learning functions) & trainbr (Bayesian regularization). Monitoring & water quality management along the river was done by establishing five sampling stations along Ganga River stretch which were selected from Devprayag-To-Roorkee city inside the Uttarakhand state of the India. These states are Bihar, Uttarakhand, Delhi, UP & West Bengal. The Hill Rivers of the Uttarakhand are Alkananda, Bhagirathi, Mandakini. ANN modeling was done using Matlab tool while performance evaluation was determined using mean square error measure. It was found that ANNs were able to forecast the water quality of the Ganga River with the trainbr function at learning rate set to 0.09 giving an accuracy of 99.5% using the best model as per the present case.

13. Kanda et al, (2016) in His study to model dissolved oxygen using ANN sought to determine the ability of feed forward back propagation in the prediction of DO in River Nzoia. This was accomplished using readily available input data of temperature, EC, turbidity and pH. The results indicated that the model combination of all the four inputs and the one which only excluded pH had good performance in predicting the DO for the river. For a country like Kenya where river water quality monitoring is hampered by insufficient funds, models such as ANN can be a good alternative to traditional process-

based modeling which may require detailed data. DO is an important parameter in determining the pollution status of the river and therefore, the model developed in the study can be used to monitor the pollution levels in the river due to industrial effluent, municipal wastewater and agricultural runoff in Nzoia catchment.

14. Khalil et al, (2012) in His study to apply ANN for the prediction of water quality variables in the Nile Delta examined the potential of the Artificial Neural Networks (ANN) on predicting interrelation between water quality parameters. Several ANN inputs, structures and training were compared and evaluated with linear regression models coupled with autocorrelated errors. The results of the ANN modeling shades light on the usefulness of ANN application in the prediction of water quality variables. Using one or two nodes in the unique hidden layer using simple ANNs. Sensitivity analysis was performed by perturbing the BOD variable. It shows that the output is sensitive to random changes of BOD concentrations. The error increase reaches 30% when the BOD concentrations is changed by 20%, while it reaches only 7% when the BOD concentrations changed by 10%.

15. Khadijah et al, (2019) investigated a technique that can automatically classify water quality using ANN. The greater part of methodologies used lies on the idea of `pattern recognition', thus, it is quite convenient to inspect carefully its ability in classification of water quality. Six environmental data were used in this study which includes: pH, total suspended solids (TSS), dissolved oxygen (DO), chemical oxygen demand (COD), biological oxygen demand (BOD), and ammonia. The data was obtained through in-site measurement and laboratory analysis. However, the data was used as the feeder of input variables in the ANN database system. After training and testing the network of ANN, the result showed 80.0% accuracy classification with 0.468 of root means

square error (RMSE). It can be concluded that, ANN is a model that can easily classify the water quality with the justifiable output.

2.15 Research Gap

This research is very important considering the fact that the major industrial cluster in Nnewi is located very close to this River and thus, effluents from these industries are discharged into it. This is the first study done to investigate the irrigation water quality on this River through pollution prediction and forecast to ascertain the future water quality characteristics at spatial and temporal intervals using the developed ANN model. Hydrodynamic modeling through determination of sediment transportation and deposition using the computational fluid dynamics model on Ele River was done for the very first time in my study having done a thorough research to find other studies on this.

CHAPTER THREE

MATERIALS AND METHODS

3.1 Description of Study Area

The study Area is Ele River Nnewi. It is located at Umudim Nnewi, Anambra State, Nigeria. Nnewi is the second largest city in Anambra State , South-Eastern Nigeria. It is a one town local government, and comprises four autonomous quarters: Otolo, Uruagu, Umudim, and Nnewichi. It is absolutely located on Latitudes 6° 16' N and 6° 55' N, and Longitudes 6° 91' E and 6° 55' E. The climate is tropical with an average annual rainfall of 200 mm and mean temperature of 27^{o}C. The months of April to October experience heavy rainfall, while low rainfall, higher temperature and low humidity characterize the months of November to March.

In 2006, Nnewi has an estimated population of 391,227 (NPC, 2006) according to the Nigerian census. From UN World Urbanization Prospects, Nnewi's 2020 population is now estimated at **1,050,860**. Nnewi has grown by 280,792 since 2015, which represents a 6.42% annual change as presented in table 3.1.

Table 3.1: Nnewi Population Data and Projections

Year	Population	Growth Rate (%)	Growth
2035	1,967,116	3.47%	308,532
2030	1,658,584	4.02%	296,741
2025	1,361,843	5.32%	310,983
2020	1,050,860	6.42%	280,792
2015	770,068	6.49%	207,665
2010	562,403	6.49%	151,664
2005	410,739	6.49%	110,739
2000	300,000	6.49%	80,920
1995	219,080	6.49%	59,080
1990	160,000	10.31%	62,027
1985	97,973	10.30%	37,973
1980	60,000	10.06%	22,854
1975	37,146	10.06%	14,146
1970	23,000	10.40%	8,974
1965	14,026	10.39%	5,471
1960	8,555	10.40%	3,339
1955	5,216	10.40%	2,035
1950	3,181	0.00%	

(Source: (United Nations, 2017)

The city spans over 1,076.9 square miles (2,789 km^2) in Nnewi, Anambra State. Umudim which is the location of the Ele River is a quarter that comprises of numerous industries such as:

(i) John White Industries Ltd, producers of fan belt ad table water.

(ii) Uru Industries, producers of motorcycle spare parts, cables and table water.

(iii) Life Vegetable Oil Industry, producers of vegetable oil.

(iv) Godwin Kris Industries, producers of tubes and tyres.

(v) Lippo table water factory, producers of tale water

(vi) Innoson Vehicle Manufacturing Ltd, producers of IVM Motors and trucks.

(vii) Chicason Group, producers of animal feeds, A-Z Oil and lubricants, plastics

(ix) Kotec Industries Ltd, producers of Tummy-Tummy noodles.

(x) Beverly Hill Hotels who are into hospitality and management business.

Ele River is located very close to the above-mentioned industries with Chicason Group of Companies as the closest industry to the River. Effluents from these industries are discharged into Ele River. This river serves as a source of water supply for the residents.

Below are figures 3.1 and 3.2 showing Map of Nnewi and Visualized raster image showing Ele River and the industrial zone in Umudim Nnewi.

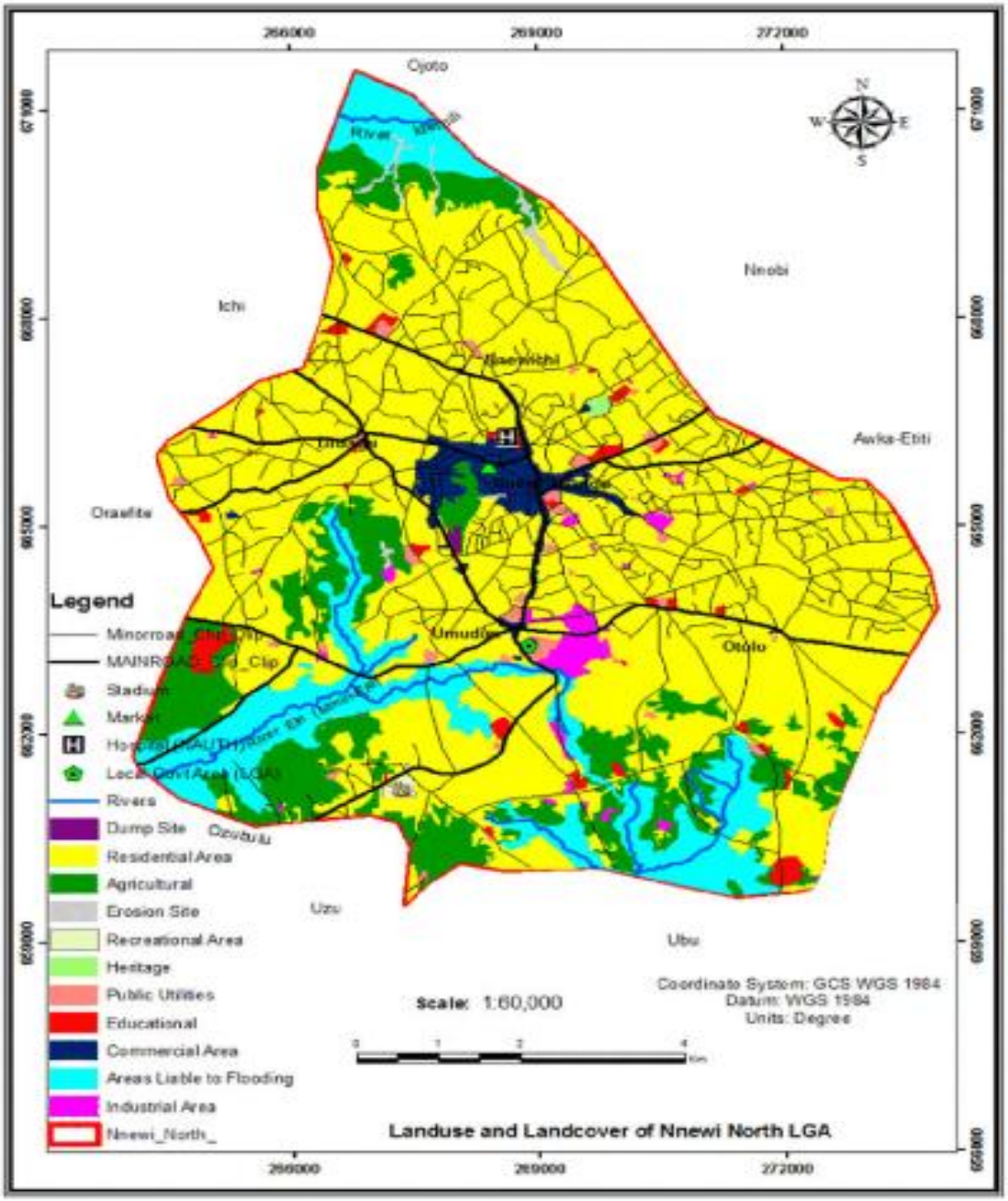

Figure 3.1: Map of Nnewi showing Ele River

Source: (Ezeomedo & Igbokwe , 2009)

Fig. 3.2: Visualized raster image showing Ele River and the industrial zone in Umudim Nnewi (Source: GIS Google image)

3.2 Water Sampling and Analysis for Time Series Modeling

Ele River based on the preliminary survey was divided into ten sampling points putting into consideration the distance from the closest point of discharge which is the discharge outlet very close to Chicason Group of Companies Uru, Umudim Nnewi. The sampling points were designated as: Point 1 (point Source/discharge point), Point 2 (10m away from the discharging effluent) , Point 3 (20m away from the discharging effluent), Point 4 (30m away from the discharging effluent) , Point 5 (40m away from the discharging

effluent),Point 6 (50m away from the discharging effluent), Point 7 (60m away from the discharging effluent), Point 8 (70m away from the discharging effluent), Point 9 (80m away from the discharging effluent), Point 10 (90m away from the discharging effluent). These ten (10) sampling points were be named P1, P2, P3, P4, P5, P6, P7, P8, P9, and P10 so as to determine/ ascertain the level of water pollution at every 10m interval from the point source to the last sampling point considering the ion dissolutions and sediment transportation from discharge point to sampling point 10. The choice of 10m interval was borne to ascertain any changes caused by pollution and sediment deposition in the water body at the closest distance from one sampling point to another. From each sampling points, duplicate water samples were collected using 1.5 litre sterile plastic bottles. These water samples were collected monthly during the six months of rainy season from April-October and six months of dry season November –March.

P1 and P2 Samples were located upstream in the River while P3 to P10 were located at the downstream section of the Ele River. Water samples were sent for analyses within 24 h after sampling. Irrigation water quality parameters to be tested are: Electrical Conductivity, Calcium, Magnesium, Sodium, Bicarbonate, Sulphate, Nitrate-Nitrogen, Ammonium-Nitrogen, and pH.

3.3 Laboratory Analysis of Irrigation Water Quality Parameters

3.3.1 Methods for the Physical Analysis of water samples

3.3.1.1 Determination of pH

pH was measured by Electrometric Method using Laboratory pH Meter Hanna model HI991300 (APHA; 1998) as follow:

i) The electrodes were rinsed with distilled water and blot dry.

ii] The pH electrodes were then rinsed in a small beaker with a portion of the sample.

iii] Sufficient amount of the sample was poured into a small beaker to allow the tips of the electrodes to be immersed to a depth of about 2cm. The electrode was at least 1cm away from the sides and bottom of the beaker.

iv] The temperature adjustment dial was adjusted accordingly.

v] The pH meter was turn on and the pH of sample recorded.

3.3.1.2 Determination of Electrical Conductivity

Analysis was carried out according to APHA 2510 B guideline Model DDS-307 (APHA; 1998) as follow:

i) The conductivity cell was rinsed with at least three portions of the sample.

ii) The temperature of the sample was then adjusted to $20 \pm 0.1^{o}C$.

iii) The conductivity cell containing the electrodes was immersed in sufficient volume of the sample

iv) The Conductivity meter was turned on and the conductivity of the sample recorded.

3.3.1.3 Determination of Total Dissolved Solids

Total dissolved solid was determined using APHA 2510 A TDS 139 tester (APHA; 1998)

(i) The fiber filter disc was prepared by placing it, wrinkled side up, in the filtration apparatus. Vacuum was applied and the disc washed with three successive 20ml washings of distilled water. Continuous suction was then applied to remove all traces of water.

ii] A clean evaporating dish was heated to 180 ± 2^{o}C in an oven for 1hr, Cooled and stored in a desiccator until needed. It was usually weighed immediately before use.

iii] A sample volume was chosen to yield between 2.5 and 200mg dried residue.

iv] 50ml of well mixed sample was filtered through the glass-fibre filter; it was washed with three successive 10ml volumes of distilled water, allowing complete draining between washings. Suction was continually applied for about 3mins after filtration is complete.

v] Filtrate was transferred to a weighed evaporating dish and evaporated to dryness on a steam bath.

vi] The evaporating dish was finally dried for at least 1hr in an oven at 180 ± 2^{o}C, cooled in a desiccator to balance temperature and weigh.

Calculation:

$$TDS = \frac{(A - B) \times 10^3 \text{ mg/l}}{\text{Sample volume in ml}}$$

Where A = weight of dish + solids (mg)

B = weight of dish before use (mg)

3.3.1.4 Nitrate-Nitrogen Determination

Nitrate-Nitrogen was determined using PD303 UV Spectrophotometer (APHA; 1998) as follow:

A known volume (50ml) of the sample was pipetted into a porcelain dish and evaporated to dryness on a hot water bath. 2ml of phenol disulphonic acid was added to dissolve the residue by constant stirring with a glass rod. Concentrated solution of sodium hydroxide and distilled water was added with stirring to make it alkaline.

This was filtered into a Nessler's tube and made up to 50ml with distilled water. The absorbance was read at 410nm using a spectrophotometer after the development of colour. The standard graph was plotted by taking concentration along X-axis and the spectrophotometric readings (absorbance) along Y-axis. The value of nitrate was found by comparing absorbance of sample with the standard curve and expressed in mg/L.

Methods for Calibration

Standard nitrate solution was prepared by collecting 50ml of the stock solution, 2ml of phenol disulfonic acid added and diluted to 500ml, to give 1ml = 10 μg. The solution of various strengths ranging from 0.0 (blank) to 1.0 mg/L at the intervals of 0.2 mg/L was prepared by diluting stock solution with distilled water.

Table 3.2 Preparation of Standard Calibration Curve for Nitrate-Nitrogen Determination

Ml of Standard Solution	Ml of Distilled water	Concentration (mg/l)	Absorbance
0.00	1.00	0.00	0.00
0.20	0.80	0.002	0.004
0.40	0.60	0.004	0.012
0.60	0.40	0.006	0.017
0.80	0.20	0.008	0.020
1.00	0.00	0.010	0.026

(Source: Spring board lab)

3.3.1.5 Sulphate Determination

Sulphate was analyzed according to APHA standard method (APHA; 1998) as follow:

A 250cm^3 of the water sample was evaporated to dryness on a dish. The residue was moistened with a few drop of Conc HCl and 30cm^3 distilled water was added. This was boiled and then filtered.

The dish was rinsed and the filter paper washed with several portions of distilled water and both filtrate and washings added together. This was heated to boiling and then 10cm^3 of 10% $BaCl_2$ solution was added, drop by drop with constant stirring. The mixture was digested for about 30minutes, filtered and the filter paper washed with warm distilled water. It was then ignited, cooled and weighed in an already weighed crucible.

Calculation:

$Mg/dm^3 SO_4^{2-}$ = mg $BaSO_4$ x 411.5$cm^3$of water sample

3.3.1.6 Determination of Calcium Hardness

Hardness was measured using standard analytical method of APHA, 1998 as follow:

$50cm^3$ of the water sample was introduced into a beaker and $1cm^3$ buffer solution of NH_3 was added. Three drops of solocrome Black T indicator was also added and the solution swirled properly. The mixture was titrated with 0.01EDTA solution until the colour changed from wine red to pure blue with no bluish tinge remaining. The total hardness of the water sample was calculated.

$$\text{Total hardness (mg/caC0}_3) = \frac{\text{Volume of Titrate x 100}}{\text{Volume of samples (cm}^3)}$$

3.3.1.7 Bicarbonate of Water Sample.

This was determined by titration method. 50mL or 100mL of the water sample was collected in a clean flask and slight excess of Barium Chloride solution was added to precipitate the carbonate which does not affect the bicarbonate. Two (2) drops of phenolphthalein indicator was added to the solution. It was then shake and titrated to the end point with 0.02m standard HCL (hydrochloric Acid). The volume of acid used was recorded and this calculation goes thus:

$$\frac{V \times M \times 100{,}000}{\text{mL of sample used}}$$

3.3.1.8 Ammonium-Nitrate Determination

The titrimetric procedure for the determination of ammonium nitrogen can be used only for samples which have been treated by the preliminary distillation into boric acid absorbing solution. In this procedure, the ammonium concentration of the boric acid solution is titrated with a strong acid titrant to the pale lavender end of methyl re-methylene blue indicator.

Equipment:

1. Distillation apparatus
2. 50ml burette

Reagents

1. Indicating boric acid
2. Methyl re-methylene blue mixed indicator
3. Hydrochloric acid standard titrant 0.01N

   % Nitrogen = Titre value × normality of titrant × atomic mass of Nitrogen × dilution factor

   % Nitrogen × kjheal factor; $\%NH_3$ % Nitrogen × 6.25

Table 3.3: FAO Water Quality Standards for Evaluation of Common Irrigation Water Quality Problems

Water parameter	Symbol	Unit[1]	Usual range in irrigation water	
Electrical Conductivity	EC	dS/m	0 – 3	dS/m
Total Dissolved Solids	TDS	mg/l	0 – 2000	mg/l
Calcium	Ca^{++}	me/l	0 – 20	me/l
Magnesium	Mg^{++}	me/l	0 – 5	me/l
Sodium	Na^{+}	me/l	0 – 40	me/l
Bicarbonate	HCO_3^{-}	me/l	0 – 10	me/l
Sulphate	SO_4^{--}	me/l	0 – 20	me/l
Nitrate-Nitrogen	NO_3-N	mg/l	0 – 10	mg/l
Ammonium-Nitrogen	NH_4-N	mg/l	0 – 5	mg/l
pH	pH	1–14	6.0 – 8.5	

Source: (FAO, 1984)

3.4 Time Series Modeling Using Artificial Neural Network

Artificial Neural Network Modeling

ANN can be described as data modeling tool which can be applied in hydrology to simulate input (rainfall) output (river flow) patterns. Artificial Neural Network (ANN) as defined by Smith (2001) describes a neural network as "a form of multiprocessor computer system" with simple processing elements, a high degree of interconnection, simple scalar messages and adaptive interaction between elements. However, ANN can also be described as a network of simple but interconnected processing units called neurons, which are able to automatically adjust to information and learn aspects of this information by storing it in the connection strengths, represented as synaptic weights between the neurons as shown in Figure 2.7. Artificial neural networks (ANN) are powerful tools for data modeling, especially when the underlying data relationship is unknown. ANNs can identify and learn correlated patterns between input data sets and the corresponding target values. After

training, ANN can be used to predict the outcome of a new independent input data. ANNs imitate the learning process of the human brain and can process the problems involving non-linear and complex data even when the data are incomplete and noisy (Chen et al., 2002). ANNs are preferably suited for the modeling of hydrologic data which are known to be highly complex and often non-linear.

These networks are "neural" in the sense that they are inspired by neuroscience but not necessarily because they are faithful models of biological neural or cognitive phenomena and have allowed scientists and researchers to build mathematical models of neurons in order to simulate neural behaviour (Fu, 1994).

3.4.1 Development of Artificial Neural Network

Practically, the network architecture contains a number of layers probably; the input, hidden and output layers, respectively. The architecture determines the number of connection weights and also the way information flows through the network. The determination of the best network architecture is one of the difficult tasks in artificial neural network model building process but one of the most important steps that must be taken. In this study, development research design was adopted. Artificial neural network shield of Alyuda Neural Network forecaster was used in the development of the ANN. Alyuda Forecaster is neural based network forecasting software with an intuitive and wizard-like interface which easily steps one through the process of creating a neural network for forecasting and prediction.

The structural block diagram that shows the flow and order for the model as well as the developmental stages of the ANN model are shown in Figures 3.3 and 3.4, respectively.

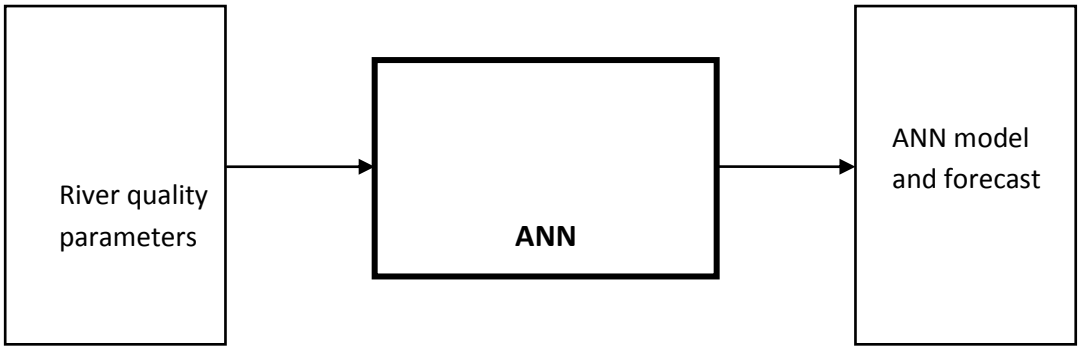

Figure 3.3: Block diagram showing flow and order of the model

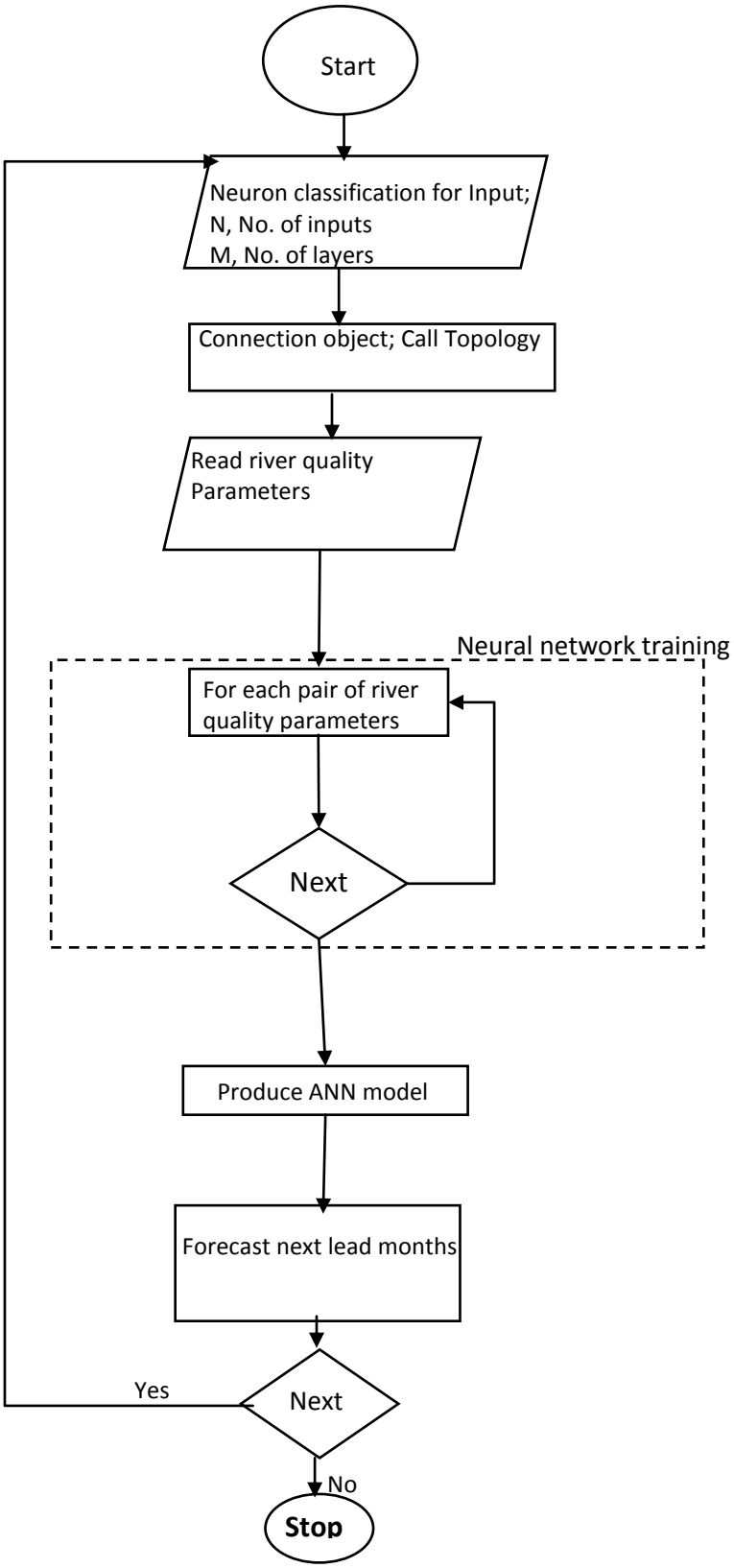

Figure 3.4: Flow Chart for the ANN development

A neural network feed-forward multilayer perceptron (FFMLP) was adopted in this study using river quality parameters at times t_{-n} to forecast the river discharge at time t_{n+1}. A feed-forward multilayer perceptron is a structure of an artificial neural network that has been proven to be the best neural network structure for hydrological modeling (Shamseldin, 1997). In the artificial neural network model development, the primary building block was the neuron classification, therefore, a neuron class was declared. The neuron class describes an entity with an (x, y) location to manage an array list of neurons, as well as its own location that are drawn relatively to the network's center. The neuron class therefore exists in the single neuron and a network of many neurons arranged in layer-by-layer basis.

A connection object was also created to connect the neurons from one layer to another. The connection object was made to connect neurons from the preceding layer to the succeeding layer. A new function called 'connect' was therefore added in the neuron class to connect object between the specified neurons.

A class that stored the array list of connections was created, just like it stored an array list of neurons. The significance of storing the array list of connections was to ensure that the synaptic weights are not changed nor lost during training.

Ultimately, a class called feed-forward was created to "feed-forward" the neurons through the network, such that the neuron objects themselves must know to which neurons they are connected in the "forward" direction. In other words, each neuron was created to have its own list of connection objects and the reference of the connections

were stored by executing the add connection function that stores the connection, so that it can pass its output to the next neuron in the next layer when the time comes.

Consequently, the input arrives at the neurons in the first layer that was drawn on the left hand side of the network and feed-forward across the connections to the neurons in the adjacent layer until it exits as output from the network itself.

Going by the new activation function and output function, a function of activation function and output function in the neuron class was created to compute the network output signals. The activation function class created computes the linear combination of the input vectors to form pre-activation signals. This was transformed using the output function to give the network output signals. The output signals were transferred to the next neurons in the layer, and the process was continued till the last output layer.

In this study, supervised back propagation training algorithm was also employed for the ANN development. All the synaptic weights in the neural network were randomized between ± 0.5 , learning rate and momentum were fixed at 0.4 and 0.5, respectively. Prior to the execution of flow of information from the input layer through the output layer, a function called "Normalization" was also created in the neuron class to normalize the inputs that was received in the input layer to values between 0 and 1. Normalization of the data set was highly essential to enable the network outputs to remain within the range of the network output function and also for all data to receive equal treatment during training as well as to enhance the efficiency of the network training algorithm. The significance of data normalization should not be underestimated. The training datae were normalized using equation 3.1.

$$N_k = \frac{R_k - Min_k}{Max_k - Min_k} \quad (3.1)$$

Where: R_k is the real value applied to neuron k,

N_k is the normalization value calculated for neuron k.

Max is the maximum number

Min is the minimum number

3.5 The Neural Network Training

In this study, supervised back propagation training algorithm was employed. The supervised back propagation training algorithm endeavours to minimize the error between the desired value and the network output value by changing the values of the synaptic weights in the network through calculating the difference between the network output values and the target values and feeding them back to the network.

To this effect, a function called "back propagation" training algorithm class was created to train the neural network. The training flowchart is shown in the block diagram in Figure 3.5. The back propagation class created takes signals from the input layer $x_i$and multiplies it by a set of fully-connected synaptic weights w_{ji} connecting the input layer to the first hidden layer using the activation function (v_j) . The computation forms the pre-activation signal for the first hidden layer. The pre-activation signal of the hidden layer was transformed using the output function y (v_j) to form the feed-forward activation signals leaving the first hidden layer x_j to the next neuron in the next layer, this process continued to the output layer.

Difference between the network output values to the desired targets d_k was calculated using equation 3.3.

$$e_k = d_k - y_k \tag{3.3}$$

Where:

e is the output error

k is the output layer notation

d_k is the desired value

y_k is the neural network output value. From the network output error term in equation 3.3, the instantaneous error energy at iteration n was computed using equation 3.4.

$$E(n) = 1/2 \sum_{k \in c} e^2{}_k(n) \tag{3.4}$$

Therefore, the average error energy of the network output was calculated using equation 3.5.

$$E_{av}(n) = \frac{1}{N} \sum_{n=1}^{N} E(n) \tag{3.5}$$

Where:

n is the number of iteration in the output layer

e is the network output error

E is the instantaneous error energy

E_{av} is the average error energy

N is the number of pattern that are been presented in the network

The network output induced field also known as the activation of the neurons in the output layer was calculated using equation 3.6.

$$v_k\ (n) = \sum_{j=0}^{m} w_{kj}(n) y_j \qquad (3.6)$$

Where:

y_j is the output of the layer previous to the output layer

m is the number of neurons in the previous layer.

Therefore, the actual network output was calculated using equation 3.7.

$$y_k(n) = \emptyset\left(v_k(n)\right) \qquad (3.7)$$

Where $\emptyset$ is the partial derivative of the local induced field.

Hence, equations 3.3 to 3.7 becomes the 5 basic equations adopted for the analysis of the back propagation training algorithm in this study. Therefore, the changes in the synaptic weights for the output layer was calculated using decent gradient rule also known as error correction mechanism through the computation of the partial derivative of the instantaneous error energy with respect to the weights connecting the output layer and the immediate preceding hidden layer using equation 3.8.

$$\frac{\partial E\ (n)}{\partial w_{kj}} \qquad (3.8).$$

Therefore, the partial derivative of the instantaneous error energy of equation was calculated by substituting equation 3.4 into equation 3.3 and equation 3.7 into equation 3.6, respectively and by employing chain rule derivatives on equation 3.8 to get equation 3.9.

$$\frac{\partial E\ (n)}{\partial w_{kj}} = \frac{\partial E(n)}{\partial e_k(n)} . \frac{\partial e_k(n)}{\partial y_k(n)} . \frac{\partial y_i(n)}{\partial v_k(n)} . \frac{\partial v_k(n)}{\partial w_{kj}(n)} \qquad (3.9)$$

Resolving equation 3.9 one after the other, equations 3.10 to 3.13 were obtained as:

$$\frac{\partial E(n)}{\partial e_k(n)} = e_k(n) \qquad (3.10)$$

$$\frac{\partial e_k(n)}{\partial y_k(n)} = -1 \qquad (3.11)$$

$$\frac{\partial y_i(n)}{\partial v_k(n)} = \emptyset' v_k(n) \qquad (3.12)$$

$$\frac{\partial v_k(n)}{\partial w_{kj}(n)} = y_j \qquad (3.13)$$

Substituting equations 3.10, 3.11, 3.12 and 3.13 into equation 3.9, to get equation 3. 14 as :

$$\frac{\partial E\ (n)}{\partial w_{kj}} = -e_k(n) . \emptyset' v_k(n) . y_j \qquad (3.14)$$

constant of proportionality known as eta which defines the network learning rate was introduced into equation 3.14, to get equation 3.15.

$$\frac{\partial E\ (n)}{\partial w_{kj}} = -\eta . e_k(n) . \emptyset' v_k(n) . y_j \qquad (3.15)$$

The learning rate was fixed 0.4, the closer the learning rate is to 1 the more oscillatory the learning rate will become.

The negative sign in front of the eta constant of proportionality signifies that the changes in the synaptic weights are moving against the direction of the decent gradient.

However, the gradient decent with respect to the induced field was substituted using equation 3.16.

$$\delta_k(n) = e_k(n).\emptyset' v_k(n) \qquad (3.16)$$

Therefore, equation 3.15 becomes,

$$\frac{\partial E(n)}{\partial w_{kj}} = -\eta.\delta_k(n).y_j \qquad (3.17)$$

Hence, the changes in the synaptic weights were calculated using equation 3.18.

$$\Delta w_{kj} = \eta.\delta_k(n).y_j \qquad (3.18)$$

Whereas the new synaptic weights were calculated using equation 3.19

$$w_{kj(p+1)} = w_{kj(p)} + \Delta w_{kj(p)} = w_{kj(p)} + \eta.\delta_k(n).y_j \qquad (3.19)$$

The eta which is also called the learning rate determined how fast a neural network learns an input to output mapping. To accelerate the training a momentum term was introduced into equation 3.19 to give equation 3.20 as,

$$w_{kj(p+1)} = \beta.w_{kj(p)} + \Delta w_{kj(p)} = \beta.w_{kj(p)} + \eta.\delta_k(n).y_j \qquad (3.20)$$

Where β is a positive number $(0 \leq \beta < 1)$ called the momentum constant.

The momentum constant which serve as the network accelerator was fixed at 0.5.

The decent gradient computation was not too difficult as long as neuron k belong to the output layer, in which case the decent gradient can be easily calculated using equation 3.16. However, the calculation of the decent gradient becomes extremely difficult for the hidden layers because their error terms $e_j(n)$are not known.

For the hidden layers, the decent gradients were computed using equation 3.21.

$$\delta_j = -\frac{\partial E(n)}{\partial v_j} \qquad (3.21)$$

Where j term is the hidden layer's notation by applying chain rule of differentiation to equation 3.21, I got equation 3.22:

$$\delta_j = -\frac{\partial E(n)}{\partial y_j}.\emptyset'_j v_j(n) \qquad (3.22)$$

The instantaneous error energy for the hidden layer was given by equation 3.23.

$$E(n) = 1/2\sum_{j\in c} e^2{}_j(n) \qquad (3.23)$$

Therefore,

$$\frac{\partial E(n)}{\partial y_j} = \sum_j e_j(n).\frac{\partial e_j(n)}{\partial y_j(n)} \qquad (3.24)$$

$$\frac{\partial E(n)}{\partial y_j} = \sum_j e_j(n).\frac{\partial e_j(n)}{\partial v_j(n)}.\frac{\partial v_j(n)}{\partial y_j(n)} \qquad (3.25)$$

By substituting equation 3.7 into 3.3, to get equation 3.26 as,

$$e_k(n) = d_j - \emptyset(v_j) \tag{3.26}$$

Therefore,

$$\frac{\partial e_j}{\partial v_j} = -\emptyset'(v_j)(n) \tag{3.27}$$

Therefore, the induced local field for the hidden layers was calculated using equation 3.28.

$$v_j(n) = \sum_{j=0}^{m} w_{ji}(n).y_j(n) \tag{3.28}$$

Likewise, the partial derivative of equation 3.28 gives equation 3.29 as.

$$\frac{\partial v_j}{\partial y_j} = w_{ji}(n) \tag{3.29}$$

By substituting equation 3.29 and 3.27 into equation 3.25, to get equation 3.30 as,

$$\frac{\partial E(n)}{\partial y_j} = -\sum e_k(n).\emptyset' v_k(n).w_{ji}(n) \tag{3.30}$$

Substituting delta δ_j into equation 3.30, to get equation 3.31 as,

$$\frac{\partial E(n)}{\partial y_j} = \sum_{j} \delta_j(n).w_{ji}(n) \tag{3.31}$$

Applying equation 3.31 into equation 3.30 to get the equation for the computation of the decent gradient for the hidden layers as.

$$\delta_j(n) = \emptyset'_j . v_j(n) \sum_k \delta_k(n) . w_{ji}(n) \qquad (3.32)$$

The back propagation training iterated until the error falls below given threshold or converged to an error point of 0.001. At this point, the back propagation training algorithm was considered to have learned the full function of the output interest and the procedure terminated. For this reason, back propagation is also known as a "steepest descent" algorithm.

During the forward and backward computational processes, the inputs were ensured to remain unchanged otherwise the neural network training would be re-trained.

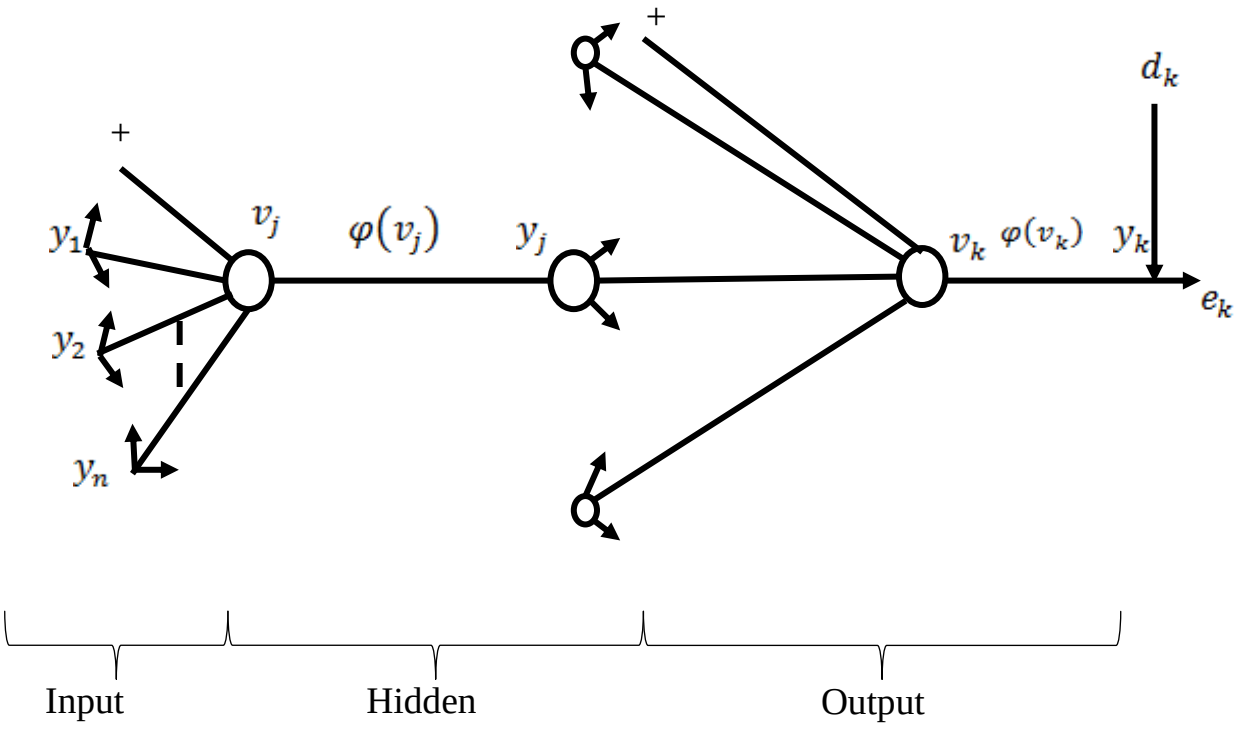

Figure 3.5: Signal flow diagram of the feed-forward neural network model (Source: Varoonchotikul, 2003)

3.6 Data Collection for Hydrodynamic Modeling (CFD)

Flow velocity was measured using Geopacks ZMFP-126S hand-held stream flow meter. Stream velocity at the inlet of the major tributary was measured at the surface midstream because flow velocity is greatest at midstream and slowest along bed and banks due to friction. The measurements were carried out in the rainy season (July and August 2018), and dry season (November and December 2018), also (July and August 2019) rainy season, and dry season (November and December 2019) to account for seasonal variation in flow. Flow velocities were also measured at five points in the river tributary and at the outlet of the channel in July, for model validation.

3.7 Modeling and Simulation of Sediment Transport in Ele River

Sediment transport is of concern when evaluating hydro-ecological problems particularly for shallow waters that experience significant pollution. Sediments significantly influence the flow properties, because not only do sediment deposition change the natural bathymetry (bed surface level/bottom configuration) they also affect storage capacity of the channel. Several studies have evaluated sedimentation and re-suspension in water bodies (Visescu *et al.,* 2016; Amoudry and Souza, 2011). Numerical modeling can play an important role towards identifying areas of a water body at higher risk of excessive deposition of sediments, as well as amounts of sediments. The use of validated numerical models can thus allow for measures to mitigate such problems. Evaluation of sedimentation and storage capacity of Ele River has become very necessary following the rapid urbanization around the river channel. Figure 3.6 shows the visualized raster image showing a major tributary of Ele River in 2003 and 2017. Expansion of the industrial zone can be clearly seen, and this has resulted to an increase in pollutants discharge to the river.

Plate 3.1: Visualized raster image showing Ele River and the industrial zone in Umudim Nnewi in 2003 and 2017. (Source: GIS Google Imaging)

The channel length of a section of the major tributary measured from the raster image was 327.38m in 2003, against the value 308.49m measured in 2017. This shows that the tributary lost 18.89m of its length to sediments from point and non-point sources. Also narrowing of the flow channel can also be seen highlighted in red. Therefore, modeling of sediments transportation in Ele River with a view to determine areas at higher risks of deposition of fine particles has become very necessary.

Investigation of sediments influence in hydraulic systems is complicated by several factors ranging from geological processes to the complex interaction of fluid and sediment particles. Due to increasing computing power, the investigation of sediment transport using computer models have increased recently. However, many of the models suffer from a range of problems, such as over-estimation due to uncertainty of the models and the unsuitability of assumptions and parameters in compliance with local conditions (Hajigholizadeh et al., 2018). Numerical simulation of sediments transportation, deposition and re-suspension is even more

complicated. Holzbecher and Hadidi, 2018 stated that sediments transport is a multiphysics problem and that water flow and sediments transport must be coupled as erosion or deposition at the bottom alters the depth of the water and thus affect the flow regime.

To accurately predict sediments dynamics in a system that is always in a state of dynamic equilibrium between deposition and erosion, a detailed knowledge of the local morphological variables such as particle sizes, settling velocities of the different particle sizes, transport rates etc. and obtaining this information will involve extensive field survey. In the study, we attempt to minimize the complexity, as well as the required computing capacity by using two dimensional (2D) Computational Fluid Dynamics (CFD). The Comsol Multiphysics® Version 5.3a used in this study is a powerful tool that allows the modeling and solving of different types of physical phenomena, based on Partial Differential Equations (PDEs) (Comsol, 2017). These PDEs are solved using Finite Element Method (FEM). Flows can be simulated in various forms like stationary or time-dependent, under laminar or turbulent conditions and models can also be built in three dimensional spaces. Different complex geometries and physical properties can be represented using the software and the graphical user interface is very flexible and contains all the tool needed to build a successful model.

3.8 Modeling Using Computational Fluid Model

Several steps are involved in the modeling process of Comsol Multiphysics. These include building up space geometry, selection of the appropriate physics that describes the problem under investigation, assigning values and defining boundaries, and finally meshing.

3.8.1 Building the Geometry of the Tributary of Ele River

A 2D geometry of the major tributary of Ele River was built for this study. The choice of 2D model in this research was because it takes a shorter time to run and requires a comparably small amount of computer memory. The first step in building the geometry of the river

tributary is georeferencing and digitization. To georeference and digitize the region of interest in the Ele River, physical vector map of Nnewi North LGA (Plate 3.2) was overlaid over the raster image of the study area in Google Earth as shown in Plate 3.3.

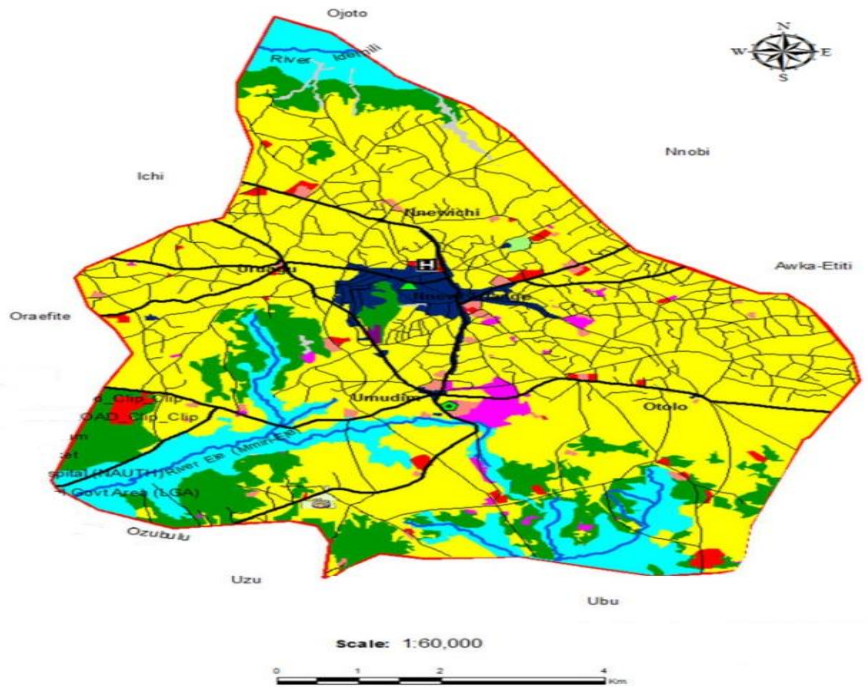

Plate 3.2 Physical vector map of Nnewi North LGA (Ezeomedo and Igbokwe, 2019)

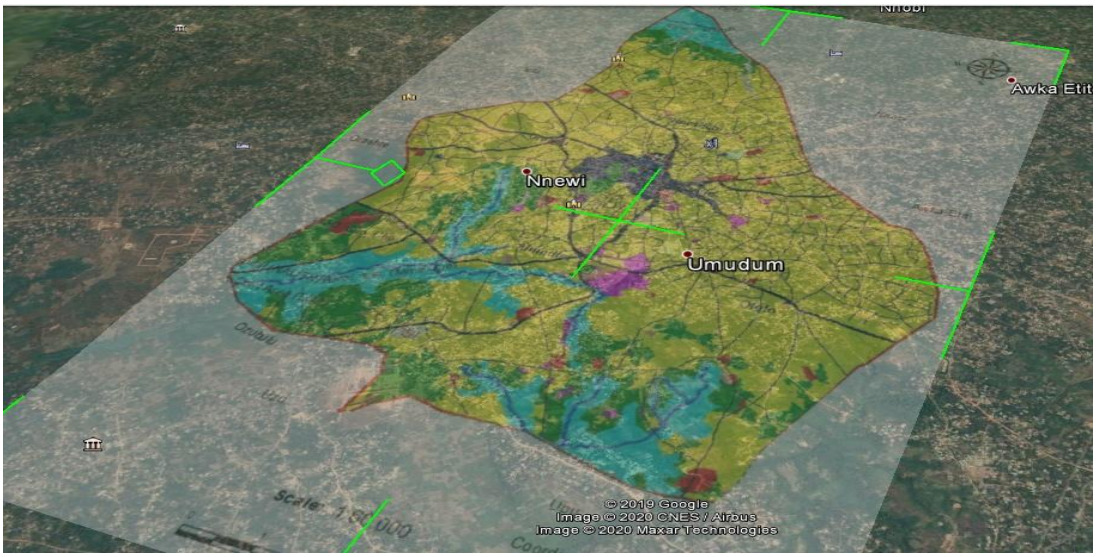

Plate 3.3 Map Overlay on Google Earth Pro

The transparency of the image was changed by sliding the tab to make the Google imagery visible beneath the overlay. The green diamond was then used to rotate the cross to reposition, and the handles to stretch the overlay until it matched the imagery beneath. When the adjustments were completed, the river tributary was digitized. The extraction of the region of interest was carried out by carefully delineating the water body from the high resolution satellite image using the polygon geometry tool.

The polygon feature depicting the boundaries of the major tributary of Ele River can be seen in Plate 3.4

Plate 3.4 Delineating the major tributary of Ele River

The polygon feature was then saved as a KML file and imported into AutoCAD Software where it was converted to .dwg format for import into Comsol Multiphysics. The 2D geometry of the tributary imported into Comsol is shown in Figure 3.10. The polygon feature was then saved as a KML file and imported into AutoCAD Software where it was converted to .dwg format for import into Comsol Multiphysics. The 2D geometry of the tributary imported into Comsol is show in Figure 3.6.

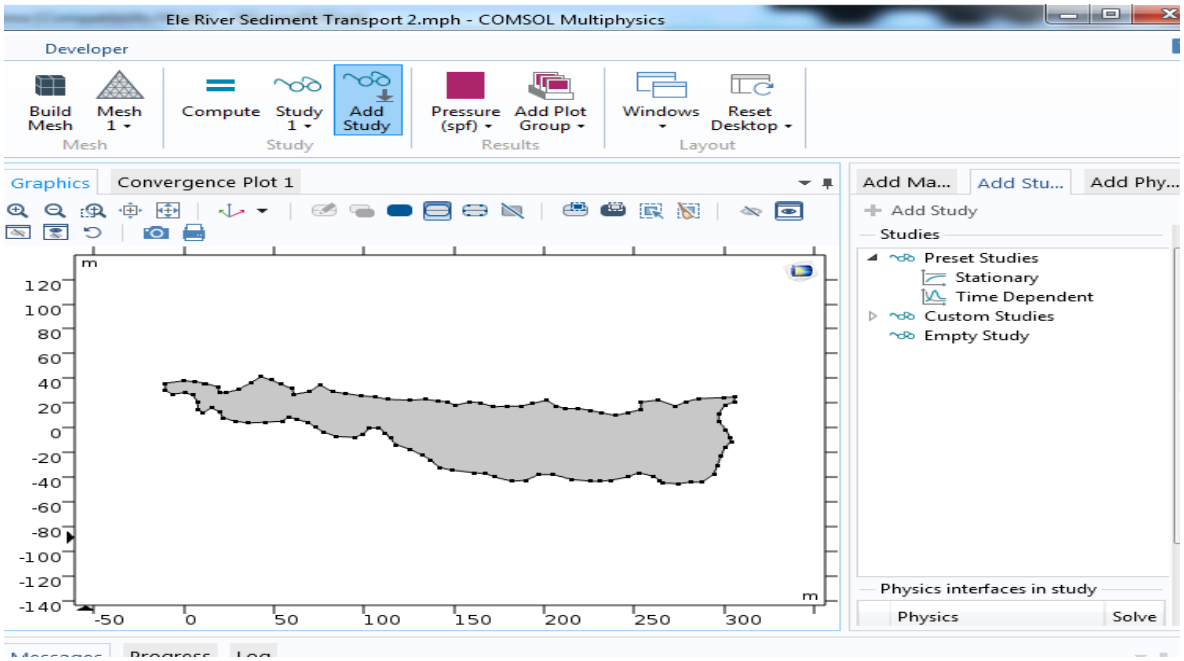

Fig. 3.6 2D geometry imported in Comsol

3.8.2 Selection of Module

The first step in selecting the appropriate module that describes the flow of water in the tributary and that models sediment transport is to evaluate the flow conditions (i.e. whether the flow is laminar or turbulent). To do that, Reynolds Number (Re) of the measured flow velocity was calculated using the following equation:

$$R_e = \frac{\rho V l}{\mu} \qquad 3.22$$

Where Re is Reynolds Number (Dimensionless); ρ is the density of water (kg/m3); V is the velocity of water (m/s); L is the characteristic of length (m) and μ is the dynamic viscosity of water.

Since the calculated Re number was greater than 2000, the flow was categorized as turbulent flow. Based on this result, the proper selection of physics module in Comsol Multiphysics was turbulent flow module. Subsequently, this module was coupled with the particle tracing module to model particle transmission. The particle tracing is used to compute the trajectory of particles in a fluid or electromagnetic field, including particle-particle, fluid-particle and

particle-field interactions. The movement is governed by either the Newtonian, Lagrangian, of Hamiltonian formulations from classical mechanics. User defined wall conditions may be specified. A wide range of predefined forces is available to describe specifically how the particle interacts with the fields. The powerful processing tools allow for sophisticated visualization of the computed particle trajectories. For each particle, an ordinary differential equation is solved for each component of the position vector.

The Navier-Stokes equations given below are the basis of flow dynamics in Comsol and are given as: (Comsol, 2017):

$$\frac{\rho}{\partial t} + \nabla.(\rho u) = 0 \qquad 3.23$$

$$\rho\frac{\partial u}{\partial t} + \rho(u.\nabla)u = \nabla.[-pI + \tau] + F \qquad 3.24$$

Where ρ is density; u is velocity; *p* is pressure; τ is viscous stress tensor and F is volume force vector

Equations 3.23 and 3.24 are conservation of mass and Equation 3.25 is conservation of momentum. For a Newtonian fluid, which has a linear relationship between stress and strain, the viscous stress tensor is given as:

$$\tau = 2\mu S - \frac{2}{3}\mu(\nabla.u)I \qquad 3.25$$

Where μ is the dynamic viscosity (Pa.s) and S is the strain-rate tensor given as:

$$S = \frac{1}{2}(\nabla u + (\nabla u)^T) \qquad 3.26$$

Thus, for a compressible flow the momentum equation becomes:

$$\rho\frac{\partial u}{\partial t} + \rho u.\nabla u = -\nabla p + \nabla.\left(\mu(\nabla u + (\nabla u)^T) - \frac{2}{3}\mu(\nabla.u)I\right) + F \qquad 3.27$$

When the temperature variations in the flow are small, a single-phase fluid can often be assumed incompressible; that is, ρ is constant or nearly constant. For constant ρ, the continuity equation (Equation 3.24) reduces to

$$\rho\nabla.(u) = 0 \qquad 3.28$$

and equation 6 becomes

$$\rho\frac{\partial u}{\partial t} + \rho(u.\nabla)u = \nabla.[-pI + \mu(\nabla u + (\nabla u)^T)] + F \qquad 3.29$$

For particle tracing, the default and most common formulation, the Newtonian formulation was employed. It defines a set of second-order ordinary differential equations for the components of the particle position based on Newton's second law of motion, given as:

$$\frac{du}{dt}\left(m_p\frac{dq}{dt}\right) = F \qquad 3.30$$

Where q is the particle position (m), m_p is the particle mass (kg), and F is the total force on the particles (N).

3.8.3 Initial and Boundary Conditions

Apart from the domain equations, proper boundary conditions were selected. For turbulent flow module, inflow velocities were specified at the inlet and outlet pressure was set as p= 0. Temperature values were also specified. While defining the boundary, no slip boundary conditions were set. For particle tracing module, the number of particles released was set at 3000. At the outlet, it was specified that the mass flow through the boundary was convective dominated ($-n.D_i\nabla c_i = 0$). This assumes that any mass flux due to diffusion across this boundary is zero. An insulation boundary condition was specified at the boundaries; thus no mass is transported across the boundaries. Beside inlet flow velocity and water temperature, turbulent flow module also requires water properties such as density and dynamic viscosity. These values

were generated for water in Comsol as default with values set at 1000 kg/m^3 and 0.001 Pa.s for density and dynamic viscosity respectively.

Meshing

The mesh partitions the model geometry into small units of simple shape or area. If the mesh is too coarse it will generate low element quality, which can cause large error in the simulation results. Conversely, if mesh is too fine the computational time for nonlinear system of equations will be longer. The physics controlled mesh sequence type was selected for this study, so as to allow Comsol select the appropriate mesh type for the specified flow condition, and the size of the element was selected to be normal.

3.8.4 Solving the Model

Once the modeling processes were completed, the simulation stage can be executed. The simulation process comprised of two stages, the first step of the simulation was the steady state determination of hydrodynamic components of flow, particularly velocity field (u) and pressure (p), using the turbulent flow interface. Determination of these components for the flow were necessary for the next step. The second stage was computing the time-dependent particle transmission using particle flow module. A simulation time of 2000s was maintained for all the scenarios to estimate the amount of particle transmitted from the inlet to the outlet. The simulations were performed on a desktop computer (Intel Core i7-2600 Processor @ 3.4GHz with 8.00GB RAM). The solution converged and produced particle positions at different times within the system.

CHAPTER FOUR

RESULTS AND DISCUSSION

4.1 Results

4.1.1 Surface Water Quality Modeling

This study employed the advanced techniques of feed-forward multilayer neural network to forecast water quality parameters of Ele River, Nnewi Anambra State. A total of ten (10) irrigation water quality parameters were selected which include; pH, Electrical Conductivity, Total Dissolved Solids, Calcium, Magnesium, Sodium, Bicarbonate, Sulphate, Nitrate-Nitrogen and Ammonium-Nitrogen. The water samples were collected for four years (4) years (May 2015 to April 2019) in ten (10) sampling points. The distance from one point to another was 10m apart. The methodology of the ANN model development and its declaration has been discussed in Chapter three.

The results are presented and discussed in four categories or sections namely; the descriptive statistics of the water quality parametric test results, time descriptive graph of the water quality parametric test results, feed-forward multilayer neural network model results, feed-forward multilayer neural network model performance evaluation results ,river water quality assessment for irrigation purposes and analysis of Variance Comparing the Level of Significance at the Sampling Points respectively.

4.1.2 The Descriptive Statistics of the Water Quality Parametric Test Results

This quantitatively describes and summarized the dataset statistically for mean, median, minimum (Min.), maximum (Max) and standard deviation, respectively.

The descriptive statistical mean values of pH which ranges from 6.34 of point 1 to 6.29 of point 10 were within the FAO permissible range (6.0-8.5). TDS showed very high

concentrations from points 1-3 above the permissible range (0-2000me/l) but decreased into the permissible range from point 4 going downstream till the 10^{th} sampling point. The increase from points 1-3 was as a result of increase of pollutants, dissolved solids, ions and inorganic salts which were too high from the discharge points to point 3 and later decreased down to the last point due to ion dissolution and dilution as it travels through the water body downstream.

Electrical conductivity increases alongside with TDS due to the presence of dissolved salts and inorganic substances which are good electrical conductors. The statistical mean values decreases from 4.24 of sampling point 1 to 1.47 of point 10. Bicarbonate mean values were all within the permissible range of 0-10me/l. This reflected in the pH values since increase or decrease in bicarbonates will have a resultant effect on the soil and water pH. The values ranges are 4.39 of point 1 to 4.35 of point 10.The mean values of Mg and Ca were within the permissible range of 0-5me/l and 0-20me/l respectively.

Sodium ion indicated a very high increase above the permissible standard which could be as a result of accumulation of sodium salts from the effluent discharges over time. The resultant effect of this causes weakening of the soil structure when its irrigation water is used for crop production which must also affect the hydraulic conductivity of water in the soil. Nitrate Nitrogen mean values were within the FAO permissible standard. The sulfate values overtime were above the permissible range of 0-20me/l. This could be as a result of the pollutant effects from effluent discharge and decayed leaves from the surrounding trees around the water body. Ammonium nitrogen values were all within the permissible standard.

Generally, just like the mean values, the total dissolved solids had the highest standard deviation value at point one (1) while magnesium had the lowest mean values at point nine (9). Hence, the very low statistical standard deviation results recorded in this study showed that the statistical data set were very close to the mean of the dataset (Wikipedia, 2020).

The descriptive statistics of the observed water quality parameters at each point are shown from Tables 4.1 to 4.10.

Table 4.1: **TIME SERIES DESCRIPTIVE STATISTICS AT POINT 1**

PARAMETERS	PH	TDS	EC	$HCO^{3—}$ Bicarbonate	Mg^{2+}- magnesium ion	Ca^{2+}- Calcium ion	Na^{+}- Sodium ion	NO_3- N	Sulphate – SO_4	NH_4-N
Mean	6.34	2458.19	4.24	4.39	1.80	8.65	39.13	3.58	93.90	2.77
Median	6.36	2439.50	4.01	4.43	1.84	8.58	37.00	2.83	95.35	2.85
Max	6.48	2742.00	5.82	4.84	1.89	9.88	64.50	6.41	97.48	3.99
Min	6.09	2199.00	3.18	3.01	1.33	7.22	24.50	2.41	87.31	1.77
Stadev	0.08	127.36	0.83	0.40	0.11	0.62	9.94	1.19	2.50	0.48

Table 4.2: TIME SERIES DESCRIPTIVE STATISTICS AT POINT 2

PARAMETERS	PH	TDS	EC	HCO^{3-} Bicarbonate	Mg^{2+}- magnesium ion	Ca^{2+}- Calcium ion	Na^{+}- Sodium ion	NO_3- N	Sulphate – SO_4	NH_4-N
Mean	6.29	2265.40	3.54	4.43	1.73	8.45	41.18	4.22	89.01	2.64
Median	6.31	2241.00	3.25	4.35	1.74	8.45	35.44	3.71	87.32	2.53
Max	6.49	2523.00	4.85	4.86	1.94	9.99	77.31	6.52	96.21	3.92
Min	6.01	2044.00	3.01	4.01	1.51	7.35	21.21	3.21	80.22	1.61
Stadev	0.13	117.07	0.49	0.24	0.10	0.60	14.06	1.17	3.84	0.43

Table 4.3: TIME SERIES DESCRIPTIVE STATISTICS AT POINT 3

PARAMETERS	PH	TDS	EC	HCO^{3--} Bicarbonate	Mg^{2+}- magnesium ion	Ca^{2+}- Calcium ion	Na^{+}- Sodium ion	NO_3- N	Sulphate – SO_4	NH_4-N
Mean	6.33	2132.88	3.35	4.23	1.74	8.86	48.01	4.62	92.51	2.37
Median	6.37	2104.00	3.25	4.15	1.74	8.86	40.95	4.51	94.12	2.22
Max	6.48	2404.00	3.84	4.74	1.96	9.74	88.45	6.41	96.10	3.99
Min	6.00	1883.00	3.01	3.12	1.52	7.94	29.24	3.51	86.31	1.22
Stadev	0.10	114.47	0.23	0.31	0.10	0.49	14.14	0.67	3.09	0.55

Table 4.4: TIME SERIES DESCRIPTIVE STATISTICS AT POINT 4

PARAMETERS	PH	TDS	EC	HCO^{3--} Bicarbonate	Mg^{2+}- magnesium ion	Ca^{2+}- Calcium ion	Na^{+}- Sodium ion	NO_3- N	Sulphate – SO4	NH_4-N
Mean	6.34	1956.21	2.89	4.36	1.80	9.28	51.06	4.16	94.60	2.46
Median	6.39	2010.00	3.14	4.52	1.83	9.28	50.25	4.00	92.16	2.21
Max	6.64	2286.00	3.78	4.74	1.96	9.87	71.24	6.41	170.80	3.98
Min	6.09	1367.00	2.01	3.61	1.42	7.86	40.24	2.01	86.31	1.99
Stadev	0.16	213.04	31.49	0.30	0.10	0.46	8.16	1.13	12.79	0.48

Table 4.5: TIME SERIES DESCRIPTIVE STATISTICS AT POINT 5

PARAMETERS	PH	TDS	EC	HCO_3^-- Bicarbonate	Mg^{2+}- magnesium	Ca^{2+}- Calcium ion	Na^{+}- Sodium ion	NO_3- N	Sulphate – SO4	NH_4-N
Mean	6.37	1678.15	2.55	4.39	1.76	8.83	45.49	4.81	90.90	2.72
Median	6.39	1616.50	2.31	4.52	1.79	8.83	43.38	5.01	89.13	2.90
Max	6.69	2154.00	3.41	4.62	1.91	9.80	70.24	6.41	175.35	3.99
Min	6.09	1064.00	2.01	3.52	1.43	8.01	30.21	4.00	80.10	1.62
Stadev	0.15	336.42	0.48	0.26	0.11	0.48	10.72	0.55	14.15	0.55

Table 4.6: TIME SERIES DESCRIPTIVE STATISTICS AT POINT 6

PARAMETERS	PH	TDS	EC	HCO_3^{-} Bicarbonate	Mg^{2+}- magnesium ion	Ca^{2+}- Calcium ion	Na^{+}- Sodium ion	NO_3- N	Sulphate – SO_4	NH_4-N
Mean	6.28	1293.94	2.22	4.30	1.77	9.20	51.55	4.56	93.88	2.89
Median	6.29	1269.00	2.12	4.32	1.81	9.22	51.21	4.25	94.21	3.02
Max	6.68	2014.00	3.12	4.74	1.95	9.99	75.21	6.42	160.21	3.62
Min	6.08	922.00	1.72	3.47	1.50	8.21	34.45	3.17	84.21	2.12
Stadev	0.14	322.46	0.36	0.23	0.14	0.45	8.26	0.79	11.79	0.41

Table 4.7: TIME SERIES DESCRIPTIVE STATISTICS AT POINT 7

PARAMETERS	PH	TDS	EC	HCO^{3-} Bicarbonate	Mg^{2+}- magnesium ion	Ca^{2+}- Calcium ion	Na^{+}- Sodium ion	NO_3- N	Sulphate – SO4	NH_4-N
Mean	6.36	963.23	1.88	4.32	1.78	9.08	50.28	4.46	93.30	2.40
Median	6.36	915.00	1.81	4.24	1.81	9.15	49.68	4.09	94.22	2.41
Max	6.79	1484.00	2.31	4.74	1.88	9.85	70.98	6.41	98.21	3.98
Min	6.08	602.00	1.12	4.01	1.54	8.05	37.98	3.09	87.31	1.06
Stadev	0.15	196.20	0.25	0.24	0.08	0.46	8.55	0.84	2.65	0.62

Table 4.8: TIME SERIES DESCRIPTIVE STATISTICS AT POINT 8

PARAMETERS	PH	TDS	EC	HCO^{3-} Bicarbonate	Mg^{2+}- magnesium ion	Ca^{2+}- Calcium ion	Na^{+}- Sodium ion	NO_3- N	Sulphate – SO_4	NH_4-N
Mean	6.28	718.98	1.55	4.28	1.77	9.38	53.77	4.72	87.86	2.59
Median	6.27	746.00	1.55	4.22	1.75	9.59	52.29	4.58	87.31	2.65
Max	6.80	940.00	2.00	4.94	1.95	9.99	72.21	6.64	97.31	3.92
Min	6.04	429.00	1.10	4.02	1.60	7.09	37.21	3.01	80.21	1.64
Stadev	0.16	119.05	0.26	0.23	0.08	0.63	7.45	0.88	5.06	0.46

Table 4.9: TIME SERIES DESCRIPTIVE STATISTICS AT POINT 9

PARAMETERS	PH	TDS	EC	$HCO3^{-}$ Bicarbonate	Mg^{2+}- magnesium ion	Ca^{2+}- Calcium ion	Na^{+}- Sodium ion	NO_3- N	Sulphate – SO4	NH_4-N
Mean	6.29	494.71	1.47	4.35	1.82	9.15	51.55	4.25	91.28	2.59
Median	6.27	499.00	1.46	4.43	1.82	9.25	50.24	3.98	87.19	2.61
Max	6.87	657.00	1.66	4.80	1.96	9.98	84.45	6.41	170.80	3.99
Min	6.07	376.00	1.21	4.01	1.67	8.02	27.99	3.38	82.22	1.61
Stadev	0.16	66.56	0.10	0.20	0.06	0.52	10.70	0.87	13.53	0.54

Table 4.10: TIME SERIES DESCRIPTIVE STATISTICS AT POINT 10

PARAMETERS	PH	TDS	EC	HCO^{3-}- Bicarbonate	Mg^{2+}- magnesium ion	Ca^{2+}- Calcium ion	Na^{+}- Sodium ion	NO_3- N	Sulphate – SO_4	NH_4-N
Mean	6.341	357.98	1.356	4.51	1.788	9.07	50.41	4.575	90.71	2.836
Median	6.35	357	1.355	4.56	1.75	9.1	50.35	4.145	91.31	2.941
Max	6.95	461	1.46	4.96	1.999	9.74	79.5	6.21	95.45	3.991
Min	6.09	254	1.23	4	1.458	7.62	30.14	3.025	82.32	1.522
Stadev	0.175	49.312	0.0568	0.294	0.115	0.57	11.49	0.929	3.994	0.556

4.1.3 Time Descriptive Graph of Water Quality Parametric Test Results

The time descriptive graph shows the trend of all the water quality parameters from point 1 to point 10 over the time under review. The descriptive graph enables researchers to see and make decisions on some dataset deviations that cannot be seen mathematically but graphically it will be shown. The dataset results for the water quality analysis of Ele River were further subjected to descriptive graph analysis to observe its trend over time under review as shown in the appendix from figures 4.1 to 4.10.

Generally, the water quality parameters evaluated over the period under review as presented in figures 4.1 to 4.10 shows a continuous variation of the parameters, although, there were indications of seasonal patterns of the parameters over the years under review.

Figure 4.1 indicates that at point 10, pH recorded the highest value in March 2019 followed by point 8 in September 2015 due to increase in bicarbonate. The lowest values of pH occurred at point 3 in September, 2015. Irrespective of the year, the highest occurrence of pH was between September to March and this period marks the beginning and end of dry season in the study area due to increase in the pollutant effect, high temperature and low turbidity during dry season which affects the water pH. Perhaps, seasonal changes could have played a role in the pH values in Ele River in Anambra State.

In Figure 4.2 and 4.3, electrical conductivity and total dissolved solids' values were high and low at most instances of which the higher concentrations occurred at the points of entry or upstream and subsides going downstream; this might be as a result of high inorganic substances at the entry points which fades away gradually along the River

downstream. Therefore, whatever be the human activities in the watershed during the dry season would have gone down into Ele River as runoff thereby causing the electrical and total dissolved solid to vary from the normal distribution of the parameters.

Figures 4.4 shows that point 1 had the lowest HCO_3^- values in October 2015, whereas in fig. 1 from the appendix, point 1, 2 and 7 recorded the lowest Mg content in November 2017, March 2017 and 2019 while point 10 had the highest Mg content in April 2019. The non-seasonal pattern representation of the HCO_3 and Mg could have been caused by the geological formation of study area.

Figure 2 from the appendix shows that there was constant distinct parametric rise of Na in December 2015, June 2016, March 2017, September 2017 and February 2019 respectively while point 9 has the lowest values of sodium from April 2017 to March 2019. Also, NO_3-N as shown in Figure 3 from the appendix shows that point 4 has the lowest values of NO_3-N in August 2015 and alternate up and down pattern with time, hence, point 1 shows lowest values of NO_3-N in May 2016 and from May 2017 to March 2019. Likewise, points 4, 7 and 8 shows the highest values of NO_3-N in August 2017, January 2018 and January 2019, respectively.

Figure 4 from the appendix, shows increased distribution of NH_4-N over time whereas many points recorded highest values of NH_4-N at different times. It was however recorded that point 7 had the lowest values of NH_4-N in July 2015, October 2016, and 2017 respectively.

Figure 5 from the appendix recorded an alternate rise and fall of SO_4 descriptive graph pattern between September to March especially at point 1 and point 8. In the study area,

the period September to March were noted to be peak of dry season, therefore, the alternate rise and fall in pattern of the parameter could be a function of high anthropogenic activities in Ele River during off rainy season.

Figure 6 from the appendix revealed that points 1, 8 and 9 had the lowest values of Ca in September 2015, November 2015 and January 2016 but point 2 shows a continues lower values of Ca from February 2018 to March 2019 while point 8 equally shows a continues higher values of Ca from May 2017 to March 2019.

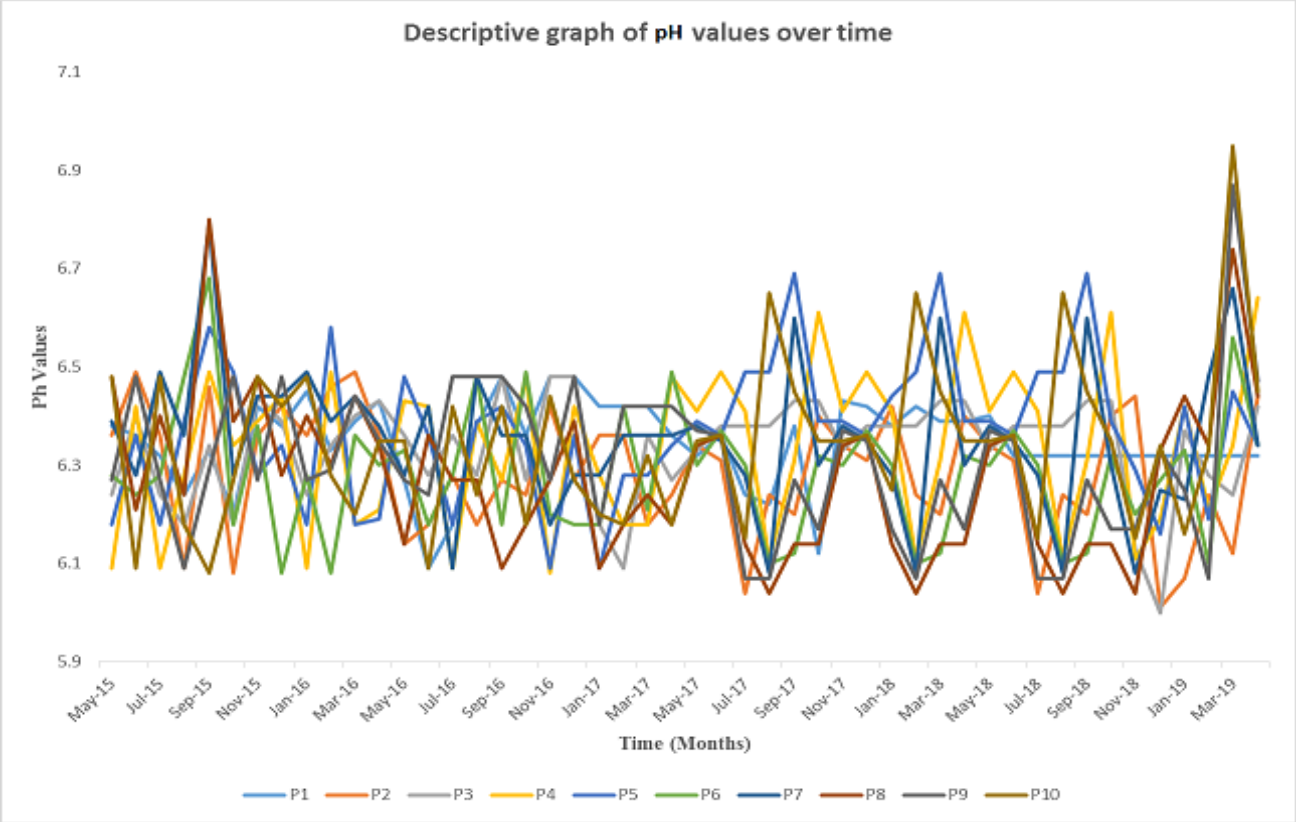

Figure 4.1: Descriptive graph of pH values over time

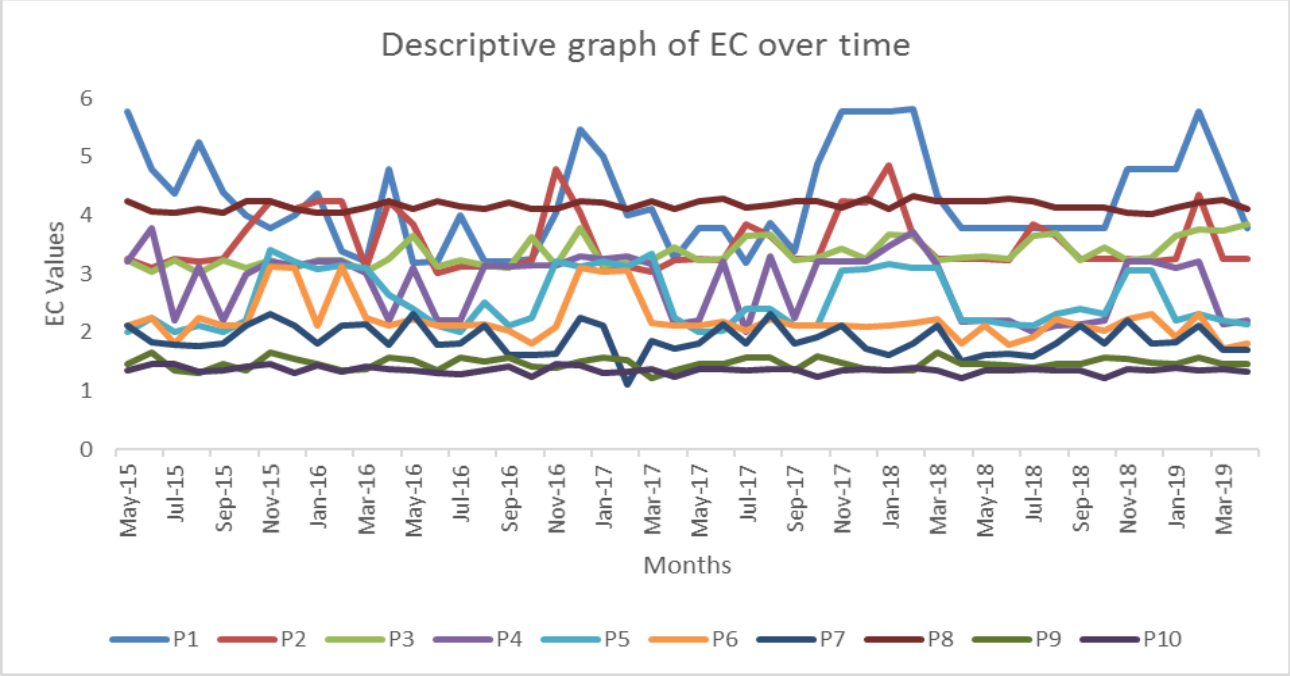

Figure 4.2: Descriptive graph of EC values over time

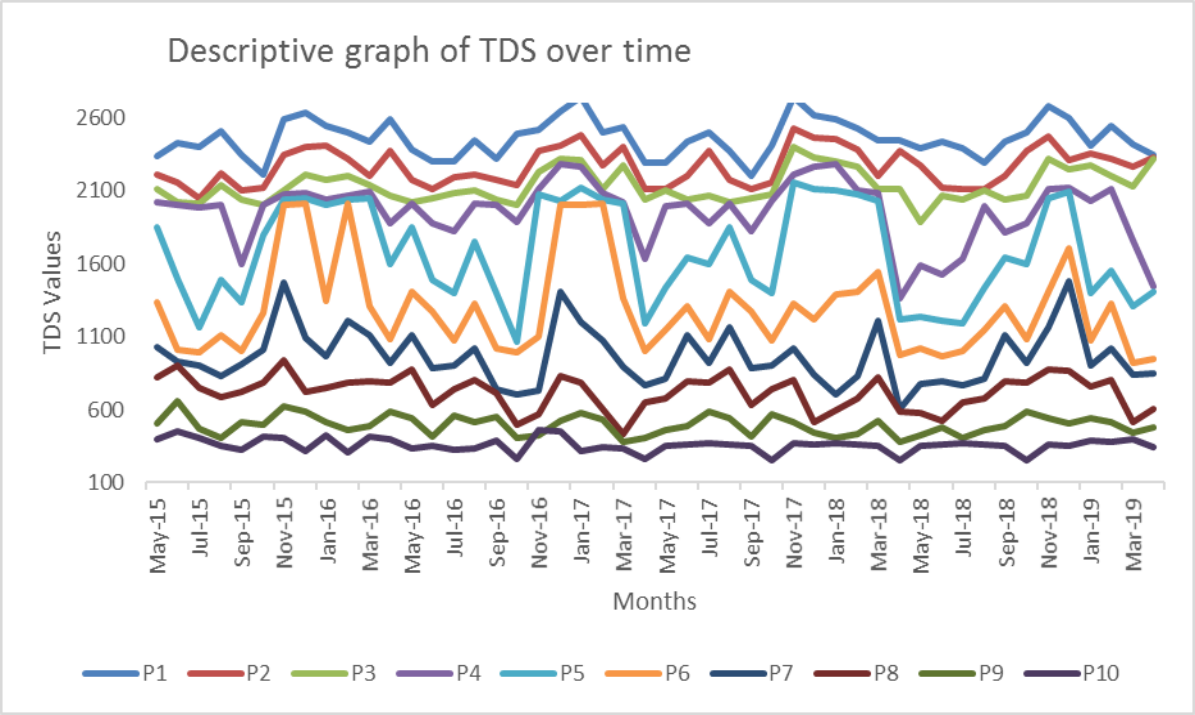

Figure 4.3: Descriptive graph of TDS values over time

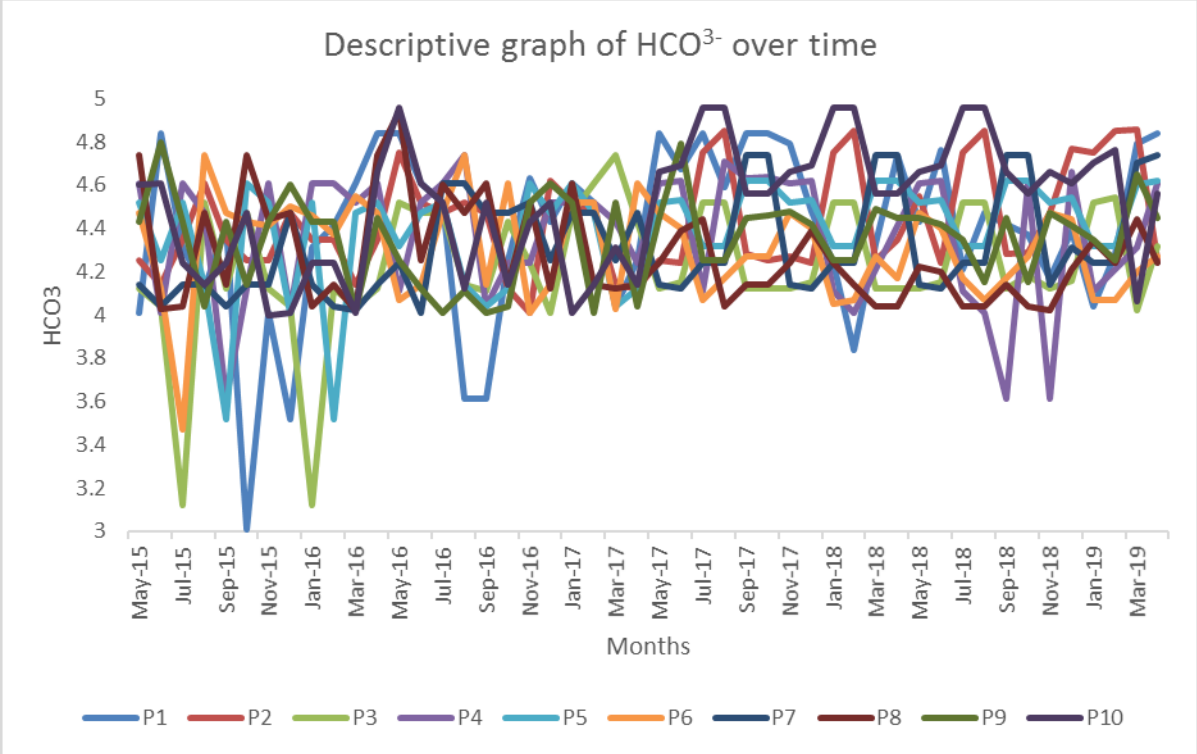

Figure 4.4: Descriptive graph of HCO^{3-} values over time

4.1.4 Feed-forward Multilayer Neural Network (FFMNN) Model Results

As discussed in chapter three, the artificial neural network architecture adopted in this study is the feed-forward multilayer neural network model. The FFMNN is used to model the water quality parameters dataset. The developed model was tested and found satisfactory before forecasting for the next one year. The ANN model descriptive scattered graphs, the actual and model graphs of the developed model, and forecast graphs for the next one year are shown in Figures 4.11 to 4.110. The Artificial neural network results are presented on point by point basis, from point 1 to point 10. At point 1, the descriptive scattered graphs, the actual and model graphs of the developed ANN model, and the forecast graphs for the next one year are shown in the Figures 4.11 to 4.110.

At point 1, it was generally observed that the ANN asymptotically modeled the water quality dataset (actual) very well as the scattered plot points were very close to the line of best fit. Comparing the ANN model with the actual, the deviations were not significant. The forecast for all the parameters at point 1 showed continuous change of the values over time of forecast.

However, the pH forecast witnessed a decrease in the 3rd month and subsequently increased at the 9th month as shown in Figure 4.11. This decrease could be as a result of variable dilution of dissolved salts at the peak of rainy season being July. Both the pH model and forecast were within the permissible range for irrigation water quality. The descriptive forecast graph of TDS increases sharply to the 6th month before decreasing to the lowest forecast value at the 2nd month as shown in Figure 4.12.This increase could be

as a result of the pollutant effects and low turbidity at the 9th month of forecast which falls within dry season.

TDS model and forecast all exceeded the FAO permissible range (0 – 2000mg/l). It was further observed that the forecast descriptive graph of the electrical conductivity shows an up and downward pattern of forecast. This is an indication that the ANN model was noisy in the time of this forecast. However, in the forecast, it went highest at the 12th month and goes lowest at 8th[th] month as shown in Figure 4.13. Both the EC model and forecast exceeded the permissible range which is always normal whenever the TDS is very high. However, the forecast shows high concentration of inorganic substances at the rainy and dry seasons of forecast thereby exceeding the permissible standard. The sharp increase at the 6th month of forecast could be as a result of low rainfall.

Figure 4.14 shows that the HCO_3^- forecast pattern had a sharp rise till the 7th month and lowest at the 12th month. The forecast and model were within the permissible range (0 – 10 me/l). Likewise, the Mg forecast pattern significantly decreased mathematically with time and later rises to the 9th month as shown in figure 4.15. Figures 4.16 and 4.17 show the forecast descriptive graph of Ca and Na, respectively. HCO_3^- , Ca, Na model and forecast were all within the permissible range. The sinusoidal movements at some points during the forecast could be as a result of fluid dynamics in the water body. The forecast pattern shows slight increase with time, especially the Na before decreasing at the 10th month. The forecast graph of NO_3-N at the beginning increased with time and subsequently decreases at the 6th months before increasing again as shown in Figure 4.18. Unlike others, the SO_4 and NH_4-N forecast decreased with time especially the NH_4-N before increasing again at the 10th months as shown in Figure 4.19 and 4.20. The high

concentration of SO_4 and NH_4-N occurred in the dry season due to pollution increase as a result of low dissolution of ions in water and rainfall effect. From the graphical representations, the forecast and model for Mg, Ca, NO_3-N, NH_4-N were within the permissible range while sulfate exceeded the permissible standard and likely with Na at most instance in the model and from 7^{th} -12^{th} month in the forecast.

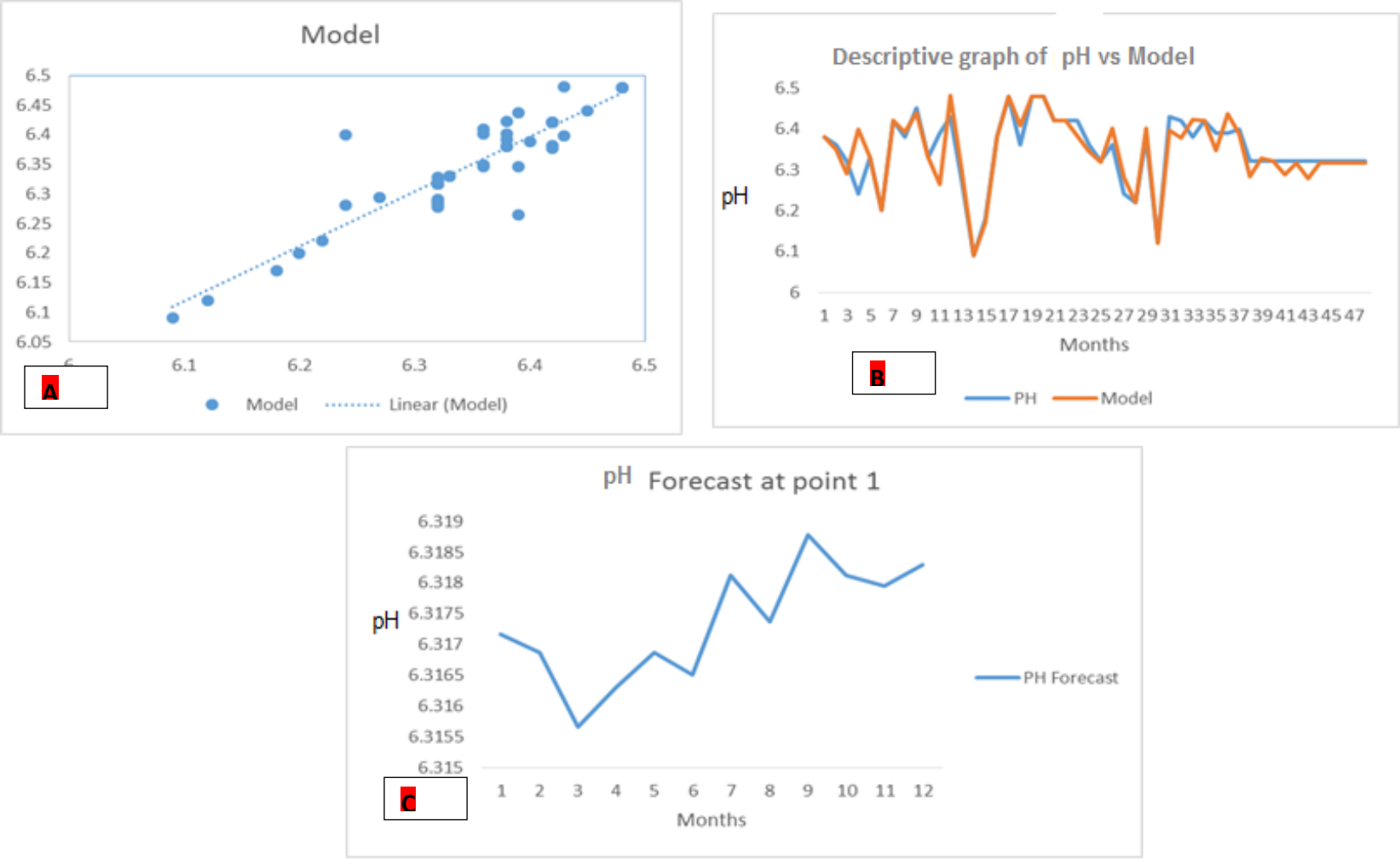

Figure 4.11 (A Band C): pH scatter, model and Forecast graph at point 1

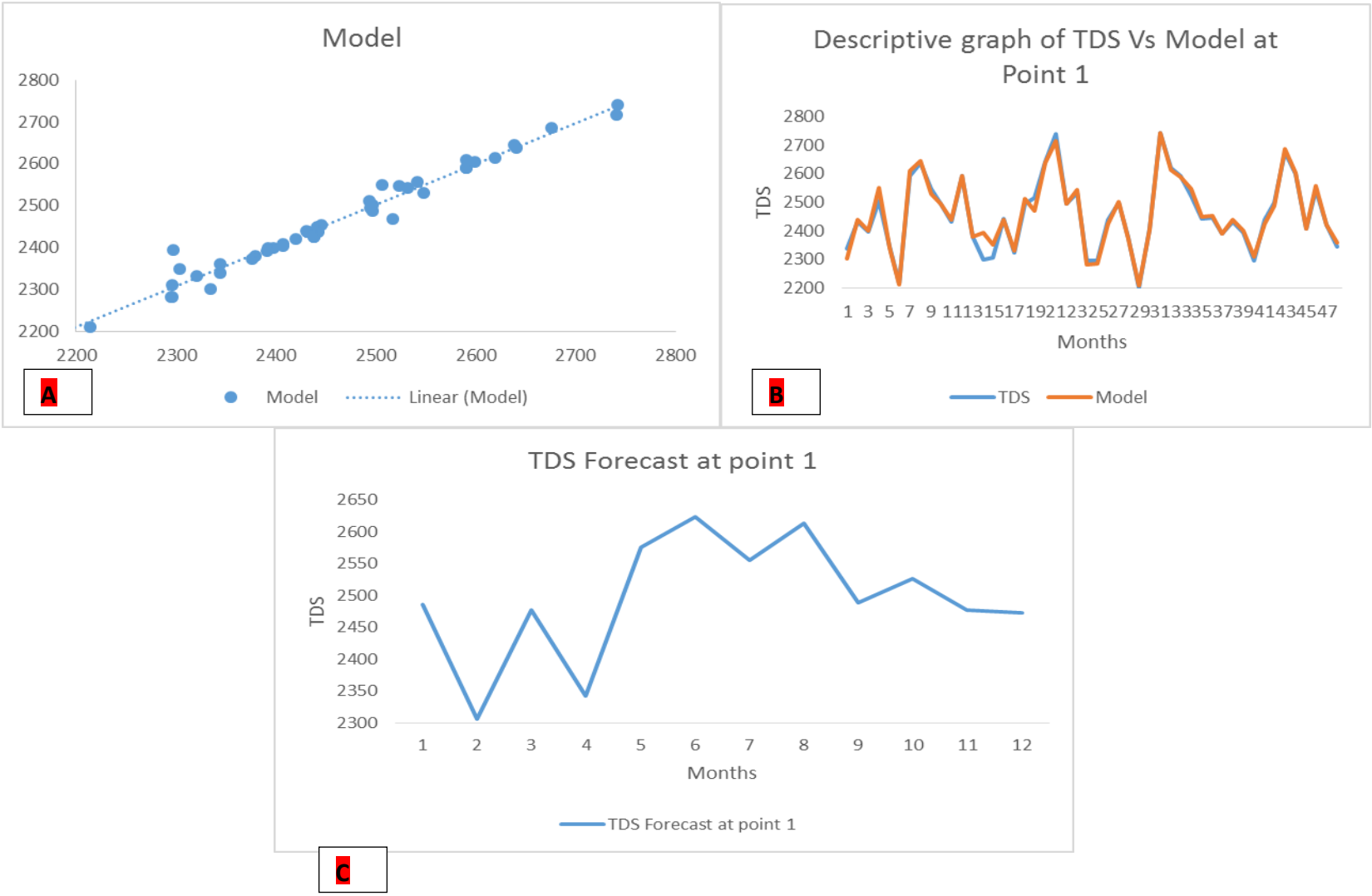

Figure 4.12 (A Band C): TDS scatter, model and Forecast graph at point 1

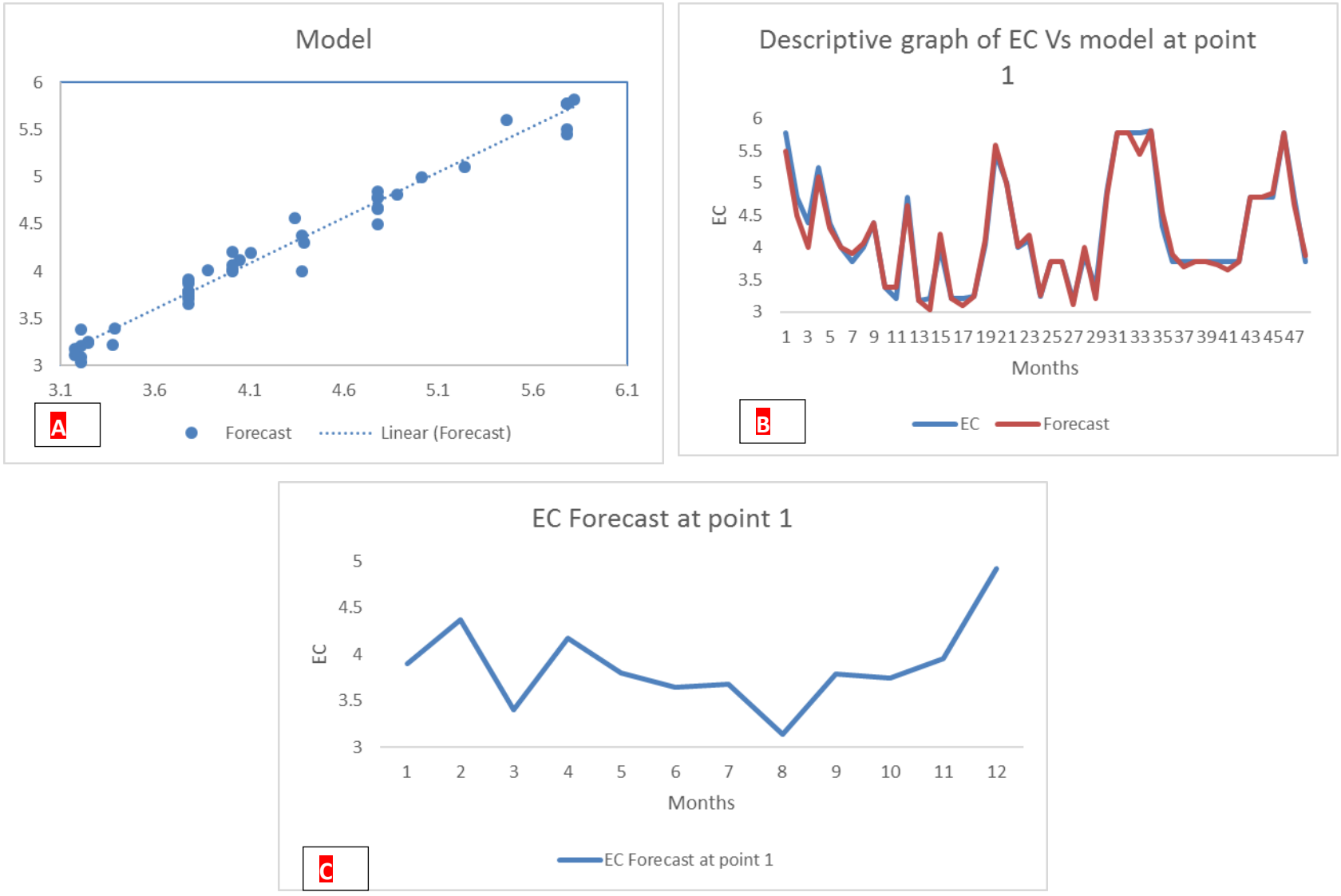

Figure 4.13 (A B and C): EC scatter, model and Forecast graph at point 1

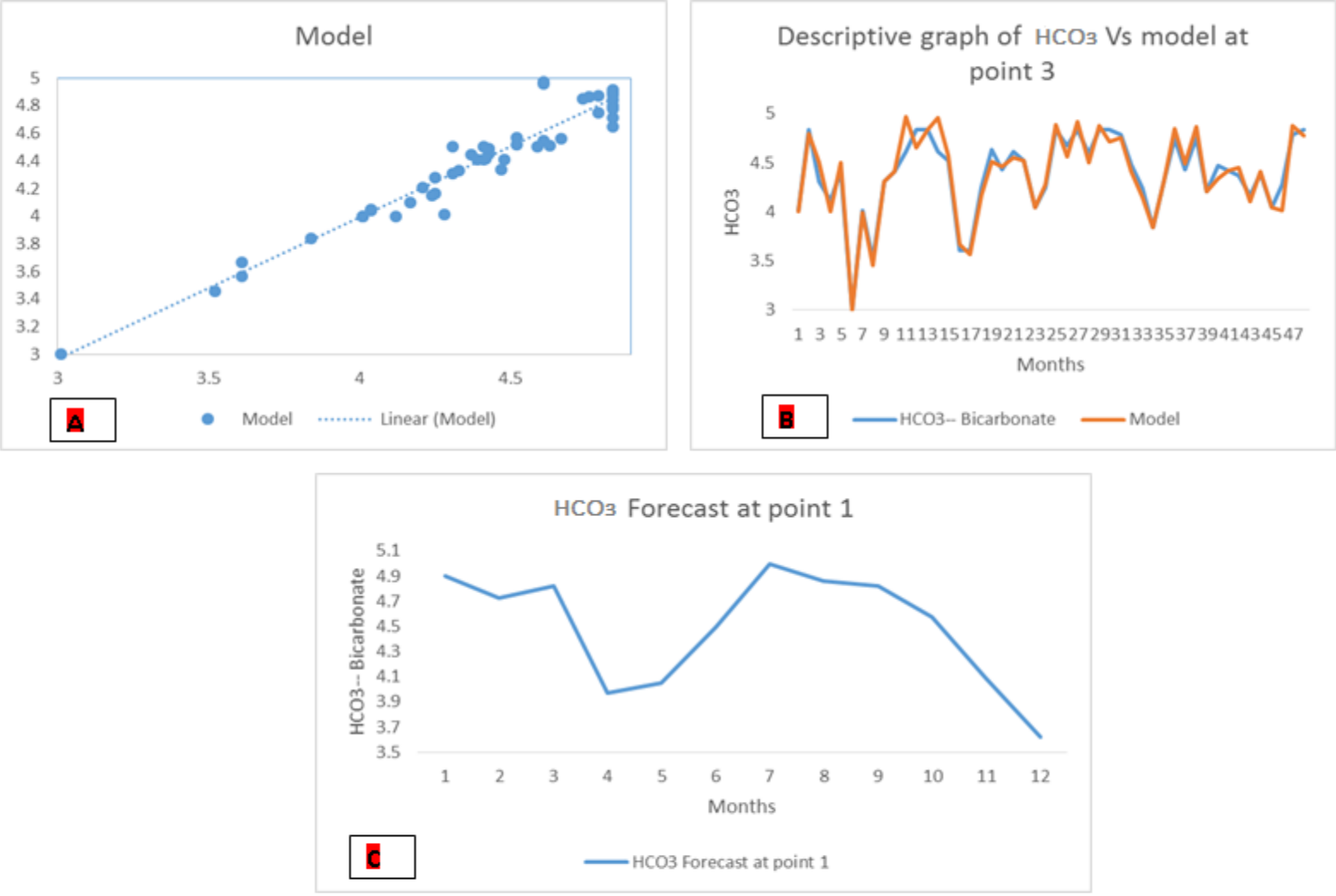

Figure 4.14 (A Band C): HCO_3 scatter, model and Forecast graph at point 1

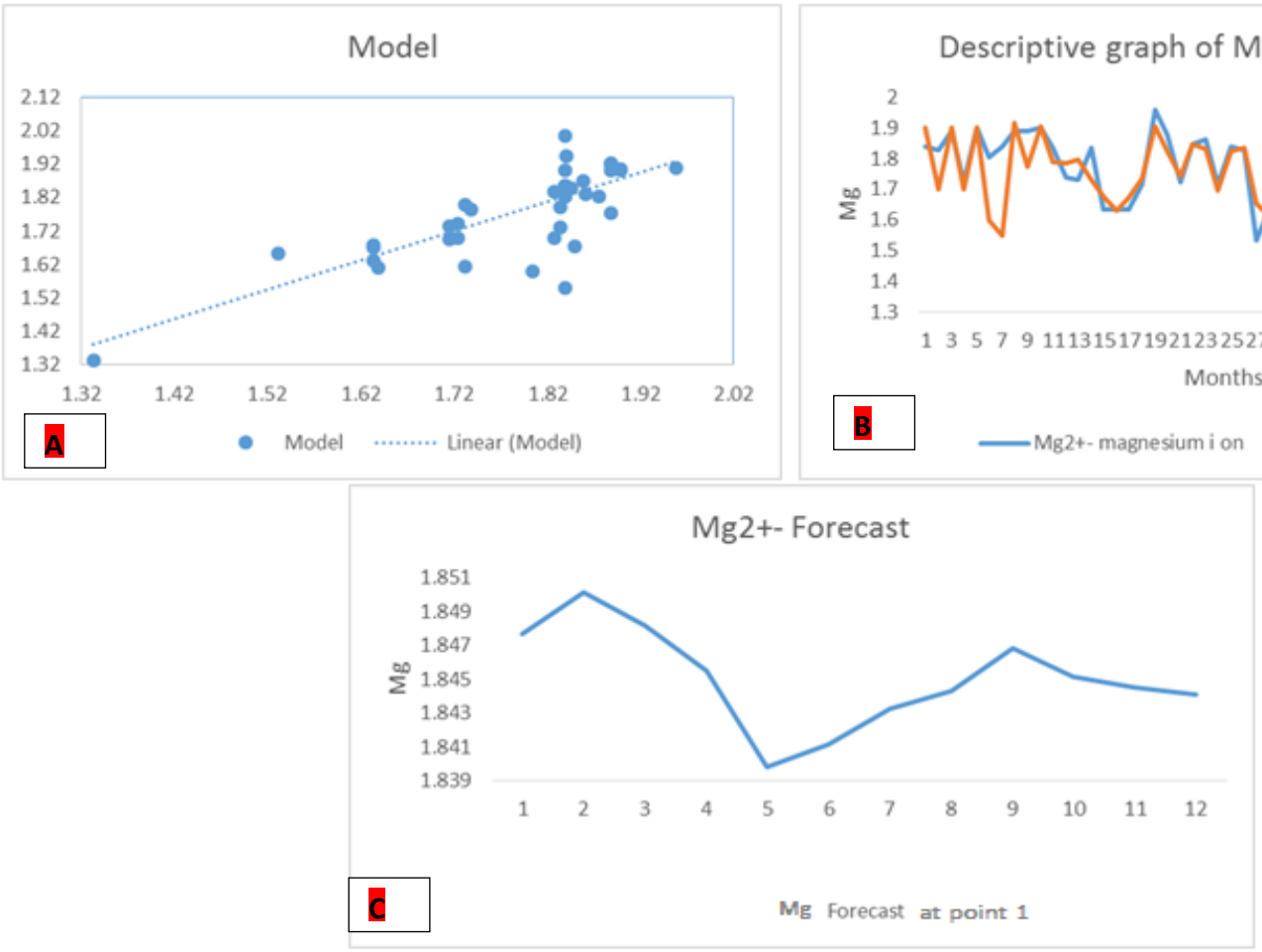

Figure 4.15 (A Band C): Mg scatter, model and Forecast graph at point 1

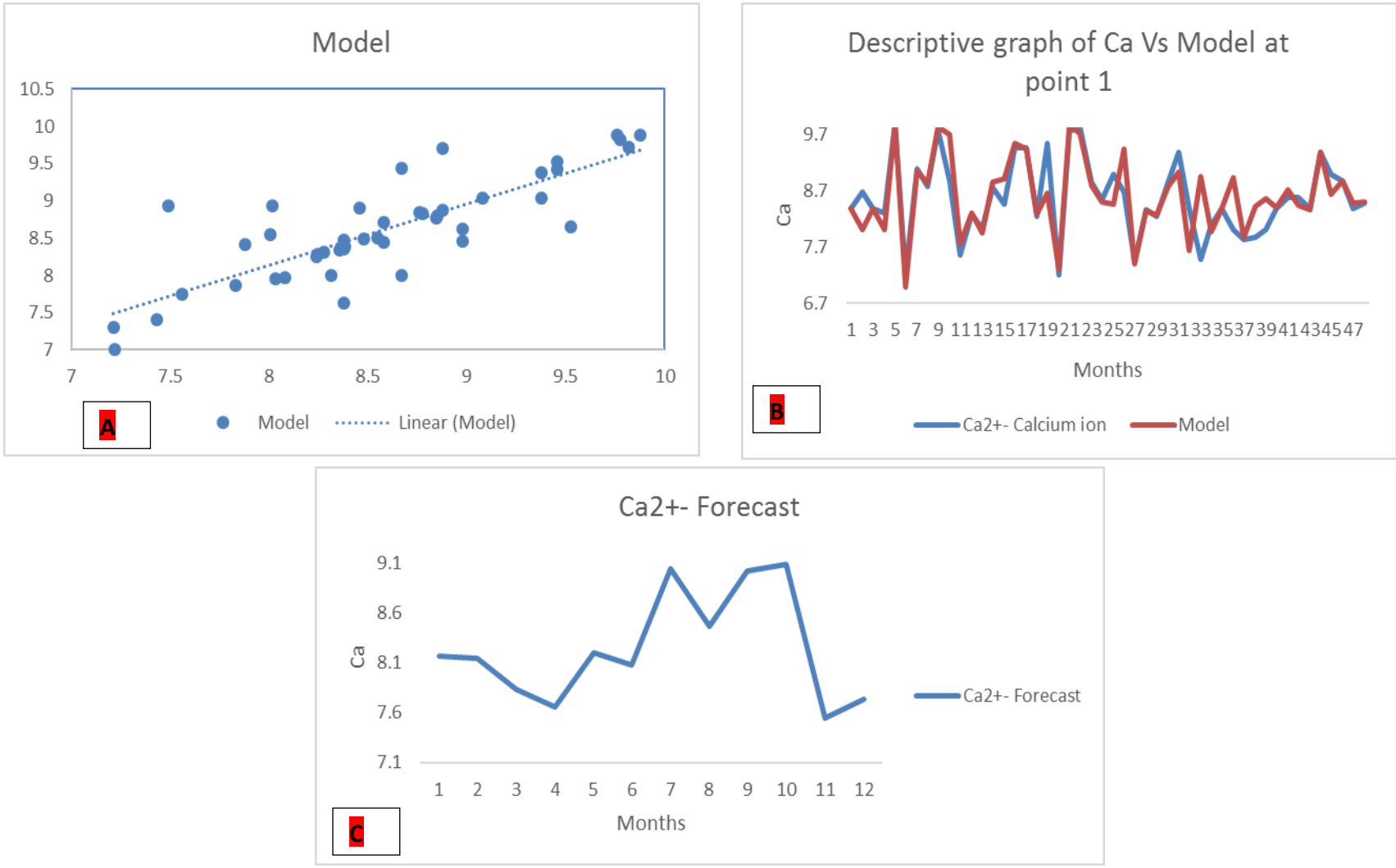

Figure 4.16 (A Band C): Ca scatter, model and Forecast graph at point 1

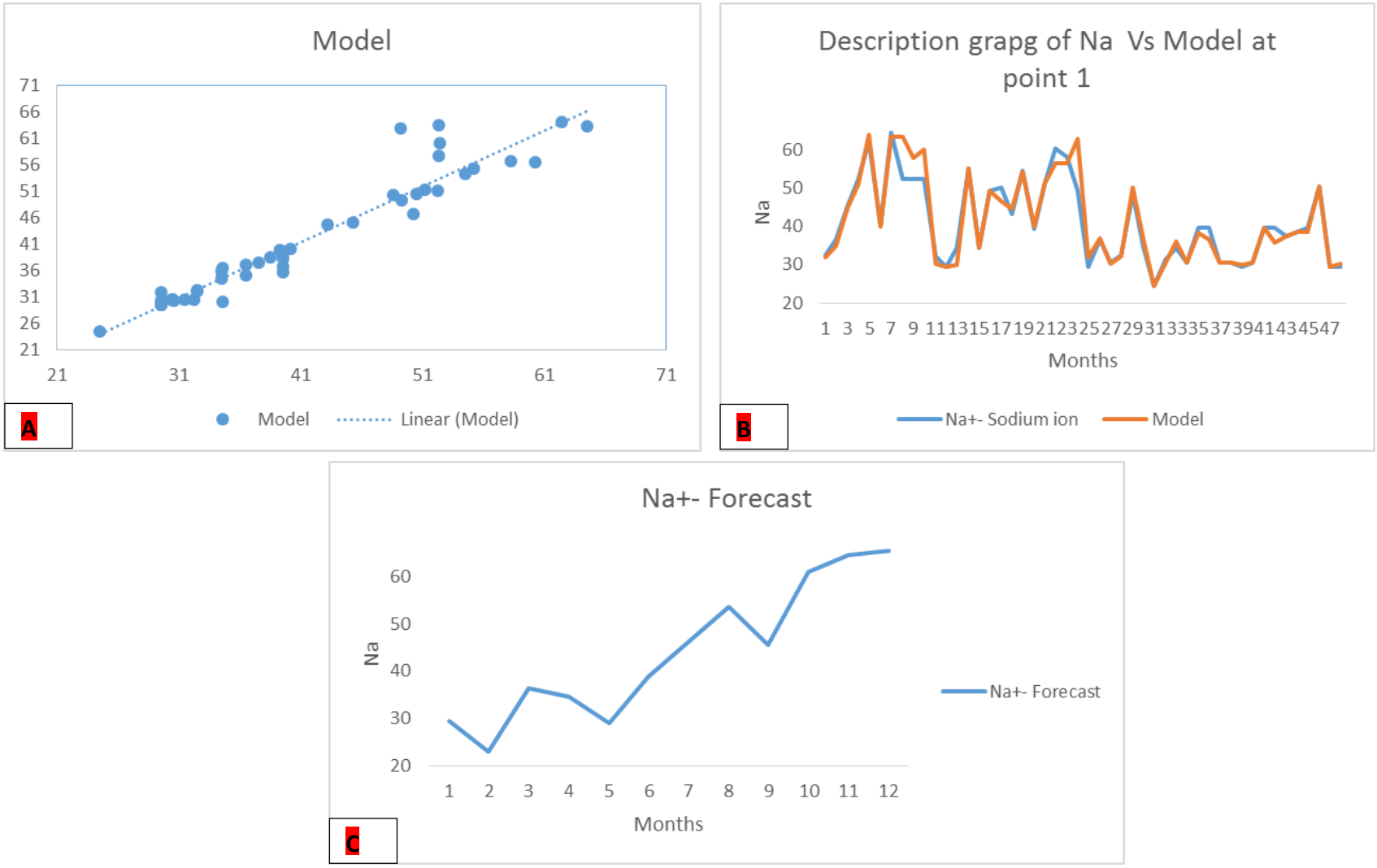

Figure 4.17 (A Band C): Na scatter, model and Forecast graph at point 1

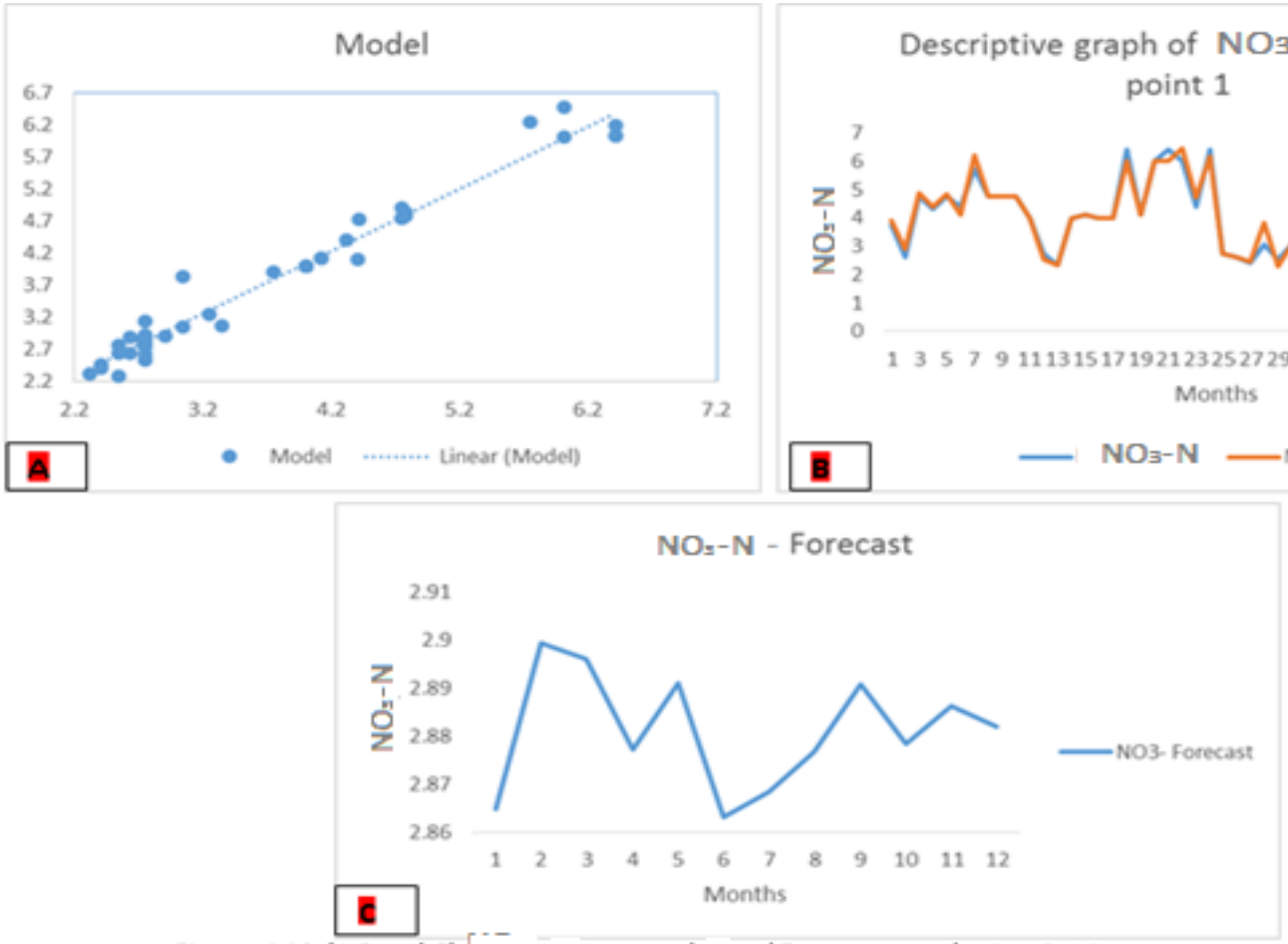

Figure 4.18 (A Band C) NO_3-N scatter, model and forecast graph at point 1

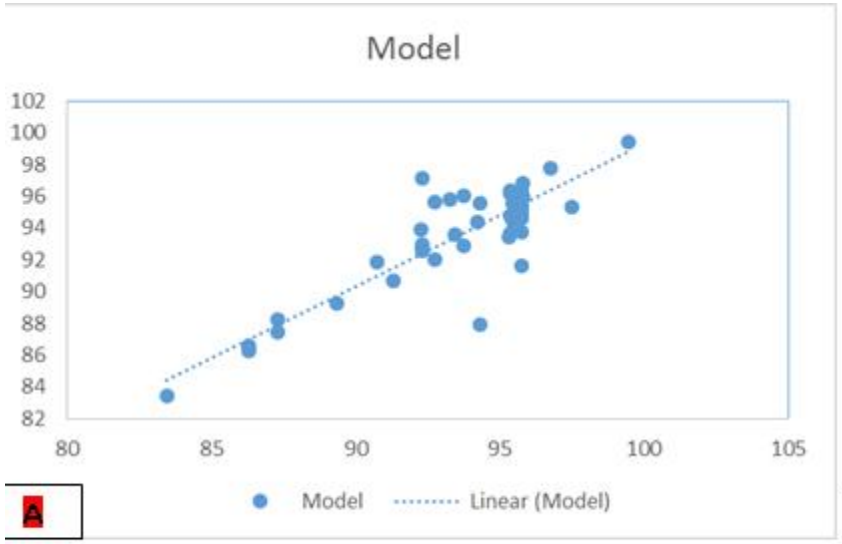

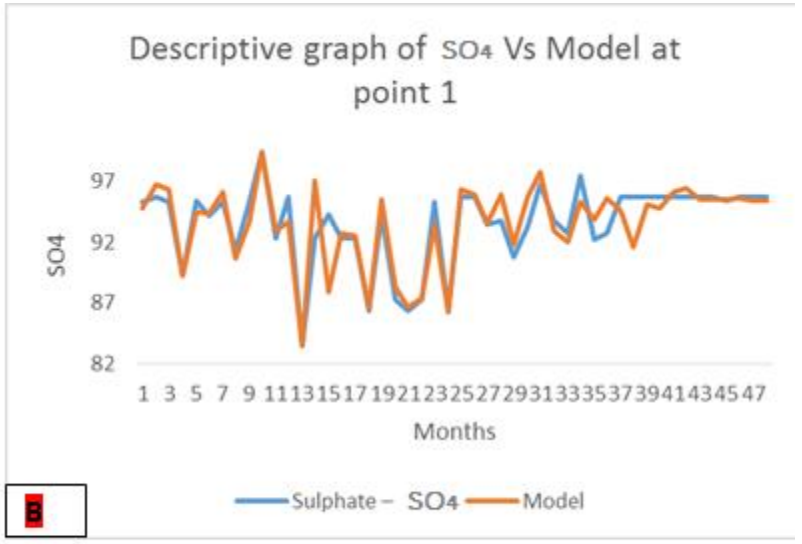

Figure 4.19 (A Band C): SO_4 scatter, model and Forecast graph at point 1

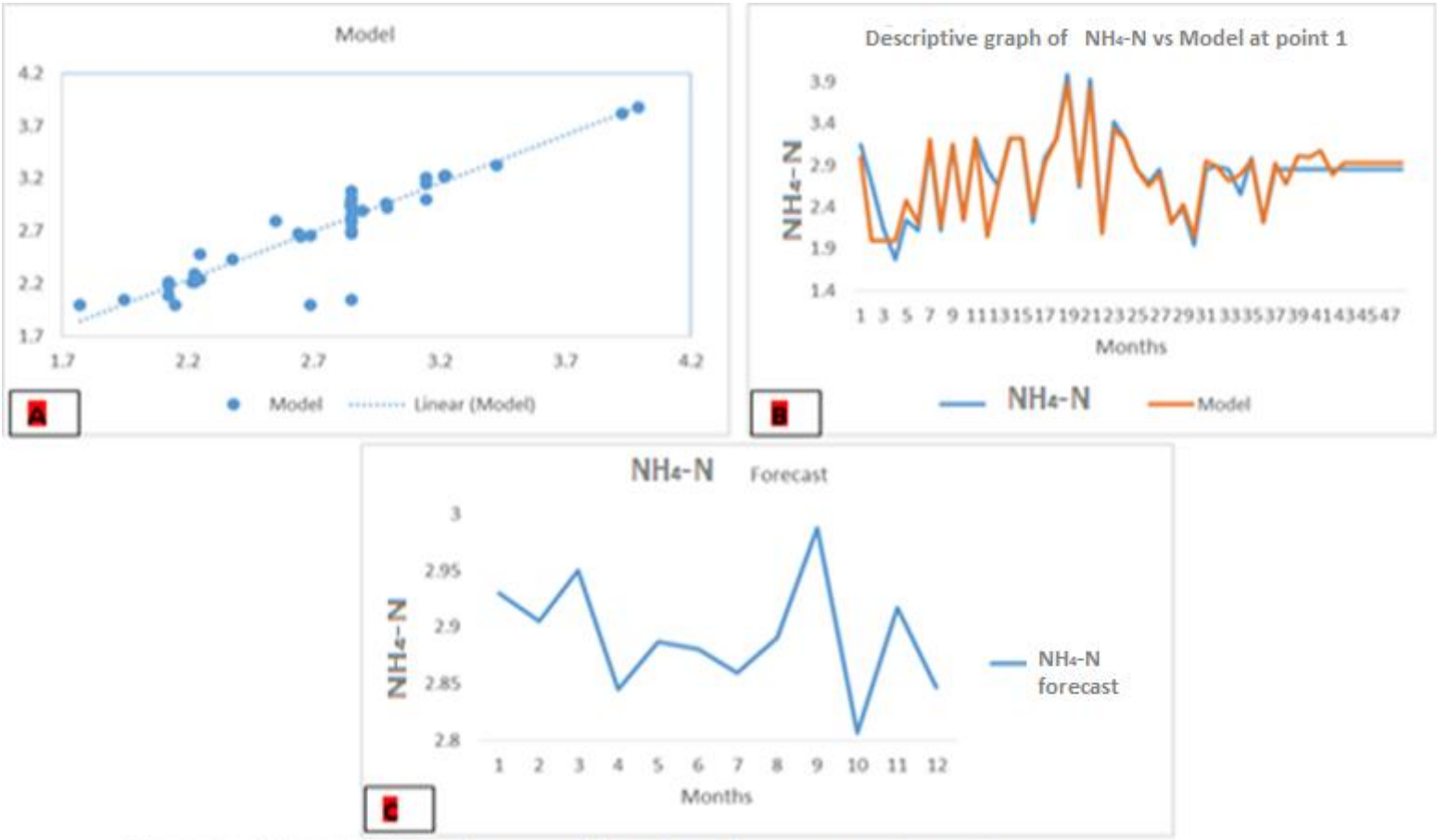

Figure 4.20 (A Band C): NH_4-N scatter, model and forecast graph at point 1

Just like the water quality parametric behaviours at point 1, it was observed generally that the ANN asymptotically modeled the water quality dataset very well, as the scattered plot points were seen to be very close to the line of best fit. Comparing the ANN model with the actual, the deviations were not significant. The forecast for all the parameters at point 2 showed continuous changes of the values over time.

The pH forecast at point 2 was observed to decrease over time in a non-linear manner, although some points were observed to have lower forecast values than other points as shown in Figure 4.22, but in all, the pH forecasts were within the permissible range. The TDS forecast was observed to have increased so high at the 9^{th} month and was lowest between 3^{rd}- 4^{th} month in Figure 4.23. TDS forecast showed high increase in the dry season due to low or absence of rainfall which in other words increases the concentration of pollutants/ inorganic substances. The low concentration of pollutants in the dry season at the 3^{rd} - 4^{th} month could be as a result of high rainfall. Figure 4.24 shows that the HCO_3 forecast increases with time of forecast but has its lowest values of HCO_3 at the 7^{th} month before rising again. Also, Figure 4.25 shows the forecast graph of Mg which shows a slight increase with time till the 3^{rd} month and sharply decreased at the 9^{th} months before rising up again till the 12^{th} month. HCO_3 and Mg showed sinusoidal movement all through which could be as a result of fluid dynamics in the water body.

The Ca and NO_3-N forecasts as shown in Figures 4.26 and 4.28 showed that their forecast descriptive graph witnessed a continuous sinusoidal pattern with time of forecast till the 9^{th} month before increasing and rising till the 12^{th} month of the forecast. However, the forecast graph of Na shows that the forecast increases with time and attains highest forecast values at the 6^{th} month before decreasing as shown in Figure 4.27. SO_4 , in figure 4.29 rose highest at point 9. Ca, NO_3-N and SO_4 showed a high concentration in the dry season since there was less ion

dissolution/ dilution due to low or absence of rainfall. The forecast graph of NH_4-N as shown in Figure 4.30 kept changing with time but in upward direction.

From the graphical representations, the forecast and model for pH, HCO_3^- , Mg, Ca, NO_3-N, NH_4-N were within the permissible range while TDS, EC, Na and SO_4 exceeded the FAO permissible standard. The Point 2 descriptive scattered graphs, the actual and model graphs of the developed ANN model, and forecast graphs for the next one year are shown in Figures 4.21 to 4.30.

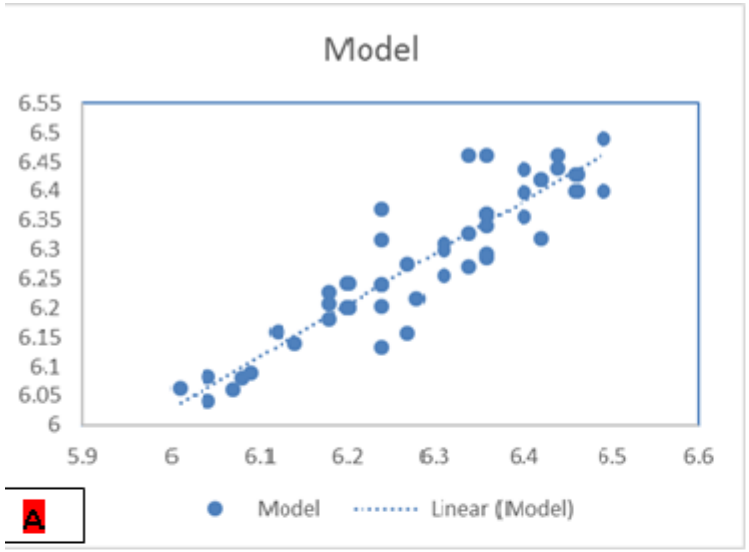

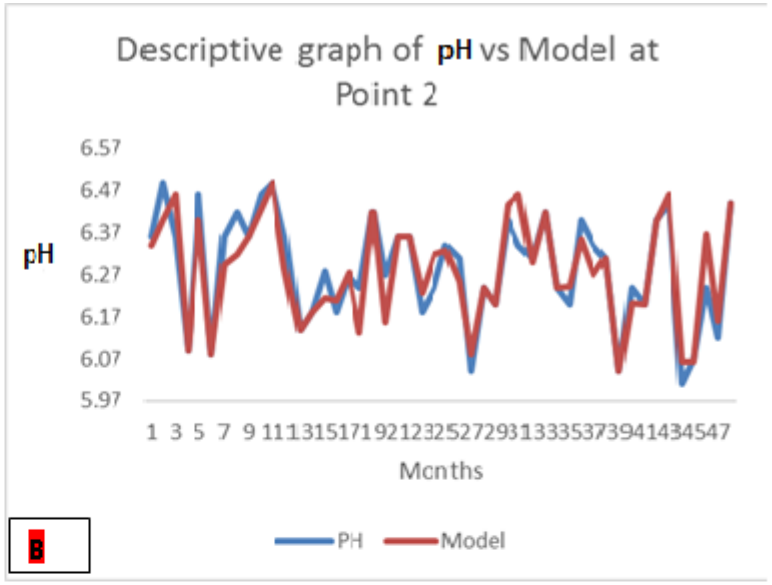

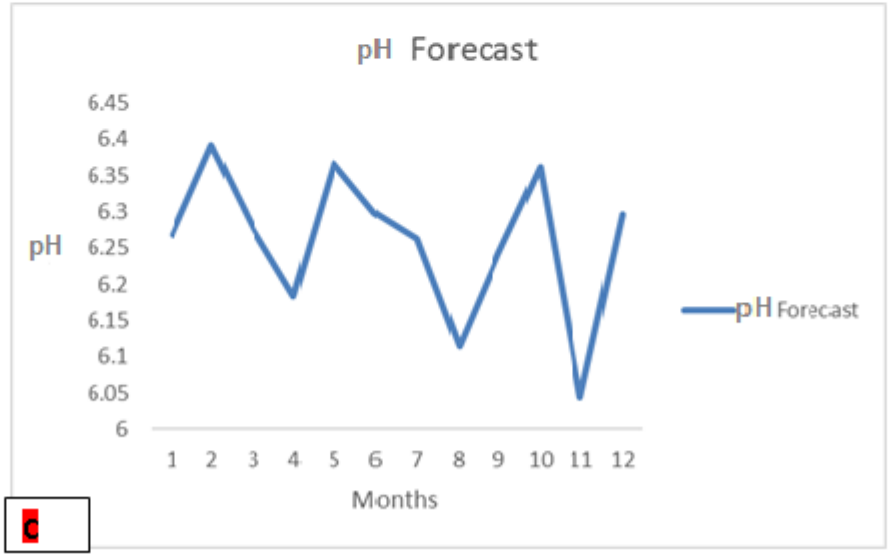

Figure 4.21 (A, Band C): pH scatter, model and Forecast graph at point 2

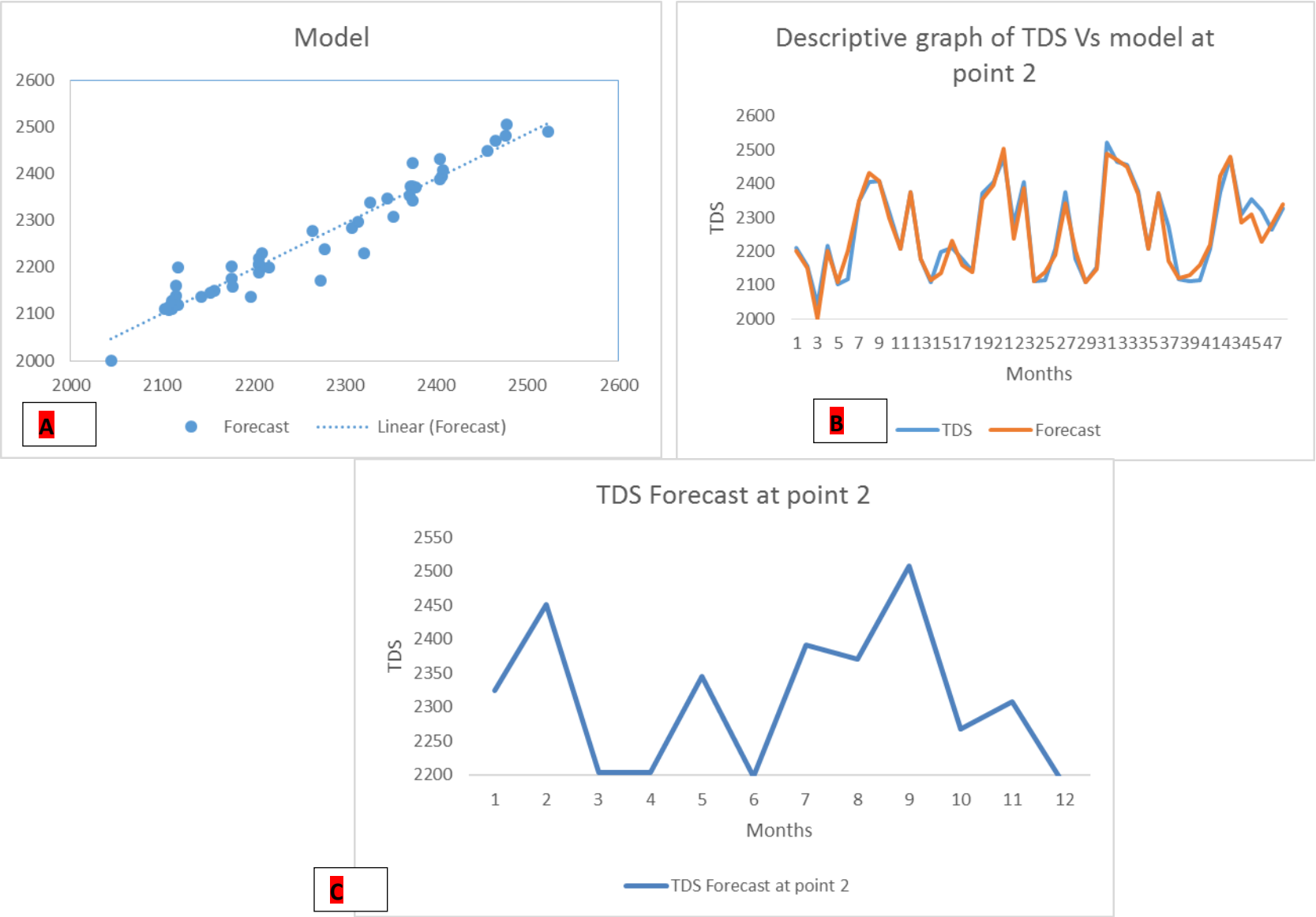

Figure 4.22 (A Band C): TDS scatter, model and Forecast graph at point

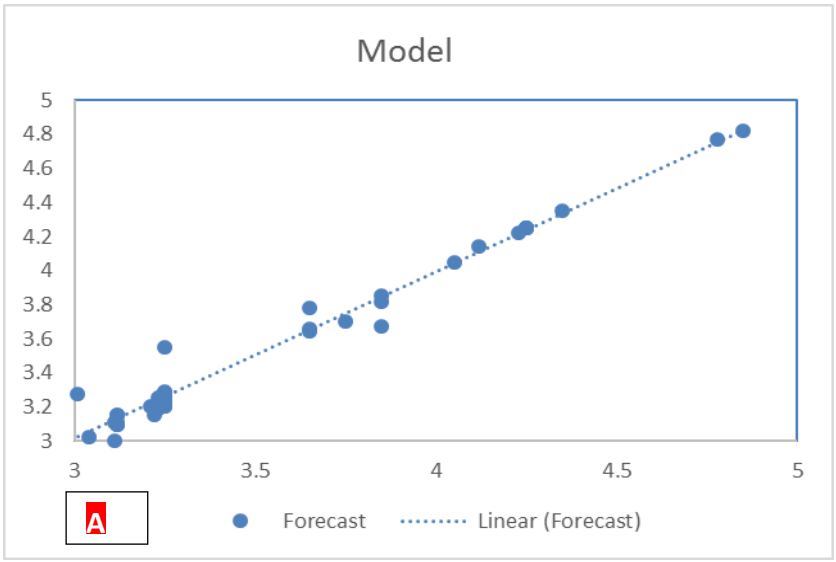

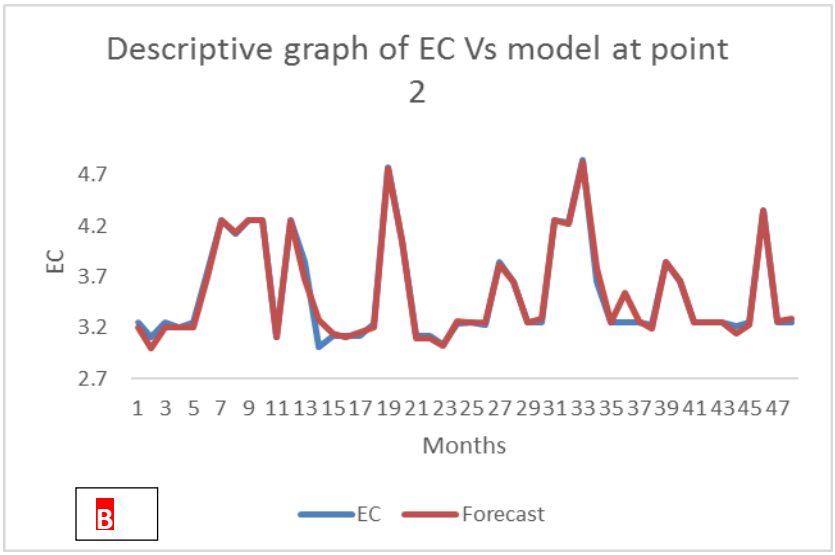

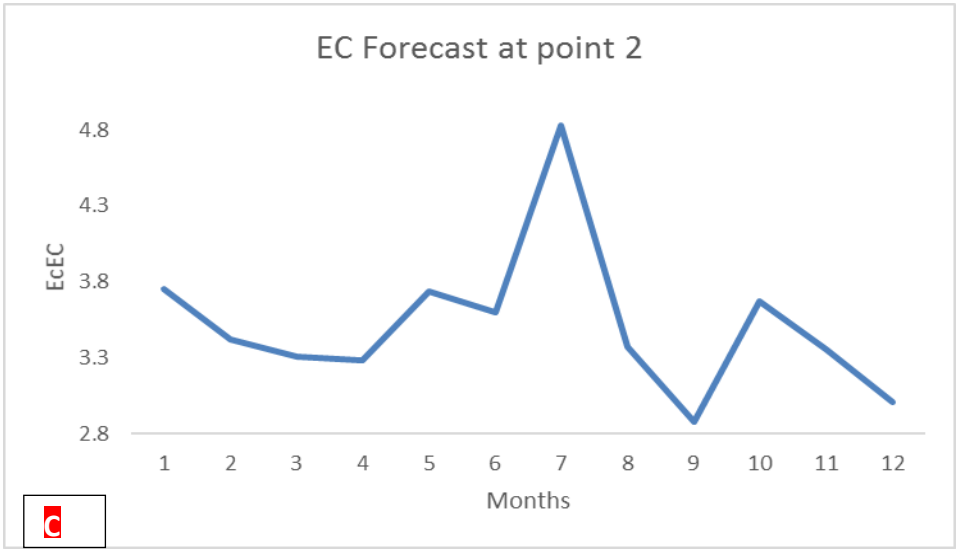

Figure 4.23 (A Band C): EC scatter, model and Forecast graph at point 2

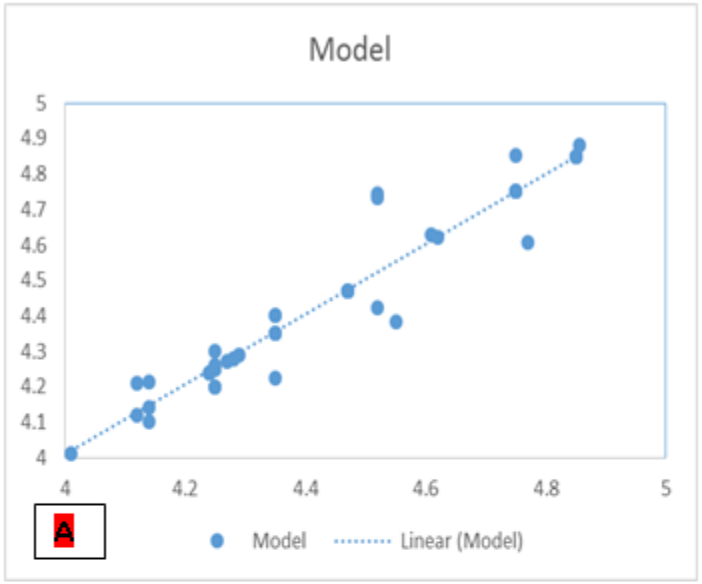

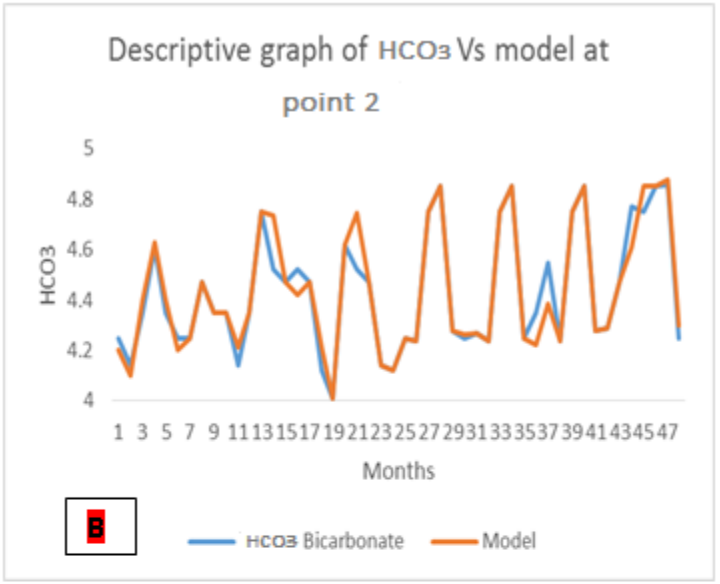

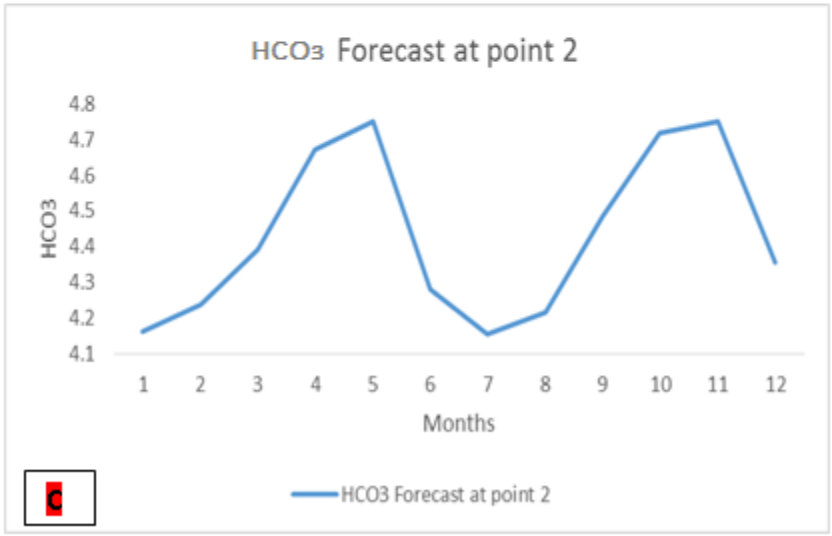

Fig. 4.24 (A Band C): HCO_3 scatter, model and Forecast graph at point 2

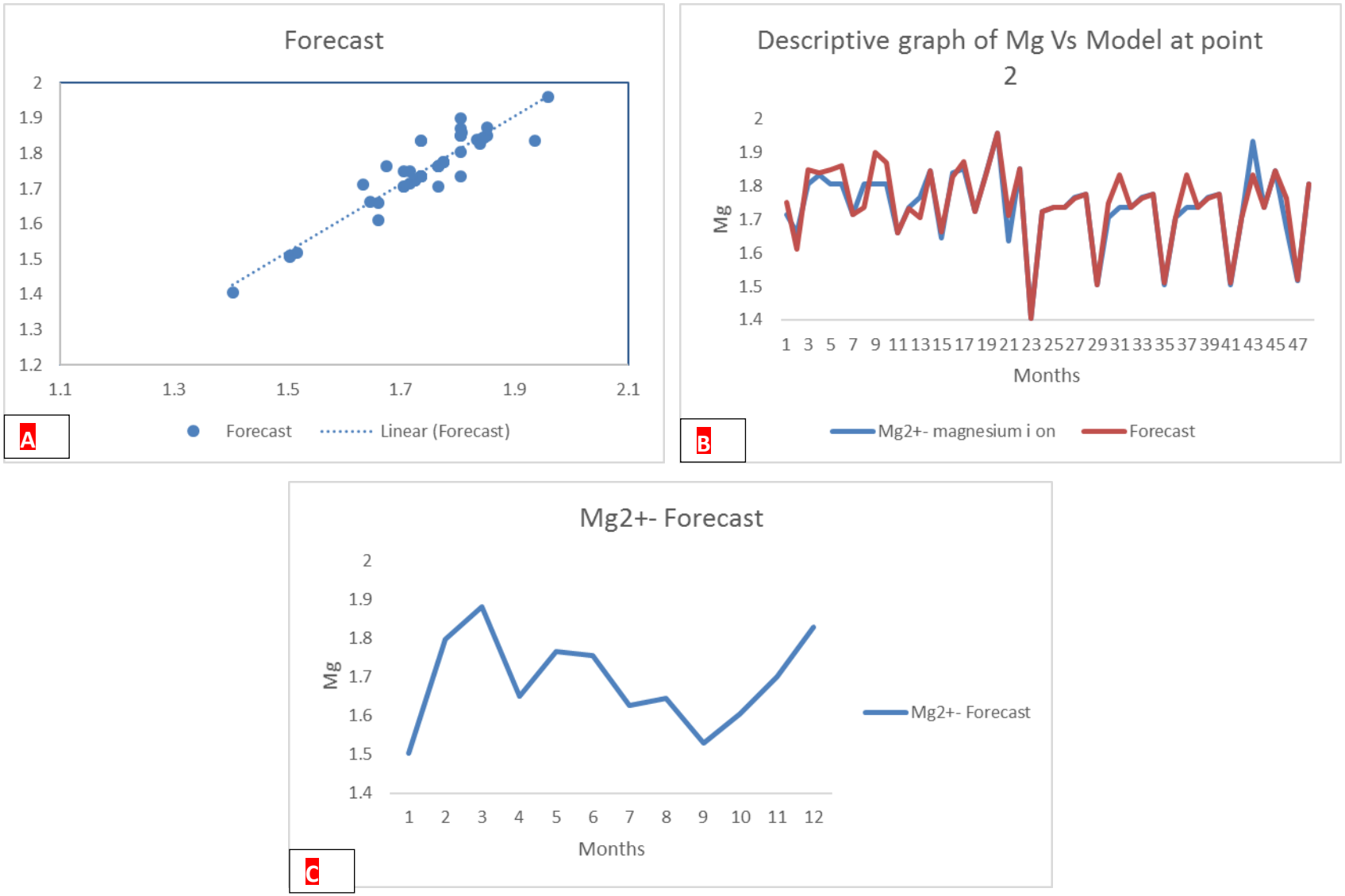

Figure 4.25 (A, Band C): Mg scatter, model and Forecast graph at point 2

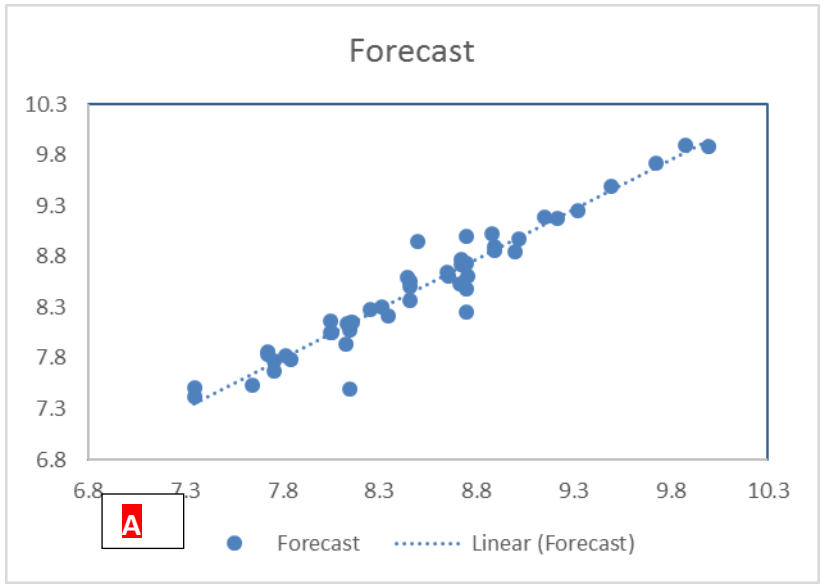

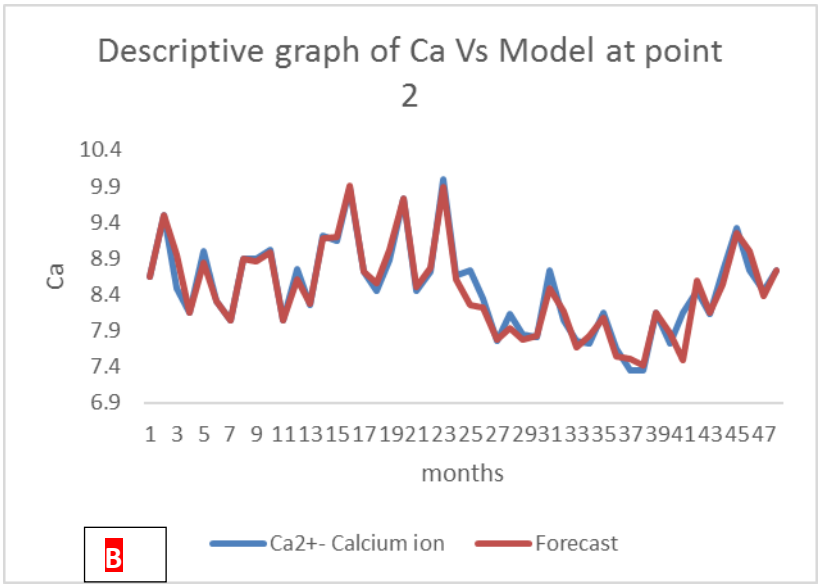

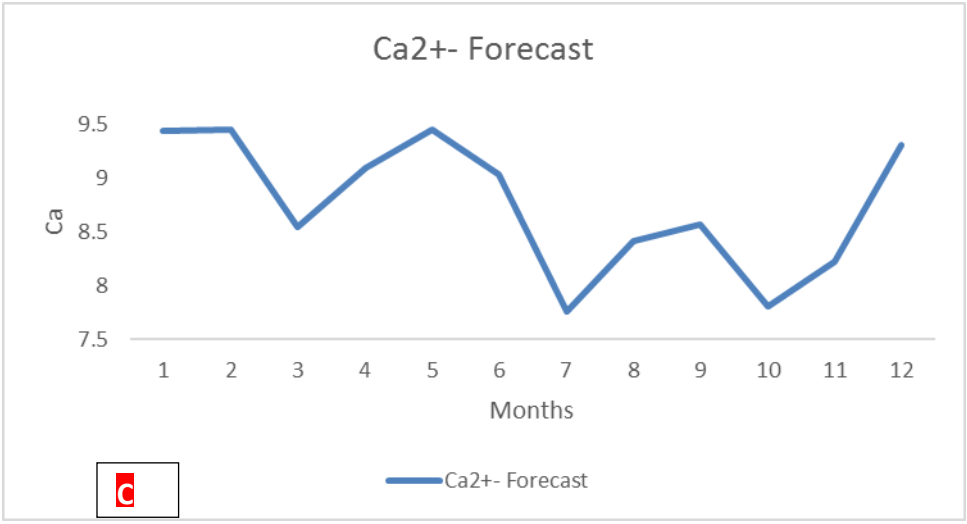

Figure 4.26 (A, Band C): Ca scatter, model and Forecast graph at point 2

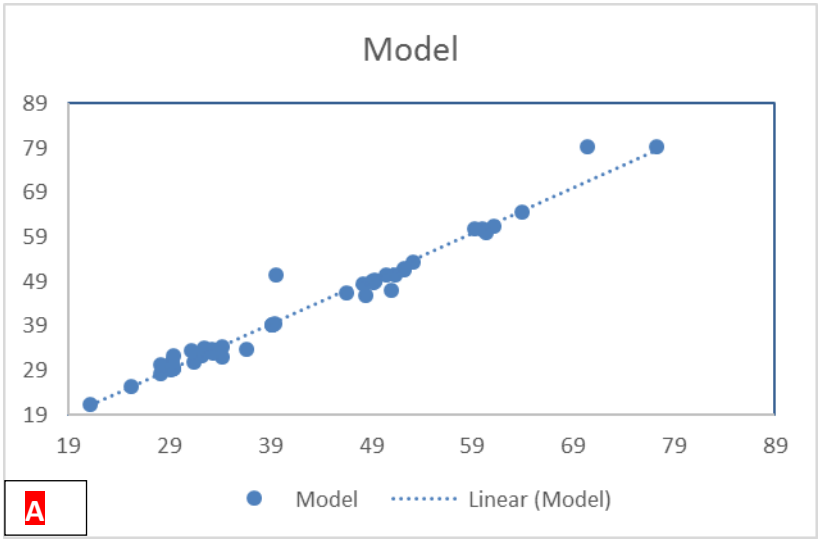

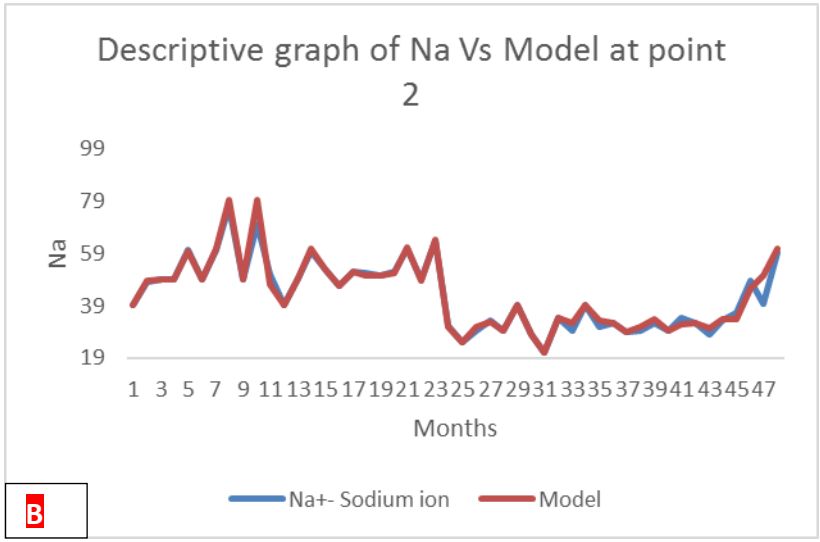

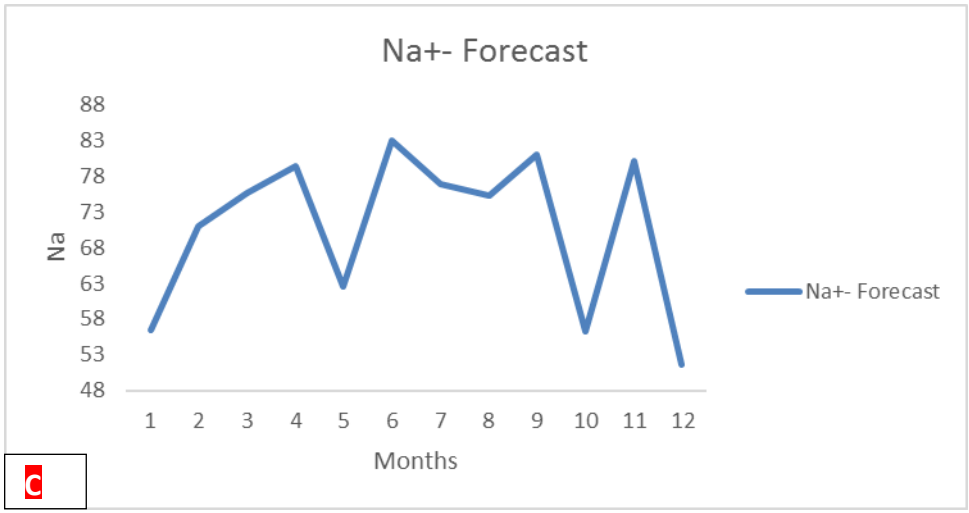

Figure 4.27 (A, Band C): Na scatter, model and Forecast graph at point 2

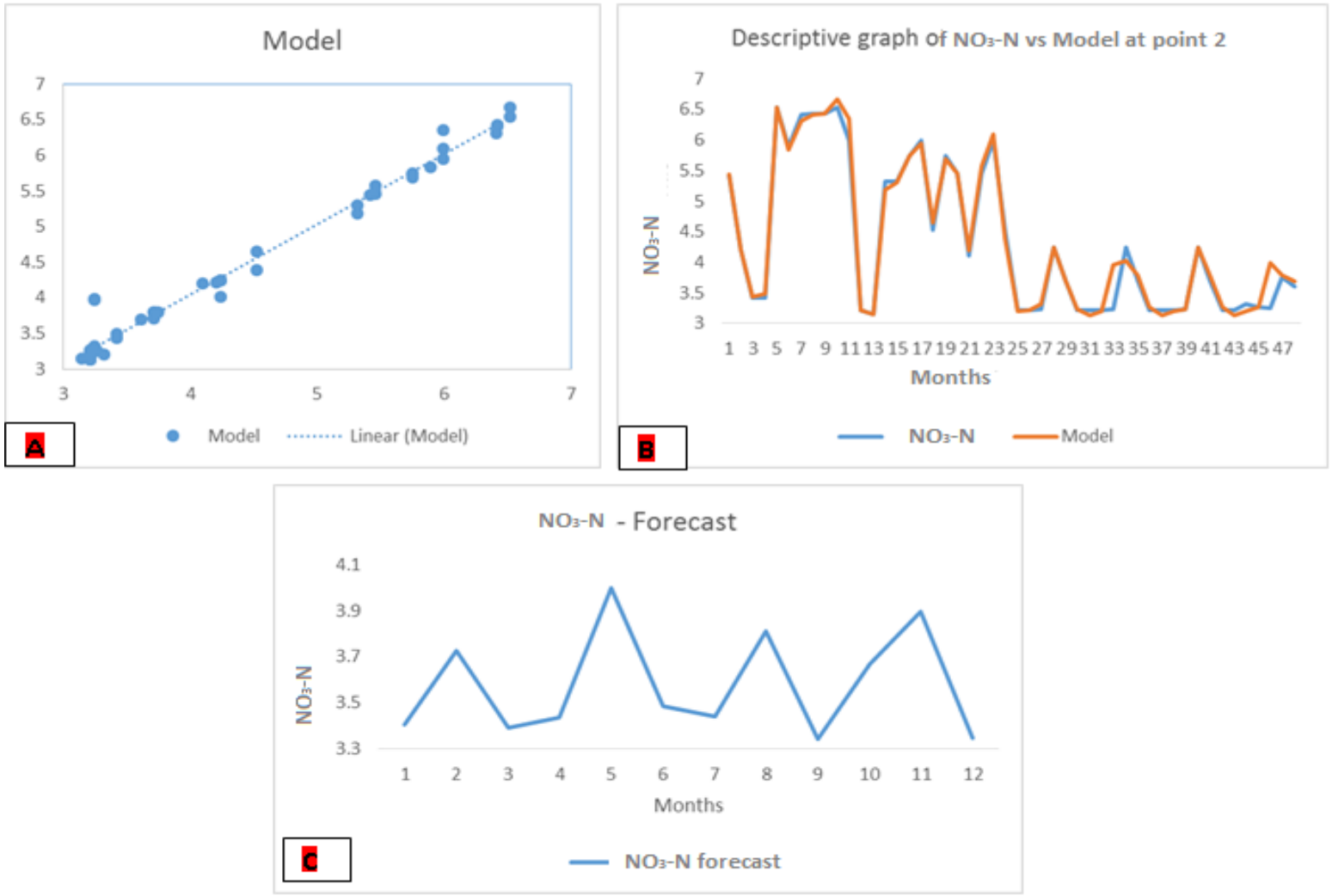

Figure 4.28 (A, Band C): NO_3 scatter, model and Forecast results at point 2

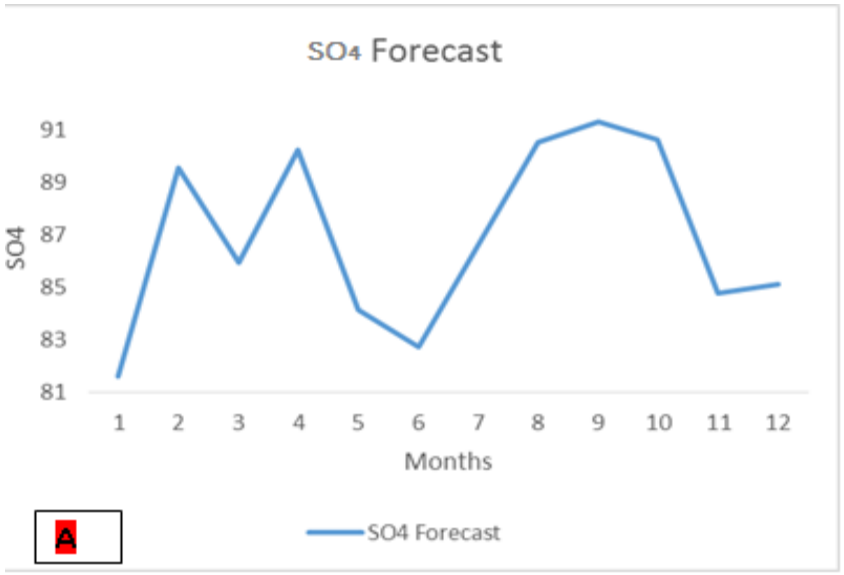

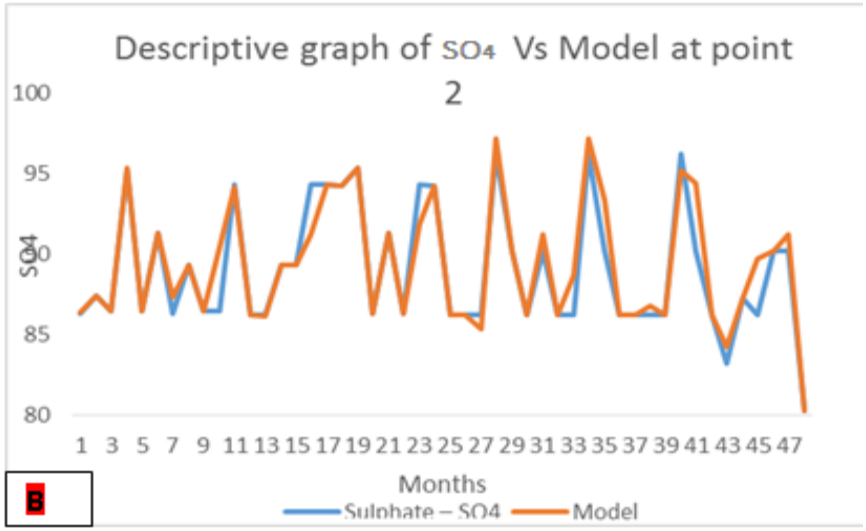

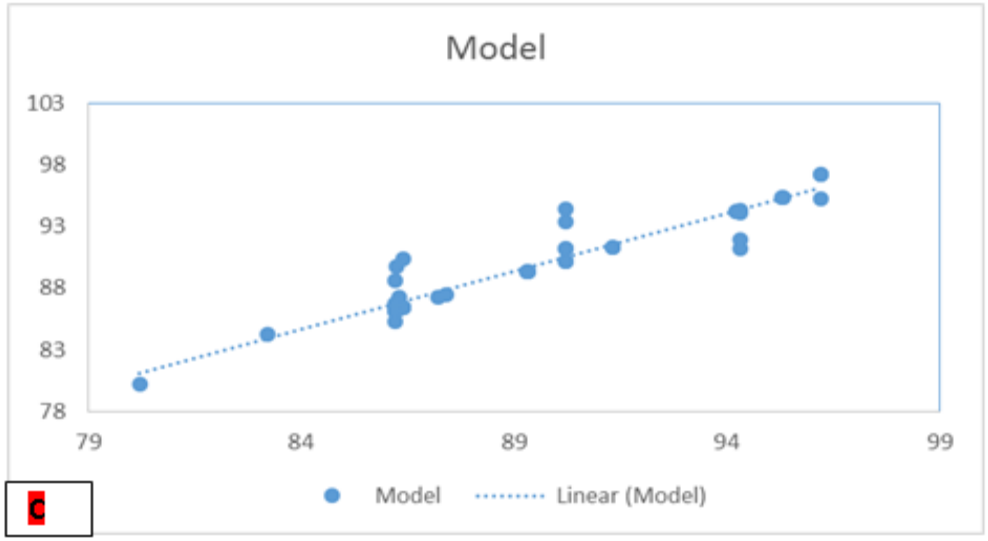

Figure 4.29 (A, Band C): SO_4 scatter, model and Forecast graph at point 2

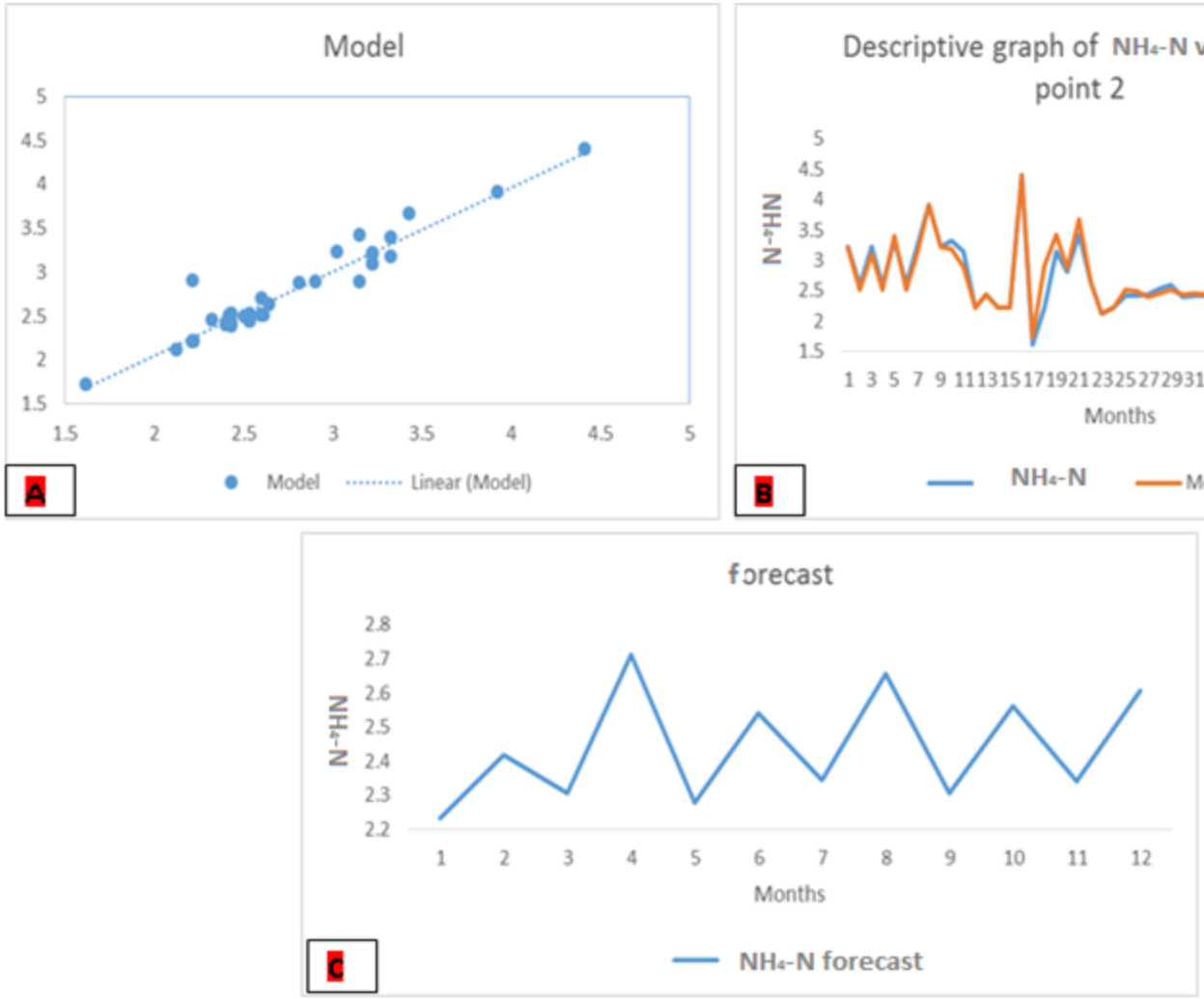

Figure 4.30 (A, Band C)NH_4-N scatter, model and Forecast graph at point 2

Just like the water quality parametric behaviors at point 1 and point 2, it was generally observed that at point 3, the ANN asymptotically modeled the water quality dataset very well, as the scattered plot points were seen to be very close to the line of best fit. Comparing the ANN model with the actual, the deviations were not significant. The forecast for all the water quality parameters at point 3 showed continuous changes of values over time as shown in Figures 4.31 to 4.40.

However, the pH forecast graph shows constant variations with time and attained the highest forecast value at the 12^{th} month and the lowest forecast values at the 5^{th} month (Figure 4.31).This high forecast value could be as a result of low turbidity and rainfall effect which adversely increased the pH concentration in the dry season. It was also observed in Figure 4.32 that the TDS forecast values non-linearly vary over time and however attained highest forecast value at the 9^{th} month due to high concentration of inorganic substances. The EC forecast graph was seen to have experienced up and down variation.

Figures 4.34 and 4.39 presented the forecast graphs of HCO_3^- and SO_4 which showed similar forecast descriptive graph shape. The forecast pattern for HCO_3^- was observed to have risen high at 2^{nd} month before making a sinusoidal movement till the 12^{th} month. SO_4^{--} was high and later came to the lowest concentration at the 6^{th} month. The Mg forecast graph as shown in Figure 4.35 revealed that the Mg forecast graph decreased with time, hence, the Ca, NO_3-N and Na as shown in Figure 4.36, 4.37 and 4. 38, respectively, showed that the forecast graph was linearly alternating up and down along the best line of fit with respect to the months of forecast. Unlike the descriptive graph of other water quality parameters in point 2, the NH_4-N forecast graph gradually increased over time and attain highest forecast value in the 7^{th} month before decreasing till the 12^{th} month.

From the graphical representations, the forecast and model for pH, HCO^{3-} , Mg, Ca, NO_3-N, NH_4-N were within the permissible range while EC, Na and SO_4 exceeded the FAO permissible standard, though in the forecast at only 3rd and 6th months, TDS was within the permissible range while at most instance in the model, it was above the permissible standard. Most variations in the model and forecast were as a result of high and low rainfall effect and also due to the effects of ion dissolution from point 1 to point 3.

The Point 3 descriptive scattered graphs, the actual and model graphs of the developed ANN model, and forecast graphs for the next one year are shown in Figures 4.31 to 4.40.

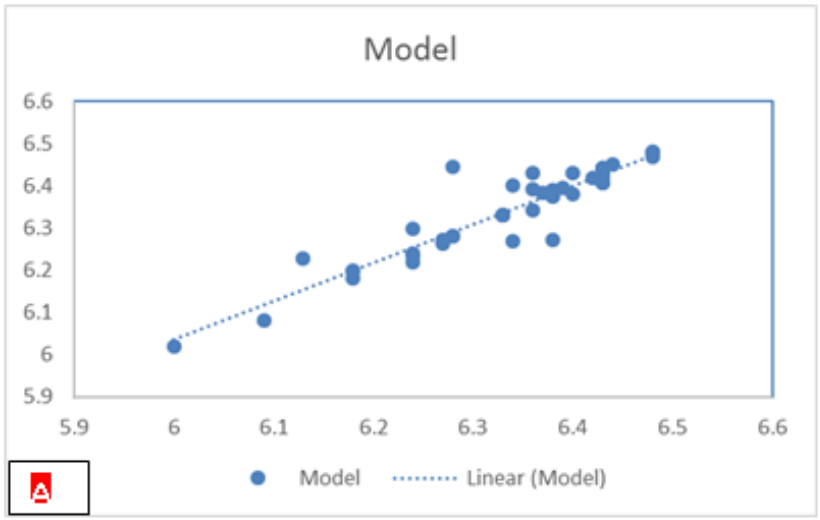

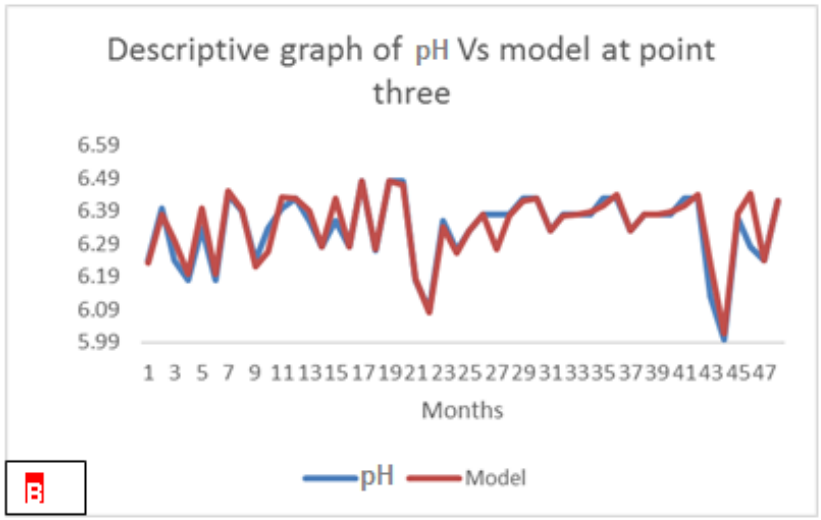

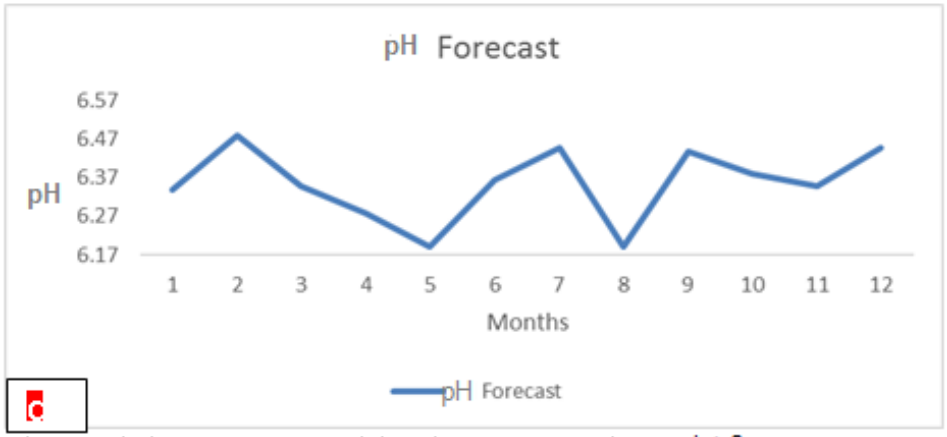

Figure 4.31 (A, Band C):pH scatter, model and Forecast graph at point 3

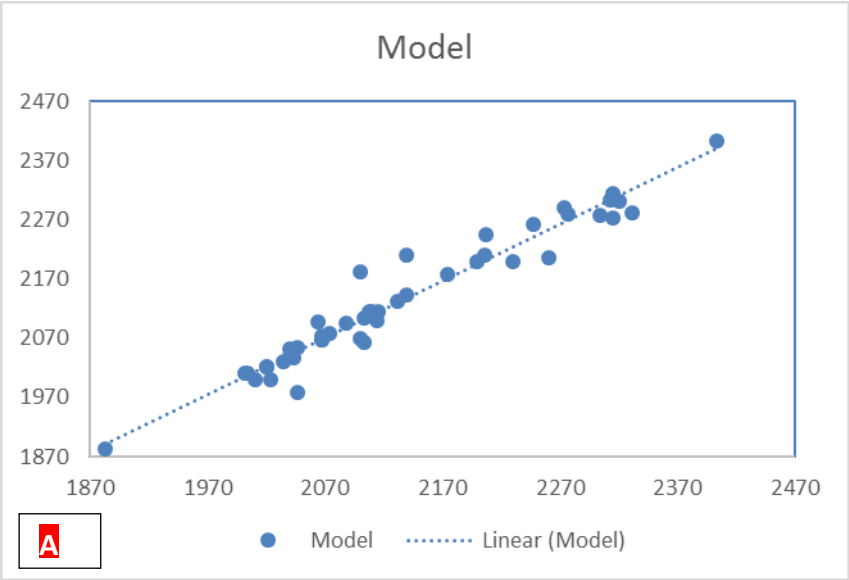

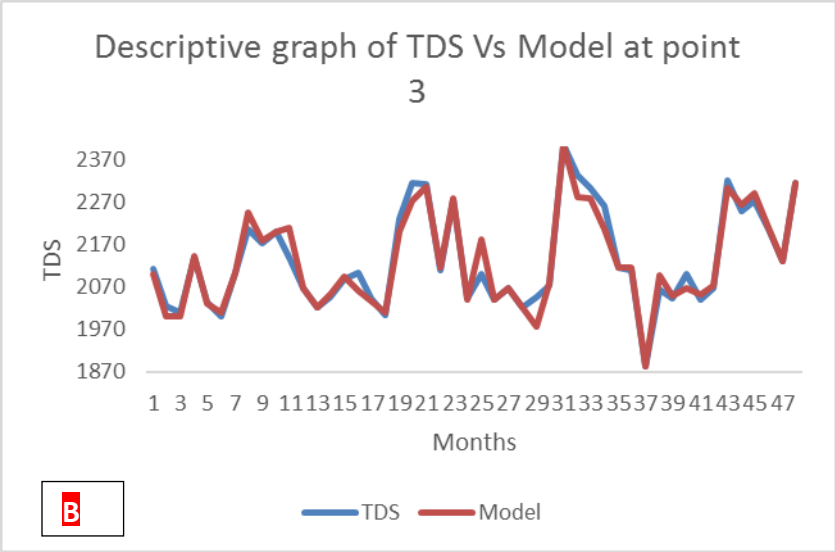

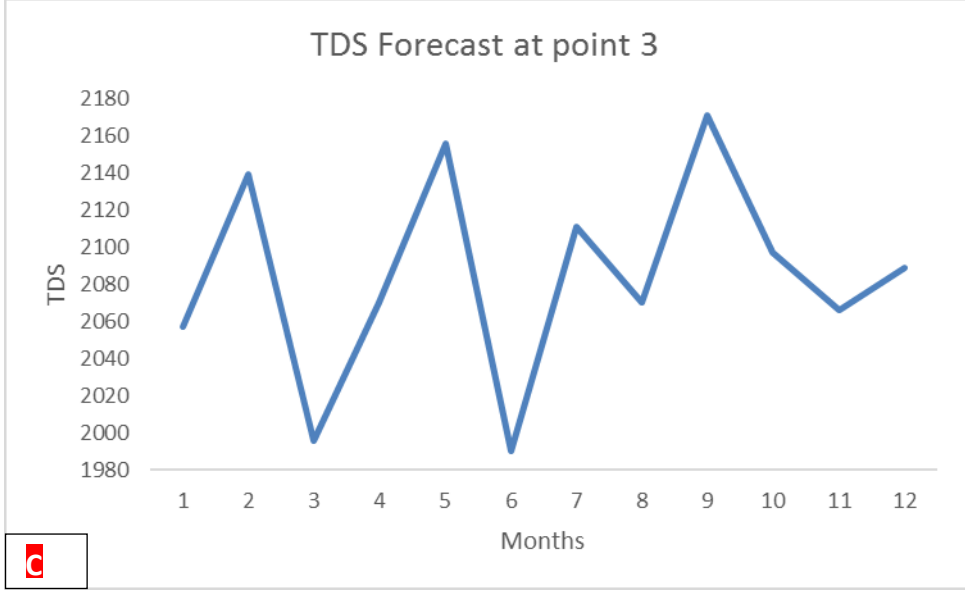

Figure 4.32 (A Band C): TDS scatter, model and Forecast graph at point 3

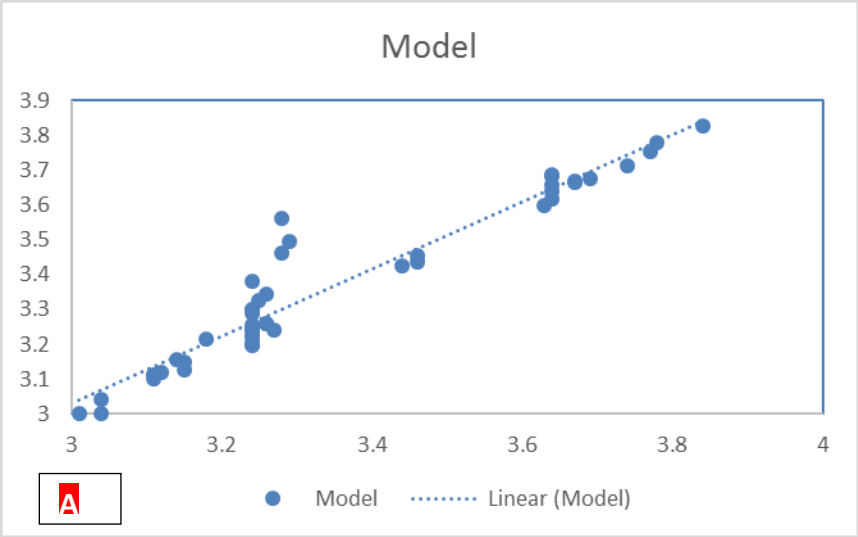

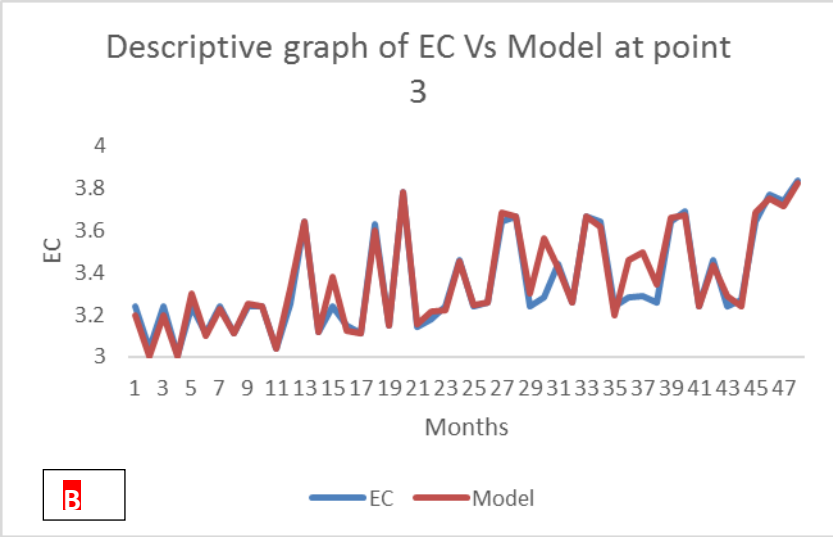

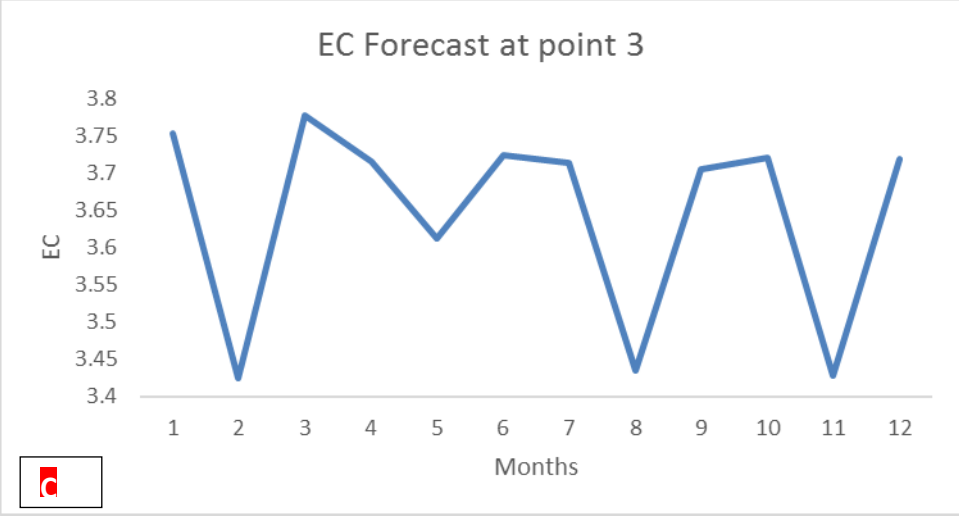

Figure 4.33 (A Band C): EC scatter, model and Forecast graph at point 3

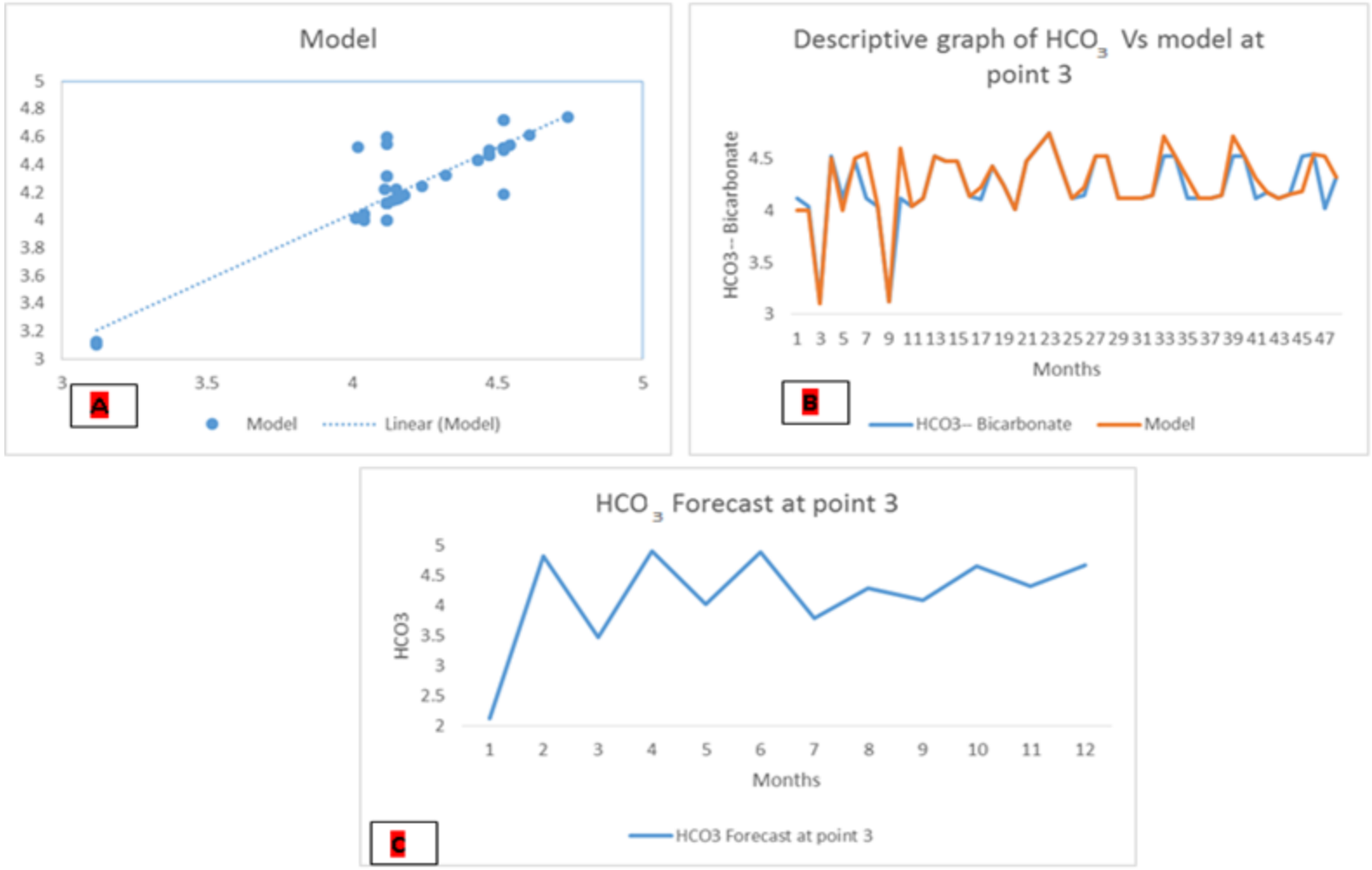

Figure 4.34 (A,B and C) HCO_3 scatter, model and forecast graph at point 3

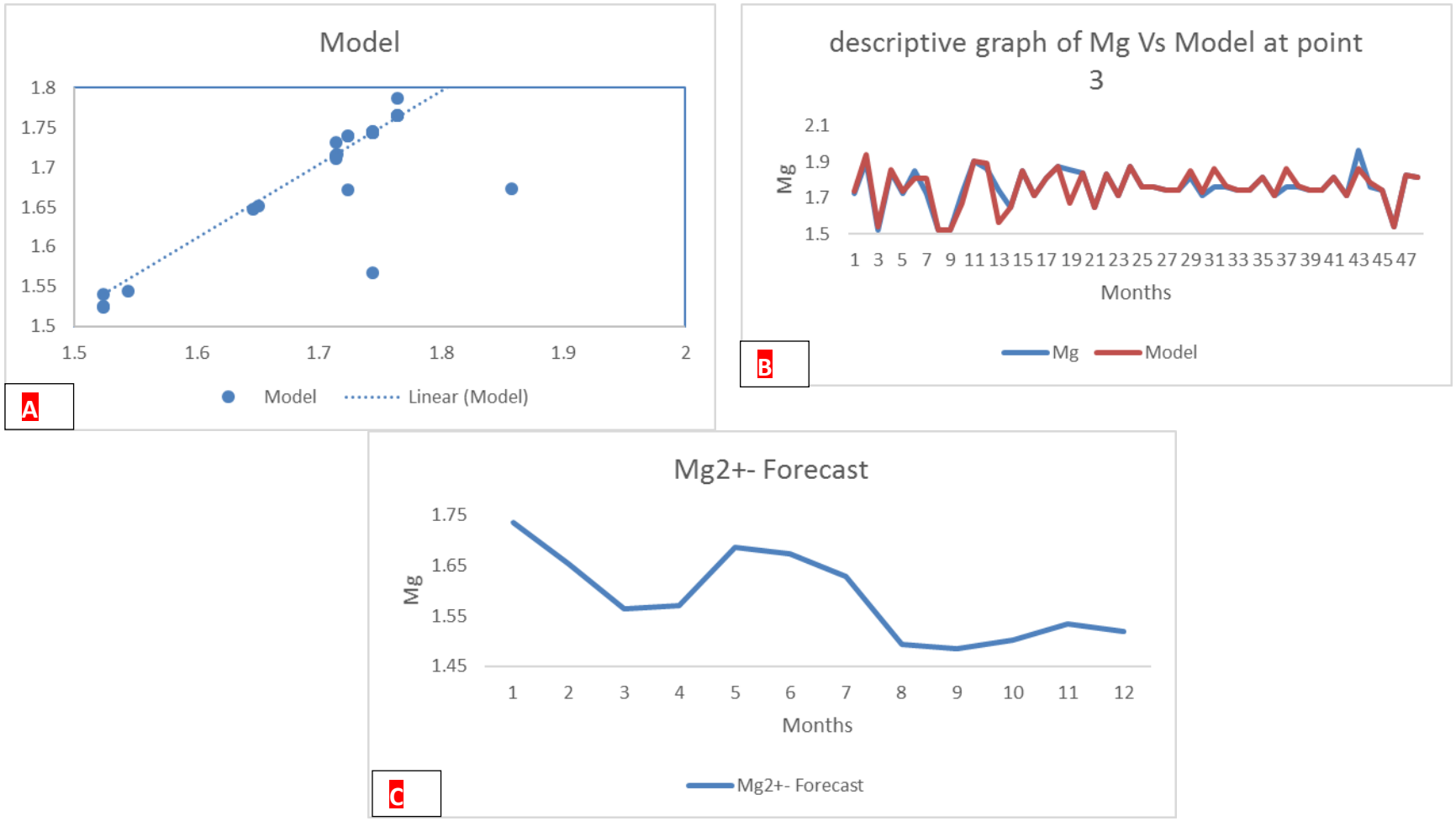

Figure 4.35 (A, Band C): Mg scatter, model and Forecast graph at point 3

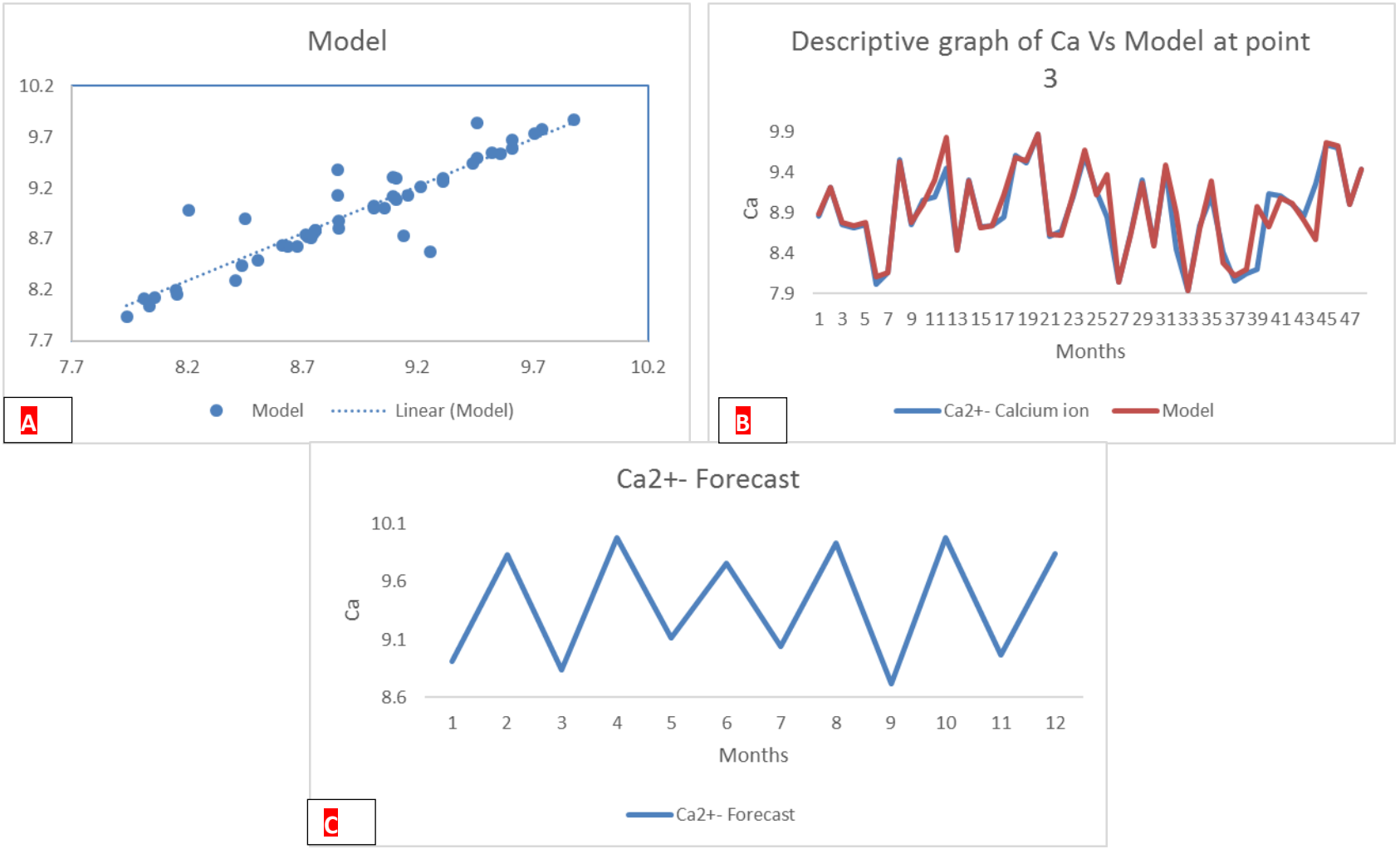

Figure 4.36 (A, Band C): Ca scatter, model and Forecast graph at point 3

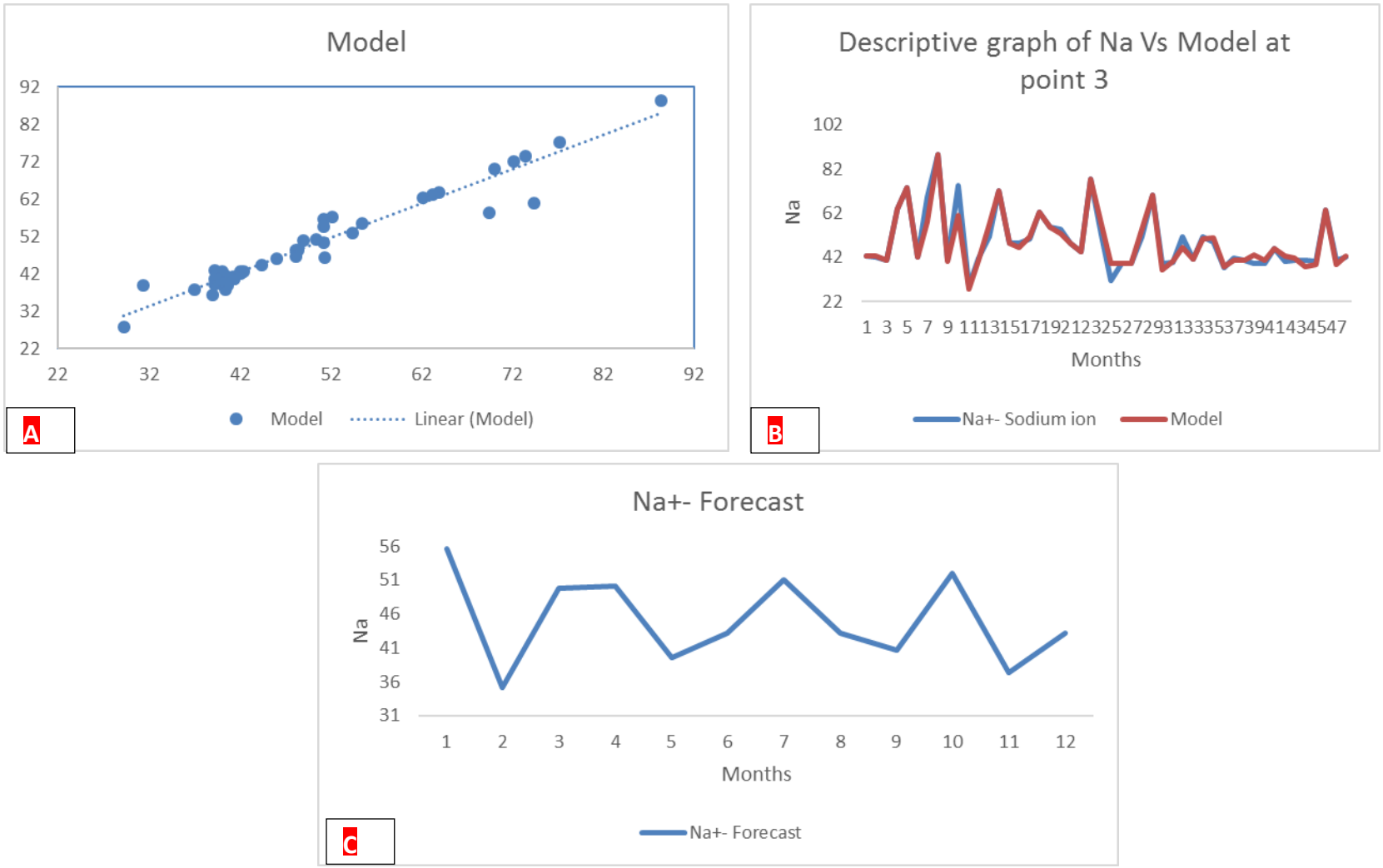

Figure 4.37 (A, Band C): Na scatter, model and Forecast graph at point 3

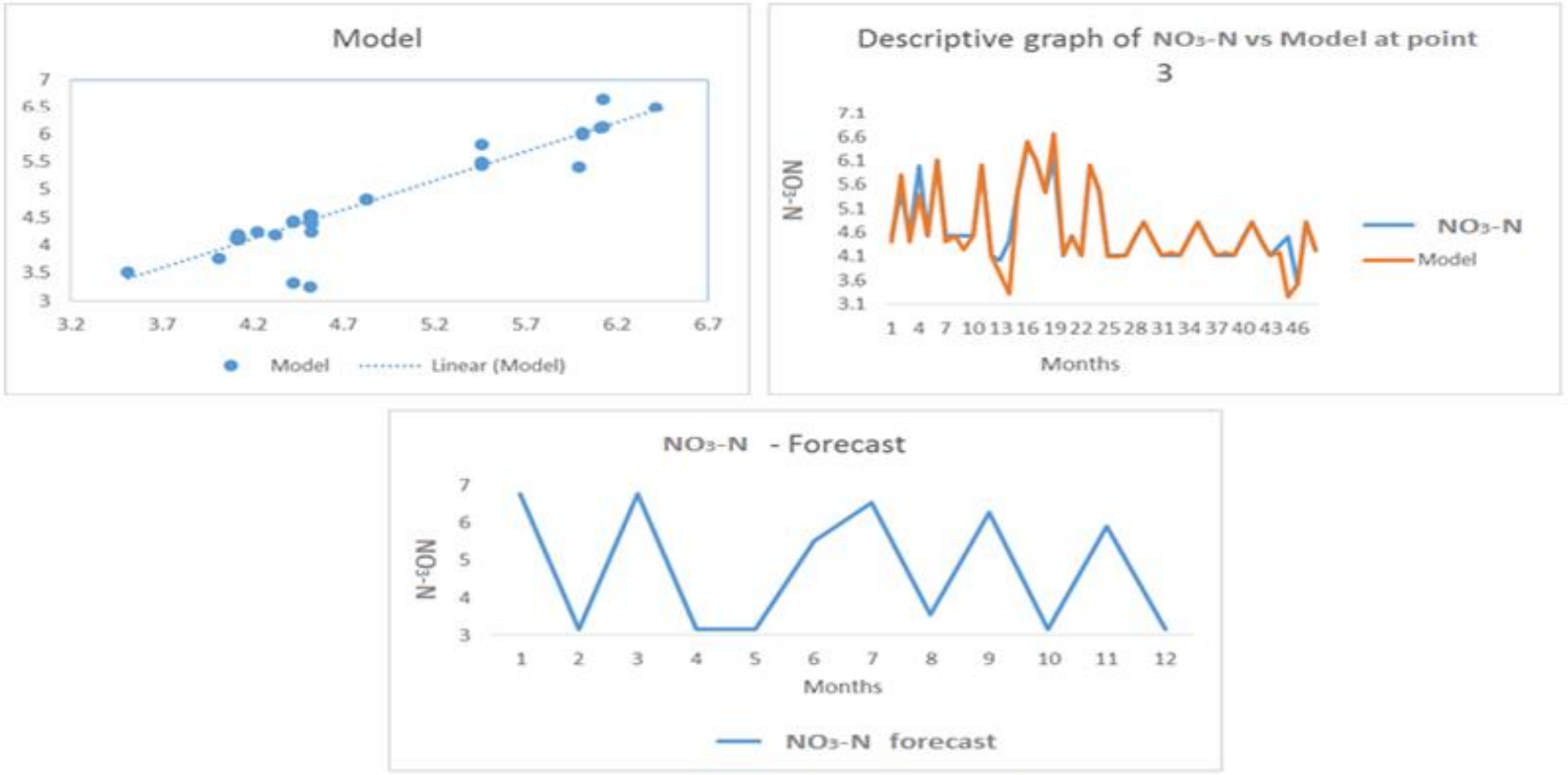

Figure 4.38 (A,B and C) NO_3-N scatter, model and forecast graph at point 3

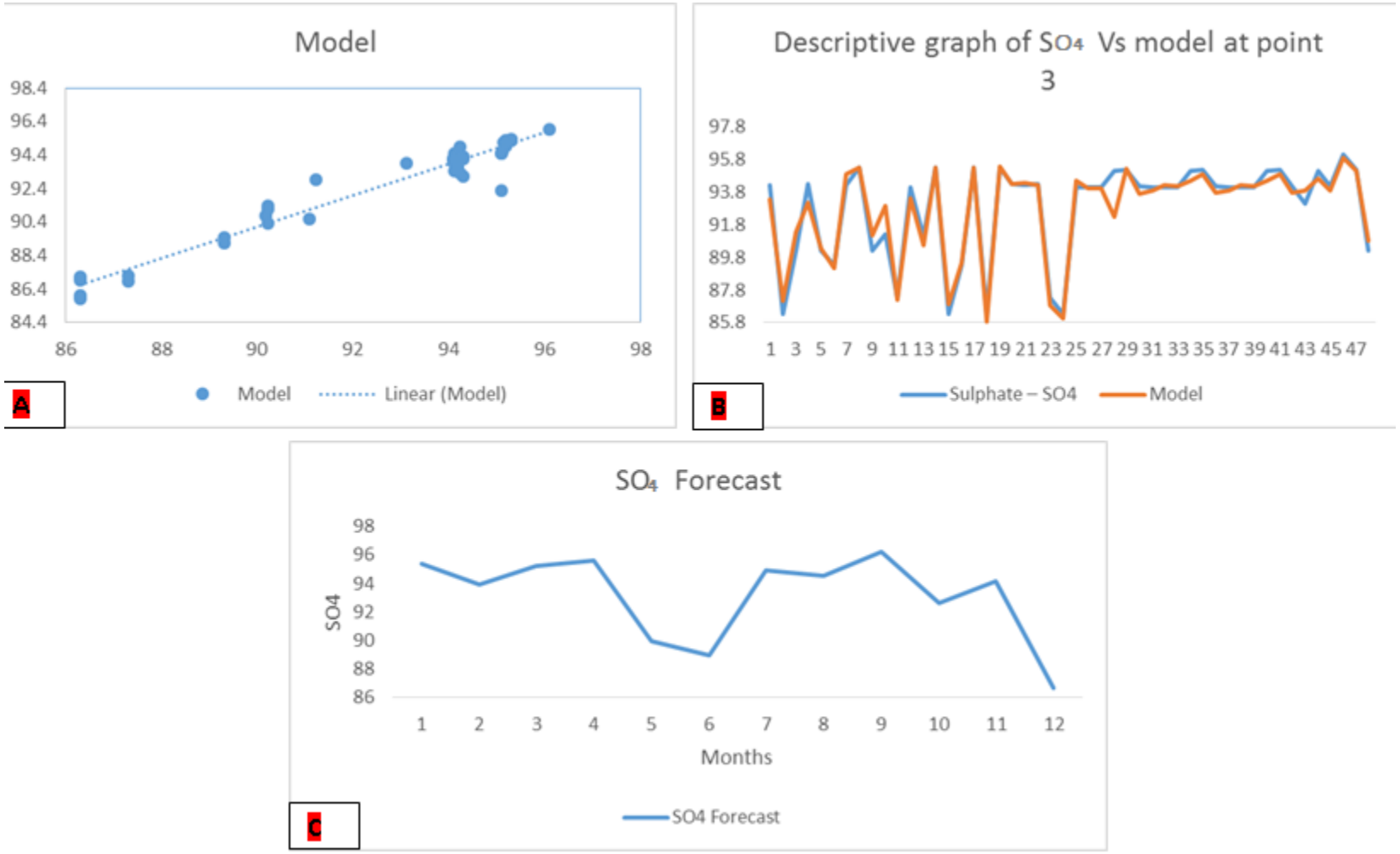

Figure 4.39 (A, Band C): SO_4 scatter, model and Forecast graph at point 3

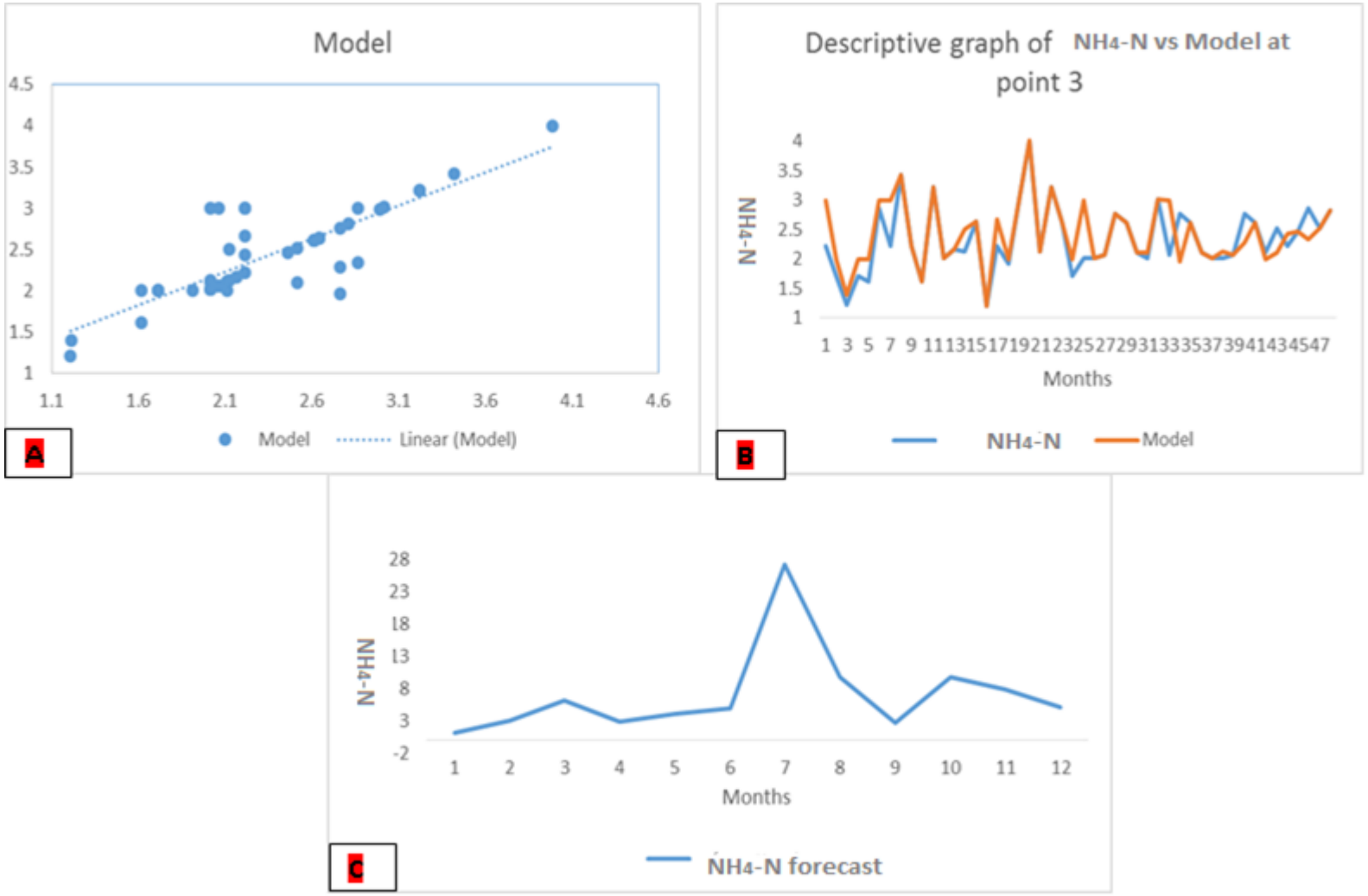

Figure 4.40 (A, Band C)NH_4-N scatter, model and Forecast graph at point 3

Just like the water quality parametric behaviors at points 1, 2, 3, it was observed generally that at point 4, the ANN asymptotically modeled the water quality dataset very well, as the scattered plot point were seen to be very close to the line of best fit. Comparing the ANN model with the actual, the deviations were not significant. The forecast for all the water quality parameters at point 4 showed continuous variations in values over time.

Conversely, the pH forecast graph as shown in Figure 4.41 reveal that the pH forecast has a sinusoidal pattern increasing with time but has the highest forecast value at the 12^{th} month which could be as a result of pollutant effects, low rainfall and turbidity. The forecast graph of TDS (Figure 4.42) started with a curved increase at the 6^{th} month which gradually decreased at the 11^{th} month due to high concentration of inorganic substances in the dry season. The descriptive graphs of EC and Na (Figures 4.43 and 4.47) showed two distinct forecast peak at the 2^{nd} and 9^{th} month but has the lowest forecast value at the 3^{rd} and 6^{th} month. The HCO_3^- graph was observed to have highly increased the 6^{th} month but attained peak forecast values at the 4^{th} month as shown in Figure 4.44. Figure 4.45 which is the forecast graph of Mg, was observed to have sharp decreased to the 2^{nd} month and gradually increased till the 12^{th} month.

The Ca forecast graph as shown in Figure 4.46 shows that the forecast graph has a linear sinusoidal pattern with respect to the forecast time along the line of best fit. It was further observed that the forecast graph of SO_4^- as shown in Figure 4. 48 at the beginning shows sharp decreased to the 3^{rd} month and highest forecast values at the 5^{th} and 11 months. The SO_4^- forecast graph (Figures 4.49) shows an alternate up and down pattern with respect to time but recorded two highest forecast values at the 5^{th} and 11^{th} month. These high concentrations at certain instance could be as a result of low rainfall effects, ion dissolutions and fluid dynamics in

the water body. The forecast graph of NH_4-N gradually increased till the 4th month before gradually decreasing till the 11th month as shown in Figure 4.50. From the graphical representations, the forecast and model for pH, HCO_{3-} , Mg, Ca, NO_3-N, NH_4-N were within the permissible range while, Na and SO_4 exceeded the FAO permissible standard. Except for the 5th, 6th and 8th months from the forecast graphs, TDS was within the permissible range while EC throughout the 12months in the forecast was within the permissible range while at few instance in the model exceeded the permissible standard. More reasons for these low and high concentrations seasonally at most sampling points were highlighted more in Fig. 4.6 (River Water Quality Assessment for Irrigation Purposes).

The Point 4 descriptive scattered graphs, the actual and model graphs of the developed ANN model, and forecast graphs for the next one year are shown in the appendix from figures 4.41 to 4.50.

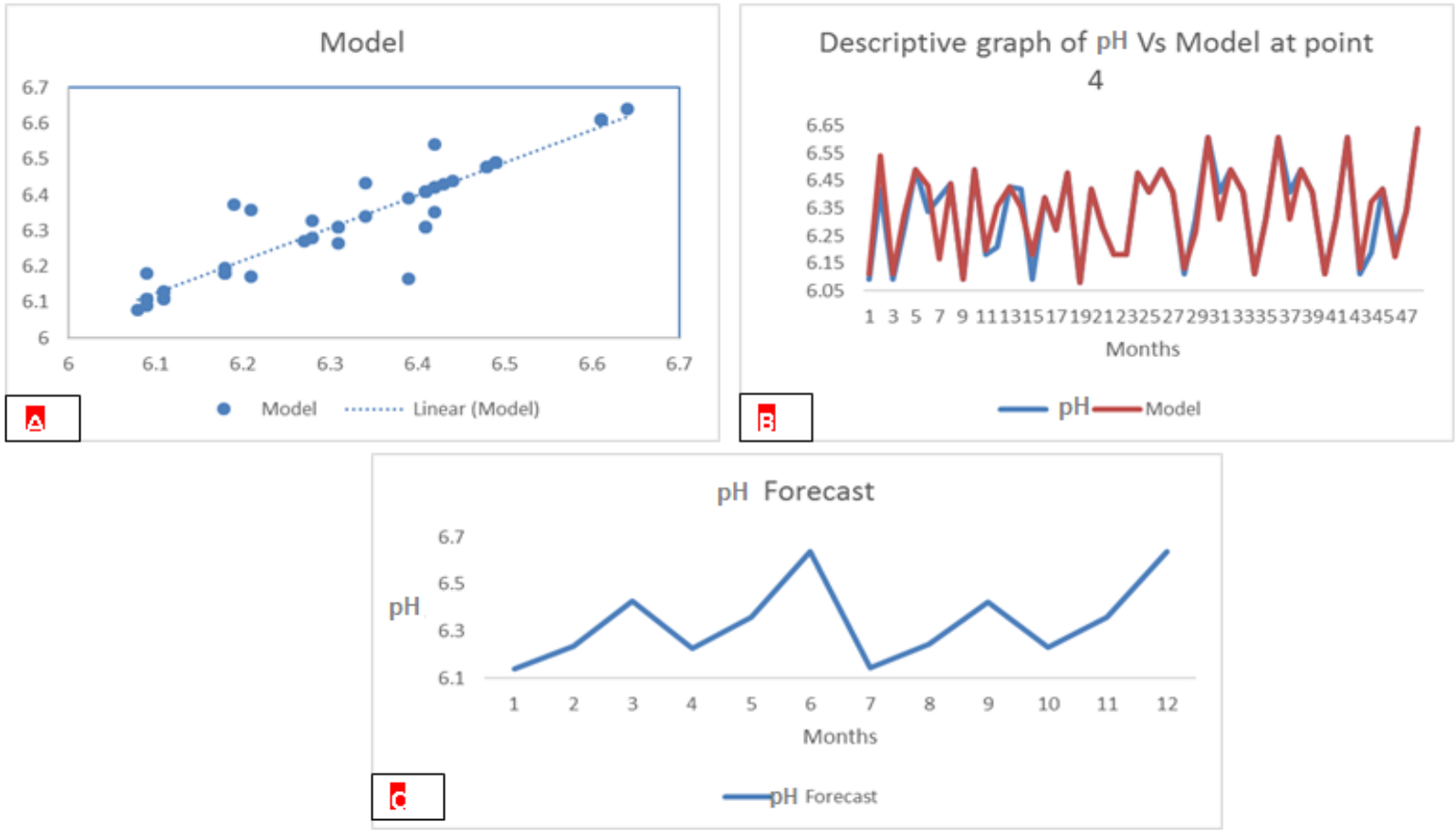

Figure 4.41 (A, Band C): pH scatter, model and Forecast graph at point 4

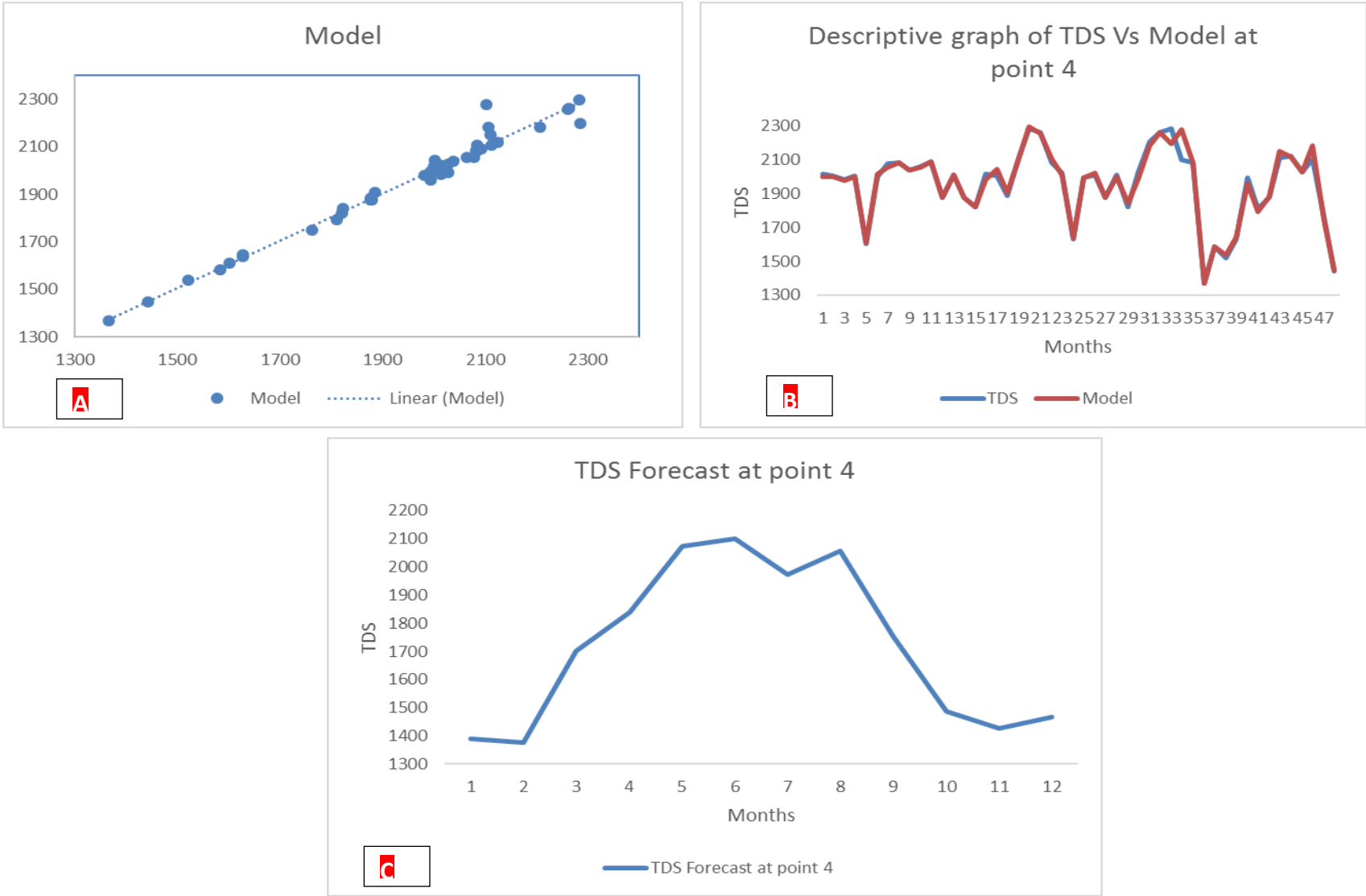

Figure 4.42 (A Band C): TDS scatter, model and Forecast graph at point 4

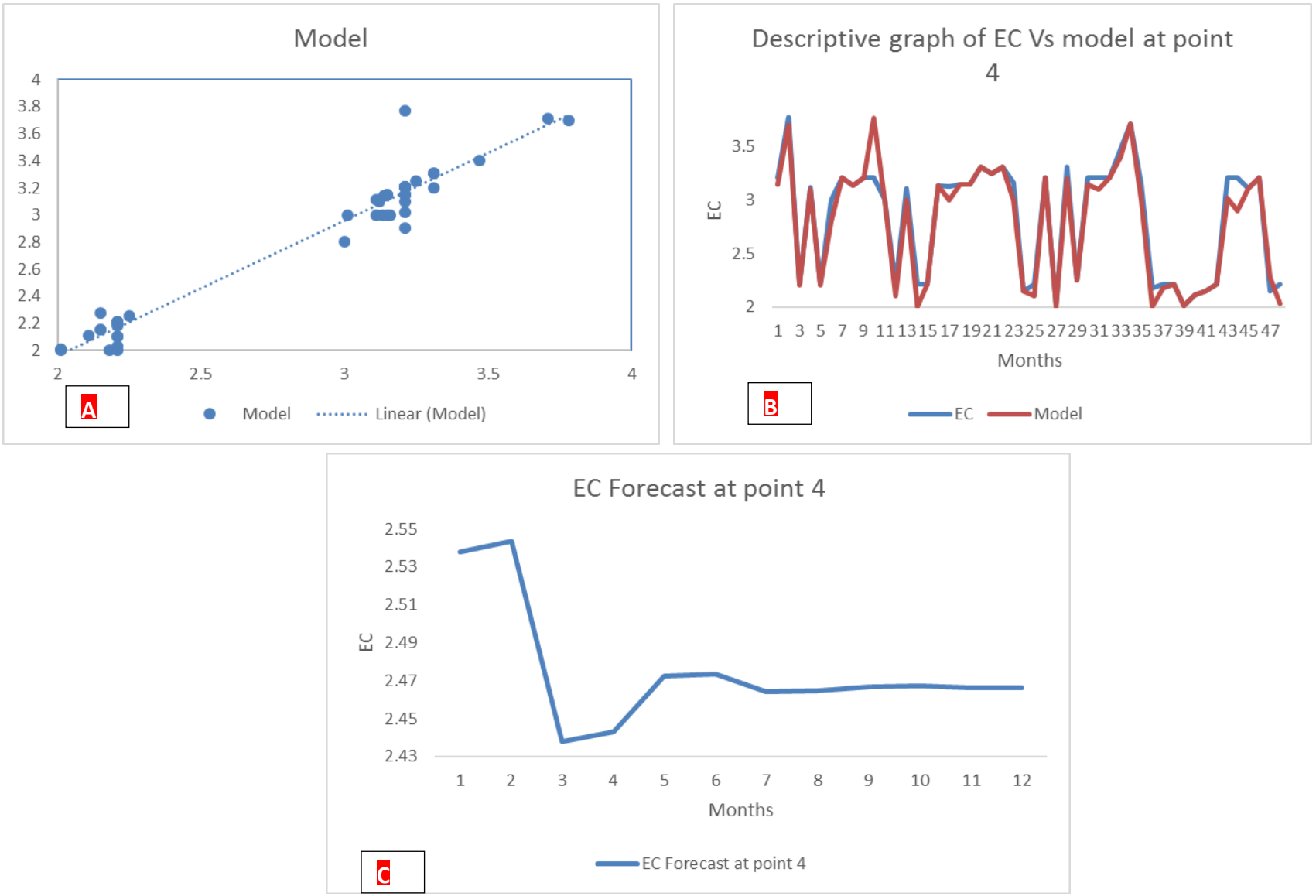

Figure 4.43 (A Band C): EC scatter, model and Forecast graph at point 4

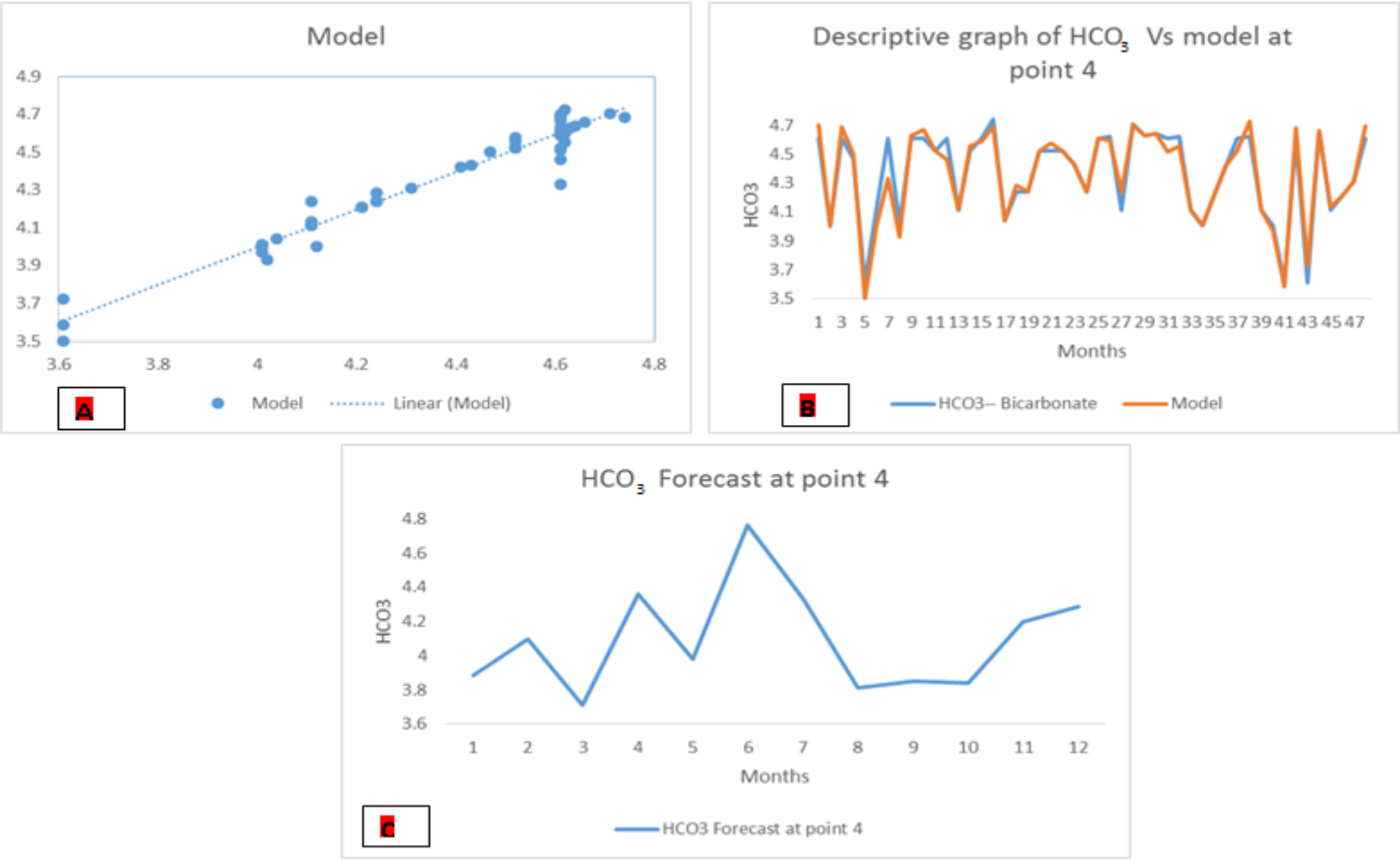

Figure 4.44 (A Band C): HCO_3 scatter, model and Forecast graph at point 4

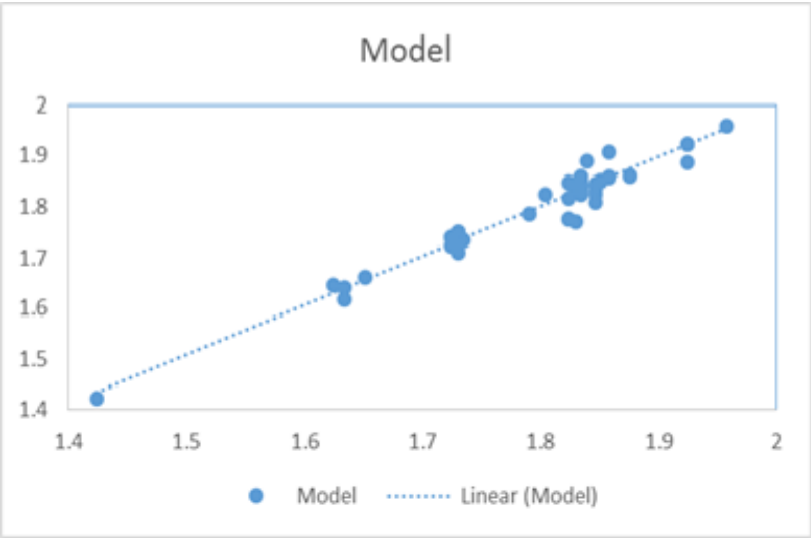

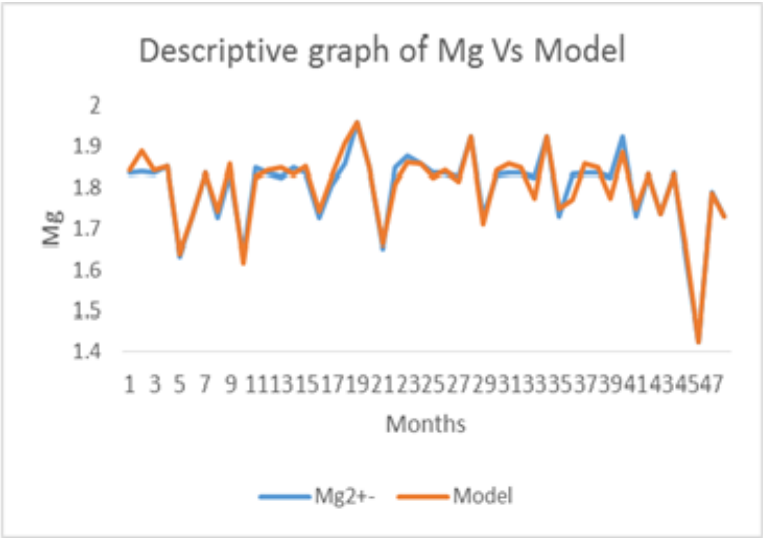

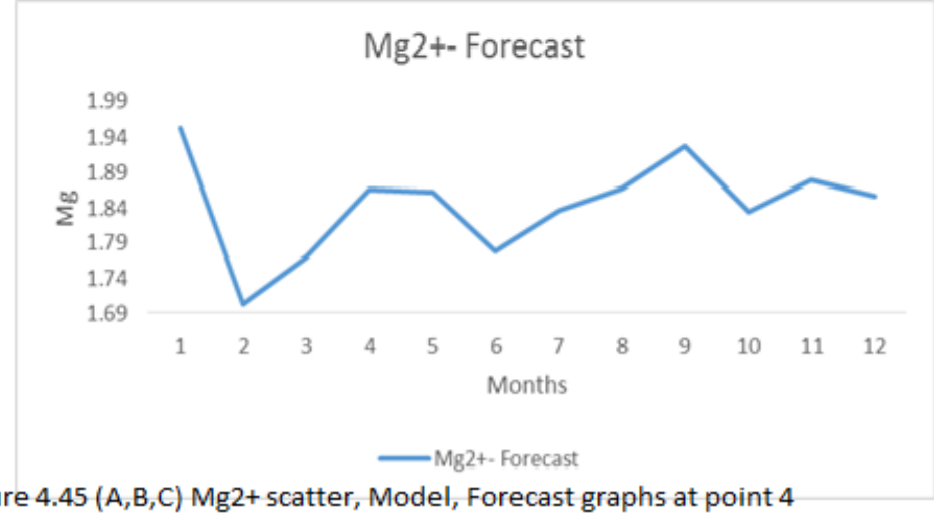

Figure 4.45 (A,B,C) Mg2+ scatter, Model, Forecast graphs at point 4

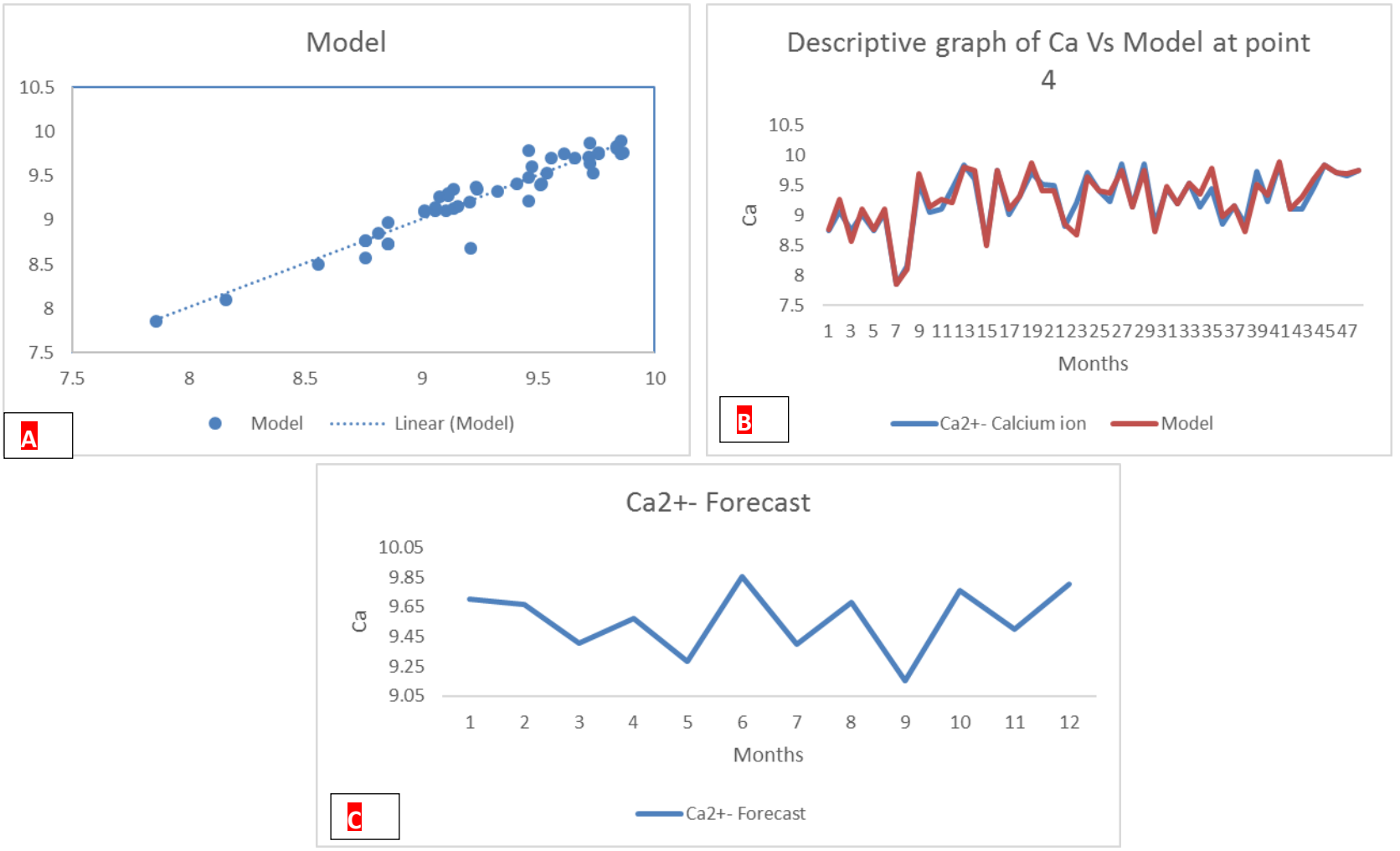

Figure 4.46 (A, Band C): Ca scatter, model and Forecast graph at point 4

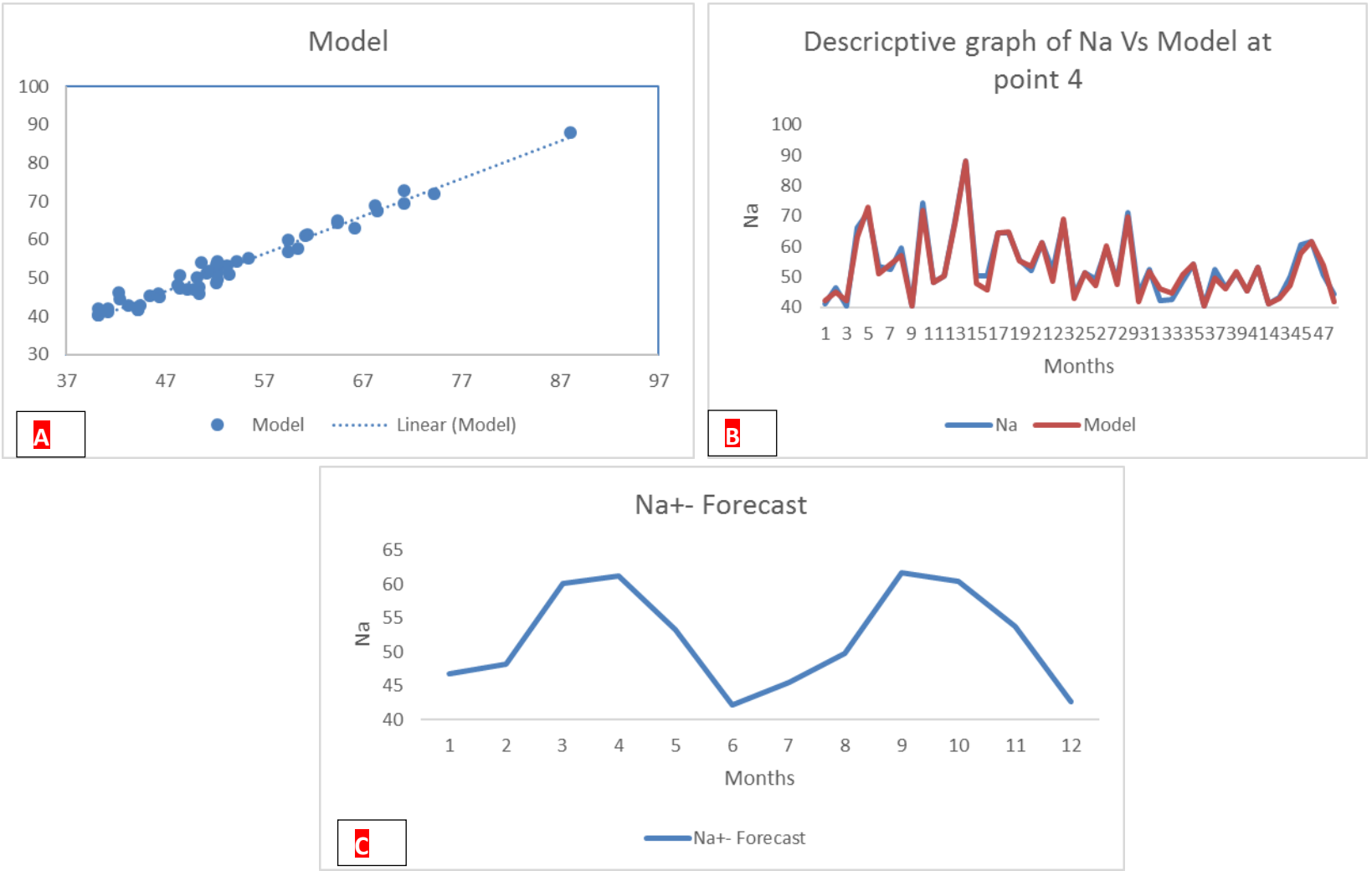

Figure 4.47 (A, Band C): Na scatter, model and Forecast graph at point 4

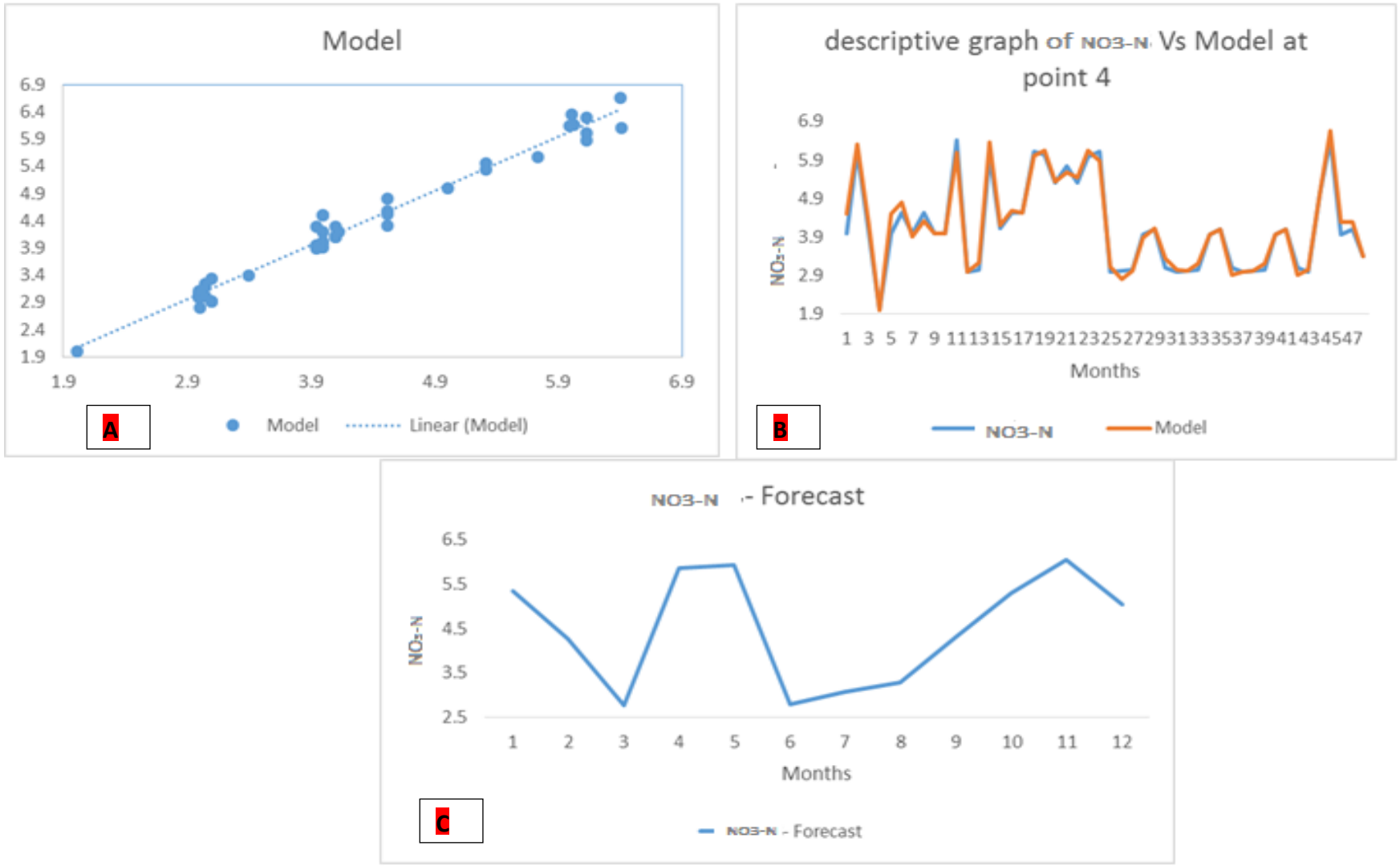

Figure 4.48 (A, Band C): NO_3-N Scatter, Model and forecast graph at point 4

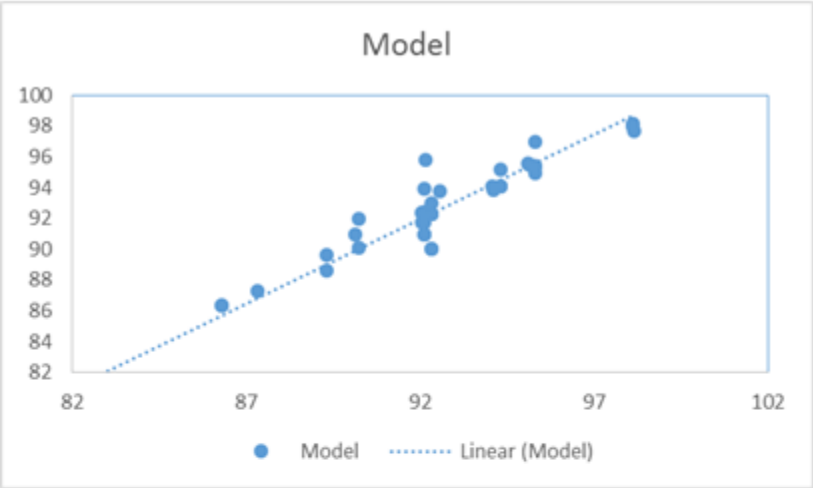

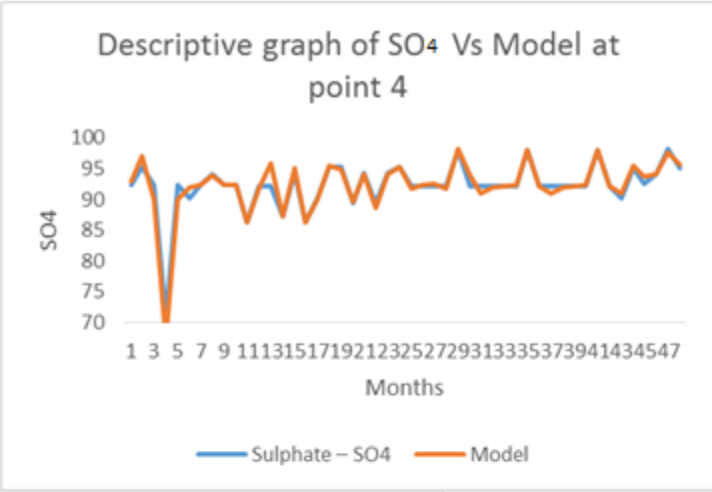

Figure 4.49 (A,B,C) : SO_4 scatter, Model and forecast point 4

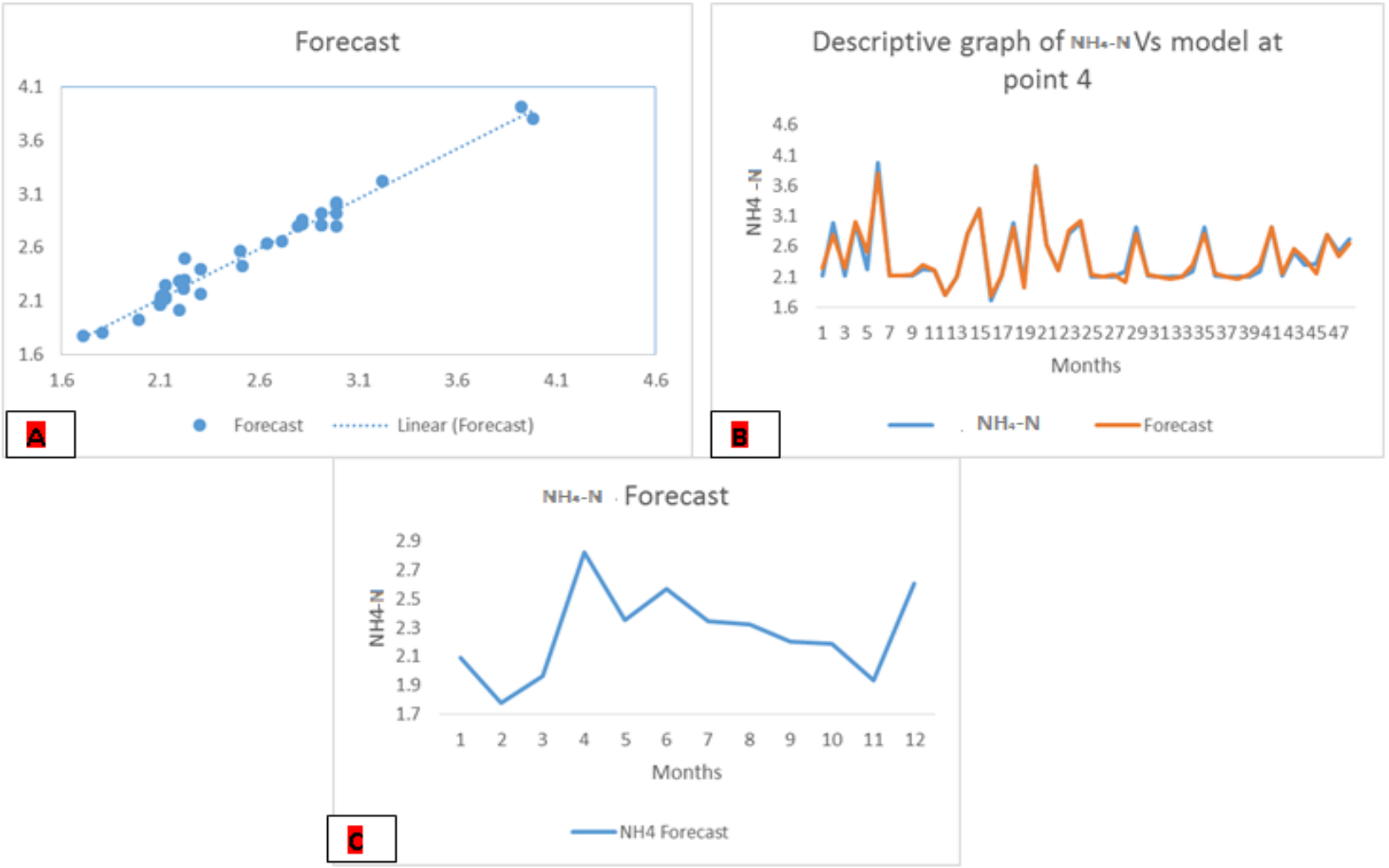

Figure 4.50 (A, Band C): NH_4-N Scatter, Model and Forecast graph at point 4

Similar to the water quality parametric behaviors at point 1 to 4, it was equally observed generally that at point 5, the ANN asymptotically modeled the water quality dataset very well, as the scattered plot point were seen to be very close to the line of best fit. Comparing the ANN model with the actual, the deviations were not significant. The forecast for all the water quality parameters at point 4 showed continues changes of the values over time.

From the graphical representations, the forecast and model for pH, HCO_{3-} , Mg, Ca, NO_3-N, NH_4-N were within the permissible range while, SO_4 exceeded the FAO permissible standard. Except for the 5th and 7th months from the forecast graphs for TDS and EC respectively, the values were within the permissible range while Na at most instance in the model and forecast exceeded the FAO permissible standard.

SO_4 exceeded the permissible range throughout the forecast due to the impacts of the discharge and dead leaves from the surrounding trees or of atmospheric deposition of water passing through rock or containing common minerals and gypsum. TDS at 5^{th} month exceeded the permissible range for the forecast. This could be as a result of the fluid dynamics and pollutant effects from nearby farmlands. EC at the 7^{th} month exceeded the permissible range due to the low rainfall effect which increased the pollution level thus promoting high electric conductivity in the water body.

The point 5 descriptive scattered graphs, the actual and model graphs of the developed ANN model, and forecast graphs for the next one year are shown in Figures 4.51 to 4.60.

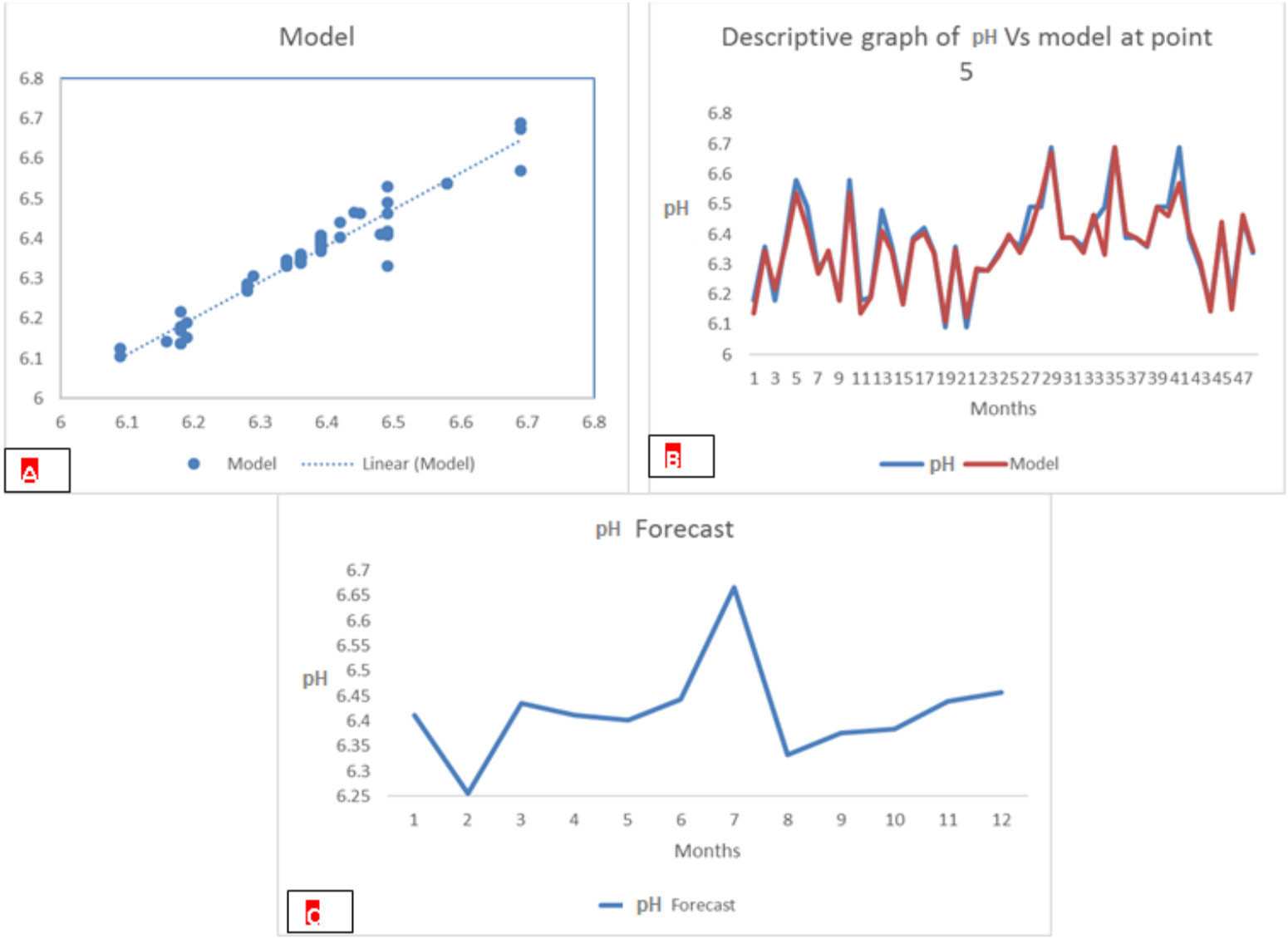

Figure 4.51 (A, Band C): Ph scatter, model and Forecast graph at point 5

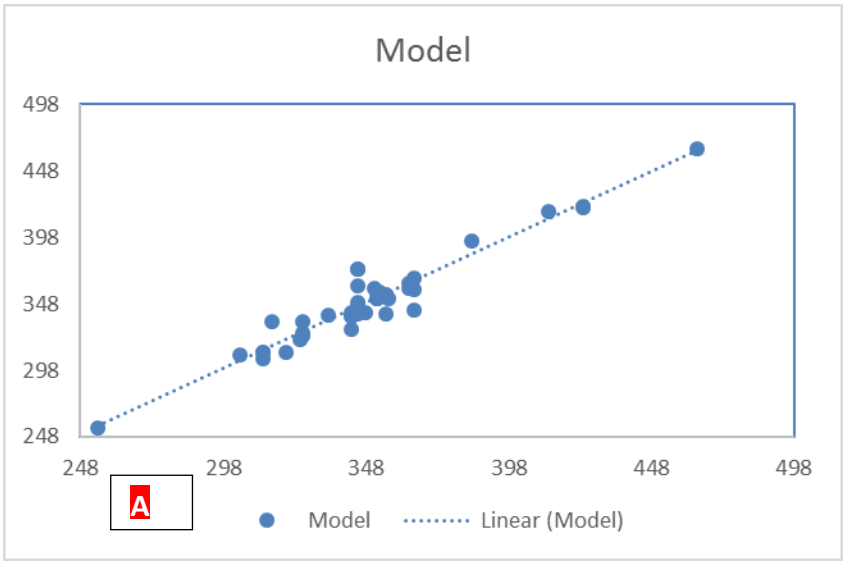

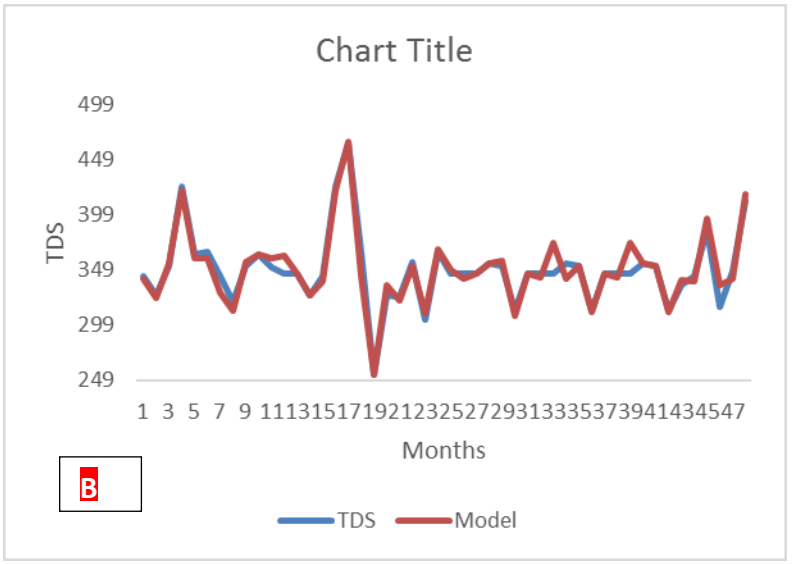

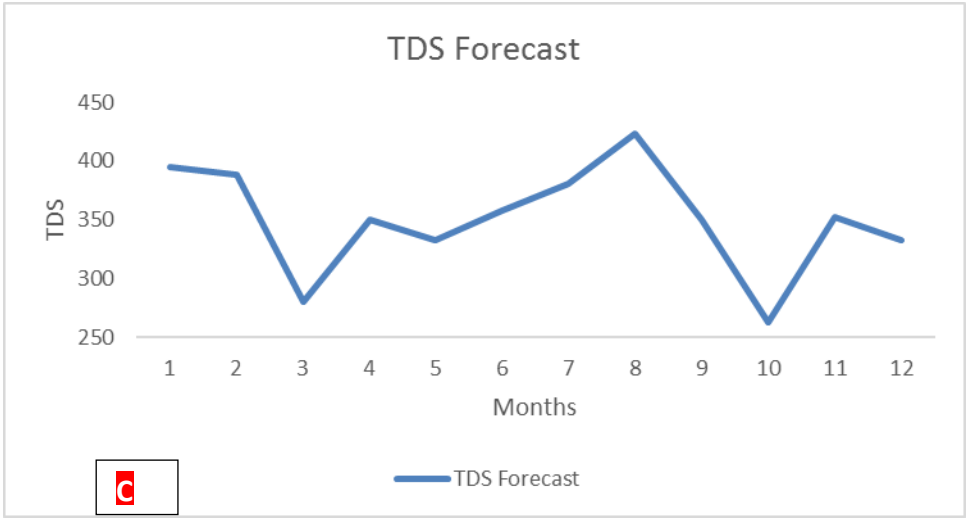

Figure 4.52 (A, Band C): TDS scatter, model and Forecast graph at point 5

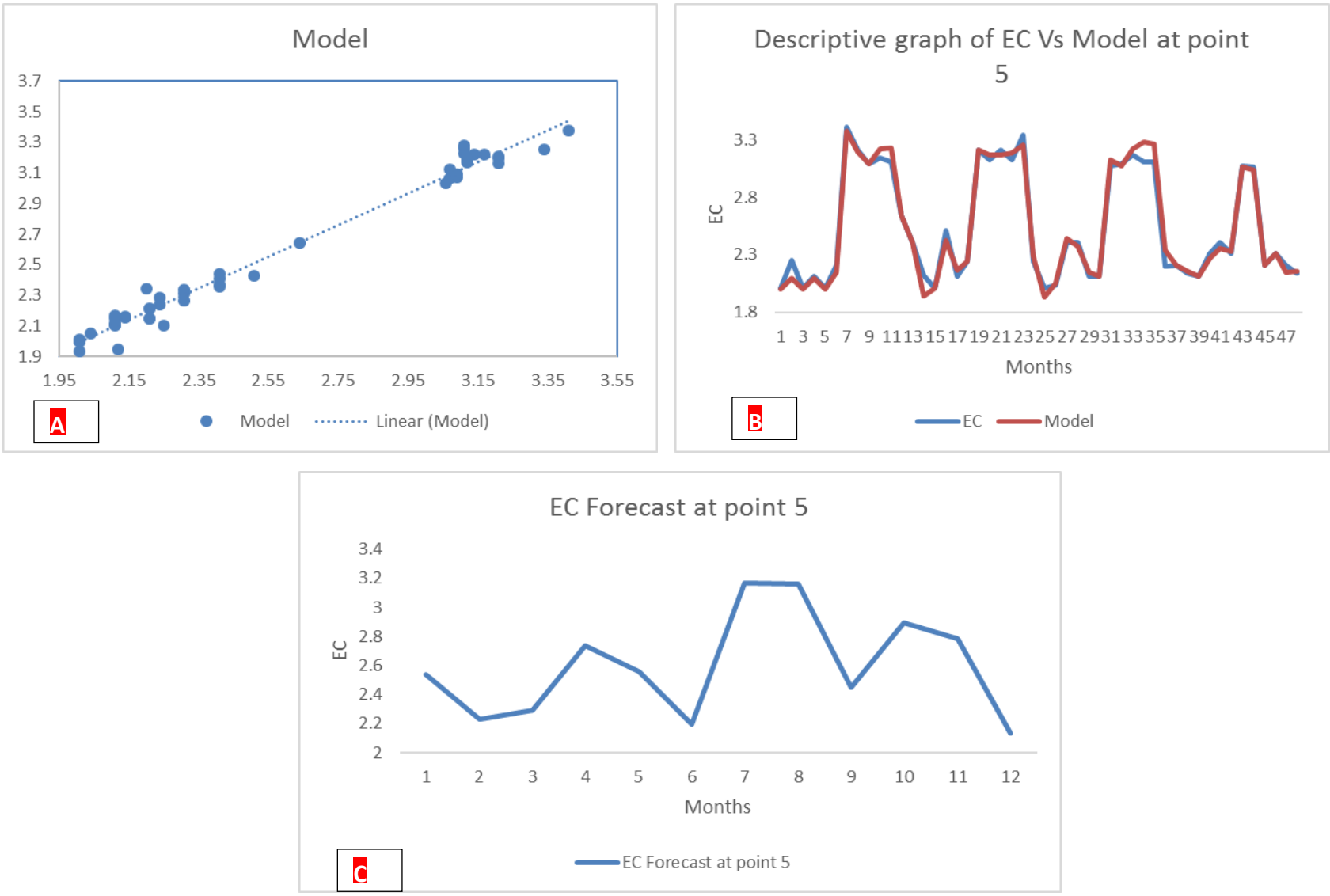

Figure 4.53 (A Band C): EC scatter, model and Forecast graph at point 5

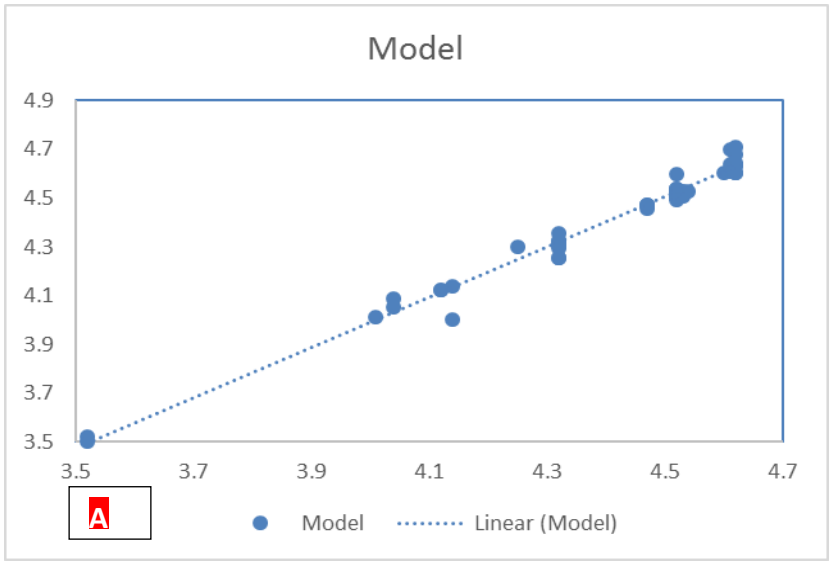

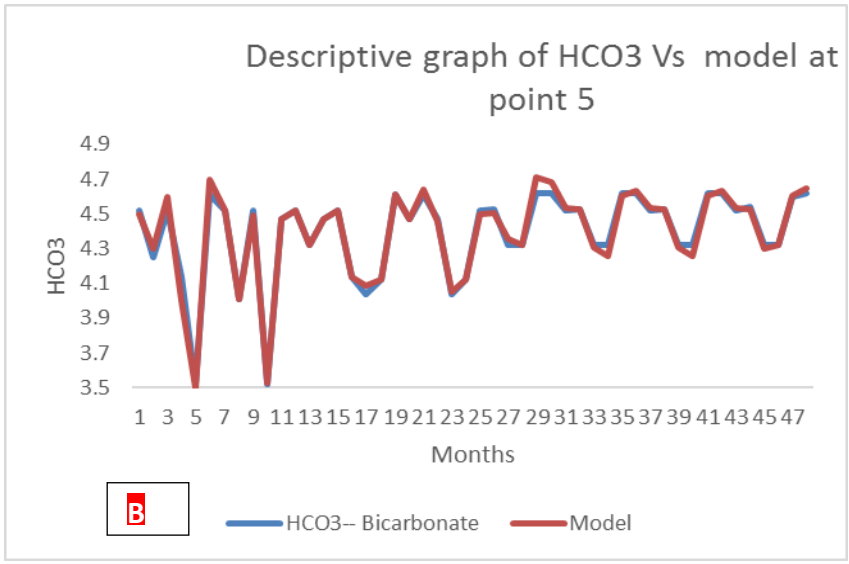

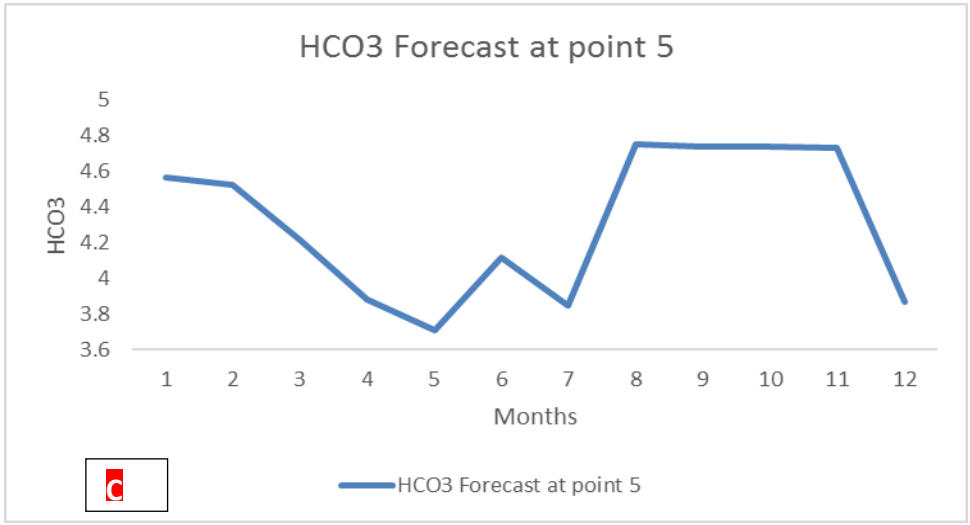

Figure 4.54 (A Band C): HCO_3 scatter, model and Forecast graph at point 5

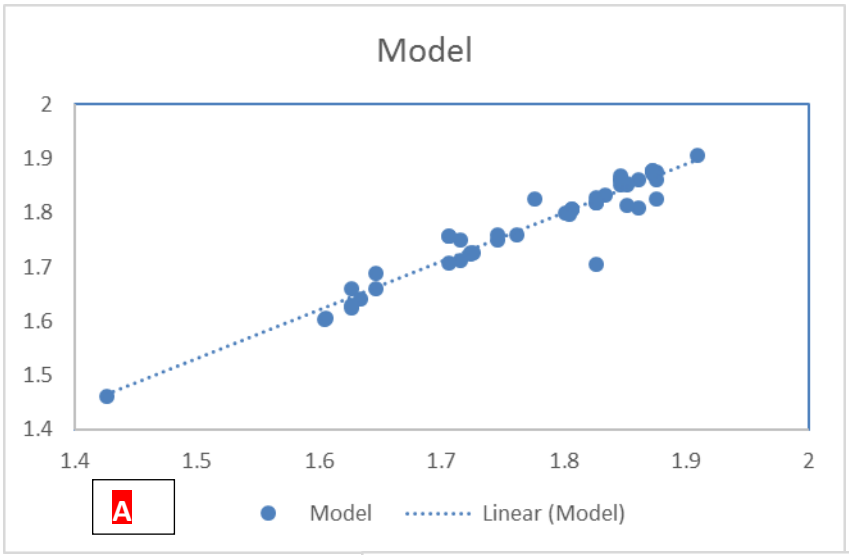

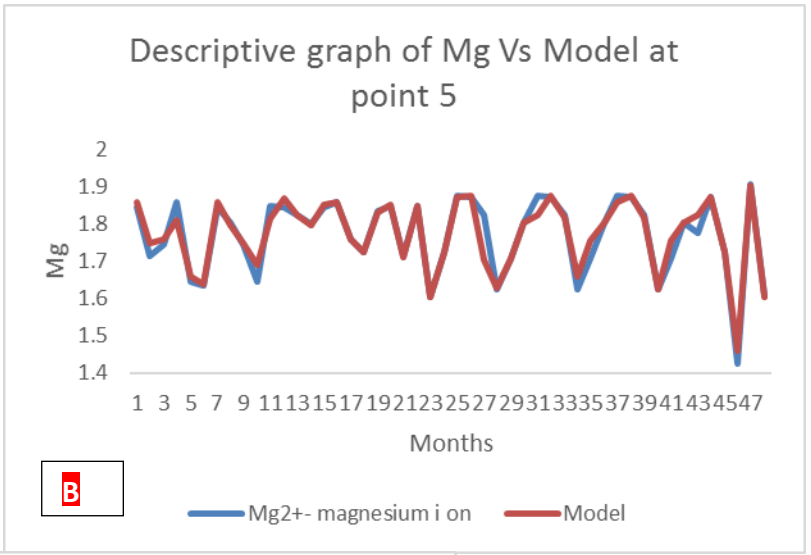

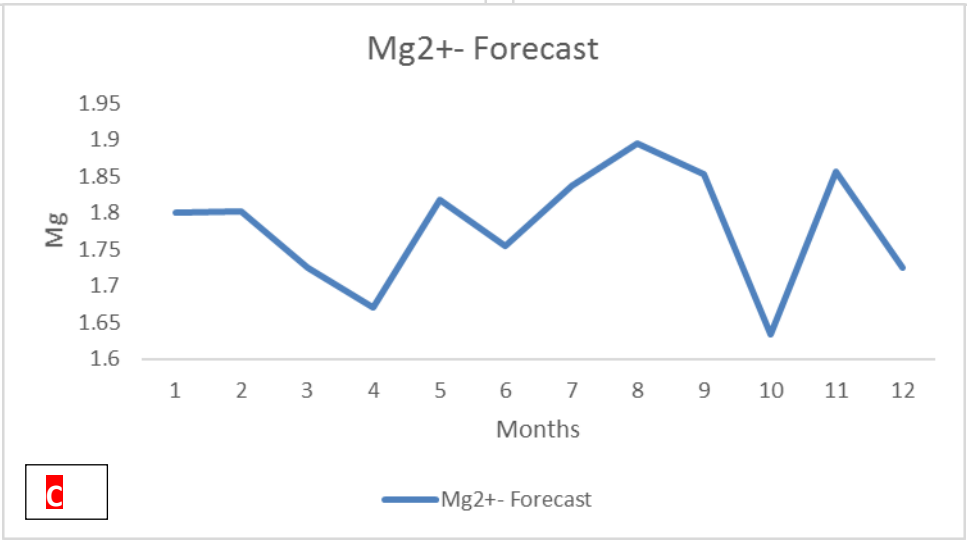

Figure 4.55 (A, Band C): Mg scatter, model and Forecast graph at point 5

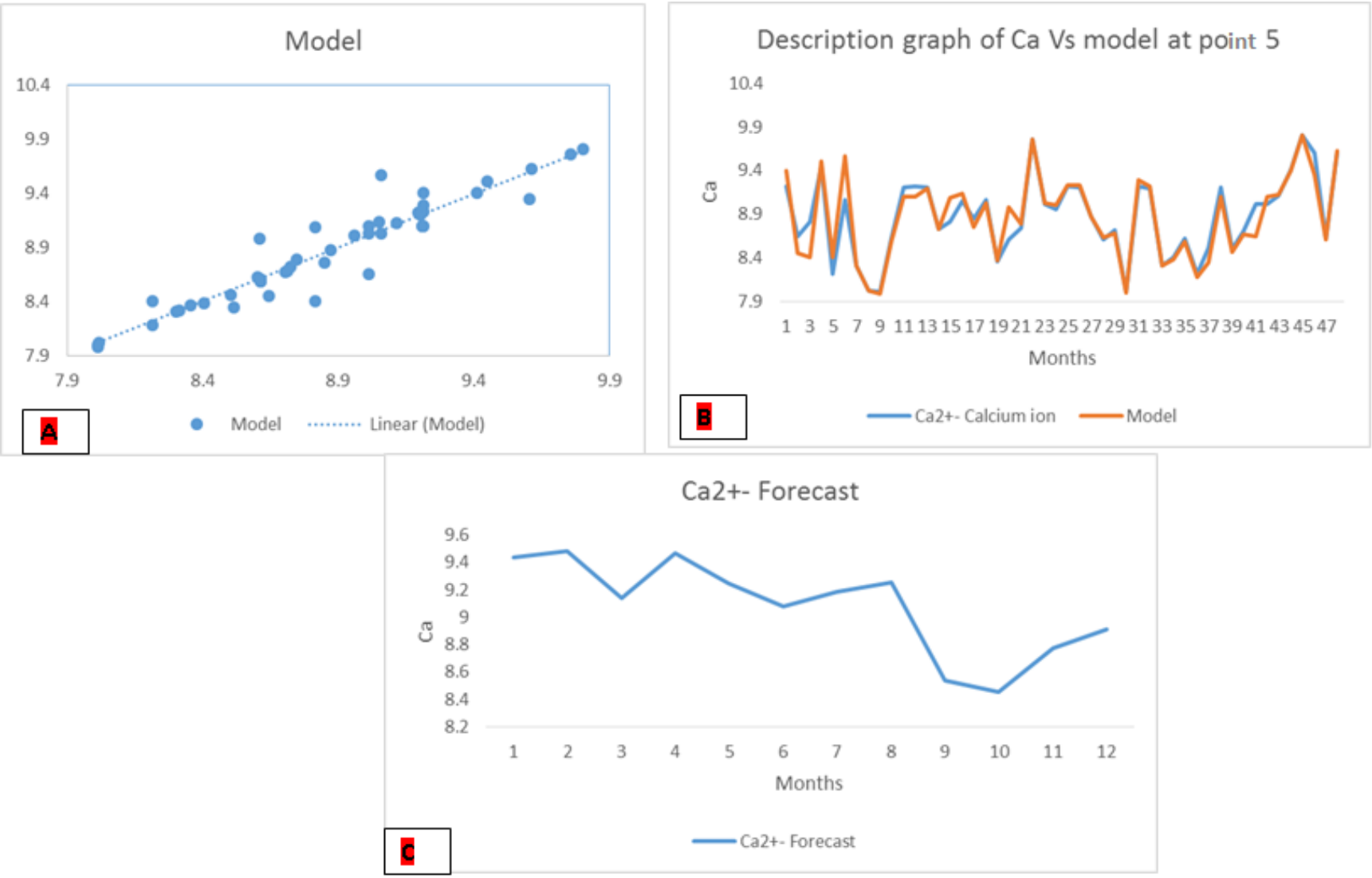

Figure 4.56 (A, Band C): Ca scatter, model and Forecast graph at point 5

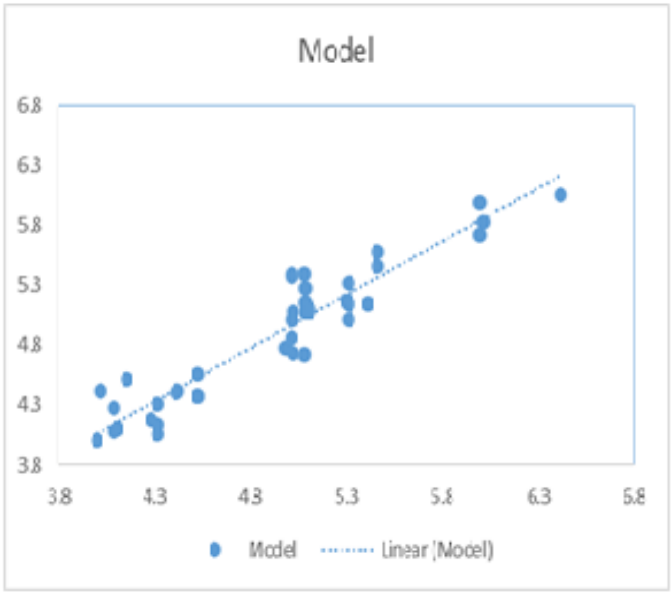

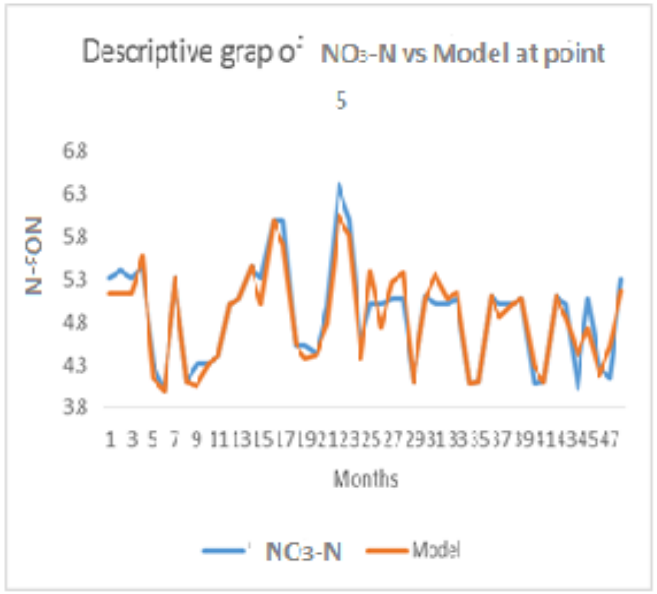

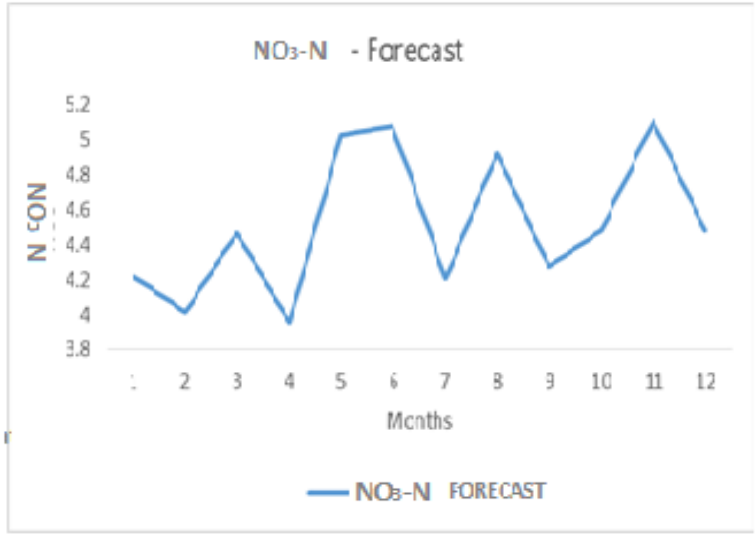

Figure 4.57 (A, Band C): NO_3-N scatter, model and Forecast graph at point 5

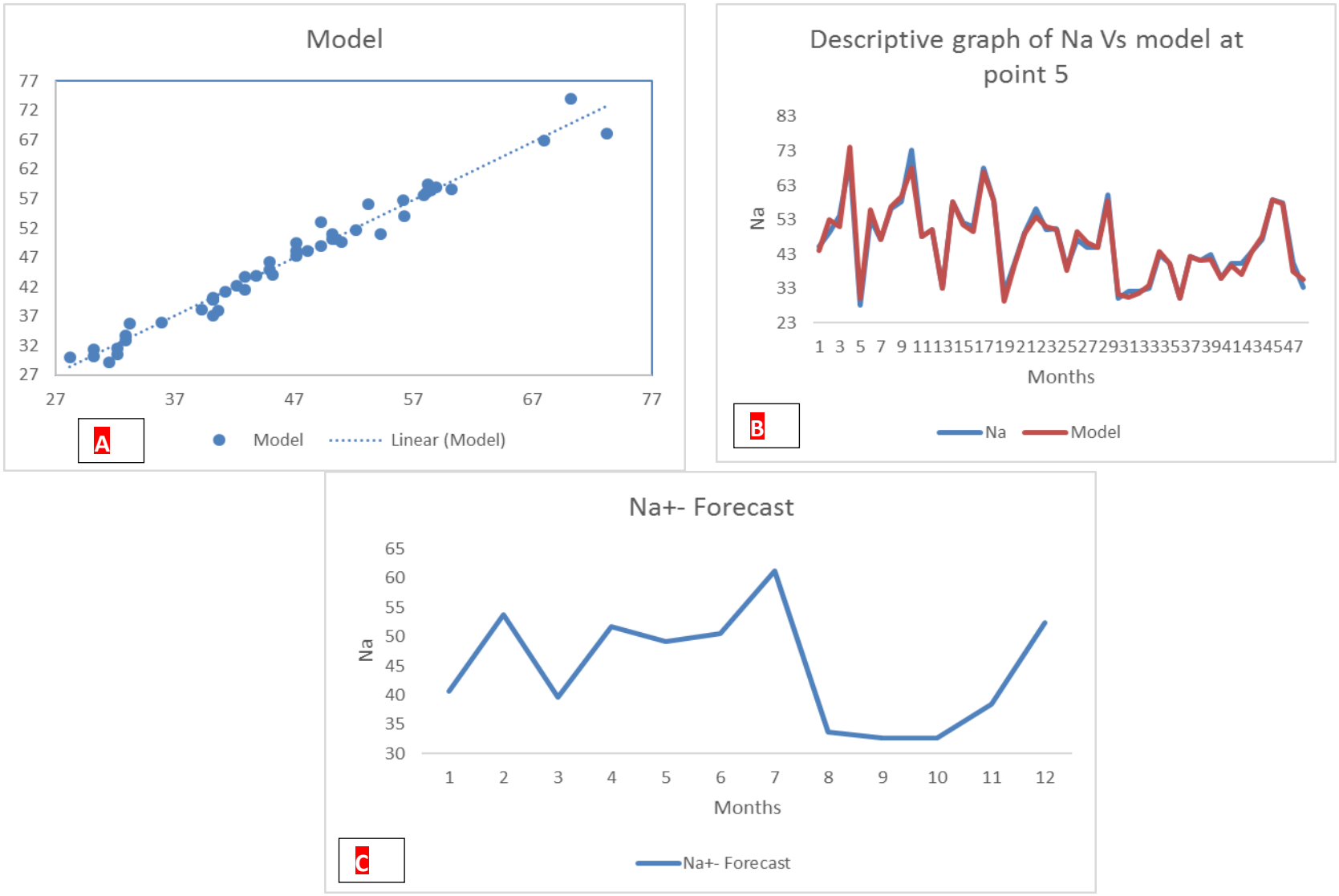

Figure 4.58 (A, Band C): Na scatter, model and Forecast graph at point 5

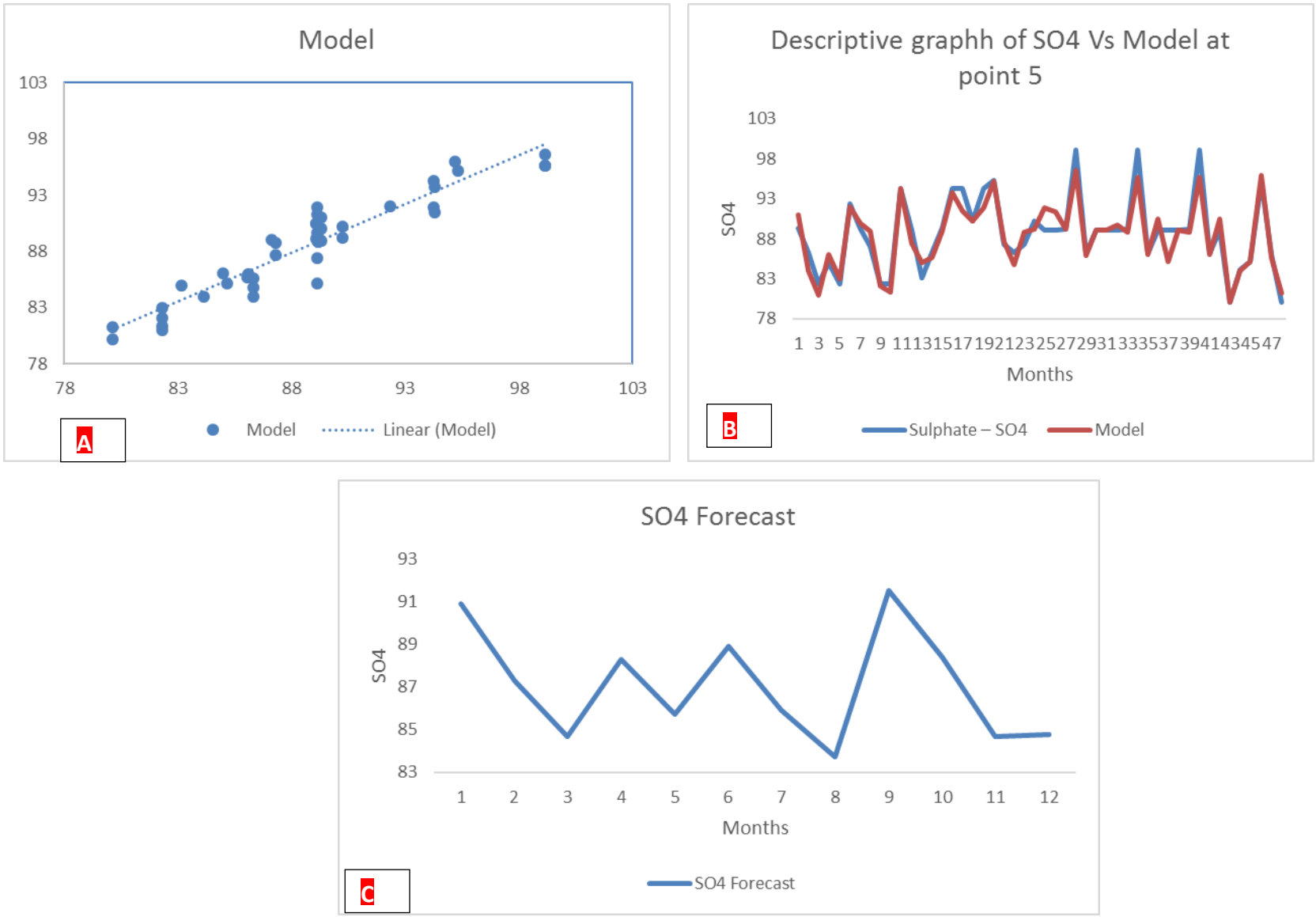

Figure 4.59 (A, Band C): SO_4 scatter, model and Forecast graph at point 5

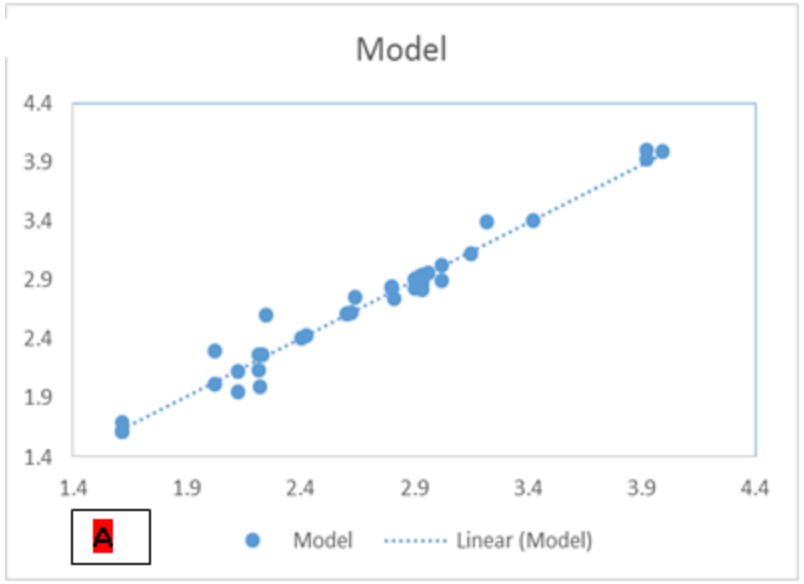

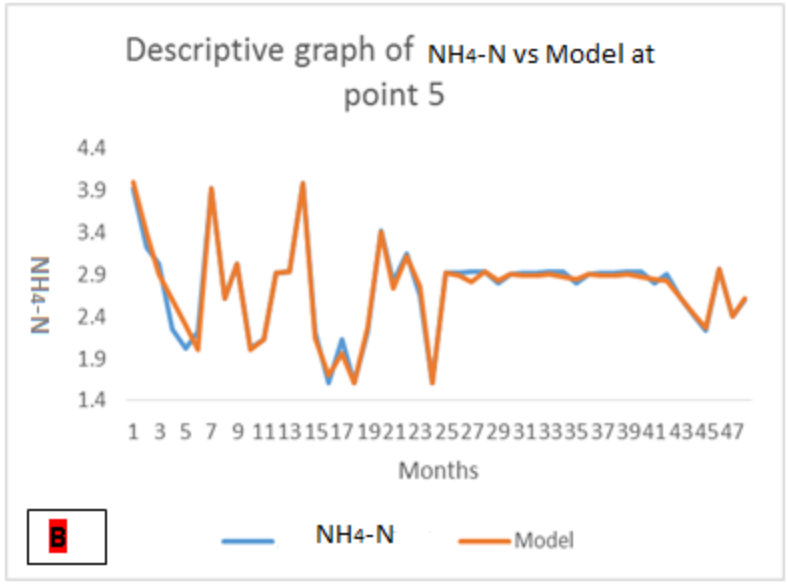

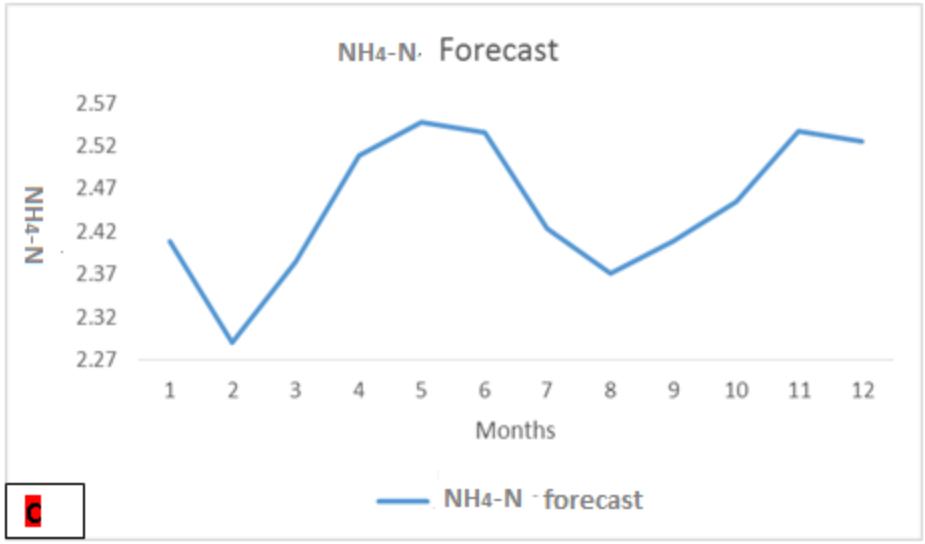

Figure 4.60 (A, Band C): NH4-N scatter, Model and forecast graphs at point 5

Akin to the water quality parametric behaviors at point 1 to 5, it was generally observed that at point 6, the ANN practically modeled the water quality dataset very well, as the scattered plots were seen to be very close to the line of best fit. Comparing the ANN model with the actual or observed dataset, the deviations were not significant. The forecast for all the water quality parameters at point 6 showed continuous changes of values over time.

However, the parameters at most instances showed sinusoidal patterns at different points due to the impacts of the rainy and dry seasons. The forecast during the dry seasonal months showed higher concentration of pollutants such as seen in the highest value of the TDS forecast at the 9^{th} month. It is noteworthy that as the water flow from point I at the upstream down to point 6 at the downstream section of the water body. The pollution impacts became lesser since most parameters were within the FAO permissible range which implies safety.

From the appendix, Ca, Na, NO_3-N in Figures 4.66, 4.67 and 4.68, respectively showed that the forecast graphs had similar pattern as they alternately moved up and down linearly along the months of forecast which could be as a result of fluid dynamics and fluctuation in the sediment transportation and deposition along the sampling points. From the graphical representations, the forecast and model for pH, TDS, EC, HCO_3^- , Mg, Ca, NO_3-N, NH_4-N were within the permissible range, while Na and SO_4 exceeded the FAO permissible standard. Sodium had a high concentration beyond the permissible standard due to the high concentration of salts from nearby processing and production industries.

The Point 6 descriptive scattered graphs, the actual and model graphs of the developed ANN model, and forecast graphs for the next one year are shown in the appendix, from fig.4.61 to 4.67.

Just like to the water quality parametric behaviors at point 1 to 6, it was generally observed that at point 7 that the ANN basically modeled the water quality dataset very well, as the scattered plot point were seen to be very close to the line of best fit. Comparing the ANN model with the actual or observed dataset, the deviations were not significant. The forecast for all the water quality parameters at point 4 showed continuous changes of the values over time.

Conversely, there was sinusoidal pattern in most of the model and forecast graphs which was clearly shown in the alternate graphical presentations in some parameters such as pH, SO_4, Mg and NO_3-N due to fluid dynamics in the water body. From the appendix, EC forecast graph as shown in Figure 4.73 revealed that the EC attained the highest forecast values in the 7^{th} month which falls in the dry season due to high concentration of ions and inorganic substances. The HCO_3^- in Figures 4.74 maintained a stable increase between the 5^{th} month till the 12^{th} month. Figure 4.76 showing the Ca forecast graph indicated that the forecast has an increasing sinusoidal relationship with time of forecast.

However, Figure 4.80 shows that the NH_4-N forecast graph has a horizontal linear variation with time till the 5^{th} month before showing a sinusoidal pattern throughout the remaining period of forecast. From the graphical representations, the forecast and model for pH, TDS , EC, HCO_3^- , Mg, Ca, NO_3-N, NH_4-N were within the permissible range, while Na and SO_4 exceeded the FAO permissible standard.

The Point 7 descriptive scattered graphs, the actual and model graphs of the developed ANN model and forecast graphs for the next one year are shown in the appendix from figures 4.71 to 4.8.

Just like the water quality parametric behaviors at point 1 to 7, it was generally observed that at point 8, the ANN practically modeled the water quality dataset very well, as the scattered plot points were seen to be very close to the line of best fit. Comparing the ANN model with the actual or observed dataset, the deviations were not significant. The forecast for all the water quality parameters at point 4 showed continues changes of the values over time.

However, from the appendix, pH, EC and Mg forecast descriptive graph as shown in Figures 4.81, 4.83 and 4.85, respectively, shows that the forecast graphs alternate up and down pattern over the entire forecast period but the Mg had its lowest forecast values at the 10^{th} month unlike the pH and EC. Equally, Figures 4.82, 4.86 and 4.87 showing the TDS, Ca and Na forecast graphs, respectively, reveal that the forecast gradually decreased with time of forecast. The HCO_3^- forecast graph as shown in Figure 4.84, shows that the forecast graph horizontally alternate up and down relationship with respect to time of forecast and however, attained to two highest forecast values at the 3^{rd} and 8^{th} month respectively. Figure 4.88 and 4.89 showing the NO_3-N and SO_4^-, gradually increase with time of forecast and had its highest forecast values at the 12^{th} month. Hence, NH_4-N as shown in Figure 4.90 revealed from the graph a sinusoidal forecast pattern along the line of best fit with respect to the time of forecast. From the graphical representations, the forecast and model for pH, TDS, EC, HCO_3^- , Mg, Ca, NO_3-N, NH_4-N were within the permissible range, while Na and SO_4 exceeded the FAO permissible standard.

The Point 8 descriptive scattered graphs, the actual and model graphs of the developed ANN model, and forecast graphs for the next one year are shown in appendix from figures 4.81 to 4.90.

Equally like the water quality parametric behaviors at point 1 to 8, it was generally observed that at point 9, the ANN practically modeled the water quality dataset very well, as the scattered plot points were seen to be very close to the line of best fit. Comparing the ANN model with the actual or observed dataset, the deviations were not significant. The forecast for all the water quality parameters at point 9 showed continues changes of the values over time.

However, the pH model and forecast graphs were within the permissible range as shown in the appendix in figure 4.91. TDS forecast descriptive graph as shown in Figure 4.92 shows alternate up and down forecast pattern along the line of best fit with respect to time of forecast, the TDS has the highest forecast value 9^{th} month due to the high concentration of inorganic substances and pollutants in the dry season. Figure 4.93 showing the EC forecast graph which was has the highest concentration at the 6^{th} month close to the dry seasonal period. It should be noted that the pollutant concentrations at point 9 were very low due to ion dissolutions from point 1 to 9 and the fluid dynamics which has less effect downstream at the 9^{th} point. Figure 4.95 which presented the forecast graph of Mg, showed an alternate up and down pattern down to the time of forecast. Also, Figures 4.96 and 4.98 which shows that the Ca and NO_3-N forecast graphs gradually increased to the highest forecast values at the 8^{th} month. It was also observed that SO_4 and NH_4-N had their highest forecast value at the 6^{th} and 7^{th} months and lowest values at 2^{nd} and 4^{th} months respectively. These graphical presentations showed the high impact of pollutants in the dry season than the wet season. From the graphical representations, the forecast and model for pH, TDS, EC, HCO_3^-, Mg, Ca, NO_3-N, NH_4-N were within the permissible range, while Na and SO_4 exceeded the FAO permissible standard due to high concentration of sodium salts and decay of dead leaves from surrounding trees respectively.

The Point 9 descriptive scattered graphs, the actual and model graphs of the developed ANN model, and forecast graphs for the next one year are shown in the appendix from figures 4.91 to 4.100.

Point 10 descriptive scattered graphs, the actual and model graphs of the developed ANN model, and forecast graphs for the next one year are shown in the appendix from figures 4.101 to 4.110.

Similar to the water quality parametric behaviors at point 1 to 9, it was generally observed that at point 10, the ANN basically modeled the water quality dataset very well, as the scattered plot point were seen to be very close to the line of best fit. Comparing the ANN model with the actual or observed dataset, the deviations were very close. The forecast for all the water quality parameters at point 10 showed continues changes in the values over time of forecast.

The pH, TDS, Ca, Na and NH_4-N descriptive forecast graph as shown in figures 4.101, 4.102, 4.106, 4.107 and 4.10, respectively, shows that there was an alternate up and down pattern of the forecast with respect to time as a result of ion dissolutions and fluid dynamics along the sampling points at different months.

The HCO_3 as shown in figure 4.104 shows slightly decrease with respect to the forecast time in an alternate up and down pattern, though the parameter was within the FAO permissible standard. From the graphical representations, the forecast and model for pH, TDS, EC, HCO_3^- , Mg, Ca, NO_3-N, NH_4-N were within the permissible range, while Na and SO_4 exceeded the FAO permissible standard.

4.5 Feed forward Multilayer Neural Network (FFMNN) Model Performance Evaluation Results

The model performance evaluation was carried out based on the ANN model training, Testing and forecast, respectively. The model performance evaluation was carried out using coefficient of multiple determinations, R^2 . The R^2 values `was generally observed to have varied in the second decimal place for the training, testing and forecast model, respectively.

The training performance evaluation shows that R^2 values ranges from 0.981 to 0.990, 0.981 to 0.988, 0.981 to 0.989, 0.982 to 0.989, 0.983 to 0.990, 0981 to 0.989, 0.981 to 0.985, 0.981 to 0.988, 0.981 to 0.988 and 0.983 to 0.990 for pH, TDS, EC, Mg, Ca, Na, NO_3-N, SO_4, NH_4-N, and HCO_3, respectively. The training results show that the Ca and Ph models have the best performance followed by EC, Mg and Na whereas NO_3-N has the least training performance.

Also, the testing performance shows that the R^2 value ranges from 0.952 to 0.967, 0.953 to 0.970, 0.951 to 0.967, 0.951 to 0.969, 0.951 to 0.968, 0.953 to 0.968, 0.952 to 0.968, 0.951 to 0.969, 0.952 to 0.968 and 0.954 to 0.964 for pH, TDS, EC, Mg, Ca, Na, NO_3-N, SO_4, NH_4-N, and HCO_3^-, respectively. However, the testing performance evaluation shows that TDS had the best performance followed by Mg and SO_4^- while the EC had the least testing performance.

The forecast performance evaluation shows that the R^2 values ranges from 0.945 to 0.968, 0.946 to 0.968, 0.944 to 0.967, 0.948 to 0.969, 0.944 to 0.967, 0.949 to 0.965, 0.944 to 0.963, 0.941 to 0.968, 0.940 to 0.967 and 0.944 to 0.970 for pH, TDS, EC, Mg, Ca, Na, NO_3-N, SO_4, NH_4-N, and HCO_3, respectively. It was however discovered that HCO_3

made the best forecast performance followed by Mg, TDS and pH, hence, NO_3-N made the least forecast performance. The water quality forecast performance was further evaluated using the Root Mean Squared Error (RMSE) which ranges from 0.022 to 0.088, 0.012 to 0.087, 0.015 to 0.085, 0.019 to 0.080, 0.010 to 0.082, 0.014 to 0.084, 0.014 to 0.086, 0.036 to 0.083, 0.030 to 0.090 and 0.032 to 0.089 for pH, TDS, EC, Mg, Ca, Na, NO_3-N, SO_4^-, NH_4-N, and HCO_3 respectively. The ANN model performed very well as their coefficient of multiple determination R^2 were very close 1, this is in agreement with the study of Awu et al (2017). On comparing the performance of the training model to the testing model and forecast, it shows that the training set performed better than the testing set followed by the forecast as its coefficient of multiple determinations, R^2, was closer to 1. The results are shown in Table 4.11.

Table 4.11: Statistical measurement of the trained, test and forecast model

Parameters	Stat. Measurement	P1	P2	P3	P4	P5	P6	P7	P8	P9	P10
pH	RSQUAD TRAIN.	0.981	0.983	0.982	0.990	0.989	0.981	0.985	0.987	0.986	0.987
	RSQUAD TEST	0.956	0.955	0.959	0.955	0.959	0.954	0.953	0.960	0.967	0.952
	RSQUAD FORECAST	0.962529	0.965922	0.959714	0.948418	0.961076	0.944764	0.949791	0.958201	0.962208	0.968347
	RMSE	0.048519	0.022088	0.026023	0.043385	0.054542	0.059115	0.087944	0.083779	0.05943	0.052658
TDS	RSQUAD TRAIN.	0.981	0.985	0.982	0.981	0.988	0.984	0.986	0.986	0.980	0.988
	RSQUAD TEST	0.959	0.970	0.964	0.954	0.962	0.954	0.955	0.956	0.953	0.954
	RSQUAD FORECAST	0.947682	0.965259	0.949851	0.945909	0.96783	0.948007	0.956011	0.962332	0.969541	0.952878
	RMSE	0.043497	0.046244	0.011687	0.055819	0.077468	0.064128	0.048192	0.087253	0.086125	0.071935
EC	RSQUAD TRAIN.	0.989	0.982	0.984	0.982	0.987	0.981	0.981	0.982	0.988	0.989
	RSQUAD TEST	0.967	0.959	0.951	0.954	0.961	0.953	0.967	0.966	0.952	0.953
	RSQUAD FORECAST	0.952864	0.95328	0.946784	0.947022	0.94404	0.944837	0.966768	0.963408	0.965003	0.944238
	RMSE	0.015462	0.017259	0.028919	0.080258	0.014895	0.06217	0.055331	0.085234	0.044357	0.069521
HCO_3	RSQUAD TRAIN.	0.989	0.986	0.984	0.985	0.983	0.99	0.987	0.983	0.986	0.983
	RSQUAD TEST	0.959	0.97	0.964	0.954	0.962	0.954	0.955	0.956	0.953	0.954
	RSQUAD FORECAST	0.968	0.959	0.944	0.957	0.943	0.970	0.963	0.959	0.954	0.944
	RMSE	0.051	0.077	0.089	0.076	0.072	0.036	0.083	0.045	0.032	0.030

Parameters	Stat. Measurement	P1	P2	P3	P4	P5	P6	P7	P8	P9	P10
Mg	RSQUAD TRAIN.	0.983	0.985	0.983	0.984	0.988	0.984	0.988	0.989	0.982	0.986
	RSQUAD TEST	0.951	0.954	0.962	0.964	0.964	0.954	0.969	0.964	0.959	0.961
	RSQUAD FORECAST	0.95379	0.950392	0.968715	0.952689	0.948963	0.965467	0.945192	0.947648	0.952362	0.956049
	RMSE	0.019363	0.05505	0.048705	0.056488	0.034202	0.075961	0.051718	0.024126	0.079541	0.060346
Ca	RSQUAD TRAIN.	0.989	0.986	0.984	0.985	0.983	0.990	0.987	0.983	0.986	0.983
	RSQUAD TEST	0.956	0.951	0.967	0.954	0.953	0.968	0.965	0.963	0.965	0.967
	RSQUAD FORECAST	0.954298	0.968227	0.955597	0.965481	0.946467	0.966722	0.955945	0.944406	0.957334	0.948506
	RMSE	0.081916	0.06988	0.07403	0.059301	0.044806	0.020855	0.02543	0.022249	0.054022	0.010422
Na	RSQUAD TRAIN.	0.986	0.984	0.988	0.985	0.987	0.981	0.987	0.980	0.989	0.983
	RSQUAD TEST	0.966	0.953	0.968	0.956	0.966	0.960	0.958	0.954	0.957	0.962
	RSQUAD FORECAST	0.961157	0.958157	0.950361	0.94929	0.965393	0.954874	0.958709	0.968416	0.956506	0.953078
	RMSE	0.031175	0.067912	0.023904	0.013521	0.02325	0.084216	0.073181	0.063805	0.040121	0.044364
NO_3-N	RSQUAD TRAIN.	0.982	0.981	0.985	0.983	0.982	0.985	0.980	0.984	0.985	0.985
	RSQUAD TEST	0.952	0.957	0.965	0.965	0.968	0.966	0.956	0.955	0.961	0.964
	RSQUAD FORECAST	0.968438	0.959323	0.944192	0.956736	0.943452	0.967848	0.963289	0.959329	0.954369	0.94399
	RMSE	0.058739	0.014253	0.031912	0.085981	0.043702	0.047589	0.054254	0.030811	0.076926	0.074946
SO_4	RSQUAD TRAIN.	0.987	0.983	0.988	0.986	0.981	0.982	0.984	0.987	0.983	0.982
	RSQUAD TEST	0.959	0.953	0.953	0.961	0.957	0.969	0.962	0.951	0.958	0.952

Parameters	Stat. Measurement	P1	P2	P3	P4	P5	P6	P7	P8	P9	P10
	RSQUAD FORECAST	0.963234	0.949192	0.941212	0.947577	0.959863	0.967899	0.947033	0.961154	0.955457	0.96385
	RMSE	0.080666	0.077558	0.04453	0.071262	0.046356	0.080473	0.084104	0.082727	0.07593	0.036253
NH_4-N	RSQUAD TRAIN.	0.982	0.980	0.984	0.982	0.986	0.981	0.986	0.983	0.984	0.988
	RSQUAD TEST	0.961	0.968	0.957	0.953	0.967	0.952	0.952	0.963	0.960	0.965
	RSQUAD FORECAST	0.965793	0.940461	0.941161	0.964714	0.952783	0.960323	0.95366	0.967191	0.956738	0.940378
	RMSE	0.05077	0.077434	0.089658	0.075673	0.071542	0.036217	0.083269	0.045091	0.032059	0.029734

4.6 River Water Quality Assessment for Irrigation Purposes

Considering the FAO Irrigation water quality permissible standards, the River water sampling points modeling and forecast will be evaluated for irrigation water quality assessment as Ele River receives effluents from industrial discharges. pH is a water quality parameter that measures the acidity or basicity of water. Mean values of pH over time were within the permissible range (6.0-8.5) for irrigation water quality assessment. At various sampling points, it shows insignificant values in deviation for the ANN model and actual. There were variations in the model and forecast over time though all were within the permissible standard. It is noteworthy that irrigation water with a pH outside the normal range may cause a nutritional imbalance or may contain a toxic ion which is harmful to crops, Westcot and Ayers, (1994).

The descriptive statistics over time shows that the TDS mean values range are from 357.98 to 2458.19, Standard deviation ranges from 49.312 to 127.36, respectively. The low values of standard deviation recorded in this study shows that the data sets were very close to the mean values of the data.

Figure 4.3 shows a continuous variation of TDS values at different instance. The highest concentrations occurred at Point 1 of November, 2017 and lowest concentration at points 10 of October 2017 and April 2018. It was observed that these high concentrations of TDS above the FAO permissible range occurred at the upstream section of the River most especially during dry season over time. These concentrations decrease along the sampling points going downstream. The potential sources of water contamination are geological formations, industrial and agricultural activities, and water treatment plants. These contaminants can be further categorized as microorganisms, inorganic, organics and disinfectants, Nollet, (2000). The decrease of the TDS concentration could be as a result of ion dissolutions and rainfall effects.

The ANN model and forecast of the TDS from points 1-10 considering the water quality permissible range, shows different variations seasonally such that the pollution levels during

dry season were higher than the rainy season since the TDS values during wet season were high from the point of discharge to points 3 due the presence of dissolved solids, ions and inorganic salts in the water at the entry points of the River which gradually decreases as the flow goes downstream due to ion dissolution which increases with the flow rate and rainfall occurrences. The presence of total dissolved solids was higher during dry season due to decrease in flow rate and absence of rainfall, thus increasing the TDS level so high beyond the permissible standard along the sampling points down to points 4 to 5. It is noteworthy that at several sampling points, there were insignificant deviations in values between the ANN model and actual. These high concentrations of TDS at the entry points towards the mid-point of the River are likely to increase the salinity and change the taste of the surface water, increase the electrical conductivity of the River system and as well decrease the dissolved oxygen level of the surface water making it difficult for survival of aquatic organisms.

Moreover, these anions and cations which increase the electric conductivity in water affect irrigation adversely since salts settle at crop root zones making it difficult for infiltration, absorption of moisture and nutrients necessary for crop production. Thus, the manageable source of water supply for irrigation can be at the last sampling points downstream which are not close to the bank of the River.

Electrical conductivity of the water is its ability to conduct electricity since the dissolved salts and inorganic substances are good electrical conductors in water. Increase in TDS mostly brings about increase in electrical conductivity of the River which in turn indicates increased concentration of sulphates and other ions which adversely affect the environmental ecosystem, Rajib et al. (2006). This high conductivity decreases along the sampling points going downstream. At high EC concentrations, the permissible range (0-3ds/m) was exceeded. High Electrical conductivity is an indicator of total salinity of which this contaminated points of the River can never be used for irrigation. When used will be harmful to crop due to absorption of salt at the crop root zone.

Bicarbonates over time showed a good range of mean values within the permissible range. It is noteworthy that high bicarbonates will possibly increase the soil, water ph and for irrigation which is detrimental to crop production due to unavailability of crop nutrients. This change in the water and soil ph will be as a result of change in the buffering capacity of soil and water. However, throughout the points modeling and forecast, HCO_3^- fall within the permissible limit. Magnesium over time was within the permissible range (0-5me/l) and at different points of modeling and forecast was also found to be normal. Same applies to the calcium level in the water.

From the descriptive statics of sodium over time in fig 4.6, it was observed that it exceeded the FAO permissible standards thereby affecting the hydraulic conductivity of soil water in crop production and weakening the soil structure (Warrence, 2003). This reduces infiltration of water into the soil of which may necessitate application of excessive water in the soil for proper absorption of moisture for crop production. At most sampling points along the River, sodium concentration was very high beyond the permissible level due to chemicals containing traces of salts from industries since sodium salts are used in water treatment, including corrosion control, pH adjustment, and coagulation, softening, disinfection in road de-icing and in the paper, glass, soap, pharmaceutical, chemical and food industries, (NAS, 1980).

From the descriptive statics of Nitrate Nitrogen over time and points modeling/forecast, the values were within the FAO permissible range. Nitrate Nitrogen refers to the Nitrogen present which is combined with nitrate ion, Westcot and Ayers, (1994). Nitrate nitrogen is the most abundant form of Nitrogen available for plant uptake due to conversion of ammonium fertilizers to nitrate by nitrification process, (Midwest, 2016). Its uptake is easily accomplished through water absorption.

The sulfate level from the descriptive statistics over time and from the point by points modeling and forecast so much exceeded the permissible range (0 – 20me/l). No doubts that these resultant effects were as a result of the effluent discharges and pollutants from the

surrounding trees. Ramp, (1996) described sulfate as naturally occurring as a result of municipal or industrial discharges since when naturally occurring, it can be as a result of breakdown of leaves that fall into the stream or of atmospheric deposition of water passing through rock or soil containing common minerals and gypsum. Its high concentrations in Ele River shows the high level of decomposition of leaves from most surrounding trees around the surface water and impacts of effluent discharges from the industrial clusters upland. Ammonium nitrogen (NH_4-N) over time and from the entire points modeling and forecast were within the permissible standard (0 – 5mg/l).

4.7 Velocity Distribution in Modeling and Simulation of Sediment Transport

Ele River flow is characterized by temporal pattern in the flow velocity, with higher values recorded during rainy season compared to the dry season values. It is widely accepted that the seasonal variation of river runoff depends on climate and catchment characteristics (Burt, 2013). Water temperature also had a temporal pattern, with high values obtained during dry season and lower values during the rainy season. The input values for velocity and temperature are as shown in Table 3.4.

Table 4.12 Input values for the turbulent flow module

No	Month	2018		2019	
		Velocity (m/s)	Temperature (^oC)	Velocity (m/s)	Temperature (^oC)
1	July	0.30	23.4	0.31	23.2
2	August	0.33	23.8	0.32	24.1
3	November	0.14	27.8	0.15	27.8
4	December	0.10	28.4	0.08	28.5

The generated 2D mesh of the river tributary is shown in Figure 4.61.

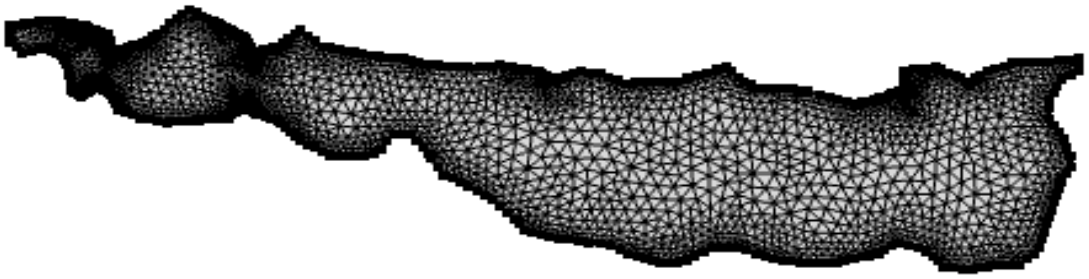

Fig 4.61: Generated 2D mesh of the river tributary

The number of elements involved in this geometry meshed model was 4,624 elements. The number of elements after the meshing process was constant for all flow conditions as the shape and the boundary position were the same for all the modeled flow conditions.

The model output for the two-dimensional velocity magnitudes in the river tributary, obtained for the different months in the first stage of simulation are visualized in figures 4.111 to 4.118. Based on colour range displayed outside the model, maximum flow velocity of the model can be determined. Flow velocity at locations within river tributary geometry can be identified by clicking at the point around the location and the system will pop-up the value of the velocity.

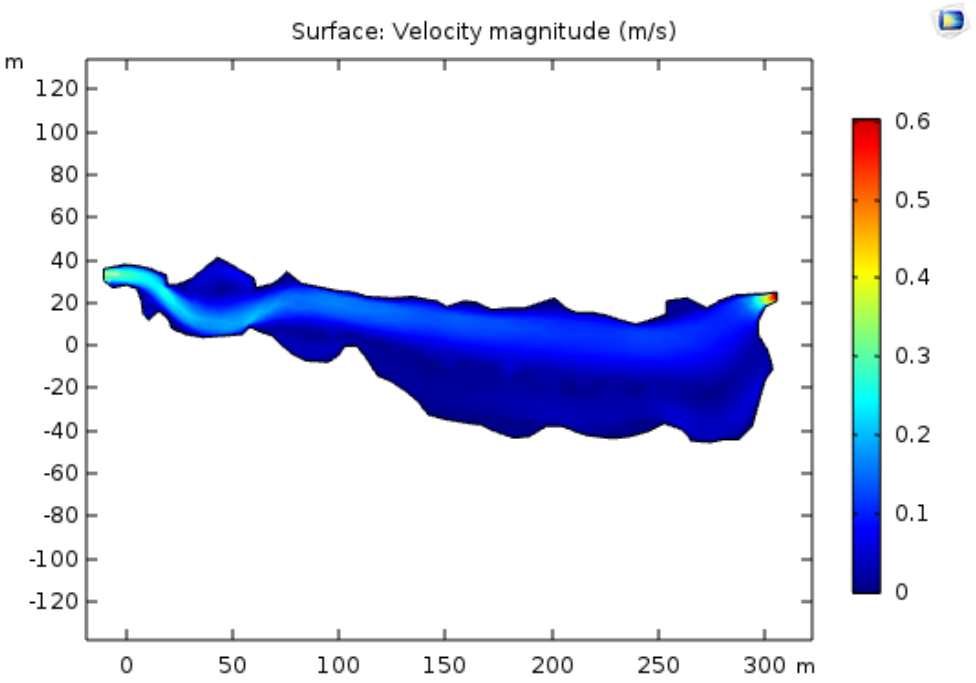

Fig. 4.62: Flow velocity distribution for July 2018 (Inflow Velocity = 0.30m/s)

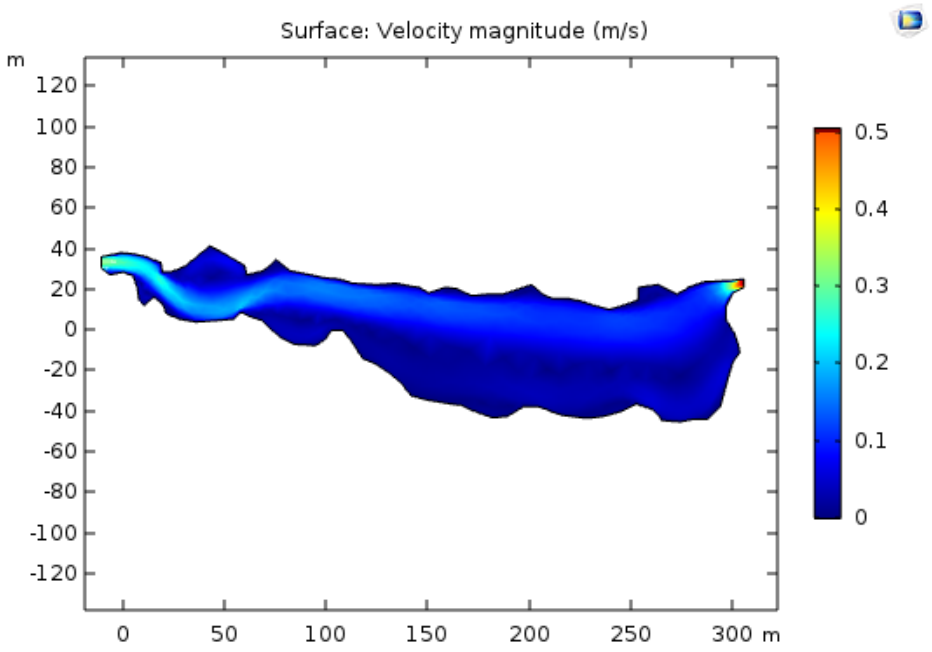

Fig. 4.63: Flow velocity distribution for July 2019 (Inflow Velocity = 0.31m/s)

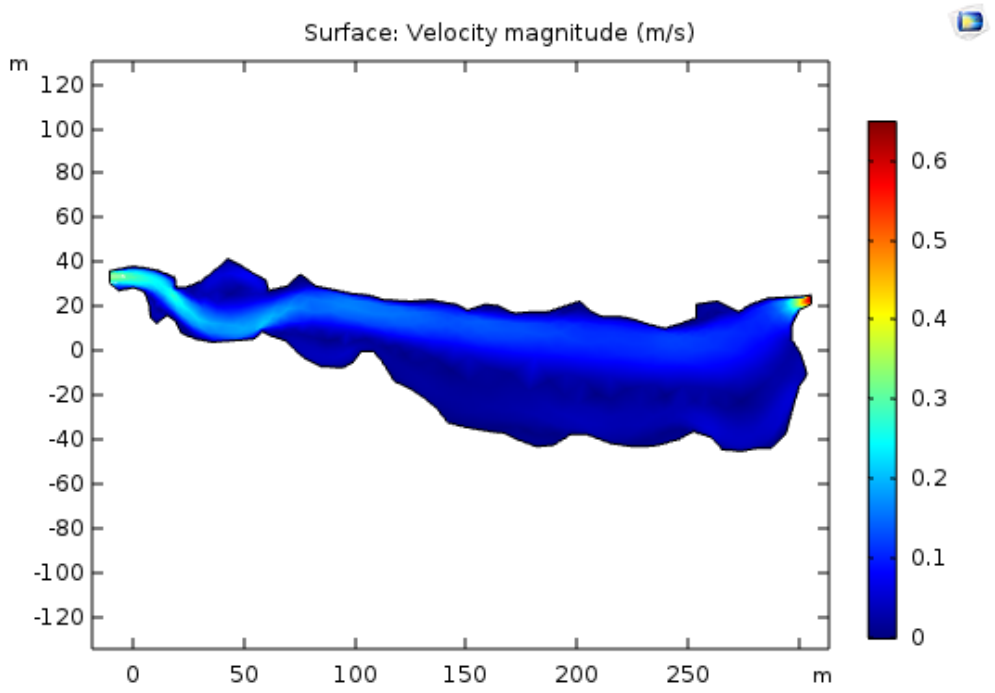

Fig. 4.64: Flow velocity distribution for August 2018 (Inflow Velocity = 0.33m/s)

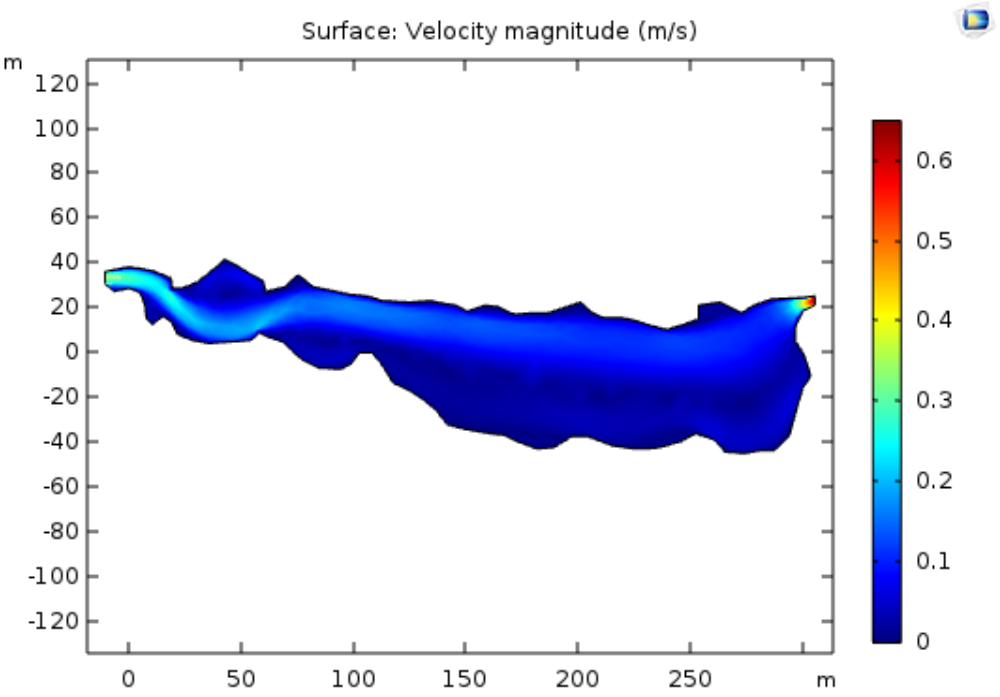

Fig. 4.65: Flow velocity distribution for August 2019 (Inflow Velocity = 0.32m/s)

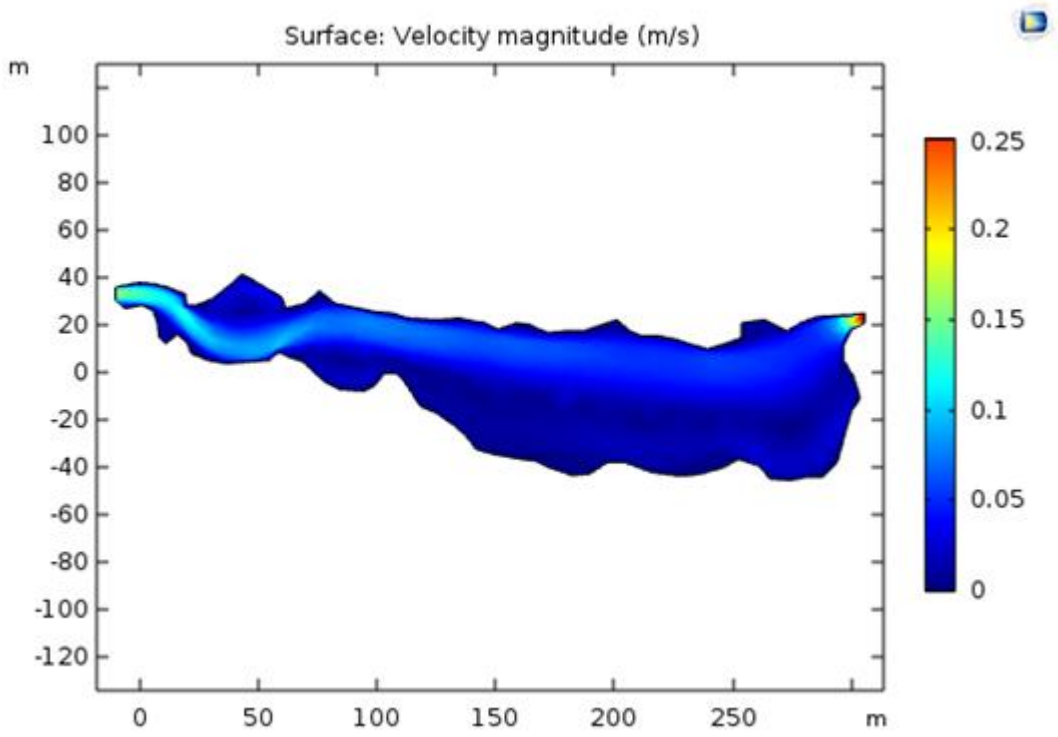

Fig. 4.66: Flow velocity distribution for November 2018 (Inflow Velocity = 0.14m/s)

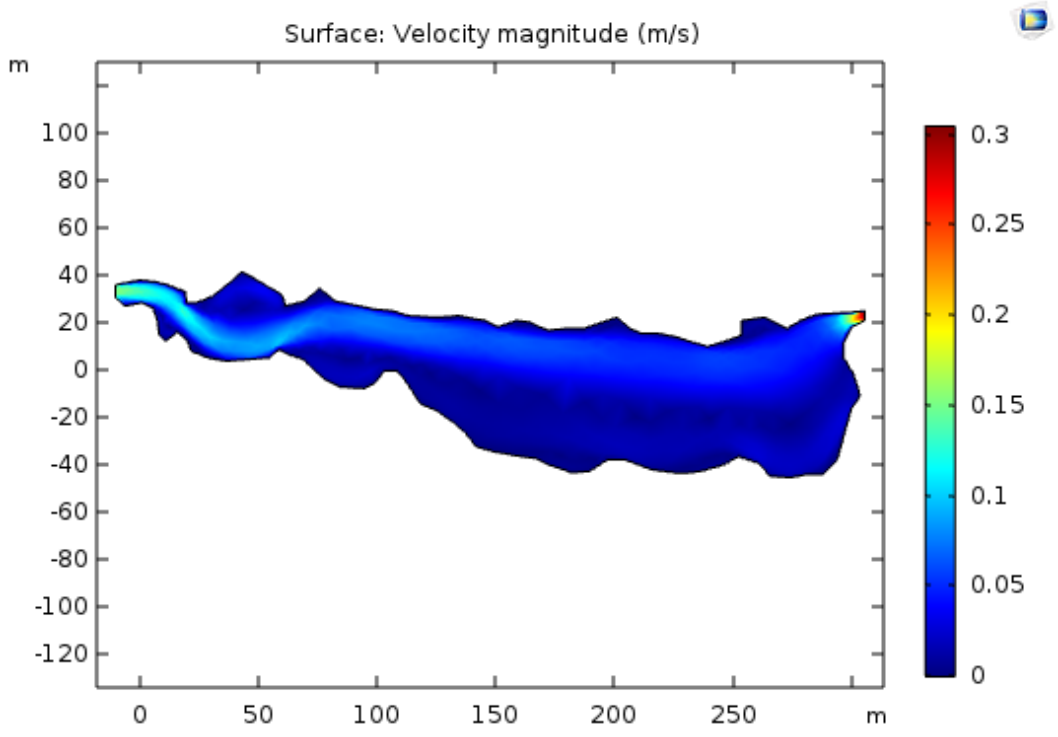

Fig. 4.67: Flow velocity distribution for November 2019 (Inflow Velocity = 0.15m/s)

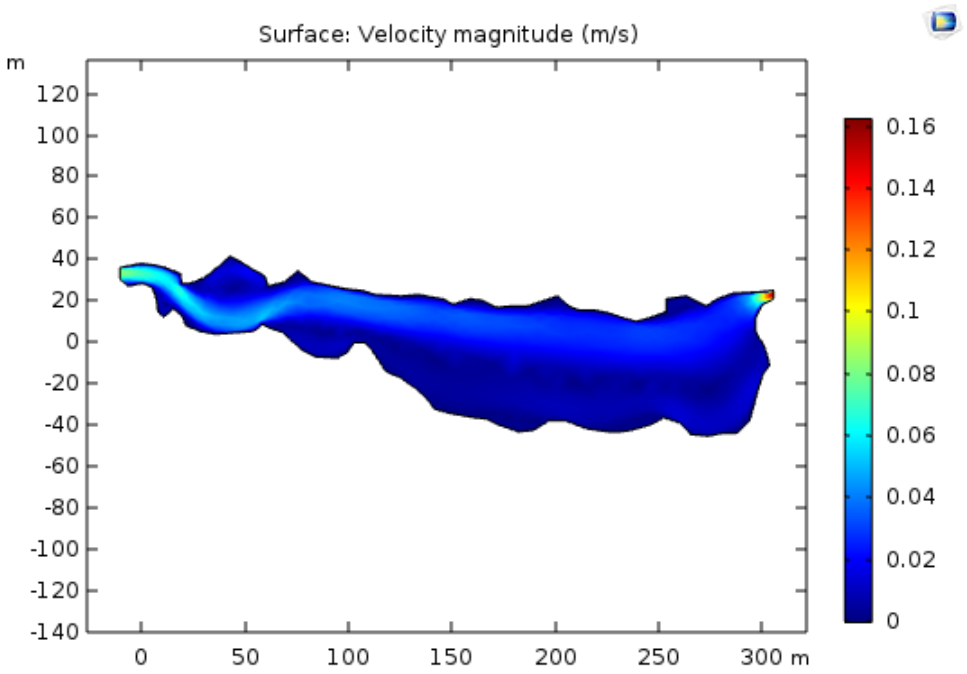

Fig. 4.68: Flow velocity distribution for December 2018 (Inflow Velocity = 0.10m/s)

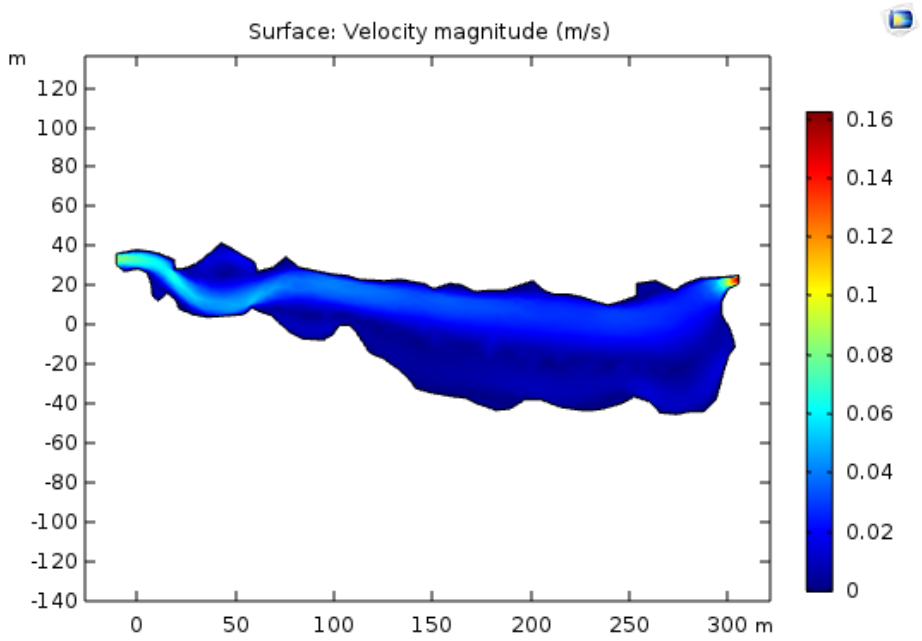

Fig. 4.69: Flow velocity distribution for December 2019 (Inflow Velocity = 0.08m/s)

Firstly, the direction of flow from the inlet towards the outlet can be identified. Furthermore, the parts of the river channel where the flow intensity was greater can be distinct. From the 2D plot, it can be seen that dead zones (i.e., areas with very low flow velocity/ regions of stagnation) occurred close to banks of the river tributary.

The model output for pressure in the water channel, obtained for the different months in the first stage of simulation are visualized in Figure 4.119 to 4.126. Pressure at different location within river tributary geometry can be identified by clicking at the point around the location and the system will pop-up the value of the velocity.

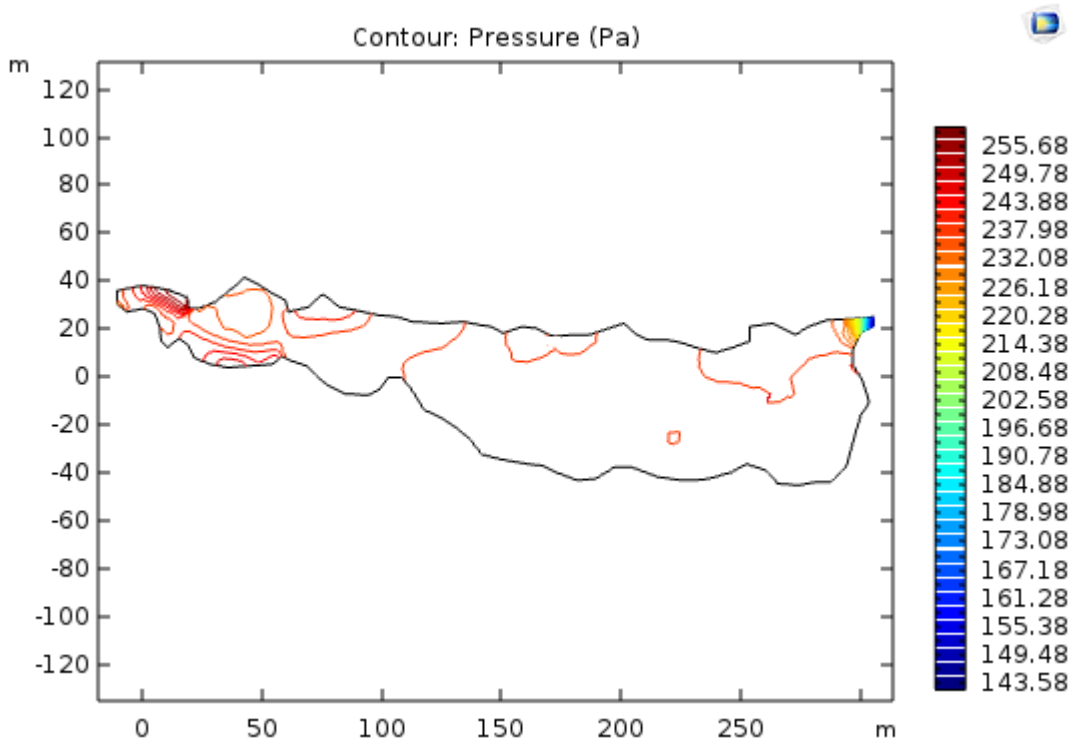

Fig. 4.70: Pressure distribution for July 2018

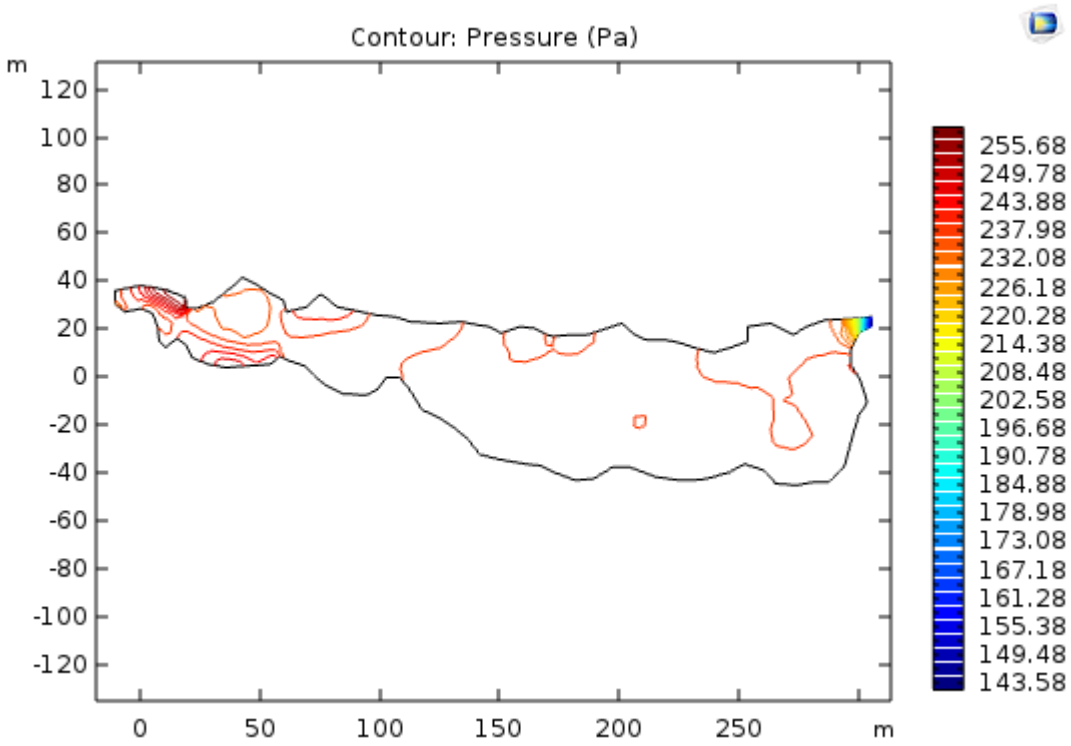

Fig. 4.71: Pressure distribution for July 2019

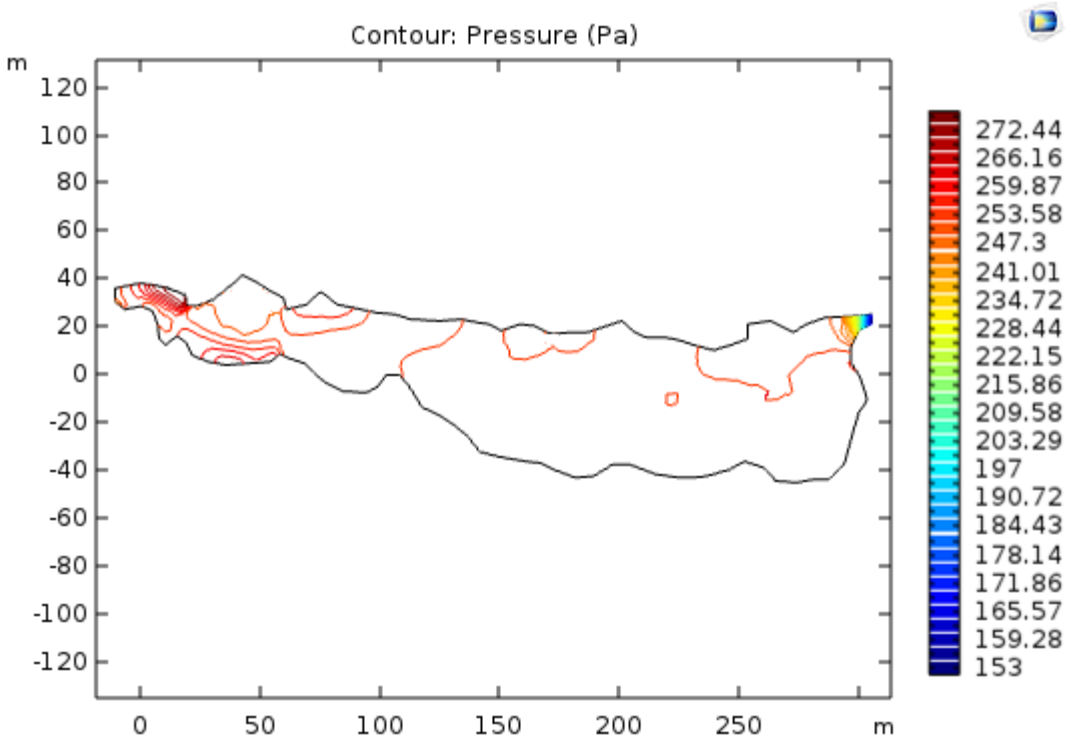

Fig. 4.72: Pressure distribution for August 2018

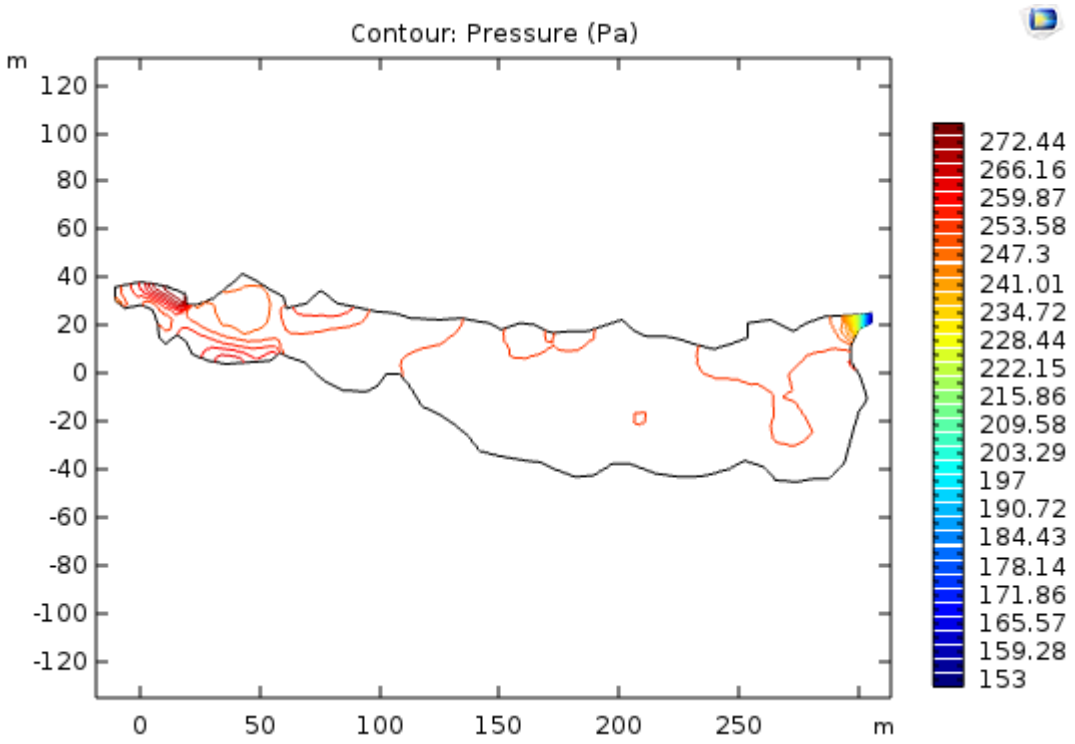

Fig. 4.73: Pressure distribution for August 2019

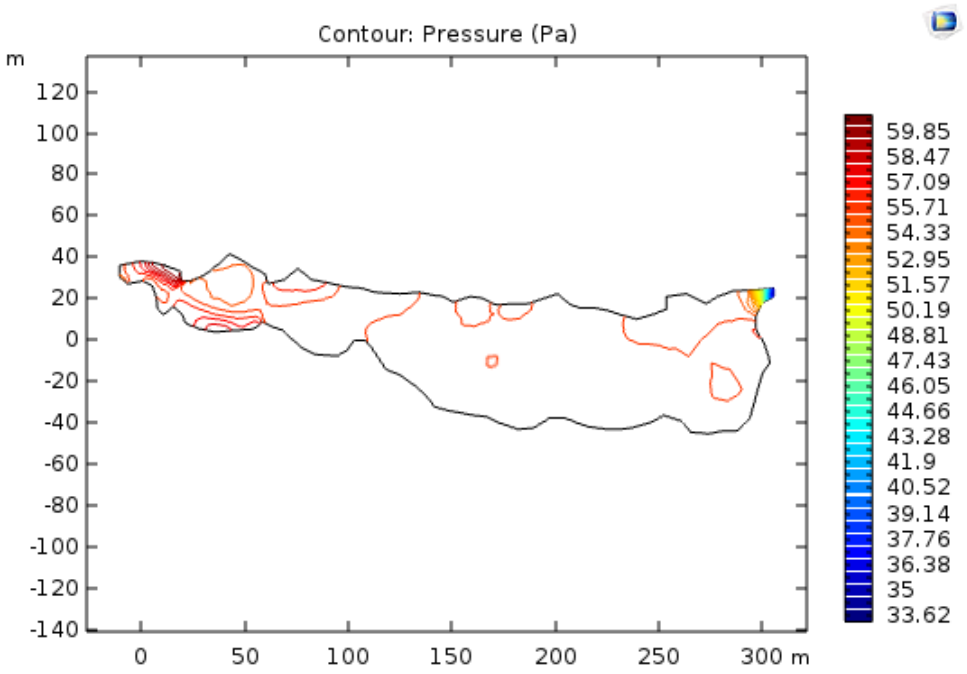

Fig. 4.74: Pressure distribution for November 2018

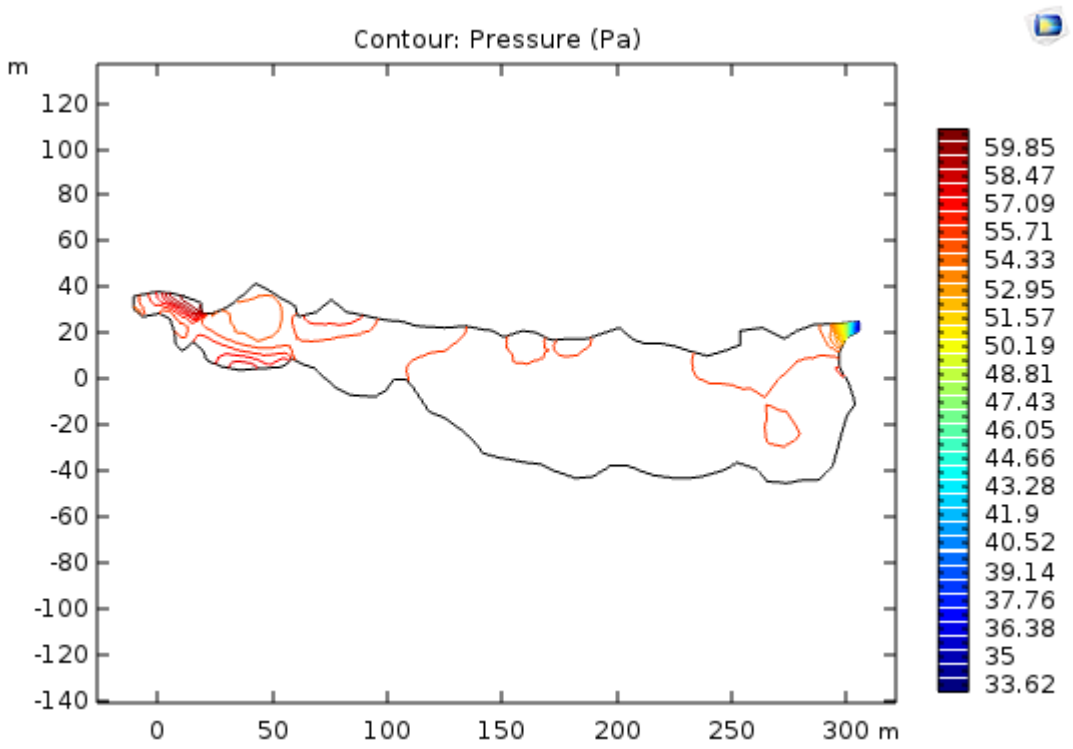

Fig. 4.75: Pressure distribution for November 2019

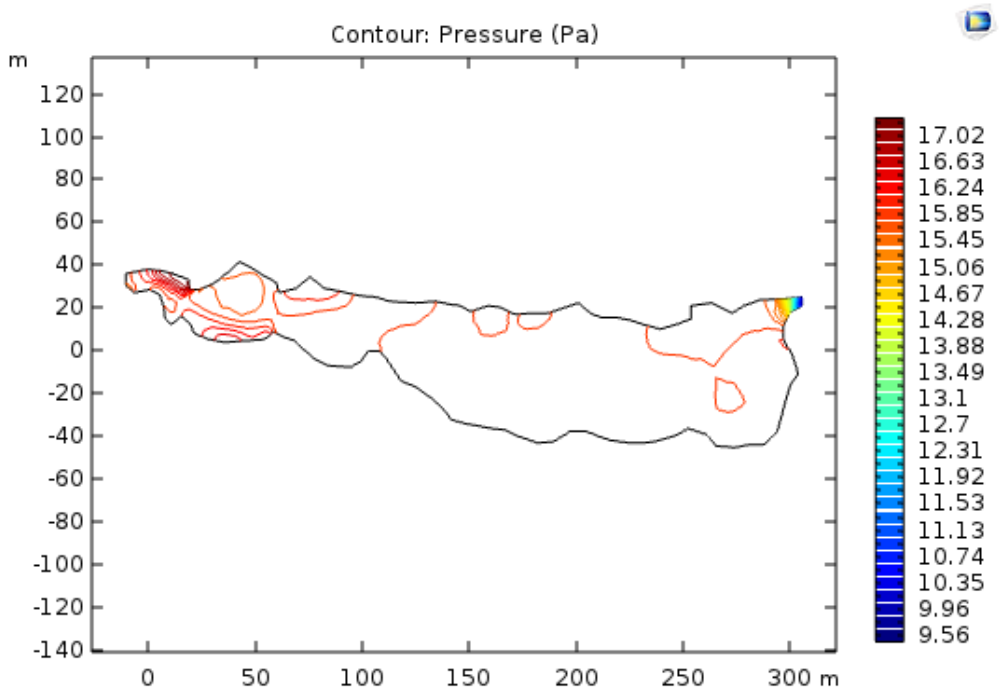

Fig. 4.76: Pressure distribution for December 2018

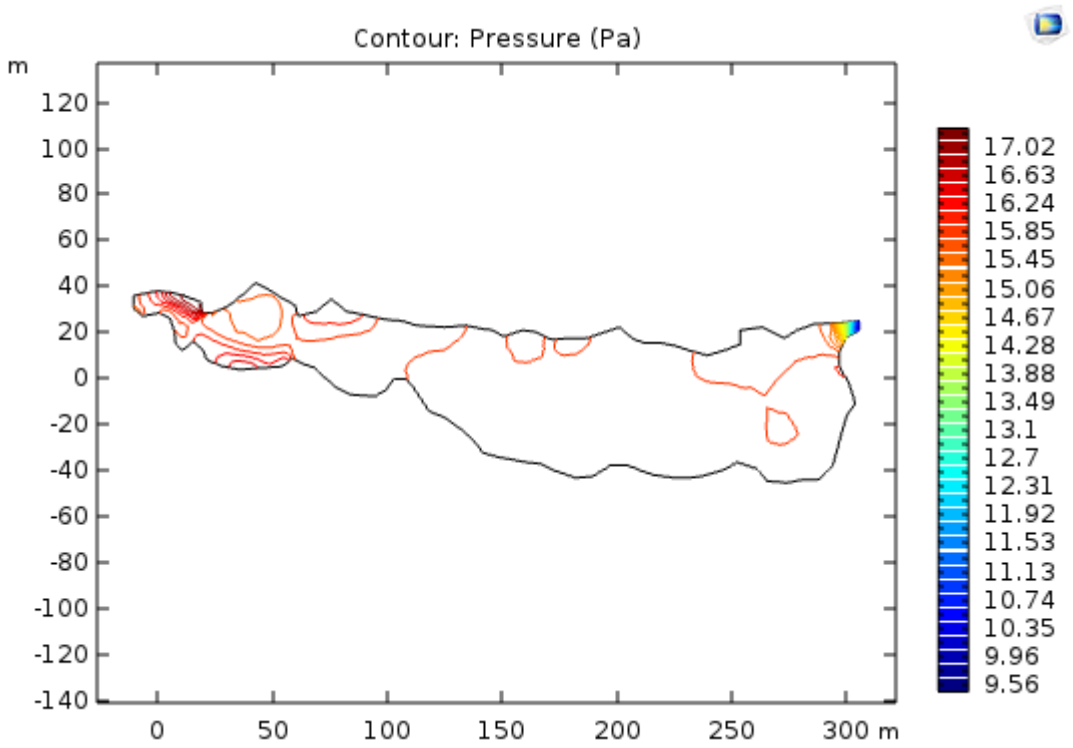

Fig. 4.77: Pressure distribution for December 2019

4.8 Validation

Particle transmission is basically governed by the flow velocity and as such it is enough to validate the flow velocity from the model. To validate the model used in the simulation, measured velocity at 6 sampling points were compared to simulated flow velocity values. The values of the two velocities and their percentage differences are presented in Table 4.12a and 4.12b.

Table 4.13a: Measured and simulated flow velocities for the year 2018.

Sampling Point	Measured Velocity (m/s)	Simulated Velocity (m/s)	% Difference
1	0.07	0.0718	2.6
2	0.31	0.3259	5.1
3	0.14	0.1321	5.6
4	0.35	0.3865	10.4
5	0.12	0.1274	6.1
6	0.18	0.1869	3.8

Table 4.13b: Measured and simulated flow velocities for the year 2019.

Sampling Point	Measured Velocity (m/s)	Simulated Velocity (m/s)	% Difference
1	0.05	0.0522	4.4
2	0.27	0.2914	7.9
3	0.12	0.1367	13.9
4	0.39	0.4091	4.8
5	0.09	0.0823	8.5
6	0.20	0.2116	5.8

The percentages difference between the measured and simulated flow velocities were in the range of 2.6% to 10.4% in 2018 and 4.4 % to 13.9 % in 2019, which is considered acceptable as it falls below the 15% tolerance suggested by Maamari *et al.* (2006). Apart from the percentage difference, the correlation between the measured and simulated velocity was evaluated using the correlation coefficient (R^2) value. The correlation between the two velocities is presented as in Figures 4.128 and 4.129.

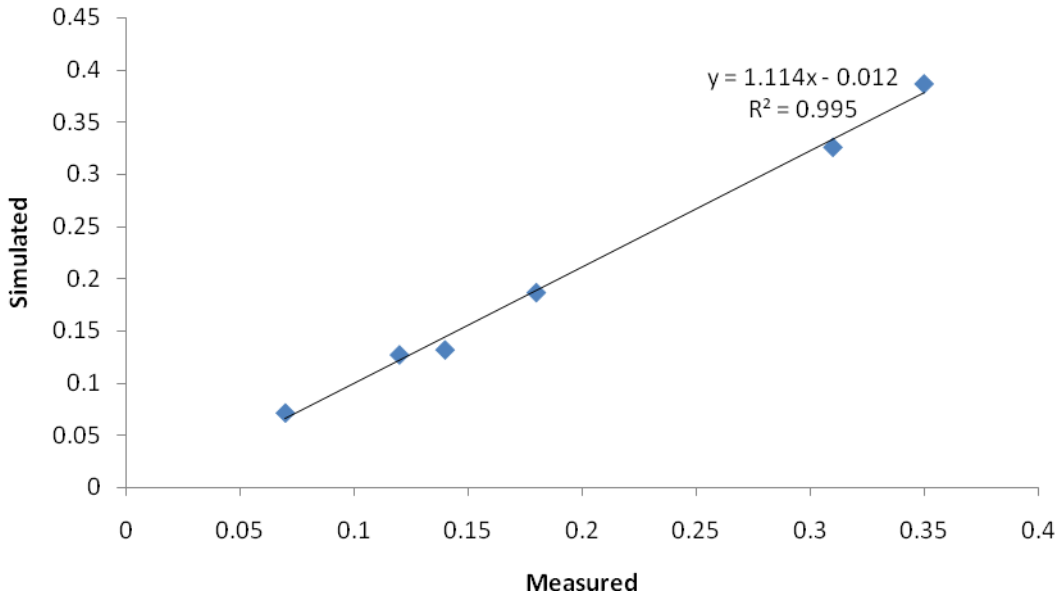

Fig. 4.78: The correlation between the measured and simulated velocity for the year 2018.

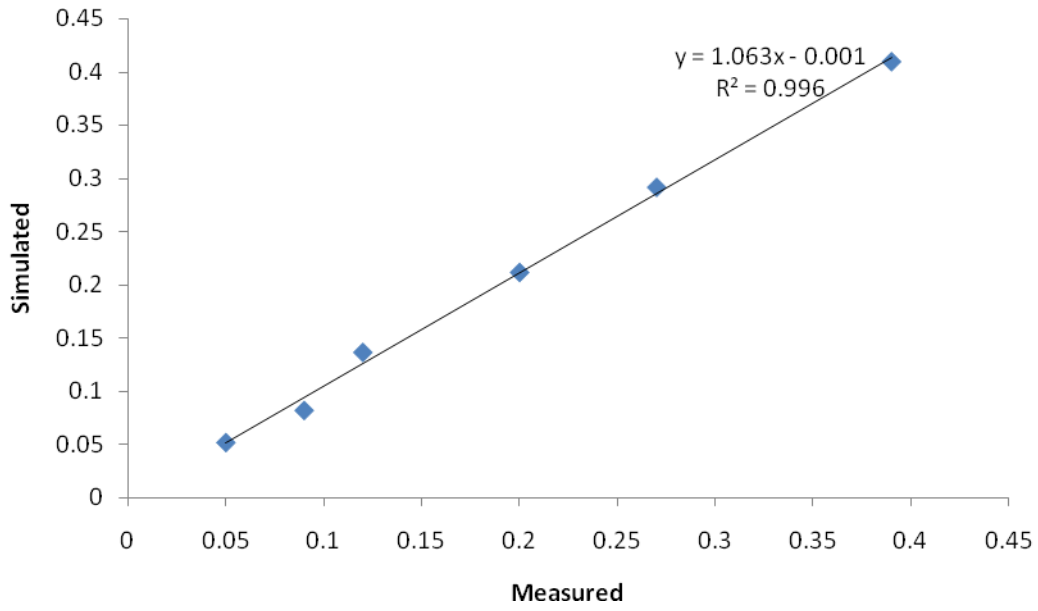

Fig 4.79: The correlation between the measured and simulated velocity for the year 2019.

According to the results, simulated velocity for all the six sampled points showed good agreement with the measured velocity, with a correlation coefficient of 0.99 and thus is considered accurate for further simulations. The convergence plot for the model solution is shown in Figure 4.120. From the plot it can be seen that residual error in the iteration process was very low and convergence occurred after just 64 iterations.

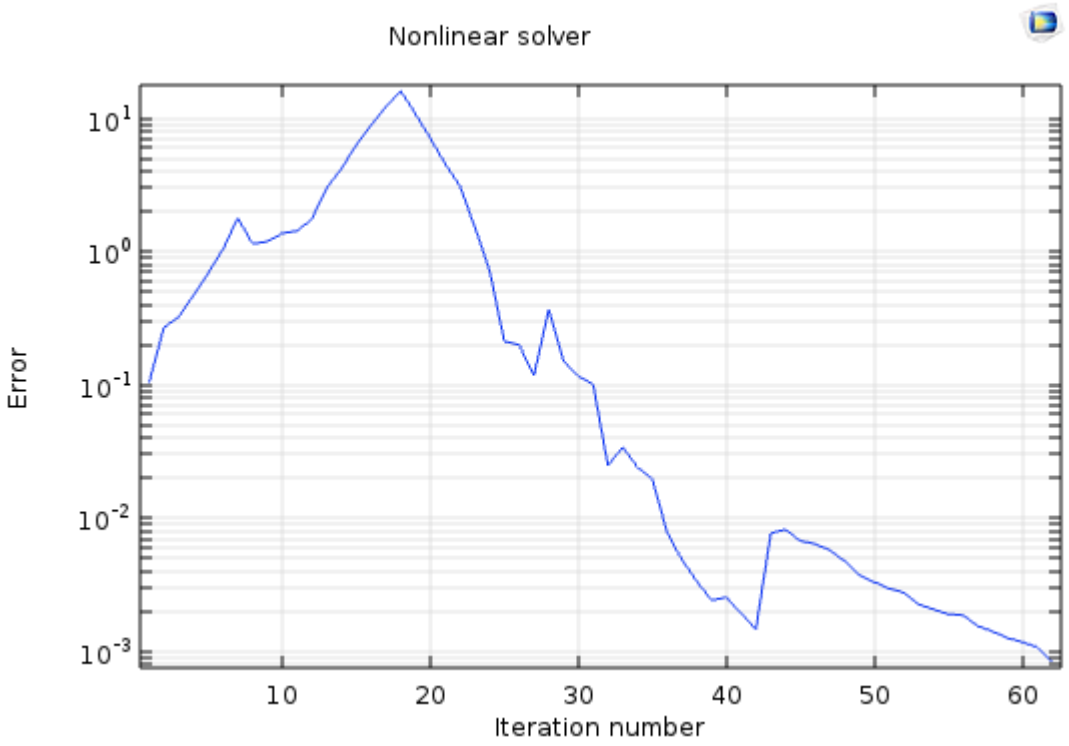

Fig. 4.80 Convergence plot for the model solution

The acceptable percentage difference and the very good agreement between the CFD simulated velocity and the measured values, typified by the high correlation coefficient, is an indication the models are validated as representation of the actual condition, thus can be used for further simulations.

Particle transmission

The particles' movement was influenced by the flow velocity within the channel. The results of the simulation of the trajectories of the particle from the inlet to the outlet of the river tributary for all the simulated conditions after 2000 sec simulation time are visualized in Figures 4.131 to 4.139.

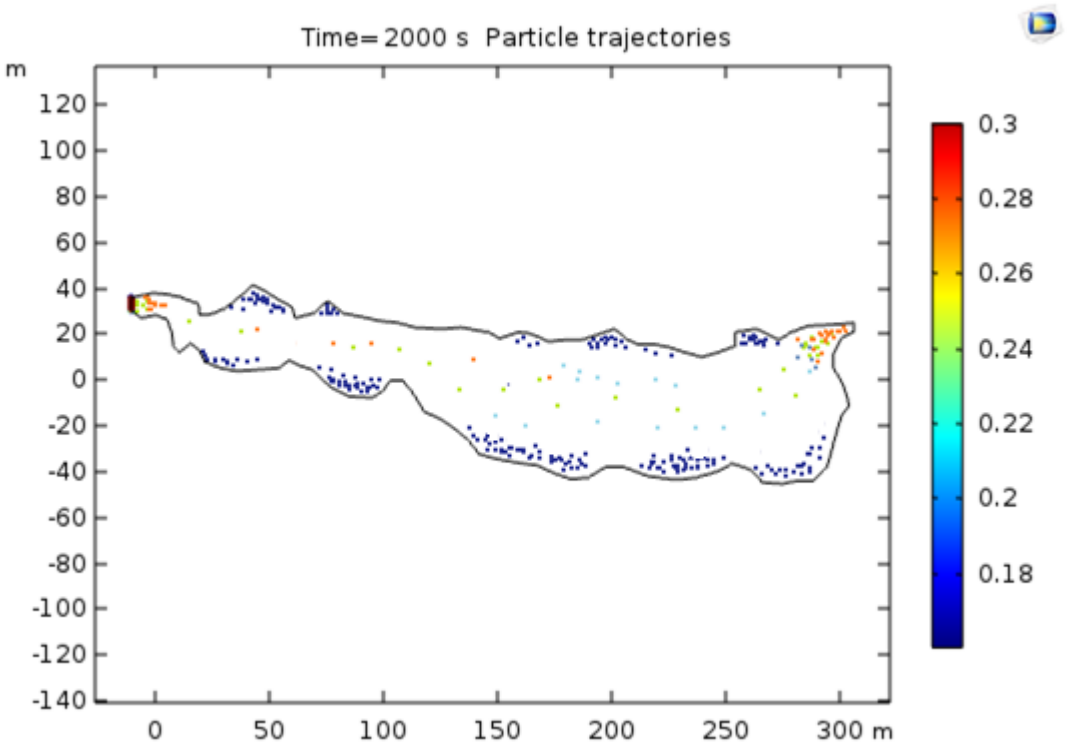

Fig, 4.81: Particle transmission for July 2018

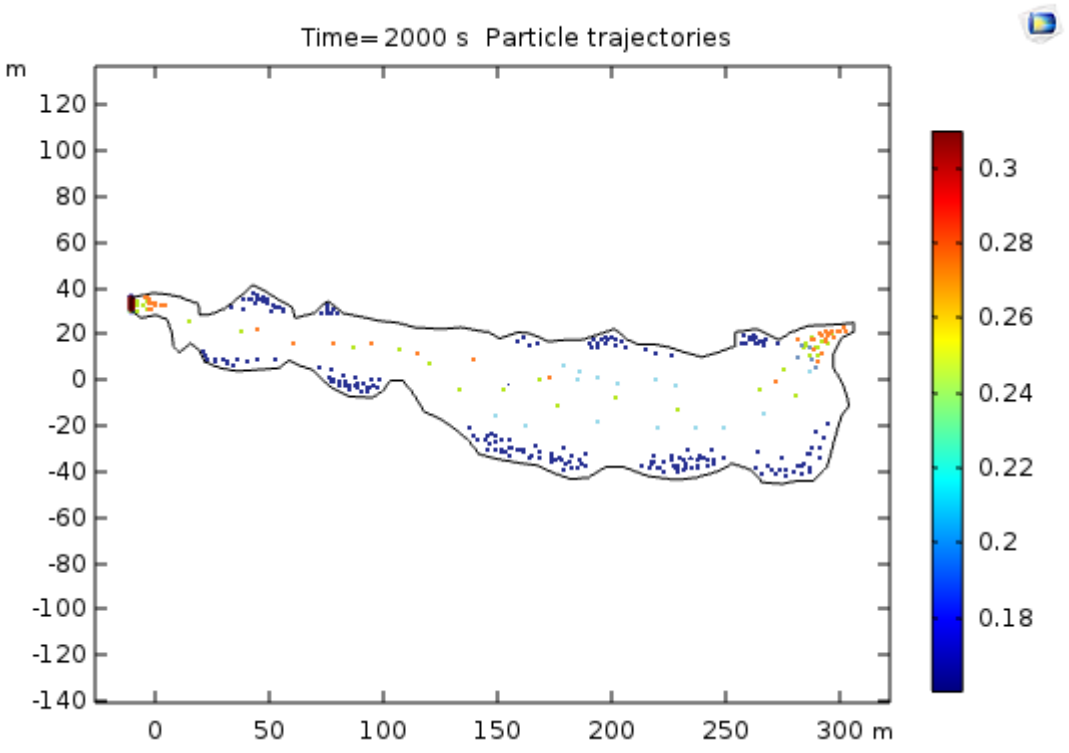

Fig, 4.82: Particle transmission for July 2019

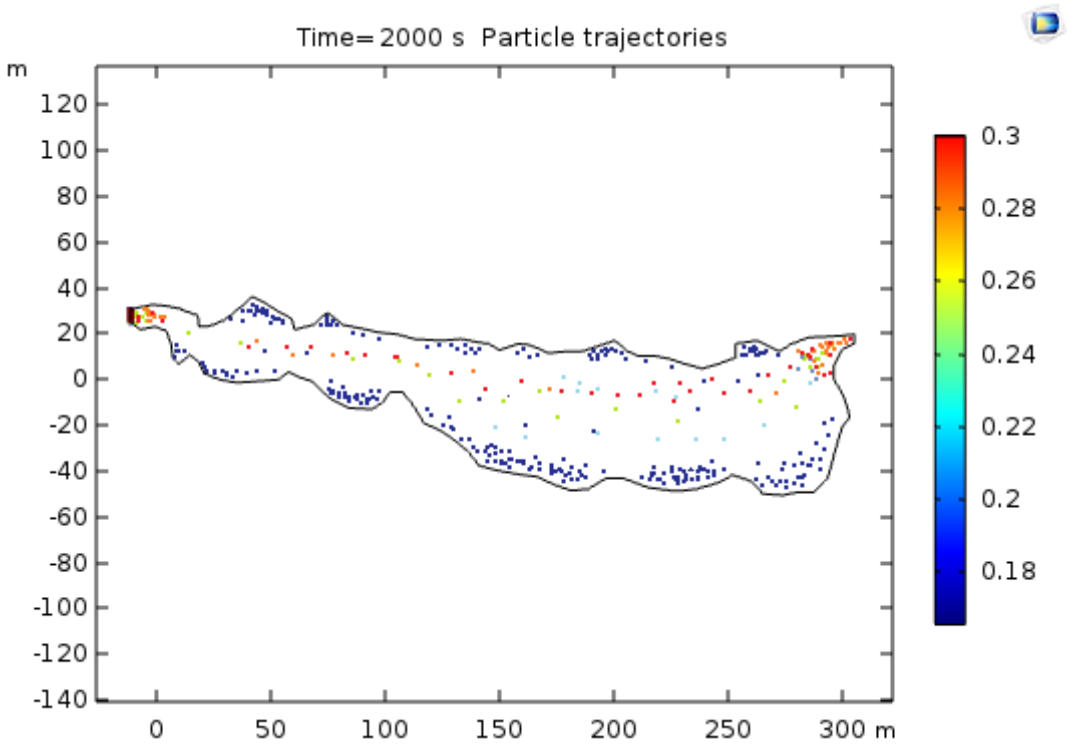

Fig, 4.83: Particle transmission for August 2018

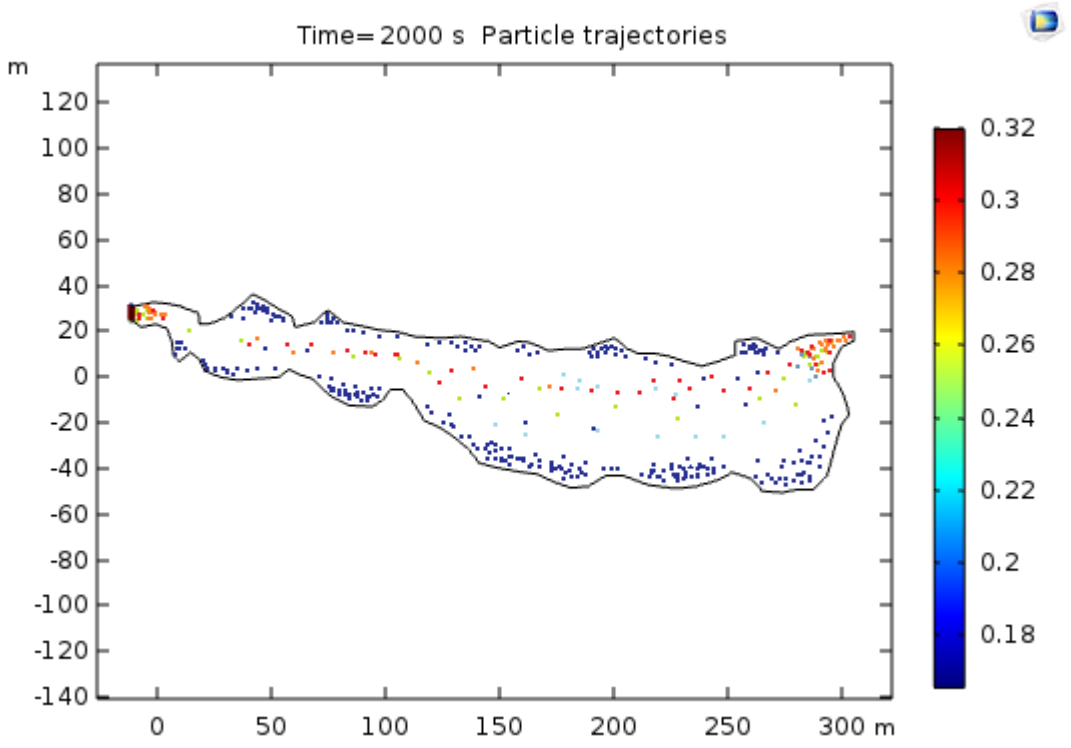

Fig, 4.84: Particle transmission for August 2019

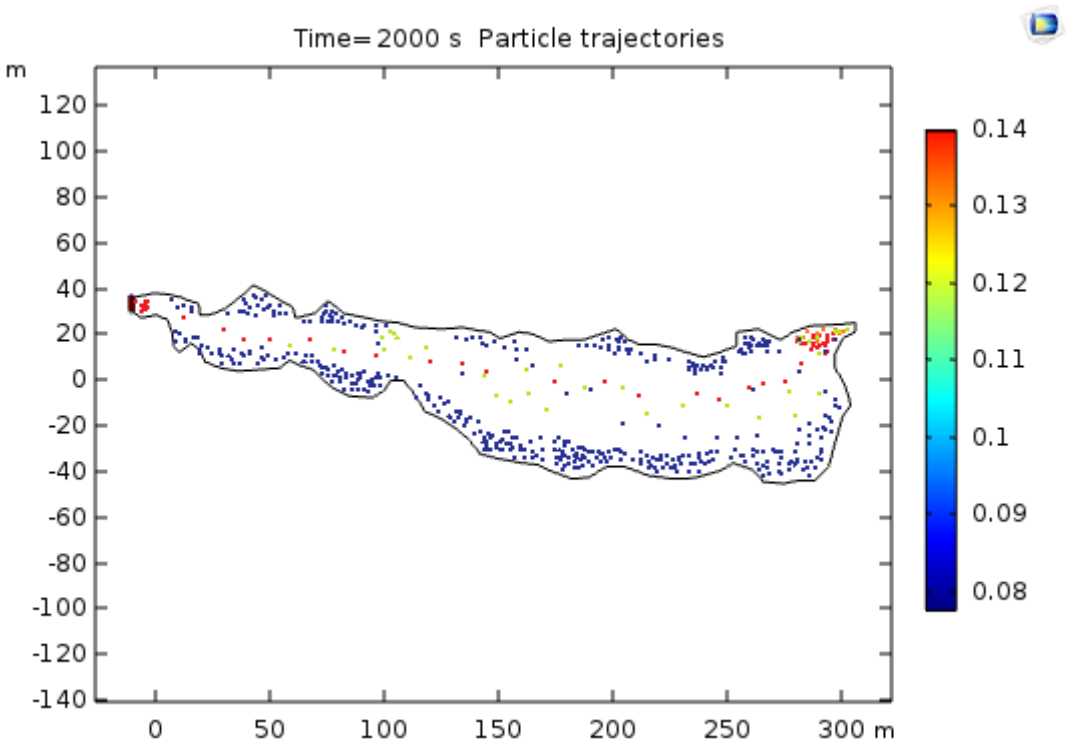

Fig, 4.85: Particle transmission for November 2018

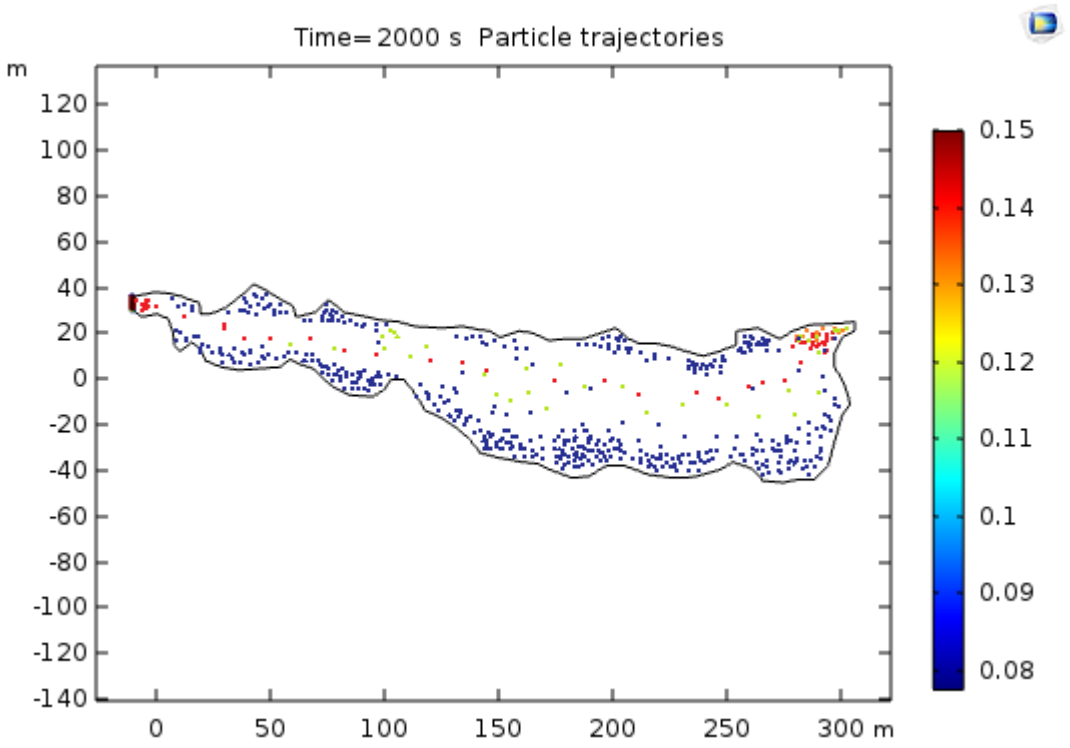

Fig, 4.86: Particle transmission for November 2019

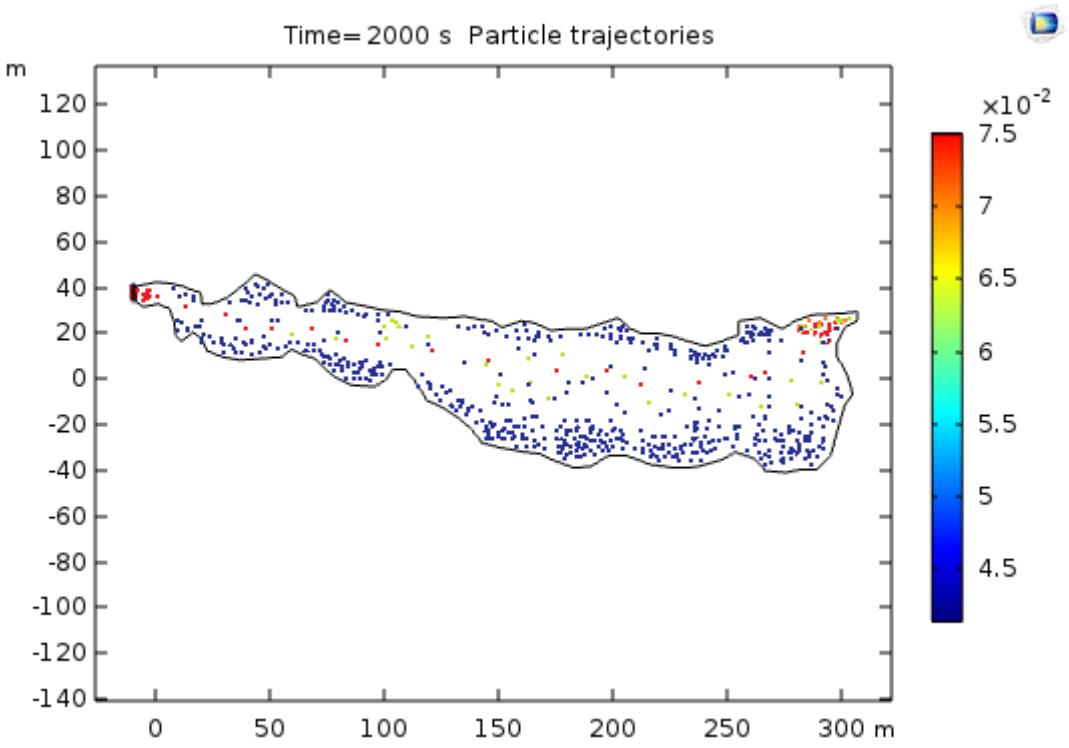

Fig, 4.87: Particle transmission for December 2018

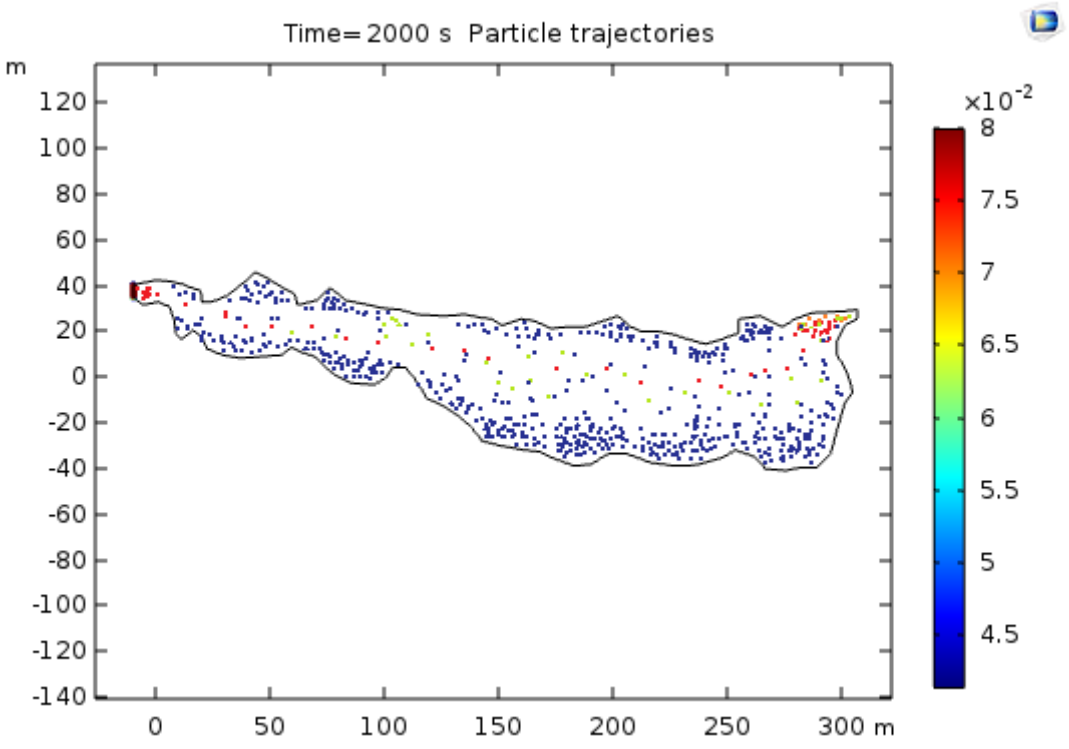

Fig, 4.88: Particle transmission for December 2019

The particles trajectory provided adequate information about sediment transport in the Ele River tributary. For all the simulated conditions, the particles at the banks had lower velocities compared to particles midstream. From the results of the simulation, it is evident that higher

sediment deposition occurs at the banks due to stagnation. By using transmission probability function in particle tracing module, it was able to estimate the number of particles. The percentage of the particle transmitted from the inlet to the outlet after 2000 sec simulation time was calculated. The results transmitted particles are presented in Table 4.14. Transmission probability results

Table 4.14: Transmission probability results

	2019		2018	
Month	% of particles transmitted to the outlet	% of particles retained in the channel	% of particles transmitted to the outlet	% of particles retained in the channel
July	77.83	22.17	73.41	26.59
August	82.79	17.21	79.63	20.37
November	65.17	34.83	63.71	36.29
December	57.32	42.68	54.36	45.64

From the Table 4.14, it can be seen that the percentage of particle retained in the river tributary ranged from 17.21% to 42.68% in 2019 and 20.59% to 45.64% in 2018, while the number of particles transmitted to the outlet was in the range of 57.32% to 82.79% in 2019 and 54.36% to 79.63%. The result also revealed a seasonal trend in flow characteristic of the river, with higher number of particles retained during the dry season when the flow velocity was lowest.

4.9 Analysis of Variance Comparing the Level of Significance at the Sampling Points

Analysis of variance used in this work is the single factor (one-way ANOVA), since it compared the level of significance at the ten sampling points. When the P-value is greater than

0.05, it shows that there is no significant difference but if otherwise stated, there is significant difference. 0.05 alpha level was used for 95% level of significance confirmation among the sampling points for the irrigation water quality parameters. POST-HOC analyses were done to show the points where the significant differences occurred. These tests are series of t tests where we can assume equal or unequal variances. Below are the analyses of variance for the irrigation water quality parameters.

Table 4.15 ANOVA table for pH

SUMMARY

Groups	*Count*	*Sum*	*Average*	*Variance*
p1	48	304.56	6.345	0.007357
p2	48	301.7	6.285417	0.016502
p3	48	304.14	6.33625	0.011007
p4	48	304.14	6.33625	0.025849
p5	48	305.77	6.370208	0.02116
p6	48	301.57	6.282708	0.017841
p7	48	304.99	6.353958	0.022241
p8	48	301.234	6.275708	0.027126
p9	48	302.71	6.306458	0.024623
p10	48	304.49	6.343542	0.028185

ANOVA

Source of Variation	*SS*	*df*	*MS*	*F*	*P-value*	*F crit*
Between Groups	0.479384	9	0.053265	2.638279	0.005485	1.899799
Within Groups	9.488943	470	0.020189			
Total	9.968327	479				

Table 4.16 ANOVA table for TDS

SUMMARY

Groups	*Count*	*Sum*	*Average*	*Variance*
P1	48	117993	2458.188	16219.77
P2	48	108739	2265.396	16146.24
P3	48	102378	2132.875	13104.11
P4	48	93898	1956.208	45385.36
P5	48	80551	1678.146	113181.4
P6	48	62109	1293.938	103979
P7	48	46235	963.2292	38492.56
P8	48	34511	718.9792	14171.81
P9	48	23746	494.7083	4429.7
P10	48	17183	357.9792	2431.68

ANOVA

Source of Variation	*SS*	*df*	*MS*	*F*	*P-value*	*F crit*
Between Groups	2.57E+08	9	28551785	776.8313	9.5E-276	1.899799
Within Groups	17274457	470	36754.16			
Total	2.74E+08	479				

Table 4.17 ANOVA Table for Electrical Conductivity

SUMMARY

Groups	*Count*	*Sum*	*Average*	*Variance*
P1	48	203.61	4.241875	0.687262
P2	48	169.87	3.538958	0.244665
P3	48	160.78	3.349583	0.053255
P4	48	135.93	2.831875	0.285024
P5	48	122.17	2.545208	0.227911
P6	48	106.33	2.215208	0.130719
P7	48	90.25	1.880208	0.060994
P8	48	200.2	4.170833	0.006493
P9	48	70.48	1.468333	0.009372
P10	48	65.09	1.356042	0.003224

ANOVA

Source of Variation	*SS*	*df*	*MS*	*F*	*P-value*	*F crit*
Between Groups	475.3163	9	52.81292	309.0429	4.2E-191	1.899799
Within Groups	80.31918	470	0.170892			
Total	555.6355	479				

Table 4.18 **ANOVA table for Bicarbonate**

SUMMARY

Groups	*Count*	*Sum*	*Average*	*Variance*
P1	48	210.53	4.386042	0.16025
P2	48	212.825	4.433854	0.057722
P3	48	238.98	4.97875	26.80573
P4	48	209.51	4.364792	0.092366
P5	48	210.76	4.390833	0.065387
P6	48	206.61	4.304375	0.05394
P7	48	207.46	4.322083	0.057179
P8	48	205.32	4.2775	0.054696
P9	48	208.93	4.352708	0.040978
P10	48	216.5	4.510417	0.086247

ANOVA

Source of Variation	*SS*	*df*	*MS*	*F*	*P-value*	*F crit*
Between Groups	17.85307	9	1.983675	0.722006	0.688869	1.899799
Within Groups	1291.301	470	2.74745			
Total	1309.154	479				

Table 4.19 **ANOVA table for Mg**

SUMMARY

Groups	*Count*	*Sum*	*Average*	*Variance*
P1	48	86.321	1.798354	0.011946
P2	48	83.406	1.737625	0.012059
P3	48	84.543	1.761313	0.009393
P4	48	86.407	1.800146	0.00866
P5	48	85.036	1.771583	0.010352
P6	48	85.389	1.778938	0.016243
P7	48	85.758	1.786625	0.006969
P8	48	85.342	1.777958	0.006759
P9	48	87.731	1.827729	0.003668
P10	48	85.953	1.790688	0.010073

ANOVA

Source of Variation	*SS*	*df*	*MS*	*F*	*P-value*	*F crit*
Between Groups	0.254596	9	0.028288	2.942954	0.002076	1.899799
Within Groups	4.517756	470	0.009612			
Total	4.772352	479				

Table 4.20 ANOVA table for Ca

SUMMARY

Groups	*Count*	*Sum*	*Average*	*Variance*
P1	48	411.22	8.567083	0.446837
P2	48	407.834	8.496542	0.378578
P3	48	427.752	8.9115	0.252923
P4	48	444.728	9.265167	0.198848
P5	48	425.622	8.867125	0.2034
P6	48	441.341	9.194604	0.215456
P7	48	434.03	9.042292	0.22052
P8	48	449.809	9.371021	0.326363
P9	48	437.922	9.123375	0.387108
P10	48	437.698	9.118708	0.311038

ANOVA

Source of Variation	*SS*	*df*	*MS*	*F*	*P-value*	*F crit*
Between Groups	35.67053	9	3.963392	13.47602	2.73E-19	1.899799
Within Groups	138.2303	470	0.294107			
Total	173.9009	479				

Table 4.21 ANOVA table for Na

Anova: Single Factor

SUMMARY

Groups	*Count*	*Sum*	*Average*	*Variance*
P1	48	1971.66	41.07625	107.5225
P2	48	2068.77	43.09938	170.9648
P3	48	2366.44	49.30083	172.1111
P4	48	2566.9	53.47708	108.6623
P5	48	2233.47	46.53063	117.522
P6	48	2513.35	52.36146	84.1988
P7	48	2462.76	51.3075	115.4622
P8	48	2572.51	53.59396	55.22999
P9	48	2548.88	53.10167	114.3531
P10	48	2546.8	53.05833	125.4819

ANOVA

Source of Variation	*SS*	*df*	*MS*	*F*	*P-value*	*F crit*
Between Groups	9124.183	9	1013.798	8.653782	4.71E-12	1.899799
Within Groups	55060.91	470	117.1509			
Total	64185.09	479				

Table 4.22 ANOVA table for Nitrate-Nitrogen

SUMMARY

Groups	*Count*	*Sum*	*Average*	*Variance*
P1	48	176.094	3.668625	1.504076
P2	48	208.098	4.335375	1.468415
P3	48	225.504	4.698	0.505335
P4	48	199.97	4.166042	1.33795
P5	48	234.605	4.887604	0.348991
P6	48	223.773	4.661938	0.707446
P7	48	223.216	4.650333	0.872978
P8	48	234.745	4.890521	0.847194
P9	48	213.774	4.453625	0.949624
P10	48	221.661	4.617938	0.86736

ANOVA

Source of Variation	*SS*	*df*	*MS*	*F*	*P-value*	*F crit*
Between Groups	59.35465	9	6.594961	7.008931	1.58E-09	1.899799
Within Groups	442.2403	470	0.940937			
Total	501.595	479				

Table 4.23 ANOVA table for Sulphate

SUMMARY

Groups	*Count*	*Sum*	*Average*	*Variance*
P1	48	4490.086	93.54346	11.38099
P2	48	4272.961	89.02002	14.98446
P3	48	4456.973	92.8536	8.571257
P4	48	4427.59	92.24146	16.94067
P5	48	4346.974	90.56196	177.169
P6	48	4501.436	93.77992	112.2068
P7	48	4479.08	93.31417	7.088958
P8	48	4235.993	88.24985	25.21977
P9	48	4373.588	91.11642	155.1335
P10	48	4366.478	90.96829	20.16645

ANOVA

Source of Variation	*SS*	*df*	*MS*	*F*	*P-value*	*F crit*
Between Groups	1585.36	9	176.1511	3.209388	0.00087	1.899799
Within Groups	25796.51	470	54.88618			
Total	27381.87	479				

Table 4.24 ANOVA table for Ammonium-Nitrogen

SUMMARY

Groups	*Count*	*Sum*	*Average*	*Variance*
P1	48	133.169	2.774354	0.211018
P2	48	128.235	2.671563	0.243778
P3	48	112.683	2.347563	0.28457
P4	48	116.342	2.423792	0.238052
P5	48	131.176	2.732833	0.280969
P6	48	139.325	2.902604	0.154344
P7	48	114.13	2.377708	0.376556
P8	48	123.827	2.579729	0.240388
P9	48	124.44	2.5925	0.284599
P10	48	135.432	2.8215	0.311203

ANOVA

Source of Variation	*SS*	*df*	*MS*	*F*	*P-value*	*F crit*
Between Groups	16.00452	9	1.77828	6.773166	3.65E-09	1.899799
Within Groups	123.3975	470	0.262548			
Total	139.402	479				

From the ANOVA tables, there were significant differences among all the parameters except for Bicarbonate where there was no level of significance among the point values since the P-value was greater than 0.05. For the parameters where there were significant differences, the P-value was less than 0.05. To ascertain the exact points where these levels of significance occurred, Post-hoc analysis was conducted of which the points of significances are shown as below:

Table 4.25 Identification of the Points of Significant Differences

S/N	Parameters	Points of Significant Difference
1.	pH	5&8**;** 8&1**;** 2&3
2.	TDS	1&2; 3&4; 9&10
3.	EC	9&10; 1&2
4.	Mg^{2+}	4&9; 1&4; 1&2; 9&3
5.	Ca^{2+}	4&8; 6&4; 8&6; 1&6
6.	Na^{+}	1&2; 2&3; 6&3; 5&6
7.	NO_3-N	1&2; 2&3; 4&1; 2&4
8.	SO_4	1&2; 1&3; 8&2;
9.	NH_4-N	3&7; 1&7

Having seen the points where the levels of significance were identified, it is worthy to note that in making decisions on the acceptability of these parameters, there should be comparisons of the ANOVA results with the FAO permissible standards of the parameters. Bicarbonate which was found to have insignificant difference between the sampling points will be acceptable. Calcium ion, Sodium ion, Nitrate-Nitrogen, SO_4, Ammonia-Nitrogen, pH, TDS, EC showed levels of significance between different points as shown in the above table 4.24. When comparing the ANOVA results with the permissible standards, calcium, Nitrate Nitrogen, pH, Ammonium nitrogen showed significant differences at certain points, but they were still within the FAO permissible level from Points 1 -10, thus they are acceptable but for Electric conductivity, Total dissolved solids, Sodium and sulfate, they showed levels of significance between some points and comparing the ANOVA results with the permissible standard, they were above the permissible limit at most instances thus will be rejected and will pose very negative effect in the river system.

Table 4.26 Summary of The ANOVA Results

S/N	PARAMETERS	P-Value	P-tab	Level of significance	Decision
1	pH	0.005485	4.60	Significant	Accept
2	TDS	0.0049	0.0046	Significant	Reject
3	EC	4.2E-191	4.56	Significant	Reject
4	HCO_3^-- Bicarbonate	0.688869	0.45	Not Significant	Accept
5	Mg^{2+}- magnesium i on	0.002076	4.50	Significant	Accept
6	Ca^{2+}- Calcium ion	2.73E-19	5.70	Significant	Accept
7	Na^+- Sodium ion	4.71E-12	5.60	Significant	Reject

8	NO_3- N Nitrate Nitrogen	1.58E-09	4.60	Significant	Accept
9	Sulphate – SO4	0.00087	4.60	Significant	Reject
10	Ammonium Nitrogen :NH4-N	3.65E-09	5.60	Significant	Accept

If the p-value is greater than 0.05, there is no significant difference; if otherwise, there is a significant difference at 5%.

CHAPTER FIVE

5.0 CONCLUSION AND RECOMMENDATIONS

5.1 Conclusion

The following conclusions were derived from the study:

1) Effluents discharged into Ele River from the industrial clusters very close to the surface water were highly contaminated. From the results obtained in the analyses and modeling of the surface water quality, there is urgent need for installation of effluent treatment facilities to reduce the health and environmental hazards these effluents might pose on the River system which will adversely affect crop production when used for irrigation.
2) Parameters such as TDS and EC at the upstream level coming from the point sources before the mid points of the river system exceeded the FAO permissible standards for irrigation water quality assessment. At downstream as the flow rate increased, the pollution level decreased within the permissible level. This was as a result of ion dissolution along the sampling points and the influence of rainfall during rainy season. The pollution level was higher in the dry than the rainy season due decrease in flow velocity and absence of rainfall. Increase in sodium and sulfate at most instances beyond the permissible standard affected the river adversely thereby increasing the salinity of the River system.
3) This study employed CFD using Comsol Multiphysics software for the modeling and simulation of the flow and particle transmission in Ele River tributary. The discrepancies between the simulated and measured values were within tolerable limits. The model was able to explain 99% of the variability in the data set.
4) The CFD model was able to highlight areas with higher risk of sediment deposition, which can be used in the management of sediment load in the river. The study also found that the very low flow velocity during the dry season had a negative effect on sediment transmission in the river channel.

5) It is evident that higher sediment deposition occurred at the banks of the River due to stagnation since the particles at the River banks had lower velocities compared to particles midstream.. This sediment deposition will also affect irrigation system for crop production considering the ability of the sediments to block sprinkler nozzles which limits it from supplying sufficient water for crop production.

Finally, these high contaminations due to water salinity which cause salt deposit in the crop root zones will require application of excess water to crops so as to meet up with the leaching requirements for crop growth. However, wastewater treatment will be most preferable for supply of good water of low conductivity for optimum crop production.

5.2 Recommendations

i. Further research should be done on modeling the River system for drinking and domestic water quality assessment.

ii. Other means of effluent disposals such as on-site/ off-site systems and full sewage systems should be resorted to so as to limit the pollutant effects on the Ele River.

iii. Soil reclamation is recommended due to the contamination by contaminated water containing salts and inorganic substances.

vii. Irrigation water should be drawn from points of low or no sediment deposition to avoid breakdown of irrigation equipment.

5.3 Contribution to Knowledge

This research work has contributed immensely to the enhancement of knowledge on water and water related issues in the following ways:

I. Through this research, a model was developed using artificial intelligence to ascertain the river water quality for irrigation purposes, thus serving as a guide on the for proper water management so as to enhance crop production

ii. The study being exploratory and predictive, forecasted the water characteristics of Ele River for another 12months into the year 2020 which will serve as a guide for irrigation.

iii. The suitability of the River for dry season irrigation water supply for crop production was shown in the work after comparing its characteristics during the Rainy and dry seasons.

iv. The level of sediment deposition was evaluated from this research using the computational fluid dynamics model so as to avoid using water from the affected points due to its contamination and possibility of affecting sprinkler nozzles for irrigation.

REFERENCES

Abbott, M.B., Bathrust, J.C., Cunge, J.A., O'Connell, P.E. and Rasmussen, J., 1986. An introduction to Europeen hydrological system - systeme hydrologique Europeen (SHE) Part 2. Structure of a physically based distributed modeling system. *Journal of Hydrology 87, 61-77*

Ahmad, A. B. M. and Ismail, S. (2004). Recurrent neural network with back propagation through time algorithm for Arabic recognition. *In Proceedings of 18th European Simulation Multiconference. Graham Harton.*

Aisien, F.A., Aisien, E.T., and Shaka, F. (2003). The Effects of Rubber Factory Effluent on Ikpoba River, *Nigerian Journal of Biomedical Engineering, 2(1), 31-35.*

Ajibola, V.O. and Ladipo, M.K. (2011). Sediment quality of effluent discharge channels from six industrial sites in Lagos, Nigeria, *htt://www.ijer.ir; 5 (4): 901-908.*

Akan, J.C., Abdulrahman, V.O.; Ogugbuaja and Reuben, K.D. (2009). Study of the physicochemical pollutants in Kano industrial areas, Kano state, Nigeria, *Journal of Applied Sciences in Environmental Sanitation; 4 (2): 89-102*

Aleksandra Z.S. and Jerzy S.,(2012) Review of Mathematical Models of Water Quality; Faculty of Process and Environmental Engineering, Technical University of Lodz, ul. *Wólczańska 213, Ecol Chem Eng S. 2012;19(2):197-211*

Alloway, B., and Ayres, D. C. (1997). Chemical principles of environmental pollution: CRC Press.

Aluyor, E.O. and Badmus, O.A.M. (2003a). Time Series Analysis of Pollutant Levels in Industrial Wastewater Effluent – A Case Study of a Beverage Industry , *Nigerian Journal of Biomedical Engineering, 3(1), 27-30.*

Aluyor, E.O. and Badmus, O.A.M. (2003b). Time Series Analysis of Pollutant Levels in Industrial Wastewater effluents – A Case Study of a Beverage Industry, *Nigerian Journal of Biomedical Engineering, 2(1), 19-32*

Ambrose, B., Wool, T.A., Martin, J.L., 2001. The Water Quality Analysis Simulation Program, *WASP6, User Manual, US EPA, Athens, GA.*

Amoudry L.O. and Souza A.J. (2011) Deterministic coastal morphological and sediment transport modeling: a review and discussion, *Reviews of Geophysics, Vol. 49, RG2002.*

Anukrati Mehta, 2020, A Comprehensive Guide to Types of Neural Networks, https://www.digitalvidya.com/blog/types-of-neural-networks/

Ashraf M.A., Maah M.J., and Yusoff I., (2012) "Morphology, geology and water quality assessment of former tin mining catchment," *The Scientific World Journal, vol. 2012, Article ID 369206, 15 pages.*

Auer P., Burgsteiner H and Maass W. (2008). A learning rule for very simple universal approximators consisting of a single layer of perceptrons. *Neural Netw. 21, 786–795. 10.1016/j.neunet.2007.12.036*

Awu J.I., Mbajiorgu C.C., Ogunlela A.O., Kasali M.Y., Ademiluyi Y.S. and James D.D. (2017). Optimization of neural network architecture and transfer functions for rainfall river flow modeling. *Journal of Environmental Hydrology. Vol. 25. Iss. 8 p. 1–15.*

Aydin, E., Sridhar, M., Oluwande, P. and Okubadeju, A.(2010). Health hazards and pollution from open drains in a Nigerian city. *Ambio, 10(1):29–33.*

Bai, J., Cui, B., Chen, B., Zhang, K., Deng, W., Gao, H., Xiao, R. (2011): Spatial distribution and ecological risk assessment of heavy metals in surface sediments from a typical plateau lake wetland, China. – *Ecological Modeling 222(2):301–306.*

Bai J.H., H.F. Gao, R.Xiao, J.J. Wang, and C. Huang, (2012a).A review of soil nitrogen mineralization in coastal wetlands: issues and methods," *Clean—Soil, Air, Water, vol. 40, no. 10, pp. 1099– 1105.*

Bai J.H., R.Xiao, K.J.Zhang, and H.F.Gao, (2012b). "Arsenic and heavy metal pollution in wetland soils from tidal freshwater and salt marshes before and after the flow-

sediment regulation regime in the Yellow River Delta, China," *Journal of Hydrology, vol. 450451,pp.244–253.*

Bakare, I. A., and Akintan, R. A. (2016) Economics of water governance-rural health survival linkages in Lagos: Evidence from badagry local government area. *Global journal of applied, management and social sciences, 11.*

Beal, L. J. and Raman, D. R. (2000). Sequential Two-Stage Anaerobic Treatment of Confectionery Wastewater. *Journal of Agricultural Engineering Research, 76, 2000, 211- 217.*

Bichi, M.H. (2000) Surface water quality in Kano industrial environment, in: Falola et al., Issues in Land Administration and Development in Northern Nigeria. *Proceedings of the National workshop on Land Administration and Development in Northern Nigeria, Department of Geography, Bayero University, Kano,: 305-313.*

Bisht Anil Kumar, Ravendra Singh, Rakesh Bhutiani and Ashutosh Bhatt, (2019), Artificial Neural Network Based Water Quality Forecasting Model for Ganga River, International Journal of Engineering and Advanced Technology (IJEAT) ISSN: 2249 – 8958, Volume-8 Issue-6.

Bowers J. A. and C. B. Shedr, (2000**).** Predicting stream water quality using Artificial Neural Networks (ANN). *Development & Application of Computer Techniques to Environmental Studies VI, ISBN1-85312-819-8*

Brown, E.J.; Kohdor, H; Hideri R.C and Rice-Evans (1998). Structural Dependence of Flavonoids Interactions with Copper (11) Ions. *Oklahoma State University Annual Science Journal, 33: p. 78 by Tripped Refuse London.Hmso vol 6.pp 20-24.*

Burt T.M. (2013). The silent river: the hydrological basis for river conservation. In: Sabater S, Elosegi A (eds) River conservation. Challenges and opportunities. *Fundacio´n BBVA, Bilbao, pp 39–60*.

Bulkley, J. W. (2011) Integrated watershed management: Past, present, and future. J*ournal of Contemporary Water Research and Education, 100(1)3.*

Canu, D.M., Solidoro, C., Umgiesser, G. (2004). Erratum to modeling the responses of the Lagoon of Venice ecosystem to variations in physical forcing. *Ecol. Model. 175,197–216.*

Cao X.J. and Zhang H., (2006). "Commentary on study of surface water quality model," *Journal of Water Resources and Architectural Engineering, vol.4, no.4, pp.18–21, (Russian).*

Carpenter, S. R., Caraco, N. F., Correll, D. L., Howarth, R. W., Sharpley, A. N., and Smith, V. H. (1998). Non-point pollution of surface waters with phosphorus and nitrogen. *Ecological applications, 8(3), 559-568.*

Castro-González, M., and Méndez-Armenta, M. (2008). Heavy metals: Implications associated to fish consumption. *Environmental toxicology and pharmacology, 26(3), 263-271.*

Cencic, O., Rechberger, H. (2008). Material flow analysis with software STAN. Sustain.*Environ. Res. 18, 3–7.*

Chen, Y., Dawson, C. W., Harpham, C., and Wilby, R. L. (2002). Evaluation of artificial neural network techniques for flow forecasting in the River Yangtze, China. *Hydrology and Earth system sciences, 6(4):619–626*

Crini, G. (2005) Recent developments in polysaccharide-based materials used as adsorbents in wastewater treatment. *Progress in polymer science, 30(1), 38-70.*

Cole, T. M., Wells, S. A. (2008), CE-QUAL-W2: A two-dimensional, laterally averaged, Hydrodynamic and Water Quality Model. *Version 3.6, Department of Civil and Environmental Engineering, Portland State University, Portland, OR.*

COMSOL Multiphysics Reference Manual Version 5.3a, (2017) .*COMSOL AB, USA.*

Dacombe James, (2017). An introduction to Artificial Neural Networks (with example), *https://www.linkedin.com/in/jamesdacombe/.*

Dada, A.Y., (1997) Evaluation of kano state environmental management program on industrial pollution a case study of challawa and sharada industrial areas.

Unpublished postgraduate diploma project, Dept. of Geography, Bayero University, Kano, 1997

Das Rajib S.N., Roy P.K.,Mitra D., (2006) 'Role of Electrical Conductivity as an Indicator of Pollution in Shallow Lakes'. *1 Jan. 2006: 143 – 146.*

David A. T., Dao N.B. and Stanley H. N., (2012) Introduction to Fuel Blending, *https://doi.org/10.1016/B978-0-12-380932-2.00001-5*.

Davis, J.B. and Reilly, P.J.A. (1980). Palm oil mill effluent -a summary of treatment methods. Oleagineux, 35:323–330.

Donald J. O'Connor. (1967).The temporal and spatial distribution of dissolved oxygen in streams. *Water Resources Research, 3(1): 65–79.*

Dwivedi, B. K. and Pandey, G. C. (2002). Physicochemical factors and algal diversity of two ponds In Faizabad, India. *Poll. Res. 21(3):361-370.*

Duflow, 2000. Duflow for Windows V3.3: Duflow Modeling Studio: Users Guide, Reference Guide. *DUFLOW, and Reference Guide RAM. Utrecht. The Netherlands, EDS/STOWA.*

Edwin K. K.,, Emmanuel C. K. , Job R. K.,(2016) Dissolved Oxygen Modelling Using Artificial Neural Network: A Case Of River Nzoia, Lake Victoria Basin, Kenya; *Journal of Water Security, 2016, Vol. 2 Article Number: jws2016004 DOI: http://dx.doi.org/10.15544/jws.2016.004.*

Egborge, A.A.M. (1994) Water Pollution in Nigeria (1) Biodiversity and Chemistry of Warri River. Ben Miller Publisher, Warri.

Egwuonwu, C. C., Uzojie, A. P., Okafor, V. C., Ezeanya, N. C. and Nwachukwu, M. U. (2012). Evaluation of the effects of industrial wastewater discharge on surface water: A case study of Nigeria Breweries PLC, Enugu. *Greener Journal of Physical Sciences, 2(3): 46 – 63.*

Eletta, O.A., Adekola, F.A. and Aderanti, M.A. (2005), "Effects of Wastewater Discharge from Soft Drink Plant into Asa River", *J. Appl. Sci. Environ. Mgt., 9(1), 187-190.*

Eremektar, S., Emongor,.V. Nkegbe, E. Kealotswe, B. Koorapetse, I. Sankwase, S. and Keikanetswe, S. (2002). Pollution indicators in Gaborone industrial effluent. *Journal of Appl Sci., 5: 147-150*

Ezeomedo I.C. and Igbokwe I.J , 2009, Mapping of Urban Features of Nnewi Metropolis Using High Resolution Satellite Image and Support Vector Machine Classifier, *Journal of Environment and Earth Science www.iiste.org ISSN 2224-3216 (Paper) ISSN 2225-0948 Vol.9, No.6, 2019 116* .

Fakayode, S.O.(2005) Impact assessment of industrial effluent on water quality of the receiving Alaro River in Ibadan, Nigeria. *Ajeam-Ragee; vol. 10, 1-3*

Faramarz D.A., Ernest B., Kumars S. P., Raghu N.S. and Behshad J.S. (2011). Application of Computational Fluid Dynamics (CFD) for Simulation of Acid Mine Drainage Generation and Subsequent Pollutants Transportation through Groundwater Flow Systems and Rivers, Computational Fluid Dynamics Technologies and Applications. *Prof. Igor Minin (Ed.), ISBN: 978-953-307-169-5, InTech.*

FAO. 1984 Trace elements in agriculture. *FAO Soils Bulletin (Draft), Soil Resources, Management and Conservation Service. FAO, Rome. 68 p*

Fath B.D, Jorgensen S.E, and Scharler U.M (2011) Ecological Modeling in Environmental Management: History and Applications. In: *Wolanski E and McLusky DS (eds.) Treatise on Estuarine and Coastal Science, Vol 9, pp. 23–33.*

Franceschini S and Tsai C W. (2010) Assessment of uncertainty sources in water quality modeling in the Niagara River. *Advances in Water Resources, 33(4): 493–503*

FEPA. (1999). Federal environmental protection agency act. Lagos, Nigeria: *Federal environmental protection agency.*

FEPA. (1991). Interim guide lines and standards for industrial effluent, gaseous emissions and noise limitations. Nigeria: *Federal environmental protection agency*

Forenshell, G. (2001). Setting basin design. *Western Regional Aquaculture Center, WRAC-106. USA: 6pp*

Förstner, U., and Wittmann, G. T. (2012) Metal pollution in the aquatic environment: Springer Science & Business Media.

Franceschini S, Tsai C W. Assessment of uncertainty sources in water quality modeling in the Niagara River. *Advances in Water Resources, 2010, 33(4): 493–503.*

Fu, L. (1994). Neural Networks in Computer Intelligence. *McGraw-Hill, Inc., University of Florida, Gainesville.*

Gayathri K Devia, Ganasri B P and Dwarakish G S,(2015), A Review on Hydrological Models: *International Conference On Water Resources, Coastal And Ocean Engineering (Icwrcoe 2015).www.elsevier.com/locate/proceedia, Aquatic Procedia 4 (2015) 1001 – 1007.*

Gbadebo, E., Nweke, O.C. and Sander, W.H. (2010). Modern environmental health hazards: *A public health issue of increasing significance in Africa. Environ. Health Persp, 117(6): 863-870.*

Gill Navdeep Singh, (2019) Artificial Neural Networks Applications and Algorithms, *https://www.xenonstack.com/blog/artificial-neural-network-applications/*

Ghosh, G. (2002) Water of India (quality & quantity): *APH Publishing.*

Gough D I. (1969) Incremental stress under a two-dimensional artificial lake. *Canadian Journal of Earth Sciences, 6(5): 1067–1075 6.*

Hafizan J., Sharifuddin M. Z., Mohd. E.T., Mazlin M., (2004).Application of artificial neural network models for predicting water quality index, Jurnal Kejuruteraan Awam 16(2): 42-55.

Hajigholizadeh M., Melesse A. M. and Fuentes H. R. (2018) Erosion and sediment transport modeling in shallow waters: A review on approaches, models and applications. *International Journal of Environmental Research and Public Health. 15(3):518*

Halliday, S. J., Wade A. J., Skeffington, R. A., Neal, C., Reynolds, B., Rowland. P., Neal, M. and Norris, D. (2012). An analysis of long-term trends, seasonality and short-term dynamics in water quality data from Plynlimon, Wales. *Science of the Total Environment 434 186– 200.*

Holanda, P.S., Blanco, C.J.C., Cruz, D.O.A., Lins, E.F., Barp, A.R.B. , Secretan, Y., 2009, "Hydrodynamic Modeling of the Lake Água Preta: Water Source of the Belém Metropolitan Area", In: COBEM 2009 – *International Congress of Mechanical Engineering, Gramado-RS, Brazil.*

Holanda SP, Blanco JC, Cruz AOD, Lopes FD, Barp BRA, Secretan Y (2011) Hydrodynamic modeling and morphological analysis of lake A´ gua Preta: one of the water sources of BelemPA-Brazil. J Braz Soc Mech Sci Eng 33(2):117

Holzbecher E. and Hadidi A., Some benchmark simulations for flash flood modelling, *COMSOL conference, Rotterdam, 2017*

Huang L.B., Bai J.H., Xiao R., Gao H.F., and Liu P.P., (2012) "Spatial distribution of Fe, Cu, Mn in the surface water system and their effects on wetland vegetation in the Pearl River Estuary of China,"*CLEAN—Soil,Air,Water,vol.40,no.10,pp.1085–1092.*

Ibekwe V.I, Ogueri N., Offorbuike J.O., (2004) Bacteriological and Physico-Chemical Qualities of Waste Water From A Bottling Company In Owerri, Nigeria, *Global journal of environmental sciences, Vol. 3 No. 1 .*

Irvine, K. N. Richey, J. E. Holtgrieve, G. W. Sarkkula, J. and Sampson, M.,. (2011). Spatial and temporal variability of turbidity, dissolved oxygen, conductivity, temperature,

and fluorescence in the lower Mekong River–Tonle Sap system identified using continuous monitoring. *International Journal of River Basin Management, 9:2, 151-168; http://dx.doi.org/10.1080/15715124.2011.621430.*

James, A. (1996). An Introduction to Water Quality Modeling. *2nd edition. John Wiley & Sons Ltd, New York.*

Ji Z G, Morton M R, Hamrick J M. (2001).Wetting and drying simulation of estuarine processes. *Estuarine, Coastal and Shelf Science, 53 (5): 683–700.*

Jimena, E., Jern, N.G. and Wun, J. (2008).Industrial Wastewater Treatment. *Imperial College Press, London.*

Juahir, H., Sharifuddin, M., Zain, M., Toriman, E., & Mokhtar, M. (2004). Use of artificial neural network in the prediction of water quality index of Langat River Basin. Malaysia. Jurnal Kejuruteraan Awam, 16(22), 42–55

Kanu, I., Achi, O. K., Ezeronye, O. U. and Anyanwu E. C. (2006). Seasonal variation in bacterial heavy metal biosorption in water samples from Eziama River near soap and brewery industries and the environmental health implications. *Int. J. Environ. Sci. Tech., 3 (1): 95- 102.*

Kanu, I. and Achi, O.K. (2011). Industrial Effluents and Their Impact on Water Quality of Receiving Rivers in Nigeria. *Journal of Applied Technology in Environmental Sanitation, 1 (1): 75-86.*

Katsuro, I., Ogunfowokan O.A and Fakankun, O.A. (2004). Physico-chemical characterization of effluents from beverage processing plants in Ibadan, Nigeria. *Inter. J. Environ. Studies. 54(2): 145-152.*

Kanda Edwin Kimutai , Emmanuel Chessum Kipkorirb and Job Rotich Kosgeib, (2016), dissolved oxygen modelling using artificial neural network: a case of river nzoia, lake victoria basin, Kenya. eISSN 2345-0363 Journal of Water Security, 2016, Vol. 2 Article Number: jws2016004 DOI: http://dx.doi.org/10.15544/jws.2016.004.

Khadijah et al (2019), Water Quality Classification Using an Artificial Neural Network (ANN). *IOP Conf. Ser.: Mater. Sci. Eng. 601 012005*

Khalil Bahaa Mohamed , Ayman Georges Awadallah , Hussein Karaman and Ashraf El-Sayed, (2012), Application of Artificial Neural Networks for the Prediction of Water Quality Variables in the Nile Delta; Journal of Water Resource and Protection, 2012, 4, 388-394 doi:10.4236/jwarp.2012.46044.

Kim I., Jeffrey E.R., Gordon W.H., Juha S., Sampson M., (2011) Spatial and temporal variability of turbidity, dissolved oxygen, conductivity, temperature, and fluorescence in the lower Mekong River–Tonle Sap system identified using continuous monitoring; *International Journal of River Basin Management 9(2):151-168 DOI: 10.1080/15715124.2011.621430.*

Kim, K.-H., Jahan, S. A., Kabir, E., and Brown, R. J. (2013) A review of airborne polycyclic aromatic hydrocarbons (pahs) and their human health effects. *Environment international, 60, 71-80.*

Kima, D., Wanga, Q., Soriala, G.A., Dionysioua, D.D and Timberlake, D., (2004). A model approach for evaluating effects of remedial actions on mercury speciation and transport in a lake system. *Sci. Total Environ. 327, 1–15*

Knight, R. L., Payne, V. W., Borer, R. E., Clarke, R. A., and Pries, J. H. (2002) . Constructed wetlands for livestock wastewater management. *Ecological engineering, 15(1), 41-55.*

Komatsu, E., Fukushima, T., Harasawa, H. (2007), A modeling approach to forecast the effect of long-term climate change on lake water quality. *Ecological Modeling, 209:351-366*

KuoJ.T.,Lung,W.S.,Yang,C.P.,Liu,W.C.,Yang,M.D.,Tang,T.S.(2006).*Eutrophicati on modeling of reservoirs in Taiwan.Environ.Model.Softw.21,829–844.*

Lai, Y.C. (2010). Development of Kaoping River Management Strategies. *Ph.D. Dissertation, National Sun Yat-Sen University, Kaohsiung, Taiwan.*

Lee, S., Ni-Mesister, W., Toll, D., Nigro, J., Gutierrez-Magness, A. L., Engman, T., (2010), Assessing the hydraulic performance of the EPA's nonpoint source water quality assessment decision support tool using North American Land Data Assimilation System (NLDAS). *Journal of Hydrology, 387(3-5):pp212-220.*

Limno-Tech, (2002). Descriptive inventory of models with prospective relevance of impacts of water withdrawals. *Prepared for Great Lakes Commission.*

Lin C E, Chen C T, Kao C M, Hong A, Wu C Y. (2011) Development of the sediment and water quality management strategies for the Salt-water River, Taiwan. *Marine Pollution Bulletin, 63(5): 528–534.*

Liu X, Huang W. (2009). Modeling sediment re-suspension and transport induced by storm wind in Apalachicola Bay, USA. *Environmental Modeling & Software, , 24(11):* 1302–1313.

Liou S.-M., Lo S.-L., and Hu C.-Y.,(2003) "Application of two-stage fuzzy set theory to river quality evaluation in Taiwan," *Water Research, vol.37, no.6, pp.1406–1416.*

Lowel and Thompson F., (1992). Biodiversity of vibrios. Microbiol. *Mol. Biol. Rev. 68: 403-431* ***34398***

Maamari, F., Andersen, M., De Boer, J., Carroll, W. D., Dumortier, D. and Greenup, P. (2006). Experimental Validation of Simulation Methods for Bi-directional Transmission Properties at the Daylighting Performance Level. *Energy and Buildings, (38), pp.878–889.*

Ma A.N., 2004 Environmental management for the palm oil industry. *Palm Oil Dev*; 30:1–9

Monteiro Magda and Costa Marco, (2018) A Time Series Model Comparison for Monitoring and Forecasting Water Quality Variables, *Hydrology 2018, 5, 37;doi:10.3390/hydrology5030037.*

Mahata, T. V. and Antil, C. (2004) Impact of refinery effluent on the physicochemical properties of a water body. *Appl. Ecology Env. Res., 3: 61-72.*

Martin . J. ,1999. Hydrodynamics and Transport for Water Quality modelling. *CRC Press,*

New York.

Marquitta K. Hill (2004). Understanding Environmental Pollution.2nd Edition. *Cambridge University Press. Pp 199-221*

Merian, E. (1991): Metals and their Compound in the Environment. *Occurrence Analysis and Biological Relevance .Uclt, Weintrein-New York.*

Midwest Lab, (2016), nitrate and ammonium nitrogen stability and uptake. *https://midwestlabs.com/wp-content/uploads/2016/11/109-Nitrate-and-Ammonium-Nitrigon-Stability-and-Uptake.pdf*

Minns, A W and Hall, M J 1996. Artificial neural network as rainfall-runoff models. *Hydrological Sciences Journal, 41(3): 399-417.*

Mohd Ekhwan T. (2002) Investigations into channel instability and river morphological change: The Langat River, Peninsular Malaysia. *Ph.D Thesis. Faculty of Science, Agriculture and Engineering, University of Newcastle upon Tyne, 255 pp.*

Morris, B., Lawrence, A., Chilton, P., Adams, B., Calow, R., and Klinck, B. (2003). Groundwater and its susceptibility to degradation (p. 140). *Retrieved from http:// www. unep.org/ dewa/water/ groundwater/pdfs/groundwater_prelims_screen.pdf*

Mujumdar P. P. and Vemula V. R. S. "Fuzzy waste load allocation model: simulation-optimization approach," *Journal of Computing in Civil Engineering, vol.18, no.2, pp.120–131, 2004*

Mura, S., Seddaiu, G., Bacchini, F., Roggero, P. P., and Greppi, G. F. (2013) Advances of nanotechnology in agro-environmental studies. *Italian Journal of Agronomy, 8(3), 18.*

Najah A. , A. El-Shafie , O. A. Karim and H. El-Shafie, (2012).Application of artificial neural networks for water quality prediction. *Neural Comput & Applic. 22 (Suppl 1):S187–S201 DOI 10.1007/s00521-012-0940-3.*

National Academy of Sciences, NAS. (1980) Drinking water and health. *Vol. 3. Washington, DC, National Academy Press: 283-293*

National Population Commission (NPC) (2006). Census figures Anambra state, Nigeria

National Pollutant Discharge Elimination System, NPDES.(2008). *Department of waste water management, Tallahassee: Florida..*

NIEA (National Institute of Environmental Analysis, Taiwan EPA) 2004. Rate Analysis, NIEA W022.51C.

Nikos J. Warrence, Krista E. Pearson, and James W. Bauder (2003). Basics of Salinity and Sodicity Effects on Soil Physical Properties. *Department of Land Resources and Environmental Sciences, Montanta State University-Bozeman.*

Nitsche, N. C., 2000, Assessment of a hydrodynamic water quality model, Duflow, for a winter rainfall river, *MSc Engineering thesis, University of Stellenbosch*

Nkwocha, A.C. and Okoye, J.I. (2007). Quality Evaluation of Industrial Liquid Effluent", *Continental J. Applied Sciences, 2, 51-55.*

Nkwocha, A.C. and Okoye, J.I. (2008). "Assessment of the Treatment Effectiveness of Industrial Wastewater Treatment Plant". *Journal of Agricultural Research and Policies, 3(4), 12- 14.*

Nkwocha, A.C., Okoye, J.I. and Okpalanma, F.E. (2010). "Quality Assessment of Fast Food Industries Effluent", *International Journal of Biotechnology and Allied Sciences, 5(1), 625- 628.*

Nollet L. M. L., (2000) Handbook of Water Analysis, *Marcel Dekker, New York, NY, USA*

Norman, E.P. and Mitchel M. (2000). Water quality degradation effects on freshwater availability: Impacts of human activities, *International Water Resources Association; Water International Journal; vol. 25 (2) 185-193.*

Novotny, V. (2003). Water quality: Diffuse pollution and watershed management: *John Wiley & Sons.*

Nwabuzor, A. (2005). Corruption and development: New initiatives in economic openness and strengthened rule of law. *Journal of Business Ethics, 59(1-2), 121-138*.

Obropta C. C., Niazi M., and Kardos J. S. (2008) "Application of an environmental decision support system to a water quality trading program affected by surface water diversions, "*Environmental Management, vol. 42, no.6, pp. 946–956.*

Odoemelam, S.A, (2005). Bioaccumulation of Trace Elements from Fishes from Oguta Lake, Nigeria. J. *Chem. Soc. Of Nigeria, Vol. 30(1).pp 18-20*

Ojiako, J.C. and Igbokwe, J.I. (2009). Application of Remote Sensing and Multimedia Geographic Information System (GIS) in the Administration of Socio-Economic Activities in Nnewi Urban Area of Anambra State, Nigeria. Environmental Research *Journal,Volume 3; Issue 2, Pp 60-67*.

Ogedengbe, K. and Akinbile, C. O. (2004). "Impact of Industrial Pollutants on Quality of Ground and Surface Waters at Oluyole Industrial Estate, Ibadan, Nigeria". Nigeria *Journal of Technological Development, 4(2) 139-144.*

Ogunkunle, C. O., Mustapha, K., Oyedeji, S. & Fatoba, P. O. (2016). Assessment of metallic pollution status of surface water and aquatic macrophytes of earthen dams in Ilorin, north-central of Nigeria as indicators of environmental health. *Journal of King Saud University-Science, 28(4), 324–331. doi:10.1016/j.jksus.2015.11.005*

Okereke, C. D. (2007). "Environmental Pollution Control". *1st Edition. Barloz Publication Owerri.*

Oketola, A. A. and Osibanjo, O. (2009). Estimating sectoral pollution load in Lagos by industrial pollution projection system (IPPS): *Employment versus output. Toxicological and Environmental Chemistry, 91(5), 799–818. doi: 10.1080/02772240802614499*

Okoye, P. A. C., Enemuoh, R. E. and Ogunjiofor, J. C. (2002). Traces of heavy metals in Marine crabs. J. *Chem. Soc. Nigeria. 27 (1) 76-77*

Okoye N.H., Obidike, G.E. and Nduka, J.K.C (2011). Analysis of untreated effluents from soap factories in Aba, Abia State, Nigeria. *Journal of Basic Physical Research, 2 (2): 21-25.*

Omole, D. O., Ndambuki, J. M. and Osabuohien, E. (2014). Nigeria's legal instruments for land and water use: Implications for national development. *In E. Osabuohien (Ed.), Handbook of research on in-country determinants and implications of foreign landacquisitions.IGIGlobal.doi:10.4018/978-1-4666-7405-9.ch018.*

Omole, D. O., and Isiorho, S. (2011). Waste management and water quality issues in coastal states of Nigeria: *The Ogun state experience. Journal of Sustainable Development in Africa, 13(6), 207–217.*

Omole, D. & Ndambuki, J. (2014).Sustainable living in Africa: Case of water, sanitation, air pollution and energy. *Sustainability, 6(8), 5187–5202. Doi: 10.3390/su6085187.*

Onuigbo A.C. and Madu, I.A., 2013. Assessment of impact of effluent discharge on the quality of Emene River, Enugu, Nigeria. *New York Science Journal. 6 (8), 34-42.*

Otukunefor, T.V. and Obiukwu, C. (2005), "Impact of Refinery Effluent on the Physiochemical Properties of a Water Body in the Niger Delta", *Applied Ecology and Environmental Research, 3(1), 61-72.*

Odokuma, L. and Oliwe, O.S.I. (2003). Toxicity of substituted benzene derivatives to four chemolithotrophic bacteria isolated from the New Calabar River. *Global J Environ Sci*.,2(2): 72-77

Patrícia S.H., Claudio J.C.B, Daniel O. , David F.L. ,Ana R.B., Yves S. , (2011) ; Hydrodynamic Modeling and Morphological Analysis of Lake Água Preta: One of the Water Sources of Belém-PA-Brazil, *J. of the Braz. Soc. of Mech. Sci. & Eng. April-June 2011, Vol. XXXIII, No. 2* .

Pei Zhao & Xiangyu Tang & Jialiang Tang and Chao Wang, 2013. "Assessing Water Quality of Three Gorges Reservoir, China, Over a Five-Year Period From 2006 to

2011," Water Resources Management: An International Journal, Published for the European Water Resources Association (EWRA), Springer; European Water Resources Association (EWRA), vol. 27(13), pages 4545-4558.

Politano M., Haque M. M., and Weber L. J., (2008). "A numerical study of the temperature dynamics at McNary Dam."*Ecological Modeling, vol.212, no.3-4, pp.408–421*.

Phiri, O., Mumba, P., Moyo, B.H.Z. and Kadewa, W.,(2005) Assessment of the impacts of industrial effluents on water quality of receiving rivers in urban areas of Malawi, *International Journal of Environmental Science Tech; Sept. 2005; vol. 2, (3) 237-244.*

Varoonchotikul (2003) Flood Forecasting using Artificial Neural Networks, *Taulor & Francis, 2003, 102 σελ., ISBN: 9058096319.*

Qinggai Wang, Shibei Li, Peng Jia, Changjun Qi, and Feng Ding, (2013), A Review of Surface Water Quality Models, *the scientific world journal, article ID 231768, 7 pages, http://dx.doi.org/10.1155/2013/231768*

RAMP, (1996). River Assessment Monitoring Project, *http://www.state.ky.us/nrepc /water /ramp/rmso4.htm*

Rehman, W., Zeb, A., Noor, N., and Nawaz, M. (2008) Heavy metal pollution assessment in various industries of Pakistan. *Environmental Geology, 55(2), 353-358.*

Rein, S. (2005). Water Quality Monitoring. *Journal of Agriculture & Social Sciences, 4:31-34.*

Rice, E., Bridgewater, L., Association, A. P. H., and Association, A. W. W. (2012). *Standard methods for the examination of water and wastewater.*

Riffat R. (2012). Fundamentals of wastewater treatment and engineering. *CRC Press, 5.*

Ritter, W. F., and Shirmohammadi, A. (2000). Agricultural nonpoint source pollution: Watershed management and hydrology: *CRC Press.*

Robbins, P., Polderman, A., and Birkenholtz, T. (2001) Lawns and toxins: An ecology of the city. *Cities, 18(6), 369-380.*

Sahaya Vasanthi, S. and Adish Kumar, S., (2018), Application of artificial neural network techniques for predicting the water quality index in the Parakai Lake, Tamil Nadu, India, applied ecology and environmental research 17(2):1947-1958

Sakshi Kohli , Surbhi Miglani , Rahul Rapariya, (2014) Basics of Artificial Neural Network, *International Journal of Computer Science and Mobile Computing, Vol.3 Issue.9, September, pg. 745-751*

Schulz, K. and Howe, B. (2003). Uncertainity and sensistivity analysis of water transport modeling in a layered soil profile using fuzzy set theory. *J. Hydroinform., 1: 127-138.*

Scoullos, M., Vonkeman, G. H., Thornton, I., and Makuch, Z. (2012) Mercury—cadmium— lead handbook for sustainable heavy metals policy and regulation (Vol. 31): *Springer Science & Business Media*.

Sevimli, E., Dejoux, C., H. Deelstra and Wizszlkinson, R. (1999) Pollution. In The ecology and utilization of African inland waters, edited by J. Symoens, M. Burgis and J. Gaudet. *UNEP Rep.Proc.Ser., (1):149–161*.

Siebert, S., Burke, J., Faures, J. M., Frenken, K., Hoogeveen, J., Döll, P., and Portmann, F. T. (2010). Groundwater use for irrigation - *A global inventory. Hydrology and Earth System Sciences, 14, 1863–1880. doi:10.5194/hess-14-1863-2010.*

Sigel, K., Klauer, B., and Pahl-Wostl, C. (2010) Conceptualizing uncertainty in environmental decision-making: The example of the water framework directive. *Ecological economics, 69(3), 502-510.*

Sirisha P., Sravanti K N and Ramakrishna V., (2008) Application of Artificial Neural Networks for Water Quality Prediction, *International Journal of ISSN 0974-2107 Systems and Technologies Vol.1, No.2, pp 115-123*

SKM 2011, Development of WQ Modelling Framework for the MDB Phase 1—Scoping

Study, *Sinclair Knight Merz, report prepared for Murray-Darling Basin Authority, Canberra.*

Susilowati Y, Mengko T R, Rais J and Leksono B E. (2004).Water quality modeling for environmental information system. In*: Proceeding of the 2004 IEEE Asia-Pacific Conference on Circuits and Systems, 2:929–932*.

Sylvia R. Esterby S R. (1996) Review of methods for the detection and estimation of trends with emphasis on water quality applications. *Hydrological Processes, 10(2):127–149.*

Taghinia, H. A., Basaravajappa, H.T. and Qaid Saeed, A.M. (2010). Heavy metal pollution in Kabiri Rivers sediments, *htt://www.ijer.ir; 4 (4) 629-636.*

Tim U.S.and Jolly R. (1994). Evaluating agricultural non point-source pollution using integrated geographic information systems and hydrologic/ water quality model. *Journal of Environmental Quality, 23 (1):25.*

Ubah, J. I., Chukwuma, G. O., Orakwe, L. C., Ogbu, K. N. and Menkiti, N. I. (2015). Seasonal Impacts of Industrial Effluents from Chikason Industries Limited on Ele-river Nnewi, Anambra State, Nigeria. *International Journal of Applied Research and Technology. 4(4): 55 – 60*

Ubawuike J.N. (2010). Effects of Industrial Wastewater on Aba River in Aba, Abia State. *Unpublished Thesis.*

Varoonchotikul P (2003) Flood forecasting using artificial neural lnetworks. Taylor & Francis, The Netherlands, p 102

Vasanthi S.S., Adish K., S., (2018) Application of Artificial Neural Network Techniques for Predicting the Water Quality Index In The Parakai Lake, Tamil Nadu, India, *Applied Ecology And Environmental Research 17(2):1947-1958.*

Versteeg, H. K., Malalasekera, W. (1995). An introduction to computational fluid dynamics, *Longman Group limited, Longman House, Essex, England.*

Visescu M., Beilicci E. and Beilicci R., (2016). Sediment transport modeling with advanced hydroinformatic tool case study - modeling on Bega channel sector, *Procedia Engineering, Vol. 161, 1715-1721.*

Wang J.Q., Z.Zhong, and J.Wu, (2004) Steam water quality models and its development trend," *Journal of Anhui Normal University (Natural Science),vol.27,no.3,pp.243–247.*

Wang Q.G., Dai W.N., Zhao X.H., Ding F., Li S.B.,and Zhao Y. (2009), "Numerical model of thermal discharge from Laibin power plant based on Mike 21,"*Research of Environmental Sciences,vol. 22,no.3,pp.332–336, (Russian).*

Wang Qinggai, Shibei Li, Peng Jia, Changjun Qi, and Feng Ding (2013), A Review of Surface Water Quality Models, The Scientific World Journal, Article ID 231768, 7 pages http://dx.doi.org/10.1155/2013/231768.

Wechmongkhonkon, N.Poomtong and S. Areerachakul, (2012) Application of Artificial Neural Network to Classification Surface Water Quality; World Academy of Science, Engineering and Technology. *International Journal of Environmental and Ecological Engineering Vol:6, No:9* .

Westcot D.W. and Ayers R.S., (1994) Water quality for agriculture, Food and Agriculture Organization of the United Nations. *M-56 ISBN 92-5-102263-1.*

Winbourne, S.(2002).Corruption and the environment. *Management Systems International and USAID, Washington*

World Health Organization (2004). *World Health Organization guidelines for drinking water quality (3rd Edition). Geneva, Switzerland.*

World Health Organization (WHO) 2004a: Guideline Values for chemicals that are of Health Significance in Drinking Water Quality. *World Health Organization Geneva,pp 491-493.*

WWAP. (2014). The United Nations World Water Development Report 2014: Water and Energy (Vol. 1).

Xiao,J.H.Bai,H.F.Gao,J.J.Wang,L.B.Huang,andP.P.Liu,(2012)"Distribution and contamination assessment of heavy metals in water and soils from the college town in the Pearl River Delta, China,"*CLEAN—Soil,Air,Water,vol.40,no.10,pp.1167–1173,*.

Xie R, Wu D, Yan Y, Zhou H. (2010).Fine silt particle path line of dredging sediment in the Yangtze River deepwater navigation channel based on EFDC model. *Journal of Hydrodynamics, 22(6): 760–772.*

Yamini Soni and Vikas Sejwar, (2019) An Estimating Model for Water quality of river Ganga using Artificial Neural Network; *International Journal of Innovative Technology and Exploring Engineering (IJITEE) ISSN: 2278-3075, Volume-8 Issue-9, July* .

Yang, C.P., Kuo, J.T., Lung, W.S., Lai, J.S. and Wu, J.T. (2007). Water quality and ecosystem modeling of tidal wetlands. *J. Environ. Eng. 133, 711–721*.

Yang Y S, Wang L. (2010) A review of modeling tools for implementation of the EU water framework directive in handling diffuse water pollution. *Water Resources Management, , 24(9): 1819–1843.*

Yetik, M.K., Yuceer, M., Karadurmus, E., Semizer, E., Calimli, A., Berber, R. (2014): interactive GIS-based software for dynamic monitoring of rivers. – *Journal of Environmental Protection and Ecology 15(4): 1767–1778.*

Yih S M, Davidson B. (1975). Identification in nonlinear, distributed parameter water quality models. *Water Resources Research, 11(5): 693–704.*

Xu Z.-X. and Lu S.-Q., (2003)."Research on hydrodynamic and water quality model for tidal river networks,"*Journal of Hydrodynamics, vol.15,no.2,pp.64–70.*

Yuyan Fan, Tianqi A, Haijun Yu, Guoru Huang, and Xiaodong Li, (2017); A Coupled 1D-2D Hydrodynamic Model for Urban Flood Inundation, *Volume 2017, Article ID 2819308, 12 pages https://doi.org/10.1155/2017/2819308*.

Zhang, M.L., Shen, Y.M., Guo, Y. (2008). Development and application of a eutrophication water quality model for river networks. *J. Hydrodyn. 20, 719– 726.*